

MIXING RATIO AND TEMPERATURE VARIATION IN THE WINNIPEG AREA

by

Charles G. Ponce

A thesis
presented to the University of Manitoba
in partial fulfillment of the
requirements for the degree of
Master of Arts
in
Geography

Winnipeg, Manitoba

1986 Charles G. Ponce, 1986



Permission has been granted to the National Library of Canada to microfilm this thesis and to lend or sell copies of the film.

The author (copyright owner) has reserved other publication rights, and neither the thesis nor extensive extracts from it may be printed or otherwise reproduced without his/her written permission.

L'autorisation a été accordée à la Bibliothèque nationale du Canada de microfilmer cette thèse et de prêter ou de vendre des exemplaires du film.

L'auteur (titulaire du droit d'auteur) se réserve les autres droits de publication; ni la thèse ni de longs extraits de celle-ci ne doivent être imprimés ou autrement reproduits sans son autorisation écrite.

ISBN 0-315-34001-0

MIXING RATIO AND TEMPERATURE VARIATION IN THE WINNIPEG AREA

BY

CHARLES G. PONCE

A thesis submitted to the Faculty of Graduate Studies of
the University of Manitoba in partial fulfillment of the requirements
of the degree of

MASTER OF ARTS

© 1986

Permission has been granted to the LIBRARY OF THE UNIVERSITY OF MANITOBA to lend or sell copies of this thesis, to the NATIONAL LIBRARY OF CANADA to microfilm this thesis and to lend or sell copies of the film, and UNIVERSITY MICROFILMS to publish an abstract of this thesis.

The author reserves other publication rights, and neither the thesis nor extensive extracts from it may be printed or otherwise reproduced without the author's written permission.

I hereby declare that I am the sole author of this thesis.

I authorize the University of Manitoba to lend this thesis to other institutions or individuals for the purpose of scholarly research.

Charles G. Ponce

I further authorize the University of Manitoba to reproduce this thesis by photocopying or by other means, in total or in part, at the request of other institutions or individuals for the purpose of scholarly research.

Charles G. Ponce

ABSTRACT

Over a two year period, 1976 - 1977, 253 itineraries of 86.3 km. were randomly conducted under all weather conditions along a well defined urban - rural traverse, encompassing all major land usage, upwind and downwind of Winnipeg's core area. The automobile mounted, dew point hygrometer provided dew point and temperature data which were then standardized to the initial traverse commencement time. Climatological parameters, such as mixing ratio, saturation deficits, and absolute humidities were then calculated.

Ward's error sum of squares hierarchic fusion algorithm was utilized to achieve cluster traverse organization. Linearly interpolated surface to 500 mb. radiosonde data aided in detecting air mass groupings. To facilitate urban - rural climatological comparisons with the established literature, the primary air masses chosen for investigated were the bench mark air masses, continental Arctic and continental maritime Arctic.

The general postulation throughout the thesis was that no hypothesis would be formulated regarding the traverse data sample distributions, the spatial distributions of the climatological parameters under investigation, or the

temporal variability of these climatic parameters without statistical supporting evidence. As background information regarding the bench air mass data was absent, non - parametric statistical techniques were used. The equivalent parametric statistics were also utilized on the same data in order to measure outcome variability.

The procedure generated unique conclusions which often were contrary to those found in the literature field dealing with urban - rural humidity and temperature islands.

In the case of Winnipeg, it was statistically proven that a mixing ratio island does exist under cA - cMA air mass conditions and that the spatial zones are significant even if the climatological differences were less than 1.0g/kg. The spatial forms do not necessarily parallel that of temperature. Furthermore, under specific combinations of pressure, wind speed, wind direction and cloud cover, the mixing ratio humidity island can exist separately.

Statistically it was found that alteration of the analysis from the parametric to the non - parametric drastically modified the resulting conclusions, especially when air mass surface layer complexity increased. Previously undetected and insignificant mixing ratio and temperature regimes become exposed with non - parametric statistics.

ACKNOWLEDGEMENTS

The author is grateful to many individuals for assistance given during the course of this research. I am especially indebted to the following persons.

My supervisor, Professor William Bell, who not only introduced me to the field of urban climatology, but also generously provided equipment, computer time, and continual assistance of all forms throughout the study.

To Doctor M. Samanta, who acquainted me with the fundamentals of non - parametric statistics. His office door was always open whenever I needed his professional opinion.

To Doctor A.J.W. Catchpole, for encouragement, suggestion and views on relevant themes.

À Monsieur le professeur Fortier, qui désirait toujours garder l'anonyme.

To R. Swain for instructing me how to maintain the equipment in first class condition with a minimum amount of tools.

To the various computer advisers who assisted in computer programming during the early stages of the research.

And finally, to my mother who understood the pressures associated with the undertaking. Her jovial character and constant support urged me onwards.

To all the above,

Bóg zapłać

TABLE OF CONTENTS

ABSTRACT.....	iv
ACKNOWLEDGEMENTS.....	vi
TABLE OF CONTENTS.....	viii
LIST OF TABLES.....	xi
LIST OF FIGURES.....	xiii
LIST OF MAPS.....	xiv
LIST OF SYMAPS.....	xv
APPENDICES.....	xvi

CHAPTER	PAGE
1 INTRODUCTION.....	1
1.1 Background	
1.2 Objectives	
1.3 Methodology	
1.4 History of the Study	
1.5 Definitions and Units of Measurements	
References for Chapter 1.....	11
2 URBAN HEAT ISLAND: FORMATION AND RETENTION.....	13
2.1 Introduction	
2.2 Albedo Comparisons	
2.3 Thermal Properties of Natural and Anthropogenic Materials	
2.4 Aerosol - Radiative Interactions	
2.5 Summary	
References for Chapter 2.....	36
3 LITERATURE REVIEW.....	41
3.1 Introduction	
3.2 The Evaluation of the Literature Sample	
3.2.1 Introduction	
3.2.2 Literature Sample Analysis	
3.2.3 Summary	
3.3 Conclusion	
References for Chapter 3.....	61

4	THE CLIMATE OF WINNIPEG.....	66
	4.1 Record Length	
	4.1.1 Topography and Location	
	4.1.2 Geographic Influences	
	4.2 Fronts and Air Masses	
	4.3 Synoptic Climatology	
	4.4 Temperature	
	4.5 Hot Spells	
	4.6 Cold Spells	
	4.7 Dry Spells and Drought	
	4.8 Winds	
	4.9 Weather During the Study Period	
	References for Chapter 4.....	108
5	METHODS OF INVESTIGATION.....	110
	5.1 Introduction	
	5.2 Choice of Route	
	5.2.1 Introduction	
	5.2.2 Power Restraints as a Limiting Factor	
	5.2.3 Control Site Location	
	5.3 Instrumentation	
	5.3.1 Introduction	
	5.3.2 Sensor Lag Response Estimation	
	5.3.3 Principle of Operation of Model 110S-M	
	5.3.4 Maintenance of Equipment	
	5.4 Error Minimization	
	5.5 Data Conversion	
	References for Chapter 5.....	134
6	CLASSIFICATION OF WINNIPEG'S DEW POINT REGIMES..	136
	6.1 Introduction	
	6.2 Classification	
	6.3 Dew Point Regimes During the Study Period	
	References for Chapter 6.....	163

7	ANALYSIS PROCEDURE.....	164
	7.1 Introduction	
	7.2 Classification	
	7.2.1 Introduction	
	7.2.2 Cluster Analysis	
	7.2.3 Canonical Discriminant Analysis	
	7.2.4 Conclusion	
	7.3 Tests of Normality	
	7.4 Statistic Applications	
	7.4.1 Introduction	
	7.4.2 The Kurskal-Wallis Oneway Nonparametric Anova Test	
	7.4.3 The Oneway Analysis of Variance	
	7.4.4 Kruskal-Wallis Multiple Comparison Rank Sums	
	7.4.5 Bonferroni Multiple Comparisons Method	
	7.4.6 Conclusion	
	7.5 Summary	
	References for Chapter 7.....	204
8	DATA ANALYSIS.....	207
	8.1 Introduction	
	8.2 Dendrogram Selection	
	8.3 Continental Arctic Air Mass Analysis	
	8.3.1 Fusion Selection	
	8.3.2 Proof of Air Mass Classification	
	8.3.3 The Analysis	
	8.3.4 Symap Comparisons	
	8.4 Continental Maritime Arctic Warm to Maritime Arctic Cold Air Mass Analysis	
	8.4.1 Fusion Selection	
	8.4.2 Proof of Air Mass Classification	
	8.4.3 The Analysis	
	8.5 The Analytic Conclusions and Summations	
9	SUMMATION.....	340

LIST OF TABLES

TABLE		PAGE
2.3.1	Thermodynamic Properties of Various Substances.	28
3.1.1	Weather Changes Resulting From Urbanization...	43
3.2.1	Distribution of Information in Selected Literature Sample.....	49
4.5.1	Number and Length of Hot Spells at Winnipeg 1933 - 1976.....	77
4.6.1	Number and Length of Cold Spells at Winnipeg 1933 - 1976.....	78
4.7.1	Frequency of Dry Periods of Various Lengths at Winnipeg.....	81
4.7.2	Frequencies of Months Either Wet or Dry 1874 - 1975.....	82
4.9.1	Winnipeg International Airport Meteorological Data Summary for 1976.....	89
4.9.2	Winnipeg International Airport Meteorological Data Summary for 1977.....	90
5.2.2	Point Location, Distance and Time Information..	130
6.1.1	Mean Hourly and Monthly Averages for January...	139
6.1.2	Mean Hourly and Monthly Averages for February..	141
6.1.3	Mean Hourly and Monthly Averages for March.....	143
6.1.4	Mean Hourly and Monthly Averages for April.....	145
6.1.5	Mean Hourly and Monthly Averages for May.....	147
6.1.6	Mean Hourly and Monthly Averages for June.....	149
6.1.7	Mean Hourly and Monthly Averages for July.....	151
6.1.8	Mean Hourly and Monthly Averages for August....	153
6.1.9	Mean Hourly and Monthly Averages for September..	155
6.1.10	Mean Hourly and Monthly Averages for October...	157
6.1.11	Mean Hourly and Monthly Averages for November..	159
6.1.12	Mean Hourly and Monthly Averages for December..	161
7.3.1	Temperatures Recorded at 127 Locations During 3 cA Traverses.....	180
7.3.2	Frequency Distribution of Table 7.3.1 Data.....	183
7.3.3	Test of Normality for Data of Table 7.3.1.....	184
7.4.3.2	Analysis of Variance of Table 7.3.1 Data.....	194
7.4.4.1	Critical Inequalities of Multiple Comparison of Table 7.3.1 Data.....	197
7.4.4.2	Multiple Comparisons of Table 7.3.1 Temperature Data.....	198

8.1	Code Assignment for Critical Alpha Levels of Kruskal-Wallis Multiple Comparison Rank Sums Data.....	217
8.2.1	Clustan-1C2 Job Fusion Variation of cA and cmA Traverses.....	219
8.3.1.1	Climatological and Cluster Information for Traverses Conducted Under cA and cmA Air Mass Conditions.....	234
8.3.1.2	Statistical Information on Traverses Conducted Under cA and cmA Air Mass Conditions.....	235
8.3.2.1	cA Tephigram Comparisons.....	248
8.3.3.1	Kolmogorov - Smirnov Goodness - of - Fit Test for Temperature Data of S - W Group and Cycle 126.....	263
8.3.3.2	The Squared Ranks Test for Variances (First Five Locations of Table 7.3.1).....	269
8.3.3.3	Significant Multiple Squared Ranks Test Comparisons for Cycle 126 Temperature Variance.....	272
8.4.1.1	Climatological Information for Traverses Conducted Under the Various cmAw to mAk Air Mass Transformation Stages.....	303
8.4.1.2a	Early cmAw - mAk Air Mass Transformation Traverse Dendrogram.....	304
8.4.1.2b	Later cmAw - mAk Air Mass Transformation Traverse Dendrogram.....	305
8.4.1.3a	Statistical Information of Traverses Conducted Under Early cmAw - mAk Air Mass Transformation Stages.....	306
8.4.1.3b	Statistical Information of Traverses Conducted Under Later cmAw - mAk Air Mass Transformation Stage.....	307
8.4.2.1	cmAw - mAk Tephigram Comparisons.....	316

LIST OF FIGURES

FIGURE		PAGE
5.3.3.1	General Block Diagram of the Automatic Meteorological Temperature and Dew Point Model 110S - M Measuring System.....	122
6.1.1	Hourly Temperature and Dew Point Means for January.....	140
6.1.2	Hourly Temperature and Dew Point Means for February.....	142
6.1.3	Hourly Temperature and Dew Point Means for March.....	144
6.1.4	Hourly Temperature and Dew Point Means for April.....	146
6.1.5	Hourly Temperature and Dew Point Means for May.....	148
6.1.6	Hourly Temperature and Dew Point Means for June.....	150
6.1.7	Hourly Temperature and Dew Point Means for July.....	152
6.1.8	Hourly Temperature and Dew Point Means for August.....	154
6.1.9	Hourly Temperature and Dew Point Means for September.....	156
6.1.10	Hourly Temperature and Dew Point Means for October.....	158
6.1.11	Hourly Temperature and Dew Point Means for November.....	160
6.1.12	Hourly Temperature and Dew Point Means for December.....	162
8.2.1	Chosen Cluster Analysis Dendrogram.....	231
8.3.3.4a	3 - Dimensional View of Symap 8.3.3.1a.....	291
8.3.3.4b	3 - Dimensional View of Symap 8.3.3.1b.....	292
8.3.3.5	3 - Dimensional View of Symap 8.3.3.2.....	293

LIST OF MAPS

MAPS	PAGE	
4.9.1	Precipitation and Temperature Abnormalities for January, 1976.....	91
4.9.2	Precipitation and Temperature Abnormalities for February, 1976.....	92
4.9.3	Precipitation and Temperature Abnormalities for March, 1976.....	93
4.9.4	Precipitation and Temperature Abnormalities for April, 1976.....	94
4.9.5	Precipitation and Temperature Abnormalities for May, 1976.....	95
4.9.6	Precipitation and Temperature Abnormalities for June, 1976.....	96
4.9.7	Precipitation and Temperature Abnormalities for July, 1976.....	97
4.9.8	Precipitation and Temperature Abnormalities for August, 1976.....	98
4.9.9	Precipitation and Temperature Abnormalities for September, 1976.....	99
4.9.10	Precipitation and Temperature Abnormalities for October, 1976.....	100
4.9.11	Precipitation and Temperature Abnormalities for November, 1976.....	101
4.9.12	Precipitation and Temperature Abnormalities for December, 1976.....	102
4.9.13	Precipitation and Temperature Abnormalities for January, 1977.....	103
4.9.14	Precipitation and Temperature Abnormalities for February, 1977.....	104
4.9.15	Precipitation and Temperature Abnormalities for March, 1977.....	105
4.9.16	Precipitation and Temperature Abnormalities for April, 1977.....	106
4.9.17	Precipitation and Temperature Abnormalities for May, 1977.....	107
5.2.1	Research Traverse Route with Point Locations (Used in Conjunction with Table 5.2.2).....	114

LIST OF SYMAPS

SYMAPS	PAGE
8.3.3.1a cA: S - W Wind Direction Group -- Temperature..	288
8.3.3.1b cA: S - W Wind Direction Group -- Mixing Ratio.	289
8.3.3.2 cA: Cycle 126 -- Temperature..	290
8.4.3.1 Early cmAw to mAk Transformation -- Temperature.....	294

LIST OF APPENDICES

LETTER		PAGE
A	Hypothetical Estimation of St. Norbert Heat Generation.....	346
B	Hypothetical Estimation of Unicity Fashion Square Heat Lose.....	351
C	Dates On Which Traverses Were Conducted.....	353

CHAPTER 1

Introduction

1.1 Background

This thesis is an analysis of the spatial and temporal horizontal distribution of humidity and temperature within an urban-rural context. The analysis, however, has been based upon the results and comparison of the results of nonparametrical and parametrical computations. Not a single assumption, climatological nor statistical, has been made without prior justification.

Emphasis has been placed upon mixing ratio variations and its relationship with temperature.

The role of humidity and temperature in meteorological-climatological studies can no longer be considered as only a prime tool for synoptic analysis (Ruskin, 1963). Although the understanding of the dynamics of the atmosphere-humidity systems is still in an embryonic stage, horizontal and vertical humidity variations, in time and space, are now major considerations in cloud physics and mechanics, weather modification¹, upper atmospheric

¹ The processes of evaporation and condensation of water vapor provide a means of transporting energy from one locale to another. A change in the mean temperature of the lower atmosphere shifts the location in which these processes take place and thus alters the distribution of atmospheric temperature over a greater portion of the area.

circulation², refraction of radio waves, aircraft condensation formation and in fog forecasting. For certain purposes, such as studies of radiative fluxes and the role humidity plays in air pollution reactions and urban heat island development, mixing ratios and absolute humidities are now an absolute requirement (Hage, 1975).

Distributional aspects of humidity are also of vital concern in fields such as agriculture, food science, medicine, air-conditioning and military. For example, the precise knowledge of seasonal and diurnal variations of humidity and temperature are critical to the specification of ventilation requirements for civil defense shelters (Ludwig, 1967).

Unfortunately, accurate representation of areal, spatial, and temporal distribution of water vapor in the atmosphere, at all levels and at all meteorological-climatological scale ranges, has lagged considerably behind representation of other climatic elements. Temperature variations have dominated and still dominate most discussions (Dodd, 1964; Oke, 1974; Yoshino, 1976). As early as the late 18th-early 19th century when Louis Cotte and Luke Howard, pioneers of urban-climatic studies, published explicit accounts on urban climate

² During the 'International Quite Sun Year' (IQSY), humidity was used as a tracer in the study of world-wide stratospheric circulation.

variations of Paris and London respectively, the humidity research gap was present. Kremser's paper entitled "Der Einfluss der Grosstade auf die Luftfeuchtigkeit" (The Influence of Large Towns on Air Humidity) was the first article since Cotte's publication that treated humidity variations not as strict dependents of temperature but as the results of urbanization (Greiger, 1961). Anthropogenic sources of water vapor were now recognized as important contributing factors.

Out of 230 papers presented at the 1963 International Symposium on Humidity and Moisture in Washington D.C., not one paper at the conference dealt with the distributional aspects of humidity (Dodd, 1964). This was paradoxical since the symposium was convened in order to provide a perspective view of the total cross-disciplinary nature of humidity and moisture studies (Rushin, 1963). Even in 1968, at the Geneva World Meteorological Organization Conference on Urban Climates, again not a single paper dealing with humidity variation and dispersion was again presented. From 1774 to 1969 only 17 articles have dealt with humidity variations, both within and between an urban and rural complex (Chandler, 1969). During the time raw data for this thesis was acquired and analyzed, only one major paper entitled "Humidity Distributions in a Small City and Their Relationships to Surface Materials" by James A. Henry, was published (Chandler, 1976).

Of the few comparative studies undertaken, analysis has been limited to those days and nights when such climatic parameters as wind speed and opacity were advantageous to the establishment and retention of intense urban heat islands, not humidity islands. Measurements of the moisture content of urban and rural atmospheres were also limited in time duration. Thus what observational evidence there is, is not completely conclusive (Chandler, 1976).

1.2 Objectives

Since cities appear to initiate complex interactions between advective, diffusive and radiative processes following local changes in boundary conditions, an understanding of the relative temporal and spatial distribution of water vapor and its relationship to temperature may provide further impetus for analysis or re-analysis of the urban mesoclimate. The probability of a re-analysis increases, not only at an urban mesoclimatic scale but at all climatic levels, when one examines the underlining reasoning behind climatological-meteorological studies. That is, the statistical framework for the majority of these studies was based upon parametric data assumptions. Assumptions which either were carried over from similar research undertakings or were assumed as valid for the data in question mainly because the field of parametric statistics is far better understood and is much better represented in computer packages. Whether or not the

assumptions were valid were not to be questioned. The results of the findings are therefore distorted unless otherwise proven.

Therefore, the objectives of this study are:

- (1) to deduce the possible anthropogenic and meteorological parameters which would influence the structure, duration and magnitude of the urban heat and mixing ratio islands with specific reference to the research zone and the climatic conditions that prevailed prior and during the acquisition of climatic data. By adopting such an approach, a theoretical foundation is built. The selected statistically significant analyzed data can thus be fitted against the hypothesis. This procedure, furthermore, prevents the fitting of numerous questionable ideals against the data.
- (2) to present, analyze and delineate statistically-significant spatial and temporal distributions of mixing ratio from original traverse data taken over a two year span under all weather conditions within a well defined urban-rural complex. Cluster analysis will be employed to achieve some sort of traverse organization while non-parametric statistical techniques will be used on the particular fusions in order to locate which of these fusions have statistically significant temperature and/or mixing ratio distributions. The selected dendrogram groupings will then be subjected to the equivalent parametric statistics. Comparisons will be made with emphasis placed upon discovering to what degree parametric assumption violations effect or alter the computed results.
- (3) to estimate and delineate the magnitude variations of the temperature and mixing ratio islands on the basis of air mass type and climatic parameter differentiation. These changes will be further investigated through the examination of case studies. However, if the selected data groupings are such that there seems to be no time unity, case studies will not be undertaken. For example, if only 5 out of 30 traverses of a particular air mass have been proven to be statistically significant on one or both of the climatic parameters under scrutiny and these 5 traverses are not within the same time

frame, it would be misleading to label this group as a general representation of temperature and/or mixing ratio variations for that particular air mass.

Fulfillment of these interrelated objectives will be achieved through an inverse hierarchical examination of the data. Scrutinization shall commence with the analysis of the most illogical climatological cluster, that is, the main cluster comprising of 253 traverses, and shall terminate with the numerous explicitly defined sub-clusters of the main air mass categories. Meteorological-temporal parameter combinations to be infused with each analysis will be introduced such that those conditions which maximize the urban mixing ratio and/or heat islands will precede those which minimize island formation.

Though scrupulous in nature, these methods ensure the dominance of statistical inferred conclusions. Hence, the prior "reference" and inductive hypothetical reasoning techniques will be rendered validless. A non-significant statistical conclusion is in itself significant because it has proven the fact of insignificance.

A static methodology is thus ruled out. New test statistics chosen for objective optimization, shall be introduced whenever greater clarification of the results

are required. However, when the nonparametric and their equivalent parametric forms yield conflicting conclusions for the same data field, conclusions which would appear as "false inadequate impressions" in the literature field of this thesis' topic, the thesis shall terminate. This of course does not connote abandonment of the objectives, but on the contrary, indicates investigation and enlightenment. Clarification will be provided in later chapters. Here themes dealing with the so-called unifying framework of urban climatological systems shall be investigated.

Revision, where required, will follow.

1.3 Methodology

The research objectives are attained through the acquisition of a large quantity of dew point and temperature data, measured by automobile mounted instrumentation, driven along a well defined traverse, encompassing all major land usage, upwind and downwind of Winnipeg's core area, over a two year sampling period. Traverse data was reduced to a constant time after conversion from millivolts to degrees Celsius was completed. Regular synoptic observations at the Winnipeg International Airport Meteorological Station were then merged to form the data base. Analysis of daily surface and upper air charts plus examination of

prognostic aviation forecasts provided the broader meteorological picture with respect to air mass type. The data base was subdivided according to season, air mass and wind quadrant direction. Fixed point estimators were grouped accordingly and subjected to para- and nonpara-metric tests of significance. Interpretation, conclusion, and assumptions were based upon those results which showed strong statistical significance.

1.4 History of the Study

The foundation of this study and interest of the author stemmed from similar research previously undertaken along a parallel traverse in Winnipeg by Bell of the University of Winnipeg. The lack of humidity research in urban-rural mesoclimatic studies intensified by the desire to examine the effect of urbanization on certain climatic parameters, provided the stimulus to undertake a few night time traverses in November 1975. Results indicated that even under cloudy, windy conditions, the heat and humidity islands exist climatologically, even though statistical significance between the average fixed point observations was less than the 95% level. Plans were therefore made with Bell to undertake further study.

Over a two year period, 253 traverses were randomly conducted, yielding 32, 131 cases of point data. There

were 127 fixed point measurements per traverse (see Map 5.2.1). From the basic data acquired, air vapor pressure also known as the saturated vapor pressure at dew point, was calculated. Formulae for the above conversions and for further conversions to mixing ratios, etc. were obtained from the Smithsonian Meteorological Tables.

The data was accordingly edited and an attempt was made to perform a comprehensive analysis of this data.

1.5 Definitions and Units of Measurements

The two climatic parameters under investigation in this study are mixing ratio and temperature. As the former climatic parameter can not be directly measured from the environment, the dew (frost)-point temperature of the air will be logged. All units in this thesis are metric.

The thermodynamic dew point temperature, T_d , of moist air at temperature, T , and at pressure, p , and mixing ratio, r , is the temperature to which the air must be cooled in order that it shall be saturated with respect to liquid water at the initial pressure, p , and mixing ratio, r . Temperature is the major climatic control determining the maximum dew point value. Other influencing factors are:

- (1) air mass type
- (2) wind direction and speed

- (3) moisture conditions on the ground
- (4) turbulent mass exchange
- (5) cloudiness as affecting the insolation of an area
- (6) water surface temperature and water body area upwind of an area
- (7) evapotranspiration and anthropogenic sources of water vapor

The thermodynamic frost point temperature's definition parallels the above in all respects except that it is determined with respect to ice.

The mixing ratio, r , of moist air is the ratio of the mass, m_v , of water vapor in grams to the mass of dry air in kilograms with which the water vapor is associated with. Together with absolute humidities, mixing ratios are the best indicators of air mass type for only condensation and evaporation can alter the values.

All definitions of the above parameters correspond to those formulated and adopted by the World Meteorological Organization. These definitions are in affect at present.

The boundaries of Winnipeg are defined as all areas located within and bounded by Manitoba Provincial Highways 100 and 101. The latter highways are locally referred to as the Perimeter.

LIST OF REFERENCES

- Chandler, T.J., 1976:Urban Climatology and Its' Relevance to Urban Design. Technical Note No. 149, World Meteorological Organization, Geneva, 36pp.
- _____, 1969:Selected Bibliography on Urban Climate. Technical Note No. 155, World Meteorological Organization, Geneva, 383pp.
- Dodd, Arthur van Zandt, 1964:Water Vapor Near the Ground in the Continuous United States. Ph.D. Theses, Pennsylvania State University, 199pp.
- Geiger, Rudolf, 1965:The Climate Near the Ground. Cambridge,Harward University Press, 611pp.
- Hage, K.D., 1975:Urban-Rural Humidity Differences. Journal of Applied Meteorology, 14, 1277-1283
- Hall, A.E. and Hoffman, G.J., 1976:Leaf Conductance Response to Humidity and Water Transport in Plants. Agronomy Journal, 68, 876-881.
- Henry, J.A., 1976:Humidity Distributions in a Small City and Their Relationships to Surface Materials. Great Plains-Rocky Mountain Geographical Journal, 5(1),47-56
- Oke, T.R., 1974:Review of Urban Climatology. Technical Note No. 134, World Meteorological Organization, Geneva, 133pp.
- Ruskin, R.E., 1963:The Measurement of Humidity in Meteorology. Weatherwise, 4, 55-61
- United States Office of Civil Defense. Office of the Secretary of the Army. Urban Climatological Studies by F. L. Ludwig. Contract OCD-PS-64-201,work unit 1235A,Washington D.C.:Government Printing Office,1967.

Yoshino, Masatoshi, 1976:Climate in a Small Area:an
Introduction to Local Meteorology. Tokyo, University
of Tokyo Press, 549pp.

CHAPTER 2

Urban Heat Island:Formation and Retention

2.1 Introduction

The following discussion on urban heat island formation and retention shall be very selective since voluminous literature has been directed towards this topic. Detailed examination of such contributing parameters to heat island formation, as:

- (1) the effect varying concentrations of gaseous pollutants have on the radiative balance.
- (2) wind velocity
- (3) cloud cover and opacity
- (4) anthropogenic heat sources
- (5) city density structure
- (6) time

have been adequately documented by Oke(1944), Yoshino(1975), Bach(1976) and Chandler(1976). These aspects, therefore, need not be mentioned here. Consequently, the discussion shall be limited to those contributing factors most prominent within the research area. Typical urban albedoes¹ and the thermodynamic properties of urban surfaces shall be compared with their rural counterparts. The possible effect aerosols might have upon the research area's radiative balance shall then be discussed. The latter control is of considerable

¹ Albedo is defined here as the decimal fraction of reflected or scattered to incident global radiation, and is used to denote the characteristic reflectivity of radiation within the range 0.36 to 4.00 microns.

importance for current studies by LaDochy et al.(1977) have shown that not only do the particulate counts for the research zone exceed the Clean Air Act standards, but also, the values rank among those cited for such cities as Los Angeles, Chicago, and Atlanta. When one examines the climatic conditions that prevailed over the research area and Western North America during the data acquisition period, aerosol contribution to the radiative balance becomes crucial.²

Results of LaDochy's analysis will later be employed in Chapters 8 to 10 as possible explanations of why under certain climatic conditions, dewpoint and temperature differences between urban and rural points were not

² It is generally accepted that within any urban or rural atmosphere, airborne concentrations, by weight, of minerals originating from such sources as sea spray, forest fires and industry, are quite low relative to soil minerals (McMullen et al. 1970). Within the research area, the above generalization is less than valid. Concentrations vary with season and climatic conditions. For instance, from early November to late May, approximately $81.65 * 10^6$ to $90.72 * 10^6$ kg of salt treated sand is present upon the city's street systems (personal communication, Ed Kyjanka, Materials and Research, City of Winnipeg). Coefficients of haze are greater over urban areas during this period with maximum values being reached after snowmelt (LaDochy et al., 1977). An increased aerosol concentration results in a reduced loss of both shortwave radiation due to less scattering and longwave radiation due to an increase in atmospheric absorption. Both processes heat the atmosphere, reducing the heat flux, and thus slightly warm the surface. Aerosols above the inversion heat the air and thus maintain the inversion strength. In so doing, the inversion height rise is suppressed, hence, aerosol dispersion is checked and the greenhouse affect strengthened over urban areas. Thus the urban factor is increased. See Chapter 3 for evidence of the above occurrence.

statistically significant.

2.2 Albedo Comparisons

Surface albedo, a fundamental surface property which can be relatively easily altered by mere surface treatment, both natural and anthropogenic, directly determines the absorptivity of any opaque surface. Thus for a given solar input and counter irradiance, albedo regulates the daytime surface shortwave and longwave absorption. Both the latter, in turn, dominate the net radiation budget. A limit to the magnitude of the surface energy balance and the inter-related water balance is therefore established. Albedo manipulation invokes a change in the thermal and moisture climate of the surface and the adjacent air and soil layers. The following discussion will indicate the magnitude of influence albedo possesses.

It has long been recognized that the lighter the colour of an object the higher its albedo. The colour of a substance is determined by the substance's chemical structure and the physical conditions effecting the substance. For fibrous or granular matter the primary physical control is moisture. Bare soil albedo is dependent mainly upon the moisture status of the soil surface.³ Aase et al. (1975) have calculated that significant

³ The major chemical controls of soil colour are the amount of organic material present and the particle size distribution. An increase in the former fosters an overall increase in the absorption of radiant energy within the

colour change in soil can increase or decrease albedo by approximately 60 percent on both smooth and rough surfaces. Approximately 14.2-18.3 percent more direct solar energy received in the 0.5-2.6 micron range will be absorbed by an increase in moisture content while the remaining increase in percentage occurs in the near infrared (Bowers et al., 1965; Kondrat'yev, 1969).

Although the albedo of natural and anthropogenic materials is less affected by moisture, similar absorption-reflectance characteristics exist per wavelength.⁴ For instance, the reflectivity of limestone, white brick and sandstone at 0.5 microns is equal to 40 percent, whereas at 2.6 microns it is 87 percent

wavelength region 0.36 to 1.80 microns while accompanying decrease soil particle size is a rapid exponential increase in reflectance (Bowers et al., 1965).

⁴ Reflectance decreases with increased wavelengths for each substance only when wavelengths are greater than a specific length. The critical wavelengths range from 1.1 to 3.0 microns. The inverse relation occurs for wavelengths below the critical length (Kondrat'yev, 1969).

Reflectance reaches a maximum at sun elevations of 10-20 degrees (Coulson et al., 1971; Kondrat'yev, 1969). It is during this elevation that the ratio between direct to diffuse light is equal, thereby producing no change in surface reflectance. When the sun is below 10 degrees elevation or below the horizon incident light is entirely diffuse and surface reflectance is relatively low varying from 22 to 26 percent. As the sun increases beyond 20 degrees elevation, direct light incident at a larger zenith angle becomes the dominant component. Hence, albedo decreases to a minimum at solar noon.

Myrup(1969), who reasoned as above, showed theoretically that the urban heat island should be most intense at solar noon and least during low solar zeniths. Although

(Kondrat'yev, 1969). With sun elevations of 10 to 50 degrees, hemispheric reflectance at 0.3 microns for tar, asphalt and macadam is 0.09 while at 0.8 microns it is 0.20 (Coulson, 1971). Absorption of wavelengths greater than 1.3 microns varies directly with wavelength.

Since albedo is generally symmetric about solar noon, with minima recorded at that time, for both dry bare soil⁵ and homogenous materials, (Idso et al., 1975), albedo value differences between bare dry soil and non-black urban fabric become negligible.⁶ Anthropogenic heat sources and an increased sensible heat flux between buildings and their air envelope due to the thermodynamics of the enormous surface area then become the prime factors maintaining an urban factor.

Values of albedo are lower over vegetated ground than for either bare soil or anthropogenic materials. Lower values occur because leaf reflectivity does not increase with increasing wavelength to a specific threshold length nor does it decrease with increasing wavelength after the threshold length has been passed. Investigation of

Goldreich's(1970) analysis of Johannesburg's heat island confirms the above possibility, most studies indicate that the temperature excess is actually greatest at night. Chapters 8 to 10 will show that there is some validity to Myrup's hypothesis in the Winnipeg Region.

⁵ Dry soil is defined as having a volumetric water content less than 0.04.

⁶ Absorption-reflectance characteristics of glass and highly polished metallic materials do not parallel those for bare soil.

numerous texts and papers have shown that on the average, reflectance remains stable at 0.5 within the range 0.34-0.50 microns, increasing to 0.13 at 0.54 microns but falling in the red to its former stable value. The maximum fall occurs at 0.65 microns. A very strong increase follows, leading to high values in the regions 0.8-1.3 microns, 1.5-1.8 microns and 2.1-2.3 microns. Reflectivity of leaves beyond wavelengths greater than 2.5 microns is minute, being less than 10 percent for an angle of incidence of 65 degrees and less than 5 percent for an angle of 20 degrees.⁷

If one compares the reflectivity of limestone, white brick and sandstone of infrared at 2.6 microns to that of green vegetation, the former groups value is 24.8 times greater than that of the latter (Kondrat'yev, 1969;Woolley, 1971).

Vegetative stand albedo is lower than the albedo value for its individual leaf because reflection now depends upon the combined influences of the radiative properties of the component surfaces,crop physiology,stand architecture and

⁷ The primary absorbing agent of the infrared beyond 2.5 microns is plant water. Leaves are classified as almost perfectly full radiators in the infrared and therefore are also very efficient emitters of longwave radiation. This high emissivity, and the portion of energy liberated in the form of latent heat of evapotranspiration aid the leaf in shedding heat to the environment. Thus the temperature of the leaf is moderated.

the angle of solar incidence. The latter four factors control the amount of shortwave and longwave penetration and escape, the internal radiative absorption, reflection, transmission and trapping as well as the mutual shading within the stand volume. For detailed examination of the influence each of the above factors possess, see Monteith(1973), Bannister(1976) and Lange et al., (1976).

The radiation budget of a plant stand is therefore quite complex. Nevertheless, the following generalizations hold valid:

- (1) The actual height of the principal active layer in a canopy lies closer to the top than to the bottom of the stand. Position of the actual height depends upon the species and the levels of the effective sources and sinks of heat, water vapor, momentum and carbon dioxide.
- (2) The transmission of shortwave and longwave radiation into a stand or canopy shows an almost logarithmic decay with depth of penetration. (Monteith, 1973). Ripley et al., (1976) measured an 85% reduction of incoming solar radiation in a 0.2m stand of native grass at Matador, Saskatchewan at solar noon on June 28th, 1972. Net all-wave radiation in Watts per square meter for the same period varied from approximately 564 above the grass canopy to 213 at ground level, a 62% reduction. Similarly, Gay et al., (1971) estimated the average transmission of shortwave radiation through a 2.3m stand of Loblolly pine to be about 18%. During the 8 hour measurement period, the total shortwave radiation intensity above the canopy was 16.1 MJ/m² while on the floor it barely approached 2.8MJ/m².
- (3) The vertical attenuation of solar radiation by foliage affects the spectral composition of the solar radiation penetrating through a stand canopy. Wavelengths less than 0.74 and greater than 2.5 microns are totally absorbed by the leaf.⁸ The intensity of the spectral range less

⁸ Plant pigments, particularly chlorophyll, have strong

than 0.74 microns is $687\text{W}/\text{m}^2$ and represents approximately 50.8% of the total intensity of the solar constant $1353\text{W}/\text{m}^2$. The greatest solar spectral irradiance for the Thekaekara standard solar curve, $0.2074\text{ W}/\text{m}^2$ per micron is within this spectral range being obtained at 0.48 micron wavelengths. The respective intensity and the fraction of the total intensity for the spectral range greater than 2.5 microns are $50\text{W}/\text{m}^2$ and 3.7%. Radiation with wavelengths between these limits can either be reflected or transmitted downwards through the leaf canopy. Although this spectral range represents 45.5% of the total solar irradiance curve and has an average intensity of $61\text{W}/\text{m}^2$, the average solar spectral irradiance of $0.432\text{W}/\text{m}^2$ per micron, centred at 1.25 microns, is approximately 21% that of the maximum received at 0.48 microns. Thus a unit area of floor surface must receive a greater quantity of lower intense shortwave energy in order to equal the amount that could have been received at shorter wavelengths if the stand or canopy did not exist. However, as stated in the introduction of this section, reflection decreases with increased wavelengths for inanimate materials only when wavelengths are greater than a specific length. The critical wavelength was referenced to range from 1.1 to 3.0 microns. Hence, vegetative stands or canopies further decrease the available shortwave energy that would have been converted to other energy forms on contact with the ground or stored in the ground. The approximate reduction varies by approximately 53.5 to 68.2 percent.

- (4) The geometry of the canopy provides a radiative trap for outgoing longwave radiation. The net loss diminishes towards the ground, however. Trapping of outgoing longwave radiation therefore tends to reduce surface cooling.

Even in winter, the above influences are present.

Federer(1970) has estimated from both theoretical and empirical data that roughly 65 percent of the incident radiation on leafless trees is absorbed by stems, branches

absorption bands in the violet and ultraviolet, the blue (0.40-0.51 microns), and the red(0.61-0.74 microns). Peak absorption is at 0.45 microns.

and trunks while approximately 20 percent is reflected upwards. The remaining 15 percent penetrates downward.

The net effect of the diurnal heating and cooling of a vegetated surface is to raise the level of the maximum diurnal temperature range from the soil surface to either the maximum leaf area in the case of tree or herbaceous plant canopies or near to the top in the case of grass-like vegetation. In the former vegetative types, the maximum leaf area is the location where radiative absorption and transpiration provide the most heat and water vapor. The maximum air temperature and mixing ratio are located here. Beneath this a temperature inversion occurs because the canopy is warmer than the floor where, as previously shown, only weak radiative absorption occurs due to the restrictive radiative nature of the canopy. The humidity profile is less intense underneath a canopy because of the contribution of evaporation from the soil, or evapotranspiration from the plants on the floor. The lapse above the canopy is not very pronounced also because of the evapotranspirational cooling at the surface of the foliage.

At night, the inverse situation occurs. The minimum temperature is in the upper portion of the canopy but the inversion is above and the lapse below. The canopy's ability to absorb almost all longwave radiation at

wavelengths greater than 2.5 microns ensures that longwave radiative losses from both the ground and the canopy are reduced. Thus relatively mild conditions are maintained within the stand as compared with those found in the open or above the canopy.

The humidity inversion remains during the night although in a weakened form provided that no dew formation occurs.

Although the climatic modification initiated by grass-like vegetation is similar to that discussed above, the degree of influence diminishes with a decrease in plant height and in plant density. Unlike canopies or herbaceous plants, the upright orientation of grass allows bodies of air to freely migrate vertically. Furthermore, mixing is aided by the fact that grasses are readily displaced by wind. Nevertheless, temperatures are never extreme as those developed over bare ground (Monteith, 1973 and Yoshino, 1976).

Evidence of the above leaf canopy and canopy influence can be found in Chapters 8 to 10. For example, the difference between the maximum urban temperature and the average temperature for readings taken within rural agricultural areas was statistically significant beyond $\alpha=0.025$.⁹ The difference between the maximum urban

⁹ The example cited is valid only when the air mass affecting the region is of a maritime Pacific-maritime Tropic admixture. The centre of the High pressure system

temperature and the average temperature for readings taken within Assiniboine Park was statistically significant at $\alpha=0.01$. The mean temperature for the treed park was less than that of the rural areas and the variance of the former was 5.5 times smaller than that of the latter.

In summary, vegetative ground cover and leaf canopies reduce temperature and humidity variability. The degree of variability reduction, however, varies with climate, season, plant physiology and many species-specific factors.

The albedo of snow is the most variable of all albedoes so far discussed. It may reach a value of almost 100 percent over clean dry snow yet in the case of typical dirty moist snow, it may fall as low as 20-30 percent. Illumination conditions, recrystallization processes on and within the snow pack during a day's time and surface roughness are the major parameters influencing the above variability.

Direct evidence of all the above albedo variations with season and time between various urban and rural morphologies is scarce.¹⁰ Aerial transects undertaken by Bray et

must be over southern Lake Michigan while a Low pressure system must approach from central Saskatchewan. The winds generated must be within the wind quadrant 90 to 180 degrees.

¹⁰ It should be noted that even though the flight lines of the following researchers were selected with a view to investigate extensive reasonably homogenous surfaces, measurements acquired were in reality those for effective albedo rather than for ground albedo. The former

al.(1966) from Bethal to St. Paul, Minnesota, on the first of September, under clear skies, yielded results indicating that as a unit, urban surfaces for that particular location were more reflective than agricultural surfaces which in turn had an higher albedo than natural vegetation. Respective mean albedoes were .074 , .067 , and .053. Category wise, the highest mean albedo was registered for commercial districts:.09. Industrial complexes followed with .08. The mean value for ploughed fields, .078, was third highest, being 9 percent higher than that registered for railway yards and 17 percent greater in value than that estimated for residential sectors. Bray's urban analysis complemented those of Kung et al.(1964) and to a limited degree, those of Barry et al.(1966). Studies by the latter group undertaken in June over Southern England showed that the average albedo for houses, .18, was 19 percent lower than that computed for fields though 11 percent greater than that calculated for heath. Seasonal differences are the causes of the latter's discrepancies.

albedo type is a result of complex interactions of solar radiation with aerosols and absorbing gases in the atmosphere, ground albedoes, solar zenith angle and pollutant concentrations. Therefore, the mean effective albedoes, classified as ground by the referenced authors, are not totally representative of ground or canopy albedo.

2.3 Thermal Properties of Natural and Anthropogenic Materials

Differences in the thermodynamic properties of urban and rural fabric combined with the enhanced sensible heat flux between buildings and their air envelope due to the enormous surface area of buildings, has resulted in the creation of a thermal lag between urbanized areas and their rural surroundings. Thermal lag is fundamental to the genesis of heat islands (Oke, 1973). The magnitude of the thermal lag depends, in part, upon the differences between the heat capacities and conductivities of the various fabrics. The following discussion explores the above relationships.

The thermodynamic properties to be compared are volumetric thermal capacity, (c) and thermal conductivity, (k). The former gives the amount of heat required to raise the temperature of one cubic meter of material by one degree Kelvin while the latter is the amount of heat, in Watts, that will flow through unit area of that material in one second when the temperature difference between opposite faces is one degree Kelvin and there are no other variations in temperature within that unit area; the plane of the area being perpendicular to the temperature gradient.

Values of the above parameters for homogeneous materials such as aluminum and iron and of types of building materials

such as stone, brick, cement, asphalt and lumber, which may be considered homogeneous, vary mainly with density and are slightly dependent on temperature (ASHRAE, 1970). For fibrous or granular materials, such as clay, sand and peat, volumetric thermal capacity¹¹ and thermal conductivity values are dependent on the following parameters:

- (1) temperature: The degree of influence depends upon whether it is above or below freezing: For moisture content greater than 0.12, conductivity of frozen soil becomes progressively greater than that of the unfrozen soil. (Judge, 1971).
- (2) density: The affects of density are constant for all soils at any moisture level and for either frozen or unfrozen conditions. For each 0.016 gram per cubic centimeter in dry density increase, the thermal conductivity increases by a factor of 0.03 (van Wijk, 1969).
- (3) moisture: An increase in moisture content, up to saturation, causes an increase in both c and k. For volumetric water content 0, the thermal conductivity of Whitemouth clays, a subdivision of Red River clays, is 0.209 watts while at 0.45 water content, conductivity increases to 1.200 watts. (de Jong, 1978).

¹¹ The total volumetric thermal capacity of a substance is equal to the sum of all density-specific heat products for each type of solid particle present plus that of water not chemically bounded to the particles. Air can be ignored because of its low density. Only changes in moisture can alter the overall density which in turn alters the volumetric thermal capacity of a substance. However, the phase state of the moisture present determines the thermodynamic properties. That is, the heat capacity of ice decreases by a factor of about 0.4 from that of water, though its conductivity increases by a factor of 3.75 over that of water.

¹² Values for both c and k have been compiled from various sources. They should be regarded as average values only. Thermal conductivities are for a temperature of 20°C.. Values of c and k for Red River clays fall within the ranges listed. The latter information was provided by Dr. C. F.

It can be seen from Table 2.3.1.¹² that the average volumetric thermal capacities and thermal conductivities of construction material are greater than those for Manitoba clays. As clays are never totally dry, this statement should only be viewed as representative for an unique condition.

Thus, the urban fabric heats slower, although the heat absorbed penetrates to a greater depth. Maximum absorption occurs at solar noon, when albedo is at its lowest. After solar noon, the urban fabric cools slowly, slower than soil or vegetated surfaces, thus inducing the thermal lag. When a pall of smoke and dust is present above the city, outgoing radiation is hindered, thus increasing the urban factor.

As the rise of soil surface temperature during the day and the fall of soil surface temperature at night varies inversely as the square root of the product of kps where p is soil density and s is specific heat (Brunt, 1945), the greatest fall of temperature from sunset to sunrise would be expected over dry soils.¹³ This was evident in summer

Shaykewich, Department of Soil Science, University of Manitoba.

¹³ Although heavy wet soils cool slower than dry soils, see Table 2.3.1, their original sunset temperatures are usually much lower so that they are capable of reaching lower night time minima. Evaporation or transpiration further reduces the temperature, thereby increasing the urban factor. Evidence of the above has been provided by Einarsson et

TABLE 2.3.1

THERMODYNAMIC PROPERTIES OF VARIOUS SUBSTANCES

<u>SUBSTANCE</u>	$(W/m \frac{K}{^{\circ}K})$	$(KJ/m^3 \frac{C}{^{\circ}K})$
AIR	0.026	1.275
WATER	0.598	4195.50
ICE	2.240	1861.87
DRY CLAY	0.209	1129.68
WET CLAY	1.200	3138.00
DRY SAND	0.293	1297.35
SATURATED SAND	1.884	2176.20
LIMESTONE	2.210	2171.13
SANDSTONE	1.947	1967.47
GRANITE	3.396	2198.25
CONCRETE(1.2.4)	1.120	1933.32
BRICK	1.080	1737.60
ASPHALT	0.698	2427.05
MASONRY PLASTER	1.047	1636.00
WINDOW SHEET GLASS	0.818	2143.0
ALUMINUM ALLOYS	104.67	2447.55
STEEL	59.313	3764.08

evening traverse results. As drying vegetation acts as an insulating layer, this upward flux of soil heat can be reduced. Fall results also indicate such an occurrence.

al.(1956).

The rate of evaporation, an important component in the energy balance of natural surfaces, also influences the decrease and increase in temperature.

2.4 Aerosol-Radiative Interactions

Direct aerosol extinction contributed more towards heat island formation, retention and variation than did its indirect counterpart due to the climatic conditions that prevailed during the acquisition of raw data.¹⁴ The magnitude of influence is, however, determined by such factors as:

- (1) chemical composition of particles present
- (2) particle shape and radius
- (3) particle concentrations and optical depth
- (4) aerosol position in relation to cloud cover
- (5) the presence and concentrations of other known infrared absorbers, such as water vapor, carbon dioxide, carbon monoxide, nitrous oxide, and methane.
- (6) vapor pressure of the atmosphere in which the aerosols are present.

With reference to (4), aerosols lead to net heating when distributed above the preexisting atmospheric scatterers. (Weare et al., 1974; Chylek et al., 1973).

Contributions by aerosols below 8 microns and above 12 microns are negligible under normal climatic conditions because the absorption coefficients of water vapor exceed those of aerosols (Grassl, 1973). The inverse

¹⁴ Aerosols can affect the radiative balance either directly through scattering and absorbing both direct and diffuse shortwave and infrared radiation or indirectly by acting as condensation or freezing nuclei if they possess the correct hygroscopic properties.

relationship, however, is valid in the 8-12 micron range.¹⁵ The average absorption coefficient in $\text{cm}^2/\text{g} \cdot 10^4$ for water vapor at wavelength 9.75 microns is approximately 39.90% of that of the estimate for sea salt; 6.87% of that of dust; 2.90% of that of water solubles collected from precipitation and 2.74% of that of soots. (Kondrat'yev, 1969; Volz, 1972a, b; Twitty et al., 1971). Roberts et al. (1970) have estimated that extinction by carbon dioxide is approximately 0.02 per km in the 8-12 micron region or 13.33% of the total extinction possible for all wavelengths for a normal average atmospheric carbon dioxide concentration.

¹⁵ Although the area under the standard solar spectral irradiance curve in the wavelength range 8.0 to 12.0 microns is $1.2\text{W}/\text{m}^2$ and represents only 0.09% of the solar constant $1353\text{W}/\text{m}^2$, for earth's corrected NACA standard atmosphere blackbody radiation curve, the area and percent of the total intensity $390.139\text{W}/\text{m}^2$ increases to $99\text{W}/\text{m}^2$ and 25.3% respectively (see Wallace et al., 1977 for calculation procedures.) The peak intensity found by Wien's displacement law for earth's mean radiating surface temperature of 15°C is 10.059 microns. The intensity of emission at this wavelength is $0.021\text{W}/\text{m}^2$ per micron. This is approximately 69 times greater than the intensity of the solar spectral irradiation averaged over the 8.0 to 12.0 micron range. The corrected blackbody emission intensity of 10.059 microns is approximately equal to that at solar wavelength 3.29 microns.

As the absolute temperature of a radiating substance on the earth's surface increases, the total energy radiated at that temperature and the intensity of the radiant energy flux at maximum emission increases while the wavelength, in microns, of maximum emission decreases. The fraction of the total area under the corrected blackbody curve in the wavelength range 8.0 to 12.0 microns, however, remains fairly

Dusts, inorganic water solubles, such as, NaCL, (NH₄)₂SO₄, CaO, and carbonaceous particles were the main aerosol types influencing radiative cooling or heating over Winnipeg during the above period. Contributions by the latter were of greatest significance.¹⁶ Since the absorption index for carbon is unsurpassed¹⁷ and the influence that water vapor would have on radiative scattering and absorption of infrared was minimal due to the drought, the urban factor within the research area was insignificant when the prevailing winds were light and had trajectories over the carbon sources.¹⁸

constant. Calculations of the fraction of the total area in the above spectral range for NACA standard atmospheric conditions at Winnipeg and for the daytime maximum thermal infrared surface temperature, 49.9°C for industrial sectors of St. Louis as determined by White et al. (1978), show only a variation of 2.7%. Respective values of total radiant energy and area in the 8.0 to 12.0 micron range for Winnipeg were 382.051 W/m² and 9.6%. For industrial sectors of St. Louis, the values are 616. W/m² and 17.2%. The following NACA standard atmosphere parameter values were used in the calculation of the above example: mean temperature, 13.5°C; pressure, 985.8mb; air density, 1.1978kg/m³; gravity acceleration, 9.810196m/sec².

¹⁶ Peat bog fires situated northwest, east and southeast of the city were the sources of carbon-ash haze which engulfed the research zone for the time period July 1976-May 1977 (Don Budesky, Air Pollution Control Section, Winnipeg, Environment Canada, personal communication, 1977).

¹⁷ Average absorption indices for dust range from 0.011 at 5 microns to 0.15 at 40 microns (Volz, 1972a, b). These values are greater than those estimated for water soluble aerosols although less than those for soots and carbons. Absorption by soots are 11.36 times greater than that of

It should be noted that although Rouse et al.(1973), Ackerman et al.(1976), Peterson et al.(1977) and Viskanta et al.(1977) have shown, both theoretically, and empirically that there is a strong tendency within the substrate-atmosphere system for self-stabilizing radiative compensation, constants used and conditions under which studies occurred were as near to average as possible. It will be shown in Chapter 4 that the climatic conditions during this study were not average but close to and beyond the alpha 0.05 critical mark. The hypothesis of the above authors thus become debatable.

2.5 Summary

In conclusion, the lack of data and research on the above discussed topics within Winnipeg prevents adequate proof of the points discussed above. However, as previously stated, the preceding discussion forms the basis for deducing why parameter variation between various urban-rural points were or were not statistically significant when traverses were conducted under particular synoptic

dust at 2.5 microns;2.67 times greater at 10 microns and 1.2 times greater at 40 microns. The absorption index of carbon is 6.88 times greater than soot at 2.5 microns and approximately 78.18 times greater than dust at the same wavelength (Bergstrom, 1972).

¹⁸ Since the atmosphere is being heated directly through aerosol absorption, the temperature differential between the surface and the atmosphere is reduced which in turn lowers the degree of heat transfer. Thus surface temperature variability is lessened (Viskanta et al., 1977).

conditions. Important points references are:

- (1) the absorption indices of carbonaceous aerosols are unsurpassed with respect to those of other aerosols. Specific indices, however, for the carbon-ash haze that engulfed the research zone from July 1976 to May 1977 were not determined (personal communication, Don Budesky, Air Pollution Control Section, Winnipeg, Environment Canada, 1977).

Indirect evidence of the magnitude of haze influence upon the radiative balance of the city, acquireable through the comparison of thermal infrared air photographs of similar grid sections of Winnipeg taken during similar synoptic conditions prior to and during the engulfment period, was not brought forward because no thermal infrared remote sensing of the city was undertaken during the engulfment period (personal communication, Su-Ann Bolette, Remote Sensing, Surveys and Mapping Branch, Government of Manitoba, 1980).

Even though data for coefficient of haze (COH) and total suspended particulate data has existed from 1970 for each of the four NAPS stations located at various sites throughout the city, the erratic and haphazard manner in which the data has been collected and logged renders the data's validity questionable. For example, although the actual percentage varies per station and per time sampling period, in many cases, less than 75% of the required COH data was available to calculate daily, weekly and monthly hourly mean values.

Total suspended particulate data for each monitoring station might have yielded useful information if long term average geographical monthly ambient suspended particulate data distributions for the Western Prairies and the Northern United States Plains and the terminal velocity of the particulate components of the haze were known.¹⁹ From the above

¹⁹ The actual terminal velocity of the carbonaceous aerosols of the carbon-ash haze could not be determined as neither the radii nor the densities were known. However, by substituting the average urban sooty dust density estimate of 1.6g/cm^3 as determined by Volz (1972) and using the peak carbon particle radius curve value of 0.07 microns (Twitty et al., 1977), the terminal velocity for a carbon based particle of the

data, an approximate proportion of the relative contribution of haze particulates to the total volume could have been determined and compared with the normal particulate contribution.

- (2) reflectivity increases with increased wavelength to a specific threshold length for most homogeneous surfaces, both natural and anthropogenic, as well as for bare dry and saturated soils.
- (3) wavelengths less than 0.45 microns and greater than 2.5 microns are totally absorbed by the leaf. Only radiation within the above wavelength limits will be reflected or transmitted downwards by the leaf.
- (4) canopy reflectance, both ground based and upper level, dominates ground reflectance. The degree of dominance varies with season, climate and physiological stimuli. For upper level canopies, the degree of influence is not dependant on season. The magnitude, however, diminishes with leaf fall, though it is always greater than that of grass and herbaceous plants.

Placing the above points in perspective, the following hypothesis may explain why no parameter variation between urban and rural points during haze conditions in autumn occurred.

The carbon-ash haze over Winnipeg, in addition to gross depletion of shortwave radiation, altered the spectral and directional character of solar beams to a greater extent than that under normal conditions. Higher energy wavelengths were filtered more readily while the proportion of diffuse beams increased.

above characteristics suspended in a 50°N. Latitude NACA standard atmosphere would be 0.001cm/sec. The time required for such a particle to sedimentate is far greater than the time required for that particle to be transported from any of the peat bog fires surrounding the research area (see footnote 18). For the required computation formulas, see Williamson, 1973.

In the rural sections of the research zone, the diffuse radiation penetrated groundwards 'unhindered' while in urban Winnipeg, with the exception of the C.B.D. and several industrial sectors, tree canopies further decreased the quality and quantity of solar radiation. Temperatures therefore should be lower under vegetative canopies than over rural surfaces. However, within the residential sectors, anthropogenic generated heat aided in maintaining equal to higher temperatures.

Although albedoes for all surfaces and the degree of multiple reflection between surfaces remained lower than normal because of the diffuse characteristic, the highest values were found within the C.B.D. and sectors not within the influence of vegetative canopies. Thus, more shortwave radiation was lost. Anthropogenic heat sources, once again, aid in maintaining slightly higher temperatures.

Other hypothesis will be discussed in future chapters.

LIST OF REFERENCES

- Aase, J.K. and Idso, S.B., 1975:Solar Radiation Interactions With Mixed Prairie Rangeland in Natural and Denuded Conditions. Arch. Met. Geoph. Biokl., Ser. B, 23, 255-264.
- American Society of Heating, Refrigerating, and Air Conditioning Engineers Inc., 1972:ASHRAE Handbook of Fundamentals. New York, New York, 1250pp..
- Ackerman, T.P., Liou, Kuo-Nan, and Leovy, C.B., 1976:Infrared Radiation Transfer in Polluted Atmospheres. Jour. of App. Met., 15, 28-35.
- Bach, W., 1976:Global Air Pollution and Climatic Change. Rev. Geophys. and Space Phys., 14, 429-474.
- Barry, R.G.and Chambers, R.E., 1966:A Preliminary Map of Summer Albedo over England and Wales. Quart. Jour. Roy. Met. Soc., 92, 543-548.
- Bannister, P..1973:Introduction to Physiological Plant Ecology. London, Blackwell Scientific Publications, 273pp.
- Bergstrom Jr., R.W., 1972:Predictions of the Spectral Absorption and Extinction Coefficients of an Urban Air Pollution Aerosol Model. Atmos. Environ., 6, 247-258.
- Bowers, S.A. and Hanks, R.J., 1965:Reflection of Radiant Energy From Soils. Soil Science, 100, 140-138.
- Bray, J.R., Sanger, J.E., and Archer, A.L., 1966:The Visible Albedo of Surfaces. Ecology, 47, 524-531.
- Chylek, P. and Coakley, J.A., 1974:Aerosols and Climate. Science, 183, 75-77.

- Coulson, K.L. and Reynolds, D.W., 1971: The Spectral Reflectance of Natural Surfaces. Jour. of Appl. Met., 10, 1285-1295.
- Eagleman, J.K., 1974: A Comparison of Urban Climatic Modification in Three Cities. Atmos. Environ., 8, 1131-1142.
- Einarsson, E. and Lowe, H.B., 1956: A Study of Horizontal Temperature Variations in the Winnipeg Area on Nights Favoring Radiational Cooling. Meteorological Branch, Department of Transport Circular No. 2647, TEC-214.
- Federer, C.A., 1968: Spatial Variation of Net Radiation, Albedo and Surface Temperature of Forests. Jour. of Appl. Met., 7, 789-795.
- Fischer, K., 1975: Mass Absorption Indices of Various Types of Natural Aerosol Particles in the Infrared. Appl. Optics, 14, 2851-2856.
- Flanigan, D.F. and Delong, H.P., 1971: Spectral Absorption Characteristics of the Major Components of Dust Clouds. Appl. Optics, 10, 51-57.
- Fraser, H.M., 1977: The Dry Fall of 1976 and Its Implications. Environment Canada, Atmospheric Environment Service, Internal Report, 22pp.
- Gates, D.M. and Tantraporn, W., 1952: The Reflectivity of Deciduous Trees and Herbaceous Plants in the Infrared to 25 Microns. Science, 115, 613-616.
- Grassl, H., 1973: Aerosol Influence on Radiative Cooling. Tellus, 25, 386-395.
- Idso, S.B., Jackson, R.D., Reginato, R.J., Kimball, B.A. and Nakayama, F.S., 1975: The Dependence of Bare Soil Albedo on Soil Water Content. Jour. of Appl. Met., 38, 109-113.
- Judge, A.S., 1972: Conductivity of Earth Materials. In Proceedings of a Seminar on the Thermal Regime

Measurements in Permafrost, 2-3 May, Ottawa. NRCC Asso. Com. on Geotech. Res., Tech. Memo. No. 108.

De Jong, R., 1978:Energy Exchange:Soil Surface and Soil Temperature Regime. Ph.D. Thesis, University of Manitoba.

Kanemasu, E.J., 1974:Seasonal Canopy Reflectance Patterns of Wheat, Sorghum and Soya Bean. Rem. Sens. of Environ., 3, 43-47.

Knipling, E.B., 1970:Physical and Physiological Basis for the Reflectance of Visible and Near-Infrared Radiation from Vegetation. Rem. Sens. of Environ., 1, 155-159.

Kondrat'yev, K.Ia., 1969:Radiation in the Atmosphere. New York, Academic Press, 912pp.

Kung, E.C., Bryson, R.A.A and Lenschow, D.H., 1964:Study of a Continental Surface Albedo on the Basis of Flight Measurements and Structure of the Earth's Surface Cover over North America. Mon. Weather Rev., 92, 543-564.

LaDochy, S., Ball, T. and Warchuk, B., 1978:The Nitty-Gritty of Winnipeg Air. Prairie Forum, 1, 135-150.

Lange, O.L., Kappen, L. and Schulze, E.D., 1976:Water and Plant Life:Problems and Modern Approaches. Heidelberg, Springer-Verlag-Berlin, 536pp.

Lin, Chin-I, Baker, M. and Charlson, R.J., 1973:Absorption Coefficient of Atmospheric Aerosol:A Method of Measurement. Appl. Optics, 12, 1356-1363.

McMullen, T.B.Morgan, G.B. and Ludwig, J.H., 1970: Trends in Urban Air Quality. American Geophysical Union:Transactions., 5, 468-475.

Monteith, J.L., 1973:Principles of Environmental Physics. London, Edward Arnold, 241pp.

- Myrup, L.O., 1969:A Numerical Model of the Urban Heat Island. Jour. Appl. Met., 8, 908-918
- Oke, T.R., 1973:City Size and the Urban Heat Island. Atmos. Environ., 7, 769-779
- , 1974:Review of Urban Climatology. Technical Note No. 134, World Meteorological Organization, Geneva, 133pp.
- Peterson, J.T. and Flowers, E.C., 1977:Interactions Between Air Pollution and Solar Radiation. Solar Energy, 19, 23-32.
- Pueschel, R.F. and Kuhn, P.M., 1975:Infrared Absorption of Tropospheric Aerosols:Urban and Rural Aerosols of Phoenix, Arizona. Jour. of Geo. Res., 80, 2960-2962.
- Rouse, W.R., Noach, D. and McCutcheon, J., 1973:Radiation, Temperature and Atmospheric Emissivities in a Polluted Urban Atmosphere of Hamilton, Ontario. Jour. of Appl. Met., 12, 798-807
- Twitty, J.T. and Wernman, J.A., 1971:Radiative Properties of Carbonaceous Aerosols. Jorn. of Appl. Met., 10, 725-731.
- Viskanta, R., Bergstrom, R.W. and Johnson, R.O., 1977:Radiative Transfer in Polluted Atmospheres. Jour. of Appl. Met., 34, 1091-1103.
- Volz, F.F., 1972(a):Infrared Absorption by Atmospheric Aerosol Substances. Jour. of Geophys. Res., 77, 1017-1031.
- _____, 1972(b):Infrared Refractive Index of Atmospheric Aerosol Substances. Appl. Optics, 11, 755-759.
- Weare, B.C., Temkin, R.L. and Snell, F.M., 1974:Aerosol and Climate. Some Further Considerations. Science, 186, 827-828.

van Wijk, W.R., 1963:Physics of Plant Environment.
Amsterdam, North-Holland Pub. Co., 382pp.

Williamson, S.J., 1973:Fundamentals of Air Pollution. Don
Mills, Ontario, Addison-Wesley Pub. Co., 472pp.

Wallace, J.M. and Hobbs, P.V., 1977:Atmospheric Science:An
Introductory Survey. New York, Academic Press

White, J.M., Eaton, F.D. and Auer, A.H, 1978:The Net
Radiation Budget of the St. Louis Metropolitan Area.
Journal of Applied Meteorology, 17, 593-599.

Woolley, J.T., 1971:Reflectance and Transmittance of Light
By Leaves. Plant Physiol., 47, 565-622.

Yoshino, Masatoshi, 1976:Climate in a Small Area:an
Introduction to Local Meteorology. Tokyo, University of
Tokyo Press, 549pp.

CHAPTER 3

Literature Review

3.1 Introduction

Although numerous studies of the climatological properties of urban heat islands and the relationships of heat island intensities to city size have been reported for various cities of the world, the results are, to a fair degree, conflicting. For instance, even though it is generally conceded that the annual cycle of heat island intensity is weak,¹ results differ concerning the diurnal and seasonal timing of the maximum and minimum intensities. Goldreich(1970), for example, has shown that the urban factor of Johannesburg, in contrast to studies by Sundborg(1950), Chandler(1965), and Oke and East(1971), to name only a few, is greatest by day, least by night, in summer. These findings provide empirical proof for Myrup's numerical heat island model. Yet studies also have shown that the maximum temperature change during winter in the city is less than that experienced in summer. The latter statement is in agreement with Chandler(1962) though in complete disagreement with Mitchell(1961) and Landsberg(1956).

¹ The annual mean urban factor for Chicago and Washington is 0.6°C.. For Los Angeles, Paris and Moscow it is 0.7°C.. For Philadelphia, Berlin, New York and Vancouver, respective values are 0.8°C., 1.1°C., 1.1°C. and 1.5°C (Landsberg, 1960; Hay et al., 1970).

Rather obvious disagreements also exist with the concept of heat island intensity in relation to city size. Chandler(1976) has consistently rejected the hypothesis that a linear relationship between the urban factor and the city area is possible even though Oke(1973) and Eagleman(1974) have shown otherwise.

Similar incongruencies are evident in studies examining possible reasons for heat island occurrence. It has been seen in the previous chapter that the differences in heat capacity between urban and rural fabric can not by themselves explain the obvious day-time patterns. An explanation based on radiative effects leads to better agreement with the observations than do the thermal mass arguments (Ludwig, 1970). Thermal lag however, has been quoted as fundamental to the genesis of heat islands (Chandler, 1976).

Inconsistencies in research findings, such as listed above, have not, nevertheless, hindered the estimation and tabulation of the relative urban contributions to local climate alterations. Table 3.1.1, after Oke(1977), illustrates the average change of various climatic parameters resulting from urbanization. Values are expressed as percentages or magnitudes of rural conditions.

TABLE 3.1.1

WEATHER CHANGES RESULTING FROM URBANIZATION
(PERCENTAGE)

<u>PARAMETERS</u>	<u>ANNUAL</u>	<u>WINTER</u>	<u>SUMMER</u>
SOLAR RADIATION	- 22	- 34	- 20
AIR TEMPERATURE(°C)	+ 1	+ 2	+ 0.5
RELATIVE HUMIDITY(frequency)	- 6	- 2	- 8
VISIBILITY(frequency)	- 25	- 34	- 17
FOG(frequency)	+ 60	+100	+ 30
WIND SPEED	- 25	- 20	- 30
CLOUDINESS(frequency)	+ 8	+ 5	+ 10
RAINFALL(amount)	+ 14	+ 13	+ 15
SNOWFALL(amount)	+ 10	+ 10	-
THUNDERSTORMS(frequency)	+ 16	+ 5	+ 30
POLLUTION(volume)	+1000	+2000	+500

SOURCE: Oke, 1977

The values attributed to the above air temperature and relative humidity parameters, should only be regarded as very crude estimates. These figures have been deduced on calculations derived from various research conclusions regardless of the particularities prevalent to each analysis. The prevailing synoptic conditions, the number of samples taken, instrument type, research procedures and the possible geographic topographic influences are major factors neglected in such relative compilations.

Furthermore, urban-rural differences stem from the integrated contrasts between town and country in each term of an energy balance equation, each undergoing diurnal, seasonal and synoptic changes through time and space. Only when the above influences are considered and only when research

findings are then grouped according to these influences can values such as those tabulated in Table 3.1.1 have meaning.

As stated in Chapter 2, voluminous literature has been directed towards analyzing, explaining and comparing the formation and retention of urban heat islands. Kratzer(1937) listed references to 533 works. Approximately 250 were added by Brooks(1951). Books by Geiger(1965) also refer to a number of other urban studies. Under the auspices of the World Meteorological Organization, Oke(1974) further referenced 375 articles while Chandler(1976) compiled bibliographies on urban climate with well over 1000 articles. It therefore becomes quite obvious that some sort of selection procedure must be developed when discussing the literature pertinent to this thesis.

After considerable thought, it was decided that the research techniques adopted by the various authors were far more important than their qualitative conclusions. Extensive summaries of their analyses have been adequately documented by Oke(1974), Yoshino(1976), Bach(1976) and Chandler(1976), to name only a few. These aspects, therefore, need not be mentioned here.

The literature review, hereto, shall concentrate upon the comparison of data collection and analysis techniques

employed by only those researchers who have acquired temperature and humidity data via automobile traverses. To this selection, the classic studies of Middletown et al.(1936), Sundborg(1950) and Duckworth et al.(1954) will also be added. Examination of research technique progression and/or digression with time necessitates their inclusion. By so doing, the present investigation techniques can be categorized within the sampled literature field.

3.2 The Evaluation of the Literature Sample

3.2.1 Introduction

The following systematic analysis of the various research methods referenced in the selected literature sample is based upon procedures adopted from Catchpole et al.(1976). The results are tabulated and given in Table 3.2.1. The authors of the selected articles and the date of publication are listed vertically while along the horizontal axis are the classification and distribution of information statements. The general topic headings of the latter are represented as Roman numerals, whereas their identification statements are noted in Arabic form. The above coded system has the following interpretations:

I Site Physique

- (1) the maximum estimated elevation difference, in meters, between areas traversed by the itinerary(ies) or between cities in which traverses were conducted. A blank indicates that information was lacking and topographic maps of the research zone could not be obtained.

- (2) as elevation differences guarantee a range of temperature and dew point of some magnitude at all times and may also mask or modify the effects caused by other factors, particularly those associated with local variations in urban land use, all logged data was reduced to their potential values at sea level pressures.

II Itinerary Choice

- (1) the itinerary was selected to traverse areas associated with varied urban-rural morphologies within, through and outside of either the heat dome or heat plume in all the major compass directions.
- (2) the route(s) crossed at several points thus providing a means of checking data variation with time.

III Synoptic Conditions Underwhich Traverses Were Conducted

- (1) traverses were conducted only on nights favoring radiational cooling.
- (2) traverses were conducted during the times of minimum and/or maximum sensible heat generation.
- (3) traverses were conducted on randomly selected days and/or nights under varied synoptic conditions.

IV General Traverse Information

- (1) if either more than one city was designated as a research zone or if there were more than one itinerary chosen per city, each traversed by a compatible mobile unit, traverses were undertaken simultaneously with respect to commencement time and synoptic conditions.

V Instrumentation

- (1) the accuracy and precision of the measuring equipment were either noted in the article or referenced to another article, report or circular.
- (2) where simultaneous measurements of temperature and a humidity parameter were taken, sensor lag was noted.
- (3) radiation shielding was present in order to either eliminate or minimize errors arising from solar heating at all radiation levels.
- (4) sensors were automatically aspirated.

- (5) the instruments were placed on the automobile in such a manner as to eliminate or minimize engine and other foreign heat influences.
- (6) in the case of manually operated apparatus, special error minimizational procedures were initiated and employed to insure that the data collected was representative of that particular site for that specific time.
- (7) all data was automatically logged on some form of continuous recording apparatus such as strip charts or ticker tape units.

VI Control Site Establishment and Location

- (1) instrumented control sites independent of first order meteorological stations were either established along the itinerary or within the research zone.
- (2) the positioning of apparatus at the control sites were discussed in terms of possible microclimatic influences as well as operational-maintenance procedures and probable problems.
- (3) first order meteorological stations were employed as control sites.
- (4) first order meteorological stations provided supplementary data only.

VII Editing, Standardization and Statistical Analysis Procedures

- (1) data editing and sorting to particular categories such as air mass type or wind direction and speed were discussed.
- (2) standardization of traverse data to a particular time was indicated by the researcher(s) to be fundamental for unique synoptic conditions only although no background information or references were given.
- (3) standardization of traverse data to a particular time was based upon the linear interpolation of first order meteorological station data logged during the traverse time period.
- (4) standardization of traverse data to a particular time was based upon the linear interpolation of the overall data variation occurring during the traverse as registered on strip charts or ticker tapes.
- (5) standardization information was not noted or referenced to other reports, articles or circulars.

- (6) standardization formulas were either noted and/or explained in detail.
- (7) statistical tests were employed in the analysis of data.

When information pertinent to the explanation of a particular identification statement has been found or referenced in a specific article, the number of that identification statement is listed in the corresponding article row position.

TABLE 3.2.1

DISTRIBUTION OF INFORMATION IN SELECTED LITERATURE SAMPLE

<u>AUTHORS</u>	<u>I</u>	<u>II</u>	<u>III</u>	<u>IV</u>
Chandler, T.J. (1962)	76 -	-2	1--	-
Chandler, T.J. (1967)	38 -	12	--3	-
Conrads, L.A. et al. (1971)	2 -	-2	--3	-
Duckworth, F.S. et al. (1954)	91 -	-2	--3	-
Einarsson, E. et al. (1954)	18 -	-2	1--	-
Eagleman, J.R. (1974)	113 -	-2	-23	-
Fonda, R.W. et al. (1971)	274 -	-2	--3	-
Garnett, A. et al. (1963)	305 2	1-	--3	-
Goldreich, Y. (1970)	300 -	-2	-2-	-
Goldreich, Y. (1974)	300 -	-2	-23	-
Hannell, F.G. (1976)	-	12	-23	-
Hartley, M. (1977)	97 -	12	--3	-
Hutcheon, R.J. et al. (1967)	525 -	-2	1--	-
Kingham, H.H. (1969)	76 -	12	--3	-
Kopec, R.J. (1970)	125 -	-2	--3	-
Kopec, R.J. (1973)	125 -	-2	--3	-
Landsberg, H.E. (1975)	70 -	-2	--3	-
Linguist, S. (1968)	81 -	-2	--3	-
Ludwig, F.L. (1967)	1603 -	12	--3	-
Ludwig, F.L. (1968)	101 -	-2	--3	-
Lyons, T.J. et al. (1975)	266 -	-2	1--	-
McBoyle, G.R. (1970)	-	-2	1--	-
Middleton, W.E. et al. (1936)	96 -	-2	--3	-
Millward, G.E. et al. (1976)	1000 2	12	-2-	-
Oke, T.R. (1967)	168 -	-2	1--	-
Oke, T.R. et al. (1968)	116 -	12	--3	-
Oke, T.R. (1973)	69 -	-2	1--	-
Oke, T.R. et al. (1975)	-	--	1--	-
Sham Sani (1973)	76 -	12	1--	-
Sisterson, D.L. (1978)	50 2	1-	--3	-
Sundborg, A. (1950)	41 -	12	--3	-

TABLE 3.2.1 (CON'T)

DISTRIBUTION OF INFORMATION IN SELECTED LITERATURE SAMPLE

<u>AUTHORS</u>	<u>V</u>	<u>VI</u>	<u>VII</u>
Chandler, T.J. (1962)	-23-5-7	----	----5--
Chandler, T.J. (1967)	-2345-7	1--4	---4---
Conrads, L.A. et al. (1971)	12345-7	--3-	-2----7
Duckworth, F.S. et al. (1954)	---45--	1--4	---4---
Einarsson, E. et al. (1954)	123-5--	---4	----5--
Eagleman, J.R. (1974)	--3-5-7	---4	---4---
Fonda, R.W. et al. (1971)	1----6-	---4	-----
Garnett, A. et al. (1963)	----5--	---4	----5--
Goldreich, Y. (1970)	--345-7	1-3-	1-34-6-
Goldreich, Y. (1974)	--345-7	1-3-	1-34-6-
Hannell, F.G. (1976)	1----6-	--3-	----5--
Hartley, M. (1977)	-23-5--	---4	---4---
Hutcheon, R.J. et al. (1967)	-----6-	---4	-----
Kingham, H.H. (1969)	-----6-	1--4	-2-----
Kopec, R.J. (1970)	-23-5--	---4	-----
Kopec, R.J. (1973)	-2345--	---4	-----
Landsberg, H.E. (1975)	----5--	123-	----5--
Linguist, S. (1968)	--3-5--	1-3-	---4---
Ludwig, F.L. (1967)	12345-7	1-3-	1--4-6-
Ludwig, F.L. (1968)	12345-7	--3-	---4---
Lyons, T.J. et al. (1975)	123-5--	1-3-	---4---
McBoyle, G.R. (1970)	-----6-	---4	-----
Middleton, W.E. et al. (1936)	-23-5--	---4	----5--
Millward, G.E. et al. (1976)	1----6-	1--4	---4---
Oke, T.R. (1967)	-----6-	---	-2-----
Oke, T.R. et al. (1968)	-----	1-3-	-----
Oke, T.R. (1973)	1-345-7	---4	----5--
Oke, T.R. et al. (1975)	1-345--	---4	---4---
Sham Sani (1973)	1----6-	---4	----5--
Sisterson, D.L. (1978)	1-345-7	1--4	---4---
Sundborg, A. (1950)	1-3-5--	---4	---4---

3.2.2 Literature Sample Analysis

At a glance, it appears that little comparative information can be extracted from the 31 selected articles. Information deemed essential for the analytic progression of this thesis is to a fair degree absent from the selected literature. However, a systematic analysis of the selection allows broad comparisons to be made.

Since considerable differences in height and hence pressure existed between fixed point locations and/or control sites along the itineraries in all the research zones with the exception of the City of Utrecht, see Conrads et al.(1971), temperature data should have been transformed to its potential values at sea level pressure. This would aid to differentiate urban-rural land use variations from relief factors. However, only three authors, Garnett et al.(1963), Millward et al.(1976) and Sisterson(1978) deemed the procedure a necessity. The foremost author's article was the first in which potential temperature assessment had been used in interpreting traverses of this kind. Oke(1967) states that the use of potential temperature could eliminate altitude effects, however, nowhere in his publications is there an explicit statement indicating the procedure's use. In many articles, statements expressing the idea that either relief is of small overall consequence, see Chandler(1967), or has little or no effect

when below a specific level, see Duckworth et al. (1954), were presented as arguments against reduction to potential values. Ludwig (1968) goes as far as to state that an elevation difference of 101m is of little consequence.

The question of whether humidity parameter data should be reduced to standard sea level pressure was not discussed in any article. This is rather unfortunate because there has been extremely heated debates about its use. European investigators choose to reduce the data to sea level whereas the American investigators choose to present the data for the levels at which they are obtained (Dodd, 1964).

Information regarding itinerary choice can best be summed up as being totally obscure. Although 11 authors state that the urban-industrial-rural complex was sampled, only Sundborg (1950) actually discusses the grounds for making the final choice. That is, the author declared that the primary investigation problem encountered was to find points within the research zone that can be expected to give representative values for the city when located in the city and representative values for the surrounding countryside when situated within a rural or open landscape. By comparing standard deviations of temperature data collected during a number of preliminary irregular traverses, transitional transitory locations within the research zone where located. The final observation route

chosen by Sundborg encompassed only those points with calculated standard deviations less than 0.3°C.

Whether or not energy requirements played an active restrictive role in determining the route chosen, can not be determined for this aspect was not discussed in any article examined.

In each article, with the exception of Garnett et al. (1963), there was adequate information proving that each route had sufficient crossings and repeated measurements in order to calculate regional temperature and humidity variations during the period of the traverse. Of the total, 14 authors use this information to aid in the standardization of data while four, Kopec (1970, 1973), Fonda et al. (1971), Hutcheon et al. (1967) and Einarsson et al. (1954) use the information as arguments against standardization. Adjustments were not required for the latter group of four because temporal temperature and humidity parameter change was minute, usually less than one or two degrees and even these contrasts were seldom experienced.

Although 9 authors have indicated that research was restricted to nocturnal situations favoring adequate intense heat island formation, only Oke et al. (1975) define what constitutes a favored nocturnal condition. Calm and clear data sets were those in which winds were <1.3m per sec. and the cloud cover was less than two-thirds Cirrus. Light

winds and scattered cloud were referred to conditions with winds <3m per sec. and a discontinuous Cirrus cloud cover of less than five tenths. Oke et al.(1975) further restricted the analysis to essentially steady state conditions. That is, no marked cloud and wind conditions must occur during the entire traverse period. If the latter condition was not met, the entire traverse was discarded.

Hannell(1976), Millward et al.(1976), Eagleman(1974) and Goldreich(1979, 1974) conducted measurements during the early morning and afternoon hours corresponding to the time of maximum and minimum temperature. The foremost researcher confined his traverses to within 1.5 hours prior to and after solar noon. Goldreich expanded upon this sampling procedure by only concentrating upon the daily extreme temperatures registered during December and June, the months when the earth's axis lean at a maximum inclination of 23.5° with respect to a line drawn to the sun.

In spite of the fact that 20 researchers clearly indicated that in order to avoid a subjective preference for any particular weather type, observations would be conducted at different times of the day, under different weather conditions, closer examination of their case studies indicated that the true statistical definition of randomness was not adhered to in the majority of cases. Hartley(1977), Fonda et al.(1971), Chandler(1969) and

Duckworth et al.(1954) concentrated on nocturnal conditions while Sisterson(1978) confined his analyses to daylight hours. Moreover, three authors, Landsberg(1975), Kopec(1970,1973) and Kingham(1969) had indicated that there was a bias towards those nights that might optimize information on the development of the heat island.

In an effort to determine the nature of temperature and humidity variations within and between urban areas,an extensive program of measurements were undertaken in a number of cities by Eagleman(1974), Ludwig(1967,1968),McBoyle(1970) and Duckworth et al.(1954). The conclusions brought forth,however,are debatable. Simultaneous and sequential traverses in each research city were not conducted by any of the above authors. Duckworth et al.(1954) directs attention to the fact that traverses were only undertaken under similar synoptic conditions though what parameter values constituted a similar condition classification were not discussed or referenced. Ludwig(1967) compared the results obtained from San Jose,California, Albuquerque,New Mexico and New Orleans,Louisiana:cities,not only having different climatic classification codes but also different geographic topographic influences. Though each urban area traversed by McBoyle(1970) is relatively free from any major altitudinal variation,each experiencing the same elements associated with a humid temperate climate,the traverse time

sequences were all erratic. Better planning would have eliminated the above unfavorable situations.

A breakdown of the type of instrumentation employed by the various researchers shows that 10 authors used electric resistance thermometers while 11 employed thermistors of various makes. Thermocouples were used only by a single examiner whereas 6 obtained data with the aid of various psychrometers. Mercury-in-glass thermometers were used by 4 authors. If the accuracy of the only data acquisition instrument used in this study, a Cambridge Systems Model 110S-M Automatic Meteorological Temperature and Dew Point Measuring Hygrometer, is set as the base for comparison purposes, see Chapter 5, the E.G.&G. Model 880 Dew Point Hygrometer employed by Kopec (1973) is the only apparatus used by any researcher whose article(s) has been sampled which has an operating efficiency greater than 90 percent of the base. Based on the information present in each article, operating efficiencies greater than 85 percent of the base value have been calculated for the instruments employed by Sisterson (1978) and Ludwig (1967). It should be noted that where adequate information regarding apparatus accuracy and precision was lacking, statements connoting that instrument sensitivity was well adjusted to the scale of the investigation, being neither so sensitive as to register unrelated short-period fluctuations or so slack to smooth out significant local differences, were present.

Less than two-thirds of the instruments had radiation shielding while in approximately 68 percent of the studies, automatic sensor ventilation was absent. Furthermore, only eight researchers indicated in their articles that data collected was automatically logged on some sort of recording device.

Virtually every author has taken several precautions to minimize outside heat influence. However, no set of precautions were similar. Data has therefore been obtained from several microclimatic layers above the ground. Instrument positioning above the ground has varied from a minimum of 0.3m to a maximum of 2m. Only four authors, Einarson et al. (1954), Chandler (1967), Kopec (1970, 1973) and Sham Sani (1973) have obtained measurements by positioning apparatus such that it would be at meteorological instrumentation screen level.

The establishment of control sites either independently operated or under the auspice of federal agencies were neither set up or solicited by half of the researchers whose articles have been sampled. Unfortunately, information explaining why control sites were not established were not cited in the articles.

Only Landsberg (1975) adequately describes the problems associated with control site usage. The considerable outlay for instruments and installation as well as the

requirement of a number of dependable observers were some of the problematic aspects discussed in the article. In fact, Landsberg has devoted several paragraphs to illustrate the vandalic nature of the anti-science element present in all research areas. The latter group deliberately inactivated instruments thus rendering data, logged over a period of one year, useless.

As can be expected, supplementary information was acquired from first order meteorological stations by the majority of authors.

When a researcher undertakes a particular study and is faced with a specific problem such as the standardization of data to a particular time, an adequate and precise description of each technique encountered in the literature bears more weight than the number of ways the problem can be remedied. Unfortunately, in the literature sampled, only Ludwig(1967) and Goldreich(1970) have painstakingly supplied sufficient information regarding data editing and standardization so as to enable the duplication of their unique procedures elsewhere.

With reference to standardization of data to a particular time, only Goldreich(1970) has provided his formulae and schematically explained his procedures. Ludwig(1967) has concentrated on the verbal aspects of his techniques. Although the latter author supplies a computer flow

chart, duplication of the technique requires a great deal of debugging.

It should be noted that eight authors have not provided any information what so ever on the topic of standardization while five have stated that this procedure was of little consequence in aiding to fulfill the research objectives.

Conrads et al.(1971) were the only researchers in the sample to use a statistical test to determine whether or not a particular difference between observation sets was statistically significant at a precise alpha level. The statistic employed was the non-parametric Sign Test.

3.2.3 Summary

The above discussion adequately illustrates the fact that there is no precise standard analytic format from which a researcher entering this specific field can formulate or derive a model. Each analyst composes his own research methods. Referencing other studies is in reality a mere formality. The conflicting conclusions obtained are the consequences of this approach.

3.3 Conclusion

It becomes apparent from the lack of investigations showing humidity variations in urban areas and the vagueness of the information found in these limited investigations that a number of problems will arise and be encountered by

researchers preparing dissertations in this specific field. Only after the conclusion of the research undertaking can the author examine, evaluate and suggest improvements. Only further research can eliminate prior discrepancies.

LIST OF REFERENCES

- Bach, W., 1976: Global Air Pollution and Climatic Change. Rev. Geophys. and Space Phys., 14, 429-474.
- Brooks, C.E.P., 1951: Climate in Everyday Life. New York, New York: Philosophical Society Library, 314pp.
- Chandler, T.J., 1962: Diurnal, Seasonal and Annual Changes in the Intensity of London's Heat Island. Meteor. Mag., 91, 146-153.
- _____, 1965: The Climate of London. London, Hutchinson Pub. Co., 292pp.
- _____, 1967: Absolute and Relative Humidities in Towns. Bull. Amer. Meteor. Soc., 48(6), 384-399.
- _____, 1976: Urban Climatology and Its' Relevance to Urban Design. Technical Note No. 149, W.M.O., Geneva, 62pp.
- Conrads, L.A. and van der Hage, J.C.H., 1971: A New Method of Air-Temperature Measurement in Urban Climatology. Atmos. Environ., 5, 629-635.
- Duckworth, F.S. and Sandberg, J.S., 1954: The Effect of Cities Upon Horizontal and Vertical Temperature Gradients. Bull. Amer. Meteor. Soc., 35, 198-207.
- Eagleman, J.R., 1974: A Comparison of Urban Climatic Modifications in Three Cities. Atmos. Environ., 8, 1131-1142.
- Einarsson, E. and Lowe, H.B., 1956: A Study of Horizontal Temperature Variations in the Winnipeg Area on Nights Favoring Radiational Cooling. Meteorological Branch, Department of Transport, Circular No. 2647, TEC-214.

- Fonda, R.W., Dahms, R.F., Fralik, J.E., and Kendall, R.M., 1971: Heat Islands and Frost Pockets in Bellingham, Washington. Bull. Amer. Meteor. Soc., 52(7), 552-555.
- Garnett, A. and Bach, W., 1966: An Investigation of Urban Temperature Variations By Traverses in Sheffield (1962-1963). Biometeorology, 2, 601-607.
- Goldreich, Y., 1970: Computation of the Magnitude of Johannesburg's Heat Island. Notos, 19, 95-106.
- _____, 1974: Observations on the Urban Humidity Island in Johannesburg. Israel Journal of Earth Sciences, 23, 39-46.
- Geiger, R., 1965: The Climate Near the Ground. Cambridge, Mass., Harvard University Press, 4th ed., 611pp.
- Hannell, F.G., 1976: Some Features of the Heat Island in an Equatorial City. Geografiska Annaler, 58A, 1-2, 95-109.
- Hartley, M., 1977: Glasgow As An Urban Heat Island. Scottish Geographical Magazine, 93, 80-89.
- Hay, J.E. and Oke, T.R., 1976: Climate of Vancouver. IN Proceedings of a Workshop, Canada Committee of Ecological (Biophysical) Land Classification, 23-23, November, Toronto, Ontario. Ecological Land Classification Series No. 3.
- Hutcheon, R.J., Johnson, R.H., Lowry, W.P., Black, C.H. and Hadley, D., 1967: Observations of the Urban Heat Island in a Small City. Bull. Amer. Meteor. Soc., 48, 7-9.
- Kingham, H.H., 1969: Surface Temperature Patterns in Christchurch at Night. New Zeal. Geog., 25, 11-22.
- Kopec, R.T., 1970: Further Observations of the Urban Heat Island In A Small City. Bull. Amer. Meteor. Soc., 51(7), 602-606.

- _____, 1973: Daily Spatial and Secular Variations of Atmospheric Humidity in a Small City. Jour. of Appl. Meteor., 12, 639-648.
- Kratzer, A., 1936: Das Stadtklima, Die Wissenschaft. Vieweg und Sohn, Braunschweig, 184pp.
- Landsberg, H.E., 1956: The Climate in Towns. IN : Man's Role in Changing the Face of the Earth, edited by W.L. Thomas. University of Chicago Press, 584-606.
- _____, 1960: Physical Climatology. DuBois, Penn., Gray Printing Co., 446pp.
- _____, 1975: Atmospheric Changes in a Growing Community: The Columbia, Maryland Experience. Institute for Dynamics and Applied Mathematics, University of Maryland, College Park. Technical Note BN 823, 53pp.
- Linguist, S., 1968: Studies of the Local Climate in Lund and Its' Environs. Geografiska Annaler, 50A, 79-93.
- Ludwig, F.L., 1967: Urban Climatological Studies. Office of Defence Office of the Secretary of the Army, Washington, D.C.. Contract OCD-PS-64-201, under work unit 1235A.
- _____, 1968: Urban Temperature Fields. IN Urban Climates. World Meteorological Organization, Technical Note No. 108, Geneva, 80-90.
- Lyons, T.J. and Cutten, D.R., 1975: Atmospheric Pollutant and Temperature Traverses in an Urban Area. Atmos. Envirn., 9, 731-272.
- McBoyle, G.R., 1970: Observations on the Effect of a City's Form and Function on Temperature Patterns. New Zealand Geographer, 26, 145-159.
- Middletown, W.E.K. and Millar, F.G., 1936: Temperature Profiles in Toronto. Jour. Roy. Astron. Soc. of Canada, 30, 265-272.

Millward, G.E. and Motte, R.H., 1976: Observations of the Plymouth Temperature Field. Weather, 31, 255-260.

Oke, T.R., 1967: Some Results of a Pilot Study of the Urban Climate in Montreal. Climatological Bulletin, 3, 36-41.

_____ and Hannel, F.G., 1970: The Form of the Heat Island in Hamilton, Canada. IN Urban Climates and Building Climatology, Technical Note No. 108, W.M.O., Geneva, 113-119.

_____ and East, C., 1971: The Urban Boundary Layer in Montreal. Boundary Layer Meteorology, 1, 411-437.

_____, 1973: City Size and Urban Heat Island. Atmos. Environ., 7, 769-779.

_____, 1974: Review of Urban Climatology. Technical Note No. 134, W.M.O., Geneva, 133pp.

_____ and Maxwell, G.B., 1975: Urban Heat Island Dynamics in Montreal and Vancouver. Atmos. Environ., 9, 191-200.

_____, 1977: The Significance of the Atmosphere in Planning Human Settlements. IN Ecological. (Biophysical) Land Classification in Urban Areas, Proceedings of a Workshop, Canada Committee on Ecological. (Biophysical) Land Classification, Nov. 23-24, 1976. Ecological Land Classification Series No. 3, 31-41.

Sham Sani, 1973: Observations on the Effect of a City's Form and Functions on Temperature Patterns: A Case of Kuala Lumpur. Journal of Tropical Geography, 36, 60-65.

Sisterson, D.L. and Dirks, R.A., 1978: Structure of the Daytime Urban Moisture Field. Atmos. Environ., 12, 1943-1949.

Sundborg, A., 1950: Local Climatological Studies of the Temperature Conditions in an Urban Area. Tellus, 2, 222-232.

Yoshino, Masatoshi, 1976: Climate in a Small Area: an Introduction to Local Meteorology. Tokyo, University of Tokyo Press, 549pp.

CHAPTER 4

The Climate of Winnipeg

4.1 Record Length

Outside of numerous references to the weather along the Red River in journals of explorers and letters of early settlers (Labelle et al., 1967), the earliest continuous records of daily observations of standard climatic parameters in the Winnipeg area were logged from 1875 at St. Johns College, then situated on the west side of the Red River approximately 3.2km. north of its junction with the Assiniboine. Since then, the observation station has been relocated four times. Even though there was no effective overlapping of records during changeovers, comparisons of average annual temperature show no large affects. An increase of 0.6°C. was calculated over the 101 year span 1875-1976. The present station is located at the Winnipeg International Airport, 49°54'N., 97°15'W.. The observation site is located on the west side of the Airport, approximately 2.8km. directly north of Portage Avenue and 7.2km. from the downtown corner of Portage and Main Street. Ground level observation is 235m. above mean sea level.

4.1.1 Topography and Location

Winnipeg is situated at Latitude 49°54'N., Longitude 97°08'W., midway between the Pacific and Atlantic

Oceans, at the confluence of the Red and Assiniboine Rivers, 231m above sea level.

The Red River Plain, on which the city has been located, is composed of deep deposits of lacustrine clays and alluvium, remnants of glacial Lake Agassiz. The plain varies in width from 24km. at the 49th Parallel to approximately 160km. near Winnipeg and is prone to lengthy inundation for the land slopes upwards away from the river at 38 - 57cm. per km.. It is probably the flattest area of its size in Canada (Weir, 1960). There is not a single topographic feature greater than 7.5m. above the surrounding countryside nor is there an increase of elevation of more than 90m. within an 80km. circumference of the city.

Owing to the flat terrain, local effects have been minimized to: channelling of winds along the Red River Valley; a slight warming and drying in subsiding southwesterly winds, and a slight increase in temperature and cloudiness in late summer and fall after winds from the north and northwest pass over the Manitoba lakes.

4.1.2 Geographic Influences

By virtue of its centrality on the continent, Winnipeg's climate is typically continental, marked by large annual, seasonal temperature variations. Irregularity of rainfall with an early summer maximum and overall low relative humidity in summer are other traits.

The city's distance from the Rockies combined with the lack of any major west-east oriented mountain barrier or massive underlying water bodies has resulted in a marked increase of continentality. Along Latitude 50°N., average winter temperatures decrease rapidly eastward. Winnipeg is 10.9°C. colder than Lethbridge; 5.0°C. colder than Swift Current; 1.1°C. colder than Regina, and 0.1°C. colder than Brandon. Due to more or less similar radiative fluxes along this latitude during summer, maximum mean temperature difference between Winnipeg and Lethbridge is only 1.2°C..

Being situated on the 50th Parallel, the Winnipeg area is in the middle of the belt of the strongest prevailing Westerlies. Variation in the average path of the Westerlies cause variation in seasonal weather from year to year as well as large variation each season. Cyclonic storms developing or reforming in troughs associated with direct west trans-Cordilleran routes or indirect west routes via the Columbia River-Snake River-Wyoming Gap in the south or the Liard River Cordilleran Gap in the north, cause day to day variations.

4.2 Fronts and Air Masses

Through the work and findings of Crocker et al.(1947), Anderson et al.(1955), and Penner(1955) on models for synoptic frontal analysis derived from frontal-contour-charts, the following fronts and the air

masses which they separate have been recognized by Canadian Meteorologists to affect the research area:

- (1) the Polar Front separating maritime Tropical (mT) from maritime Polar (mP).
- (2) the maritime Arctic Front separating maritime Polar (mP) from maritime Arctic (mA) or wmP (mP moving over a warm surface) from cmP (mP moving over a cold surface).
- (3) the continental Arctic Front separating maritime Arctic (mA) from continental Arctic (cA) or cold maritime Arctic (cmA) from continental Arctic (cA).

During the summer months June-August, cA has been modified to mA over North America and hence only the prior two fronts exist. During autumn (September-November), maritime Arctic air crosses the Cordillera through the Liard River Gap and ridges with modified cA hence all three fronts may exist.

Bryson (1966) suggested a new air mass classificatory system while investigating climatic-biotic relationships within the tundra-boreal forest. By analyzing the frequency distribution of July daily maximum temperatures, compiled from a total of 120 Canadian and American stations for the ten year period 1948 through 1957, Bryson, using partial collective methods, delimited ten air mass categories. Relative frequency of occurrence of July air masses affecting the Winnipeg area show only 5 dominant, however. These, in order of importance, are:

- (1) North Rockies Pacific (NR)-westerly air masses crossing the Cordillera through the Columbia River-Snake River-Wyoming Gap. This air mass has an occurrence frequency of 39%.

- (2) Canadian Rockies Pacific (CR)-direct trans-Cordilleran routes near Latitudes 45° - 50° N., due to increased Westerly velocities. CR has a frequency of occurrence of 24%.
- (3) Maritime Tropic (mT)-standard definition, mostly from the Gulf of Mexico. mT has a frequency of occurrence of 15%.
- (4) Yukon Pacific (Y)-Westerlies that cross the Cordillera through the Liard River Gap. The frequency of occurrence is 15%.
- (5) Eastern Arctic (Ae)-develops over the Canadian Arctic Archipelago, modified as tracks southward. It has a frequency of 6%.

Continental Tropic (cT) air masses only affect the research area if the Colorado Plateau High, a small high with moderate variation in size, versatile in that it can change into a number of other features, intensifies moving northeastward to the Middle Plains. It must be associated with either upper level meridional ridges or closed upper Highs of high stability (Sands, 1966). The latter's warm air inhibit cumulus and cumulonimbus cloud development. This in turn allows maximum ground heating through increased insolation. Northern migration of the above synoptic features triggered the intrusion into Southern Manitoba of the drought area centred in South Dakota by July 1976.

Bryson correlated the existence and location of mean fronts of the above air masses by constructing resultant streamline charts of surface wind for each month using data for 1930-1945. It must be noted, however, that these are the mean or resultant flows and as illustrated above, other

varieties of air clearly are quite frequent. Similar research undertaken by Barry(1967), Krebs et al., (1970), and Larsen(1971) resulted in conclusions complementary to those of Bryson's. The following discussion of Winnipeg's relationship to frontal position is based on Bryson's findings.

From November to January, the research area lies in the Pacific Air Wedge. The Polar Front lies deep south in a curve from Fort Collins, Colorado, through Missouri, then across Southern Ontario to Central Maine, while cold air converges with Pacific air along a broad sweeping line from the Yukon, through Central Saskatchewan, to the Great Lakes and then parallel 40°N .. Even though mP and cA alternate at irregular intervals, as the fronts shift around their mean location, the former dominates, generally in the form of NR air masses.

The relaxation of pressure gradients attributed to the weakening of the heat sources along the coast lines as the temperature difference from land to ocean diminishes, results in the gradual dissipation of the Pacific Air Wedge in February. Alaskan (A1) air masses entering the northern Mackenzie Valley through the Peel and Pelly River Valleys, ridge out the Athabaskan High and displace the Pacific Wedge and its associated cyclonic storm tracks south of the research area during February.

Eastern Arctic (Ae) air masses replace Al in March while mT air from the intensified Bermuda High has replaced the modified mP or cA of the southern anti-cyclonic zone. The wedge of Pacific air between these two fronts reaches its maximum eastern extent to Northern Illinois during this period. Air flows north of cyclonic storms of the Central-Eastern Wyoming and the expanded northerly positioned Trinidad Low type carry moisture into the research area resulting in heavy snow fall accumulations (Longley, 1972).

During the time period April-June, Pacific air is gradually pinched out between the southward expansion of the Arctic air stream and the northward expansion of the Tropical airstreams. By May, the latter has bulged into the former in the Southern Minnesota-Lake Traverse, N.D. area. The gradient of net radiation from the tropics to the Arctic and the limited heat transfer from soil to air, however, maintains sufficient slope to the isentropic surface so that mT air continues northward aloft (Bryson and Hare, 1974). Infrequent surface penetration occurs from mid-June to August.

Due to the changing inclination of the sun, the Polar area of net radiation cooling has reached its minima in July. The Arctic Front is now situated over the Northern Ice Caps. A wedge of Pacific air once again extends

eastward south of the Arctic airstream, . Its maritime Front sweeps from east of Aklavik, District of Mackenzie across the eastern tips of Great Bear Lake and Great Slave Lake to the southern coasts of Hudson Bay and into Northern Quebec, approximately 400-500km. north of Winnipeg. The Tropical Front is approximately 160-240km. north and northeast of the research area. This is far north of the main Westerly jet, thus implying extreme instability that expresses itself in the form of extensive spring and early summer storms, violent thunderstorms, and a tornado maxima (Bryson and Hare, 1974; McKay and Lowe, 1960)

The winter pattern discussed previously commences to re-establish itself in September. Pacific air masses, NR and CR, dominate the research area while mT air is replaced by modified mP and/or cA flowing northward from the southeastern anticyclone. By November, the latter is firmly established.

4.3 Synoptic Climatology

Sands(1966) performed a synoptic climatic study of the Western United States and adjacent areas over the period 1958-63 inclusive. Analyzing two surface charts 12 hours apart and a 500-mb upper air chart for 75 meteorological stations, he categorized 105 different but repetitive circulation features. Sixty were classified as upper air and 45 were classified surface features. Detailed

examination of the synoptic conditions affecting the research area have been documented by Bell(1974) and need not be mentioned here.

4.4 Temperature

The characteristic traits of a continental climate namely large annual, daily, and diurnal changes in temperature, are evident in the climatic records of Winnipeg. Under the normal temperature curve, January is the coldest month (mean temperature, $-18.1^{\circ}\text{C}.$) with the lowest temperature being recorded in the week of the 22nd. The normal monthly temperature range is $9.8^{\circ}\text{C}.$ while the extreme maximum-minimum range, based upon records 1872-1976, is $52.2^{\circ}\text{C}.$ ($7.8^{\circ}\text{C}.$ to $-44.4^{\circ}\text{C}.$). The greatest extreme range, however, is recorded for March with $62.2^{\circ}\text{C}.,$ ($23.2^{\circ}\text{C}.$ to $-38.9^{\circ}\text{C}.$) with April and November following. Respective extreme ranges are $61.7^{\circ}\text{C}.$ for April and $60.6^{\circ}\text{C}.$ for November. July is the warmest month (mean $19.7^{\circ}\text{C}.$) with temperatures reaching a maximum during the week of the 25th. The normal temperature range is $12.4^{\circ}\text{C}.$ while that for extremes is $41.1^{\circ}\text{C}.,$ ($1.1^{\circ}\text{C}.$ to $42.2^{\circ}\text{C}.$). The absolute minimum on record occurred in December with $-47.8^{\circ}\text{C}.$ while the absolute maximum was $42.2^{\circ}\text{C}.$ in July, giving an absolute temperature range of $90.0^{\circ}\text{C}..$

The average yearly temperature over the period 1874-1976 is $2.3^{\circ}\text{C}..$ Out of 9490 days (1951-1976) only 169 were

recorded to have maximum temperatures greater or equal to 32.2°C., a frequency of 0.02. The greatest frequency of occurrences, in respective order, occurred in July, August, and June. Maximum temperatures less or equal to 0.0°C. were recorded for 3193 days during the time span 1951 - 76. Approximately 24.4% occurred in January; 22.6% in December, and 20.9% in February. March and November followed with 16.2% and 12.7% respectively. During the same time period, 5027 days were recorded to have minimum temperatures less or equal to 0.0°C.. The months November-March each had a frequency of occurrence of 0.08. April had 0.05 occurrence frequency; October 0.04; March 0.02, and September 0.01. No minimum, temperatures less or equal to 0.0°C. were reported for June, July, or August. Of the November-March span, 78.8% of the minimum temperatures were also less or equal to -18.0°C.. February followed with 63.4%; December with 58.3%; March with 37.9%; November with 14.9%, and April with 2.3%.

The above data clearly illustrates that the three core winter months in the research area are December, January, and February. June, July, and August are the core summer months.

Even monthly means show great variations. The highest monthly mean for January has been -8.9°C(1973), whilst the lowest was -27.8°C(1974). Corresponding values for July

are 28.9°C(1974) and 10.1°C(1972). The greatest range occurs in December with 22.5°C. (-3.0°C. to -25.9°C.), the least in July, 15.7°C..

The records also reveal large daily temperature ranges with an average of 25.6°C. for December-February;24.5°C. for April and March, and 23.8°C. for September and October. The month of May has the greatest frequency occurrence of large daily temperature ranges;0.28. December, January, and April follow with 0.16 inclusive. The largest diurnal variation occurred on January 25, 1889 when 34.8°C. was recorded.

4.5 Hot Spells

A hot spell, defined locally, begins on a day when the maximum temperature of that day is more than 2.8°C. above the normal maximum temperature for that month and at least one day within the hot spell time span must be 5.6°C. above the normal mean maximum. A hot spell is considered to end on the day prior to the day that the maximum temperature dropped below the normal mean maximum or on the day prior to the first of two consecutive days that had or have maximum temperatures less than or equal to 2.8°C. above the normal mean maximum (Labelle et al., 1966;Junson, personal communication). Since neither relative humidities nor any other humidity indicies are accounted for in the definition, no differentiation is made between heat waves or hot wind spells.

Hot spell data, Table 4.3.1, has been compiled for the months April-October for the years 1963-1976 and combined with that extracted by Labelle et al.(1966) for the years

TABLE 4.5.1

NUMBER AND LENGTH OF HOT SPELLS AT WINNIPEG 1933-1976

	<u>APRIL</u>	<u>MAY</u>	<u>JUNE</u>	<u>JULY</u>	<u>AUG</u>	<u>SEPT</u>	<u>OCT</u>
NUMBER PER MONTH	1.5	2.4	1.7	1.3	1.8	2.0	1.7
AVERAGE Length (in days)	7.9	5.9	5.5	4.2	5.3	5.6	5.9

1933-1962.

No hot spell has ever lasted more than 11 days in the research area prior to 1976. With the northerly advancement of the South Dakotan drought and its associated cT like air masses, hot spell duration, in days, increased over the average length by a factor of 2.2 for the months April to June, 1976 and by a factor of 1.9 and 3.6 for August and September 1976 respectively. Associated with the latter months' heat waves were the lowest humidities since records began in 1913.

Heat waves also brought an early spring and a few record breaking high temperatures in April 1977. With the exception of the first seven days, all days of the month

were hot spell defined. Afternoon temperatures averaged seven degrees warmer than usual.

4.6 Cold Spells

A cold spell is defined to begin on a day when the minimum temperature of that day is more than 2.8°C. below the normal mean minimum temperature for that month and at least one day within the cold spell time span must be 5.6°C. below the normal mean minimum. A cold spell is considered to end on the day prior to the first of two consecutive days that had or have minimum temperatures less than or equal to 2.8°C. below the normal mean minimum. Cold spell data compiled for the winter season, December 1st to March 1st is shown on Table 3.6.1 for 30 years of records (1947-76).

TABLE 4.6.1

NUMBER AND LENGTH OF COLD SPELLS AT WINNIPEG 1947-1976

	<u>DEC</u>	<u>JAN</u>	<u>FEB</u>
NUMBER PER MONTH	2.6	2.7	2.9
AVERAGE LENGTH IN DAYS	10.4	10.4	8.7

Ridges along the eastern front of the Rockies extending into the Southern Plains combined with ridges from Central Canada

transport very cold Arctic air southwards into the research area. These are the major synoptic features that influence cold spell formation and duration. The former is highly prevalent in December-January while the latter becomes increasingly prevalent in February (Bell, 1974)

Twenty-two winter traverses were conducted during cold spell periods. Although the duration of the above traversed cold spells were well below the 20 year average, temperature minimization was not affected. The average temperature for traverses conducted during the 5 day cold spell February 1-5, 1976 ranged from -24.1°C . to -26°C .. The latter were 8.4°C . and 10.6°C . below the monthly normal respectively. An average temperature of -27.2°C . was recorded for the first 3 days of the 9 day cold spell December 4-13, 1976. The latter average was 13.6°C . below the monthly normal. The second lowest Airport and traverse temperature of 1976, -34.7°C . was recorded on the 8th of the latter cold spell period.

4.7 Dry Spells and Drought

There is no precise nor widely accepted definition of either drought or dry spells in Canada (Fraser, 1976). The latter term is generally defined as a period during which measurable rain fall is less than or equal to 0.2mm., while the former is defined as a period of abnormally dry weather sufficiently prolonged for the lack of water to cause a

serious hydrological-ecotone imbalance. Potential evapotranspiration must be higher than the amount that can be supplied by either precipitation, inflow, or irrigation. Soil moisture must diminish continuously until exhausted or be located at such a depth that its usability for domestic consumption is unsafe and below the root systems of plants. In terms of precipitation, less than 50% of the long term monthly average constitutes a drought.

Table 4.7.1, modified from Labelle et al.(1966), shows the frequency of dry periods of various lengths at Winnipeg based on records 1874-1975. There is a general tendency for dry periods to be longer than 10 days in April and October, while in June and July, only 2% of the total number of dry periods experienced during 1874-1975 were of durations longer than 10 days.

The average annual dry spell duration, in days, within the research area increased by a factor of 2 during the drought. The greatest increases occurred in the months of May, November, February, August and October. Respective dry spell lengths in days were 13.5, 14.5, 9.5, 7.7, 7.7, and 9.3. The least increase in duration occurred in the months of June and July. The latter had an increase of 1.3 days while the former experienced 0.8 more days of dry spell. The months of March and April 1977 had longer dry

TABLE 4.7.1

FREQUENCY OF DRY PERIODS OF VARIOUS LENGTHS AT WINNIPEG

<u>DURATION</u> <u>(IN DAYS)</u>	<u>JAN</u>	<u>FEB</u>	<u>MAR</u>	<u>APR</u>	<u>MAY</u>	<u>JUN</u>	<u>JUL</u>	<u>AUG</u>	<u>SEP</u>	<u>OCT</u>	<u>NOV</u>	<u>DEC</u>
1	.32	.29	.25	.23	.29	.40	.36	.30	.30	.22	.31	.30
2	.19	.20	.17	.18	.20	.20	.20	.22	.17	.17	.13	.17
3	.13	.10	.13	.11	.11	.13	.13	.15	.12	.12	.11	.14
4-6	.19	.19	.22	.22	.25	.18	.21	.20	.24	.22	.22	.19
7-9	.10	.11	.09	.11	.08	.07	.08	.07	.10	.10	.12	.10
10-14	.05	.07	.08	.10	.06	.02	.02	.04	.04	.12	.09	.07
15-19	.01	.02	.04	.03	.01	-	-	.01	.02	.04	.02	.03
20-29	.01	.02	.02	.02	-	-	-	.01	.01	.01	-	-
AVERAGES	3.5	3.7	3.9	3.9	3.5	3.2	3.3	3.3	3.7	4.0	4.1	3.7

spells than did their corresponding months in 1976. The inverse occurred for January and February 1977.

June and July also have the smallest percentages of dry months (based upon records 1874-1975). Frequency of occurrence of dry months for each is 0.18. It is also seen from Table 4.7.2 that June, July, and August have relatively small percentages of months that are wet - monthly precipitation is 50% greater than the normal monthly precipitation. Respective percentages are 8.9, 15.8 and 11.9. Thus it may be concluded that precipitation during these months are relatively reliable.

January, April, and December have the highest frequency of dry spell occurrence: 0.37, 0.28 and 0.27 respectively. The foremost month also has the greatest wet month frequency, 0.27 and almost equal range frequencies if greater than 100% is used. November and October are the only months with relatively large frequencies in the 50.5-100.5% range. Both months tend to be dry a high percentage of the time and have the longest dry spell durations. The longest dry spells have occurred during these months: 33 days from October 26-November 27, 1904 and

TABLE 4.7.2

FREQUENCIES OF MONTHS EITHER WET OR DRY 1874-1975

<u>% OF NORM</u>	<u>JAN</u>	<u>FEB</u>	<u>MAR</u>	<u>APR</u>	<u>MAY</u>	<u>JUN</u>	<u>JUL</u>	<u>AUG</u>	<u>SEP</u>	<u>OCT</u>	<u>NOV</u>	<u>DEC</u>
<50.5	.37	.23	.25	.28	.29	.18	.18	.27	.25	.26	.21	.27
50.5-												
100.5	.37	.37	.31	.34	.38	.41	.43	.33	.31	.37	.42	.32
100.5-												
150.5	.05	.25	.25	.20	.21	.33	.24	.29	.23	.20	.19	.20
>150.5	.30	.15	.20	.19	.17	.09	.16	.12	.22	.18	.19	.22

47 days from October 9-November 24, 1976.

The following synoptic conditions are favourable to drought formation over the research area. During the recharge season, taken to be that part of the year when rainfall and snowfall exceeds the amount being lost through evapotranspiration and runoff (Fraser, 1976), persistent ridges (features 102-104, Bell 1974), shift the Maritime and Polar Fronts further south than normal, thus deflecting cyclonic storms further southeastward. Below normal precipitation occurs. As the Polar Front migrates northward in April, an eastward shift of the Bermuda Anticyclone or a weakening of the Bermuda Anticyclone can restrict mT airflow along the southeastern States (Namias, 1955). When this occurs, dry, hot cT air descends from northern Mexico into New Mexico, Texas, and beyond. Persistent upper level meridional ridges and/or closed upper Highs of high stability, can block the jet streams northward, displacing its eastern segment northwestward; its western segment southeastward. Its sinking circulation draws cT air northwards and dry northwestern air southeastwards. Cumulus and cumulonimbus cloud development is inhibited. Due to greater insolation, the drought conditions are perpetuated by increased heat thermals from the ground.

This classical Dust Bowl pattern reoccurred during the periods November 1960-February 1962, and September 1976-early May 1977. Approximately 66% of the annual

normal precipitation was recorded at Winnipeg during the former period. The recharge season yielded only 89mm. of precipitation, 75% of the normal. March-May precipitation totalled 66mm. or 55.2% of the normal. June, August and December received the lowest percentages of the normal: 4.1%, 5.5% and 15.9% respectively. Altogether, losses over the Eastern Prairies were estimated to exceed 100 million dollars during this drought period (Labelle et al., 1966)

The latter period is the driest ever recorded over much of the Eastern Prairies and Northwestern Ontario (Fraser, 1977). After a near normal recharge season (90.2%) precipitation began to show extreme variability over the Eastern Prairies. Precipitation for the months April-May was 44.4% of the normal while that of June was 227.3%. Similar variations occurred for July and August: 46% and 80% of the normal respectively. By September 1st the drought had engulfed all the Eastern Prairies-Northwestern Ontario regions. There was a slight recovery in December but a return to subnormal amounts in every succeeding month till early May followed (see Maps 4.9.1-4.9.17) Approximately 80mm. or 33% of the normal precipitation was recorded from September 1976 to April 1977. The drought ended in the Winnipeg region on the 4th of May when thunderstorms released 50.8mm. of rain over the city.

4.8 Winds

The following mean monthly wind speed frequencies by direction were based upon data 1957-1966 collected from various Atmospheric Environment Publications, Canada, Department of the Environment.

The primary wind direction is south in all months with the exception of January, March and April when it is secondary. Northern winds dominate in the latter month while northwesterlies dominate in the former two. Excluding the month of June, all winds of secondary importance are from the northwestern direction. Secondary winds of June are from the north, while those of May are from the north-northeast.

Lowest average wind speeds occur from the northeast (15.3km./hr.), east-northeast (14.6km./hr.), east (15.4km./hr.) and southwest (15.5km./hr.). Greatest wind speeds based upon the records 1957-1966 occur from the north-northwest (23.3km./hr.), south (23.0km./hr.), northwest (22.9km./hr.), south-southeast (21.3km./hr.), and north (20.9km./hr.). Winds from the northwest-north sector have the greatest average speeds for all months excluding January and February. In the latter two months, southerly winds have greater speeds. Approximately 0.94 of 1% of all winds recorded at Winnipeg are greater or equal to 51.5km./hr. Winds from the northwest-northeast account for

68.5% of this amount while those from the southeast-southwest account for 21.6%. The strongest winds are from the northwest with highest frequency of occurrence in November-February, and April-May.

The average annual wind speed in Winnipeg, 19.8km./hr., is quite high compared to its Prairie neighbors to the southwest, west, and northwest. Average speeds for several stations are as follows: Williston, N.D., 15.9km./hr.; Pilot Mound, Man., 18.8km./hr.; The Pas, Man., 16.3km./hr.; Weyburn, Sask., 17.1km./hr.; Edmonton, Alb., 14.2km./hr., and Helena, Montana, 12.7 km./hr..

4.9 Weather During the Study Period

The commencement and cessation of temperature and dewpoint data acquisition for this study closely parallels the invasion of the drought area, from its centre in South Dakota, into the Eastern Prairies-Northwest Ontario regions and its eventual dissipation in early May.

The mean hourly temperature and its associated standard deviation per month and the mean monthly temperature and its associated standard deviations are represented in Tables 6.1.1 - 6.1.12, pages 138-161. Calculations were based upon records 1953-1975, obtained from the Winnipeg Meteorological Station.

During the 1976 portion of the data acquisition period, 8 months were within 0.5 standard deviations, the remaining four, February, April, October, and December within 1 standard deviations. February-April temperature means were within 1 standard deviation while that of May was within 2.5 standard deviations. The latter month's heavy rainfall (310.7% of the normal) and above normal temperatures (the mean monthly temperature was 7.2°C. higher than the long-term normal) resulted from the penetration of mT air at the 750mb and 500mb surfaces and the penetration of modified mP and mT air at the surface level. All levels were unstable.

The mean hourly dewpoint temperature and its associated standard deviation per month and the mean monthly dewpoint temperature and its associated standard deviations are also presented in Tables 6.1.1 - 6.1.12. Calculations were also based on records 1953-1975.

During the 1976 portion of the data acquisition period, the three months of March, July, and August were within 0.5 standard deviations of the mean. October's and November's mean dewpoint were within the 2.0 and 1.5 standard deviation ranges respectively, while the remainder were within 1.0 standard deviations. Because monthly means were used in calculating standard deviations, the fact that the lowest vapor pressures on record occurred during

October-November, is not statistically shown. The 1977 portion parallels that of the temperature.

The Annual Meteorological Summaries for Winnipeg, for the years 1976, and 1977 have been reproduced in Tables 4.9.1 to 4.9.2. (Atmospheric Environment Service 1976, 1977, 1978). Maps 4.9.1-4.9.17 show monthly departure from normal temperatures and percentage of normal precipitation over North America from January 1976-May 1977 (Canada Weather Reviews, Vol. 14, no.1-12; Vol 15 no. 1-5:Atmospheric Environment Service) The latter maps illustrate that the drought was not isolated to the Canadian Prairies but also occurred in the areas of the Mississippi Valley and Western Great Plains of America. This fact must be considered for any air mass trajectory over these areas will be modified temperature wise to a greater extent than moisture wise. It will be shown later that mT air masses over the research area during the data acquisition period had similar low mixing ratios yet extreme temperature variations, even though the trajectories were similar in most respects.

TABLE 4.9.1 : WINNIPEG INTERNATIONAL AIRPORT METEOROLOGICAL DATA SUMMARY FOR 1976

pour WINNIPEG INT'L AIRPORT / AEROPORT INTERN. DE WINNIPEG YEAR/ANNEE 1976

METEOROLOGICAL DATA FOR THE YEAR / DONNÉES MÉTÉOROLOGIQUES POUR L'ANNÉE

NOTE: The following units are used throughout this summary -
 Temperature: Degrees and tenths Celsius (°C)
 Degree Day: Difference of Daily Mean Temperature from 18.0°C
 Rain: Millimetres and tenths (mm)
 Snow: Centimetres and tenths (cm)
 Total Precipitation: Millimetres and tenths (mm)
 Wind Speed: Kilometres per hour (km/h)
 Wind Direction: Direction (true north) from which the wind is blowing.
 Barometric Pressure: Kilopascals and hundredths (kPa)
 Sunshine: Hours and tenths of bright sunshine.

AVIS: Unités Utilisées
 Température: Degrés et dixièmes Celsius (°C)
 Degré Jour: Différence entre la température moyenne journalière et 18.0°C
 Pluie: Millimètres et dixièmes (mm)
 Neige: Centimètres et dixièmes (cm)
 Précipitation Totale: Millimètres et dixièmes (mm)
 Vitesse du vent: Kilomètres par heure (km/h)
 Direction du vent: Direction (Nord géographique) d'où le vent souffle
 Pression Barométrique: Kilopascals et centièmes (kPa)
 Insolation: Nombre d'heures et dixièmes d'insolation effective

MONTH MOIS	TEMPERATURE / TEMPÉRATURE										DEGREE DAYS DEGRES JOURS	
	MEAN / MOYENNE			NORMAL / NORMALE			EXTREME / EXTRÊME				BELOW 18.0°C AU DESSOUS DE 18.0°C	NORMAL NORMALE
	MAXIMUM	MINIMUM	MONTHLY MENSUELLES	MAXIMUM	MINIMUM	MEAN MOYENNE	MAXIMUM MAXIMALE	DATE	MINIMUM MINIMALE	DATE		
JAN/JAN	-12.1	-24.1	-18.1	-13.4	-23.2	-18.3	3.3	28	-35.8	6	1120.3	1125.6
FEB/FÉV	-5.8	-17.4	-11.6	-10.4	-21.1	-15.7	5.5	9	-31.1	29	859.6	951.1
MAR/MAH	-3.9	-16.1	-10.0	-2.9	-13.3	-8.1	6.2	29	-32.7	5	868.8	806.1
APR/AVR	12.8	-0.9	6.0	8.6	-1.9	3.3	22.8	13	-7.2	11	362.3	438.9
MAY/MAI	20.2	3.3	11.8	17.1	4.1	10.6	29.5	30	-8.2	3	198.4	233.3
JUN/JUIN	24.2	12.3	18.3	22.7	10.3	16.5	31.3	4	2.6	16	47.0	73.3
JUL/JUIL	26.6	12.7	19.7	25.9	13.5	19.7	31.5	18	6.1	31	15.7	20.6
AUG/AOÛT	26.3	12.2	19.3	25.0	12.2	18.7	36.3	24	3.8	29	30.7	36.7
SEPT/SEP	21.2	5.4	13.3	18.4	6.6	12.6	34.5	6	-3.6	21,27	159.8	172.8
OCT/OCT	9.3	-3.6	2.9	11.9	1.1	6.6	28.1	3	-16.6	26	470.1	354.4
NOV/NOV	-0.2	-11.5	-5.9	-0.5	-8.4	-4.4	13.3	1	-26.7	30	714.7	670.0
DEC/DÉC	-12.0	-24.9	-18.5	-9.2	-18.2	-13.7	3.0	14	-34.7	8	1131.3	981.1
YEAR ANNÉE	8.9	-4.4	2.3	7.8	-3.2	2.3	36.3	Aug. 24	Jan. 6		5978.7	5863.9

MONTH MOIS	PRECIPITATION / PRÉCIPITATIONS													
	MONTHLY / MENSUELLES			NORMAL / NORMALE			EXTREME / EXTRÊME							
	RAINFALL HAUTEUR DE PLUIE	SNOWFALL HAUTEUR DE NEIGE	TOTAL	RAIN PLUIE	SNOW NEIGE	TOTAL	RAIN / PLUIE			SNOW / NEIGE				
JAN/JAN	Tr.	37.2	29.8	0.3	24.9	23.6	Tr.	18	Tr.	18	6.1	12	9.1	12
FEB/FÉV	.3	30.3	23.0	0.8	19.8	19.1	.3	17	.3	17	4.3	28	7.6	17
MAR/MAH	3.8	29.2	23.1	6.1	21.1	26.2	2.3	20	2.5*	20	7.1	2	19.3	2
APR/AVR	29.3	2.3	31.6	25.4	11.9	37.3	8.6	16	13.2*	16	2.0	18	2.3	18
MAY/MAI	10.4	Tr.	10.4	54.6	2.5	57.2	3.8	14	5.3	14	Tr.	1,2	Tr.	1,2
JUN/JUIN	182.5		182.5	80.3	Tr.	80.3	24.1	16,2	28.7*	25	---			
JUL/JUIL	36.9	----	36.9	80.3	0.0	80.3	24.1	29	24.6*	29				
AUG/AOÛT	59.0		59.0	73.7	0.0	73.7	24.9	26	24.9*	26				
SEPT/SEP	9.9		9.9	52.6	0.3	52.6	4.3	12	4.3*	12				
OCT/OCT	2.5	Tr.	2.5	29.2	5.6	34.8	1.0	2	1.0*	3,8	Tr.	SVR	Tr.	SVR
NOV/NOV	Tr.	1.7	0.8	7.1	21.3	27.2	Tr.	1,18	Tr.	1,18	.8	25	.8	25
DEC/DÉC		20.6	18.2	0.8	23.9	22.9	---				2.8	26	4.8*	9
YEAR ANNÉE	334.6	121.3	427.7	411.2	131.3	535.2	24.9	Aug. 26	June 25	7.1	Mar. 2	19.3	Mar. 2	2

*24 hour period - Climatological Day • Other Dates
 Mar. 19-20 3.5 mm; Apr. 16-17 13.5 mm; June 24-25 42.7 mm; July 29-30 24.9 mm;
 Aug. 26-27 33.0 mm; Sept. 12-13 5.3 mm; Oct. 7-8 1.5 mm; Dec. 26-27 4.8 cm snow

SOURCE

: CANADA

DEPARTMENT OF FISHERIES AND ENVIRONMENT

ATMOSPHERIC ENVIRONMENT

ANNUAL METEOROLOGICAL SUMMARY - WINNIPEG INTERNATIONAL AIRPORT, 1976

pour WINNIPEG INT'L AIRPORT / AEROPORT INTERN. DE WINNIPEG YEAR/ANNEE 1976

METEOROLOGICAL DATA FOR THE YEAR / DONNÉES MÉTÉOROLOGIQUES POUR L'ANNÉE

MONTH MOIS	SUNSHINE / INSOLATION					WIND / VENT								
	DURATION IN HOURS DUREE D'HEURES	PERCENTAGE OF POSSIBLE DAYS POUR UN POURCENTAGE DES JOURS POSSIBLES	NO. OF DAYS WITHOUT SUNSHINE NOMBRE DE JOURS SANS SOLEIL	NORMAL NORMALE	AVERAGE SPEED VITESSE MOYENNE	PREVAILING DIRECTION DIRECTION DOMINANTE	NORMAL NORMALE		MAX FOR 1 MIN MAX POUR 1 MIN		HIGHEST GUST RAFALE MAXIMUM			
							SPEED VITESSE	DIRECTION	DIRECTION AND SPEED DIRECTION ET VITESSE	DATE	DIRECTION AND SPEED DIRECTION ET VITESSE	DATE		
JAN/JAN	108.7	40.7	8	112.5	19.6	S	19.5	NW	S	60	27	S	79	27
FEB/FÉV	127.2	43.5	7	139.4	18.3	W	18.8	S	N	48	28	WNW	60*	7
MAR/MAH	186.1	50.6	1	170.4	16.9	S	19.6	S	N	61	20	N	76	20
APR/AVR	280.3	67.9	2	208.5	17.2	S	21.7	S	E	44	16	E	63	16
MAY/MAI	356.9	74.8	0	246.4	14.6	SSE	21.1	NNE	N	44	1	S	59	18
JUN/JUIN	261.3	53.5	0	258.9	18.8	S	18.5	S	S	54	4	WSW	100	6
JUL/JUIL	348.4	70.7	0	310.8	16.9	S	16.3	S	WNW	46	15	SSE	69	25
AUG/AOÛT	307.9	68.7	1	276.2	15.5	SSE	17.1	S	WNW	43	27	WSW	70	27
SEPT/SEP	227.5	59.9	2	182.6	18.5	S	18.8	S	WNW	54	3	WNW	76	3
OCT/OCT	130.0	38.9	3	158.4	18.3	WNW	20.3	S	WNW	54	15	SSW	91	3
NOV/NOV	139.7	51.2	3	81.2	20.3	NW	20.3	S	WNW	56	2	WNW	78	2
DEC/DÉC	106.4	42.0	5	86.2	19.1	S	19.5	S	S	52	21	S	74	21
YEAR ANNÉE	2580.4	57.5	32	2231.5	17.8	S	19.3	S	N	61	Mar. 20	WSW	100	June 6

*February S 60, 8 N 60, 28 Most sunshine ever recorded

Annual possible sunshine 4486.7

BAROMETRIC PRESSURE / PRESSION BAROMÉTRIQUE

MONTH MOIS	STATION LEVEL / NIVEAU DE LA STATION										SEA LEVEL / NIVEAU DE LA MER				
	MEAN MOYENNE	MAXIMUM MAXIMALE	DATE	MINIMUM MINIMALE	DATE	NORMAL NORMALE	MEAN MOYENNE	MAXIMUM MAXIMALE	DATE	MINIMUM MINIMALE	DATE	NORMAL NORMALE			
													JAN/JAN	98.75	100.19
FEB/FÉV	98.29	100.45	4	95.78	9	98.90	101.38	103.65	4	98.67	9	102.01			
MAR/MAH	98.31	99.83	1	95.19	20	98.82	101.37	103.06	1	98.05	20	101.87			
APR/AVR	98.79	100.60	11	96.54	17	98.59	101.75	103.66	11	99.42	17	101.55			
MAY/MAI	98.61	99.91	7	96.67	4	98.53	101.51	102.92	7	99.53	4	101.44			
JUN/JUIN	98.15	99.28	30	96.09	13	98.31	101.01	102.16	30	98.89	13	101.17			
JUL/JUIL	98.47	99.56	3	97.21	13	98.47	101.34	102.46	31*	100.01	13	101.33			
AUG/AOÛT	98.61	99.75	29	97.21	27	98.49	101.51	102.73	29	100.03	27	101.35			
SEPT/SEP	98.55	99.73	14	96.83	2	98.51	101.46	102.71	14	99.68	2	101.41			
OCT/OCT	98.78	100.68	26	96.06	14	98.51	101.78	103.79	26	98.91	14	101.45			
NOV/NOV	98.72	100.62	12	96.44	18	98.63	101.76	103.73	12	99.36	18	101.65			
DEC/DÉC	98.61	100.46	20	96.39	13	98.77	101.75	103.64	20	99.36	13	101.86			
YEAR ANNÉE	98.55	100.68	Oct. 26	95.19	Mar. 20	98.62	101.54	103.79	Oct. 26	98.05	Mar. 20	101.60			

*1 Kilopascal = 0.29529 inches of mercury / 3.386 kilopascals = 1 inch of mercury
 = 0.29529 pouces de mercure / 3.386 kilopascals = 1 pouce de mercure

* Not 3rd due to correction factor

TABLE 4.9.2 : WINNIPEG INTERNATIONAL AIRPORT METEOROLOGICAL DATA SUMMARY FOR 1977

pour WINNIPEG INT'L AIRPORT / AEROPORT INTERN, DE WINNIPEG YEAR/ANNÉE 1977

METEOROLOGICAL DATA FOR THE YEAR / DONNÉES MÉTÉOROLOGIQUES POUR L'ANNÉE														
NOTE: The following units are used throughout this summary - Temperature: Degrees and tenths Celsius (°C) Degree Day: Difference of Daily Mean Temperature from 18.0°C Rain: Millimetres and tenths (mm) Snow: Centimetres and tenths (cm) Total Precipitation: Millimetres and tenths (mm) Wind Speed: Kilometres per hour (km/h) Wind Direction: Direction (true north) from which the wind is blowing. Barometric Pressure: Kilopascals and hundredths (kPa) Sunshine: Hours and tenths of bright sunshine.														
AVIS: Unités Utilisées - Température: Degrés et dixièmes Celsius (°C) Degré Jour: Différence entre la température moyenne du jour et 18.0°C Pluie: Millimètres et dixièmes (mm) Neige: Centimètres et dixièmes (cm) Précipitation Totale: Millimètres et dixièmes (mm) Vitesse du vent: Kilomètres par heure (km/h) Direction du vent: Direction (nord géographique) d'où le vent souffle. Pression Barométrique: Kilopascals et centièmes (kPa) Insolation: Nombre d'heures et dixièmes d'insolation effective														
MONTH MOIS	TEMPERATURE / TEMPÉRATURE						DEGREE DAYS DEGRÉS JOURS							
	MEAN / MOYENNE			NORMAL / NORMALE			EXTREME / EXTRÊME							
	MAXIMUM	MINIMUM	MONTHLY MENSUELLE	MAXIMUM	MINIMUM	MEAN MOYENNE	MAXIMUM MAXIMALE	DATE	MINIMUM MINIMALE	DATE	BELOW 18.0°C AU DESSOUS DE 18.0°C	NORMAL NORMALE		
JAN/JAN	-16.1	-25.9	-21.0	-13.4	-23.2	-18.3	-1.2	22	-38.0	17	1208.4	1125.6		
FEB/FÉV	-6.6	-16.7	-11.7	-10.4	-21.1	-15.7	3.8	8	-33.7	6	830.2	951.1		
MAR/MAR	2.3	-7.9	-2.8	-2.9	-13.3	-8.1	16.0	28	-22.5	3	644.7	806.1		
APR/AVR	16.0	-1.3	7.4	8.6	-1.9	3.3	29.7	30	-11.1	5	321.7	438.9		
MAY/MAI	24.4	11.1	17.8	17.1	4.1	10.6	32.6	13	-1.8	7	63.7	233.3		
JUN/JUIN	22.0	11.3	16.7	22.7	10.3	16.5	29.5	25	5.6	2	53.1	73.3		
JUL/JUIL	25.7	13.0	19.4	25.9	13.5	19.7	31.6	18	8.3	25	11.1	20.6		
AUG/AOÛT	20.8	8.0	14.4	25.0	12.2	18.7	28.9	9	2.0	23	113.9	36.7		
SEPT/SEP	16.6	8.1	12.4	18.4	6.6	12.6	25.4	14.15	0.1	30	170.5	172.8		
OCT/OCT	13.6	1.4	7.5	11.9	1.1	6.6	23.3	25	-4.9	22	324.3	354.4		
NOV/NOV	-0.5	-9.0	-4.8	-0.5	-8.4	-4.4	17.8	2	-25.3	24	682.6	670.0		
DEC/DÉC	-13.1	-21.7	-17.4	-9.2	-18.2	-13.7	1.8	18	-33.8	10	1098.7	981.1		
YEAR ANNÉE	8.8	-2.5	3.2	7.8	-3.2	2.3	32.6	May 13	-38.0	Jan 17	5522.9	5863.9		
MONTH MOIS	PRECIPITATION / PRÉCIPITATIONS													
	MONTHLY / MENSUELLES			NORMAL / NORMALE			EXTREME / EXTRÊME							
	RAINFALL HAUTEUR DE PLUIE	SNOWFALL HAUTEUR DE NEIGE	TOTAL	RAIN PLUIE	SNOW NEIGE	TOTAL	RAIN / PLUIE			SNOW / NEIGE				
JAN/JAN	Tr.	12.9	12.5	0.3	24.9	23.6	Tr.	19	Tr.	19	5.5	19	5.5	19
FEB/FÉV	Tr.	23.5	20.9	0.8	19.8	19.1	Tr.	11	Tr.	24	4.1	24	11.5	24
MAR/MAR	7.3	4.3	9.9	6.1	21.1	26.2	3.0	12	3.6	12	1.3	26	2.0	26
APR/AVR	4.7	1.4	5.2	25.4	11.9	37.3	3.4	17	3.6	17	1.4	5	1.4	5
MAY/MAI	177.7	Tr.	177.7	54.6	2.5	57.2	37.1	26	50.8*	4	Tr.	6	Tr.	6
JUN/JUIN	88.4	Tr.	88.4	80.3	Tr.	80.3	15.8	17	28.5	17	Tr.	Tr.	Tr.	Tr.
JUL/JUIL	85.3	Tr.	85.3	80.3	0.0	80.3	20.2	13	41.0	13	Tr.	Tr.	Tr.	Tr.
AUG/AOÛT	89.6	Tr.	89.6	73.7	0.0	73.7	13.8	6	18.6	29	Tr.	Tr.	Tr.	Tr.
SEPT/SEP	148.2	Tr.	148.2	52.6	0.3	52.6	34.0	8	52.6	8*	Tr.	Tr.	Tr.	Tr.
OCT/OCT	30.2	Tr.	30.2	29.2	5.6	34.8	15.0	30	15.0	30	Tr.	Tr.	Tr.	Tr.
NOV/NOV	0.6	28.4	28.4	7.1	21.3	27.2	0.2	29	0.2	29*	7.0	20	17.2	20
DEC/DÉC	1.6	18.3	18.8	0.8	23.9	22.9	0.8	18	1.1	18	7.5	17	9.9	17
YEAR ANNÉE	633.6	88.8	715.1	411.2	131.3	535.2	37.1	26	52.6	8	7.5	17	17.2	20

*Other Days - January 23, 24
February 12
November 7, 30
*May 4-5 56.6 mm
*September 8-9 59.1 mm

pour WINNIPEG INT'L AIRPORT / AEROPORT INTERN, DE WINNIPEG YEAR/ANNÉE 1977

METEOROLOGICAL DATA FOR THE YEAR / DONNÉES MÉTÉOROLOGIQUES POUR L'ANNÉE												
MONTH MOIS	SUNSHINE / INSOLATION						WIND / VENT					
	DURATION DUREE D'HEURES	PERCENTAGE POUR CENT DU TOTAL POSSIBLE	NO. OF DAYS NOMBRE DE JOURS D'INSOLATION	NORMAL NORMALE	AVERAGE SPEED MOYENNE	PREVAILING DIRECTION DOMINANTE	NORMAL MORALE	MAX FOR 1 MIN MAX POUR 1 MIN	HIGHEST GUST RAFALE MAXIMUM	DATE	DIRECTION AND SPEED DIRECTION ET VITESSE	DATE
	JAN/JAN	116.3	43.5	5	112.5	16.0	NW	19.5	NW	N 57	25	N 76
FEB/FÉV	122.7	43.6	6	139.4	16.7	S	18.8	S	N 56	24	N 72	24
MAR/MAR	189.8	51.6	2	170.4	20.1	S	19.6	S	NNE 67	29	NNE 93	29
APR/AVR	279.8	67.8	0	208.5	21.0	SE	21.7	S	W 56	30	WSW 80	30
MAY/MAI	286.8	60.1	2	246.4	21.2	SSE	21.1	KNE	NW 56	1	S 104	15
JUN/JUIN	240.0	49.0	1	258.9	18.4	S	18.5	S	NW 59	30	NW 93	30
JUL/JUIL	340.5	69.1	1	310.8	16.1	S	16.3	S	ESE 46	2	W 74	13
AUG/AOÛT	234.6	52.3	0	276.2	13.9	WNW	17.1	S	WNW 41	10	NNW 69	9
SEPT/SEP	136.3	35.9	9	182.6	16.1	S	18.8	S	NNW 52	9	NNW 80	9
OCT/OCT	203.9	61.1	2	158.4	18.1	S	20.3	S	NW 44	5	NW 63	17
NOV/NOV	102.1	37.4	10	81.2	19.9	S	20.3	S	N 70	20	N 85	20
DEC/DÉC	84.8	33.5	11	86.2	16.9	NW	19.5	S	NNW 41	1, 8	S 56	11
YEAR ANNÉE	2337.6	52.2	49	2231.5	17.9	S	19.3	S	N 70	Nov. 20	S 104	May 15
Total Possible - 4475.8												
MONTH MOIS	BAROMETRIC PRESSURE / PRESSION BAROMÉTRIQUE											
	STATION LEVEL / NIVEAU DE LA STATION						SEA LEVEL / NIVEAU DE LA MER					
	MEAN MOYENNE	MAXIMUM MAXIMALE	DATE	MINIMUM MINIMALE	DATE	NORMAL NORMALE	MEAN MOYENNE	MAXIMUM MAXIMALE	DATE	MINIMUM MINIMALE	DATE	NORMAL NORMALE
JAN/JAN	98.86	100.53	17	96.56	25	98.96	102.00	103.75	17	99.51	25	102.10
FEB/FÉV	98.51	100.59	6	96.29	24	98.90	101.60	103.84	6	99.23	24	102.01
MAR/MAR	98.30	99.84	23	96.93	27	98.82	101.26	102.93	23	99.81	27	101.87
APR/AVR	98.70	100.37	24	97.03	30	98.59	101.65	103.38	24	99.83	30	101.55
MAY/MAI	98.19	99.69	7	96.38	5	98.53	101.07	102.66	7	99.18	5	101.44
JUN/JUIN	98.42	99.49	6	96.31	30	98.31	101.26	102.40	6	99.13	30	101.17
JUL/JUIL	98.38	99.85	21	96.73	11	98.47	101.25	102.74	21	99.53	11	101.33
AUG/AOÛT	98.35	99.52	17	97.14	25	98.49	101.23	102.45	17	99.95	25	101.35
SEPT/SEP	98.44	99.43	2	96.43	9	98.51	101.34	102.34	23	99.24	9	101.41
OCT/OCT	98.59	100.25	6	96.86	16	98.51	101.51	103.24	6	99.72	16	101.45
NOV/NOV	98.46	100.25	11	96.41	2	98.63	101.46	103.27	11	99.29	2	101.65
DEC/DÉC	98.59	101.13	9	96.92	18	98.77	101.67	104.40	9	99.84	18	101.86
YEAR ANNÉE	98.48	101.13	Dec. 9	96.29	Feb 24*	98.62	101.44	104.40	Dec. 9	99.13	June 30*	101.60

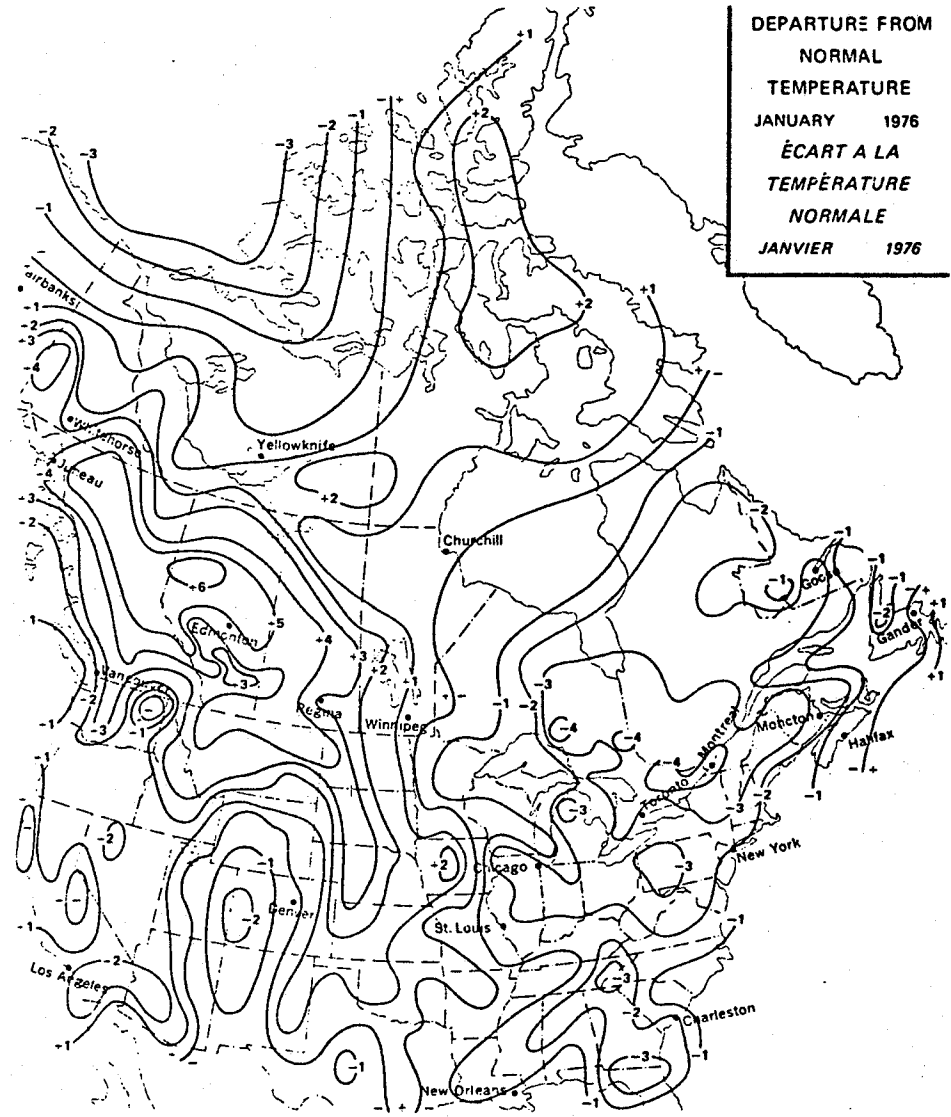
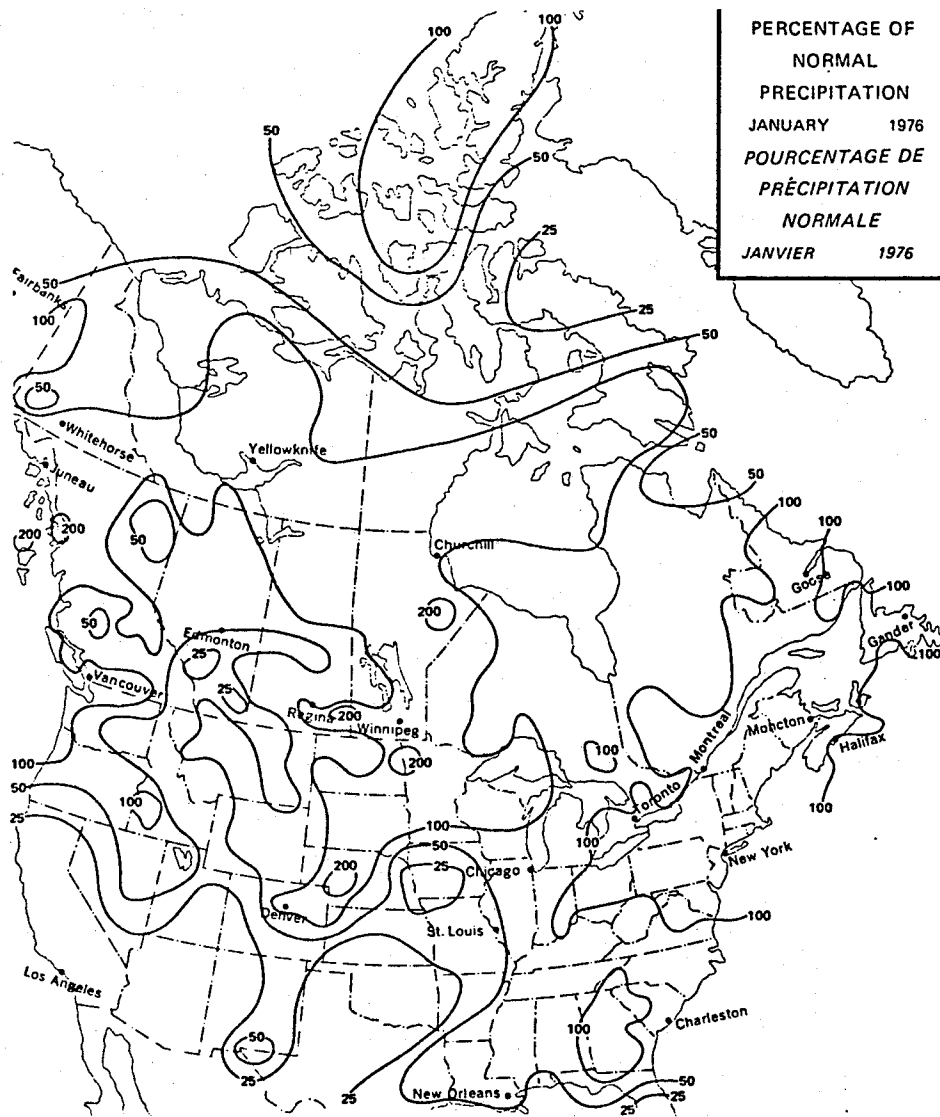
*1 kilopascal = 0.29529 inches of mercury / 3.386 kilopascals = 1 inch of mercury
= 0.29529 pouces de mercure / 3.386 kilopascals = 1 pouce de mercure

*Difference in dates of low station sea level pressure is due to different correction factors to station pressure.

SOURCE : CANADA
DEPARTMENT OF THE ENVIRONMENT
ATMOSPHERIC ENVIRONMENT
ANNUAL METEOROLOGICAL SUMMARY - WINNIPEG INTERNATIONAL AIRPORT, 1977

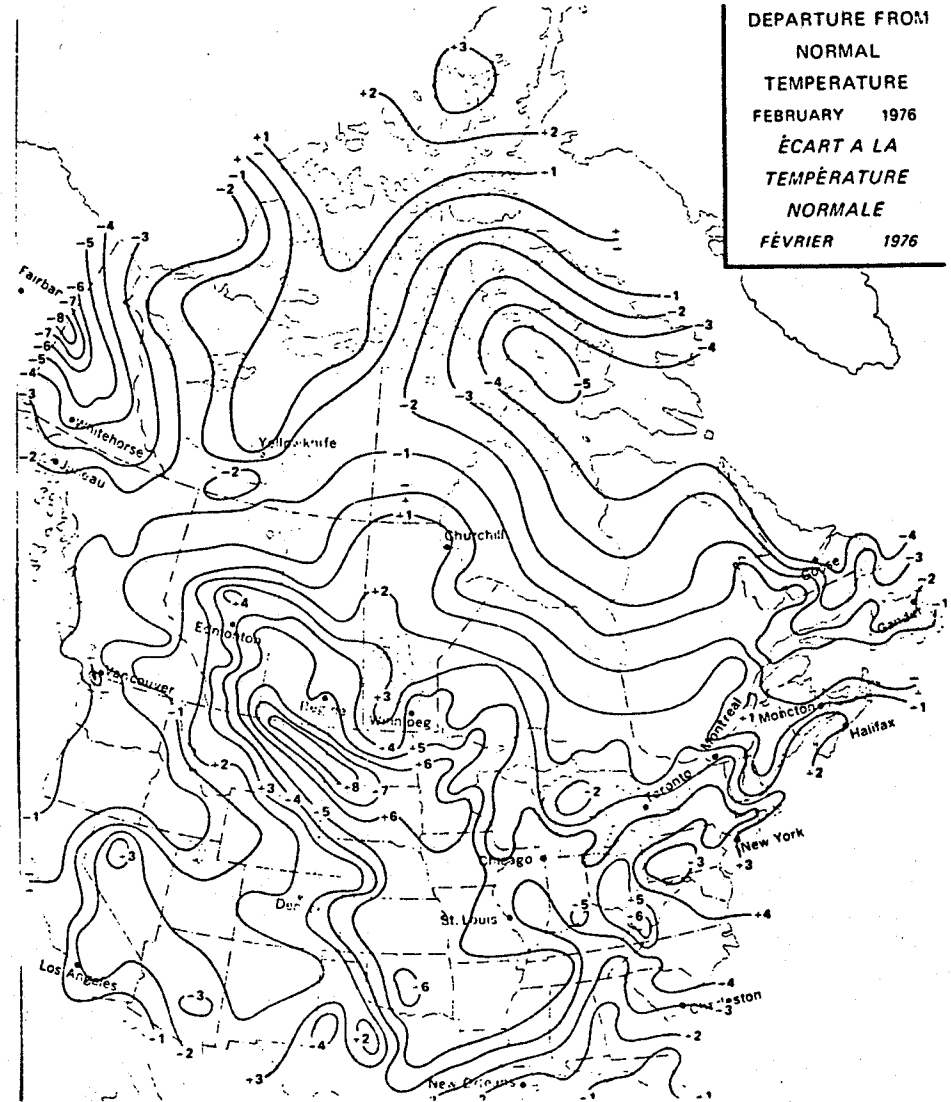
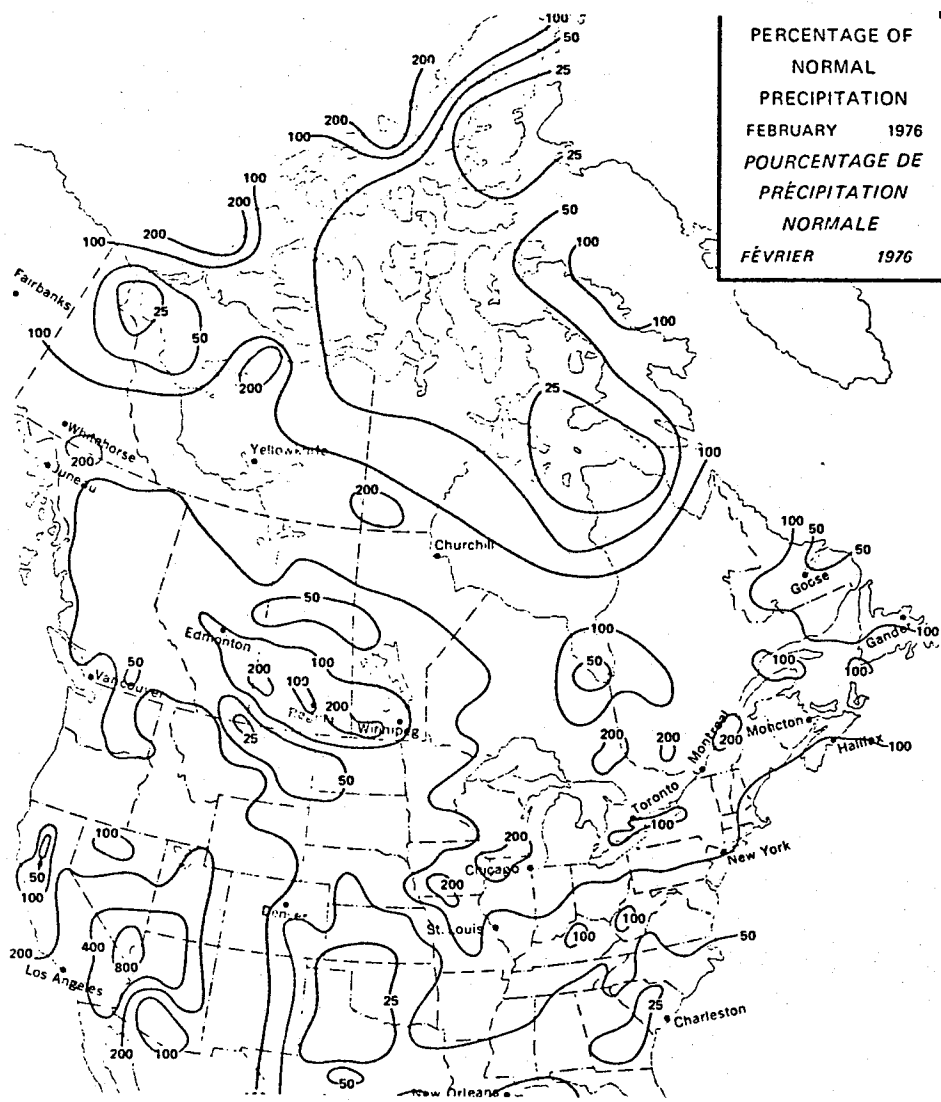
MAP 9.4.I : PRECIPITATION AND TEMPERATURE ABNORMALITIES FOR JANUARY, 1976

91



SOURCE : CANADA
DEPARTMENT OF THE ENVIRONMENT
ATMOSPHERIC ENVIRONMENT SERVICE
CANADIAN WEATHER REVIEW, Vol. 14, 1976, No. 1

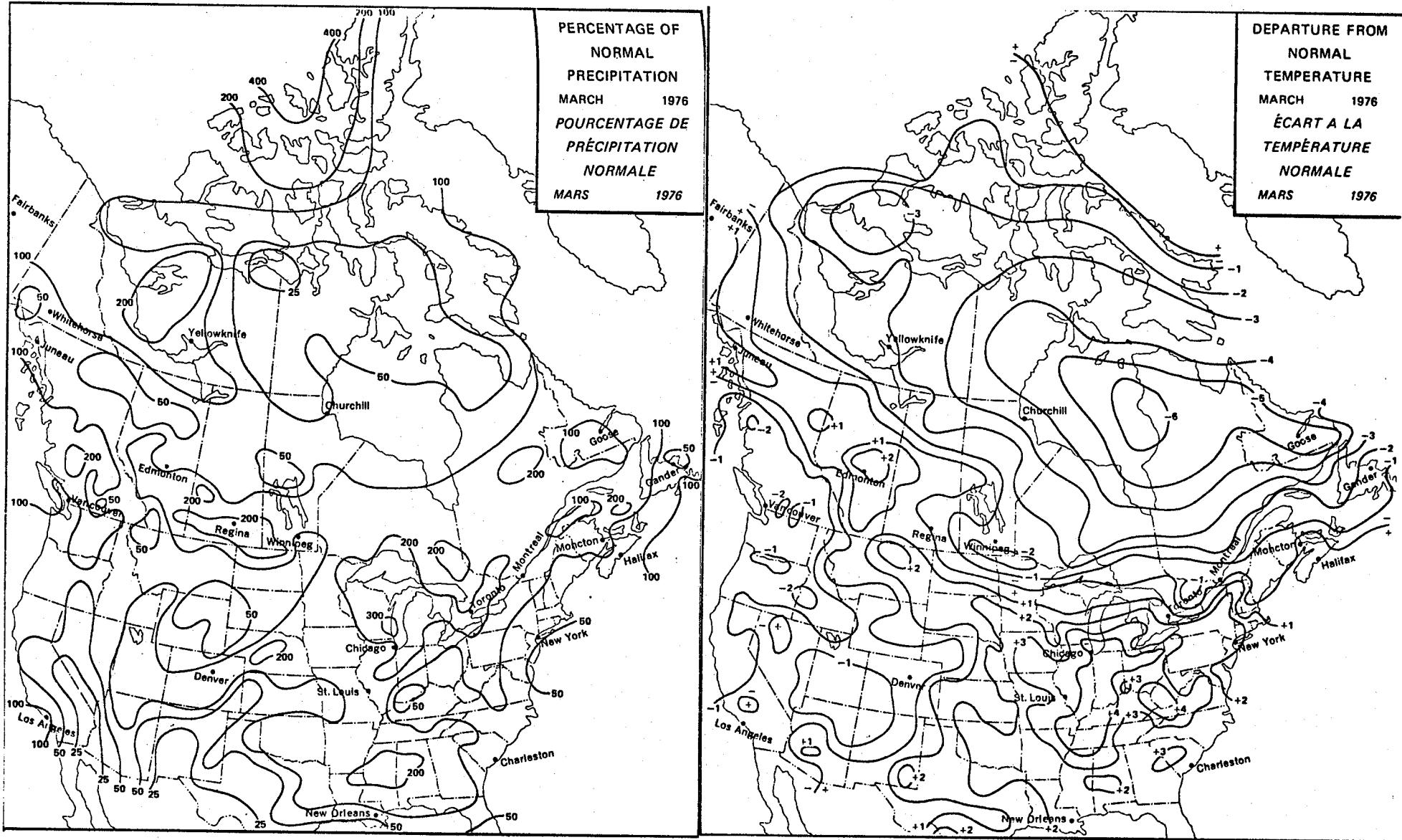
MAP 9.4.2 : PRECIPITATION AND TEMPERATURE ABNORMALITIES FOR FEBRUARY, 1976



92

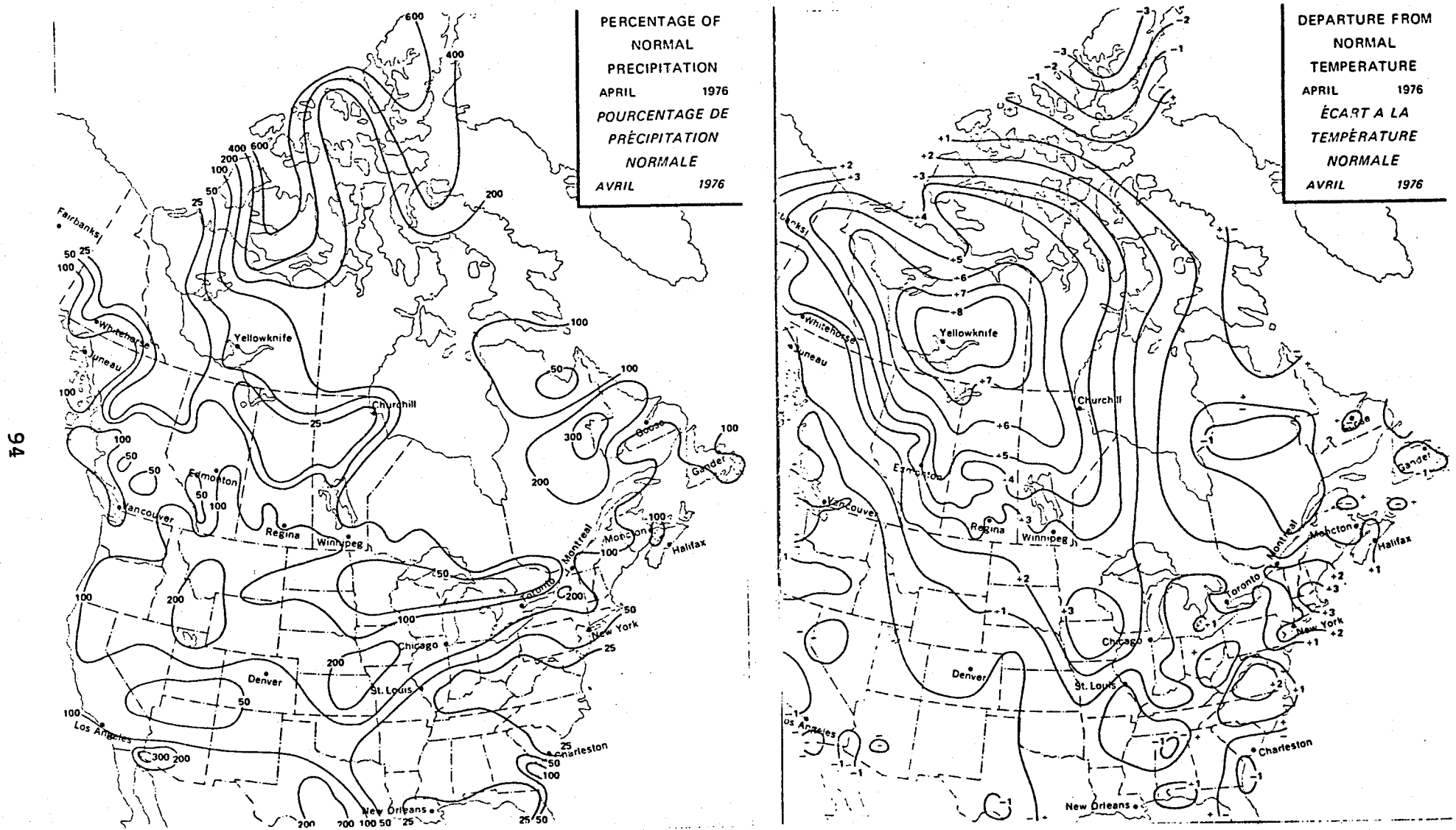
SOURCE : CANADA
DEPARTMENT OF THE ENVIRONMENT
ATMOSPHERIC ENVIRONMENT SERVICE
CANADIAN WEATHER REVIEW, Vol. 14, 1976, No. 2

MAP 9.4.3 : PRECIPITATION AND TEMPERATURE ABNORMALITIES FOR MARCH, 1976



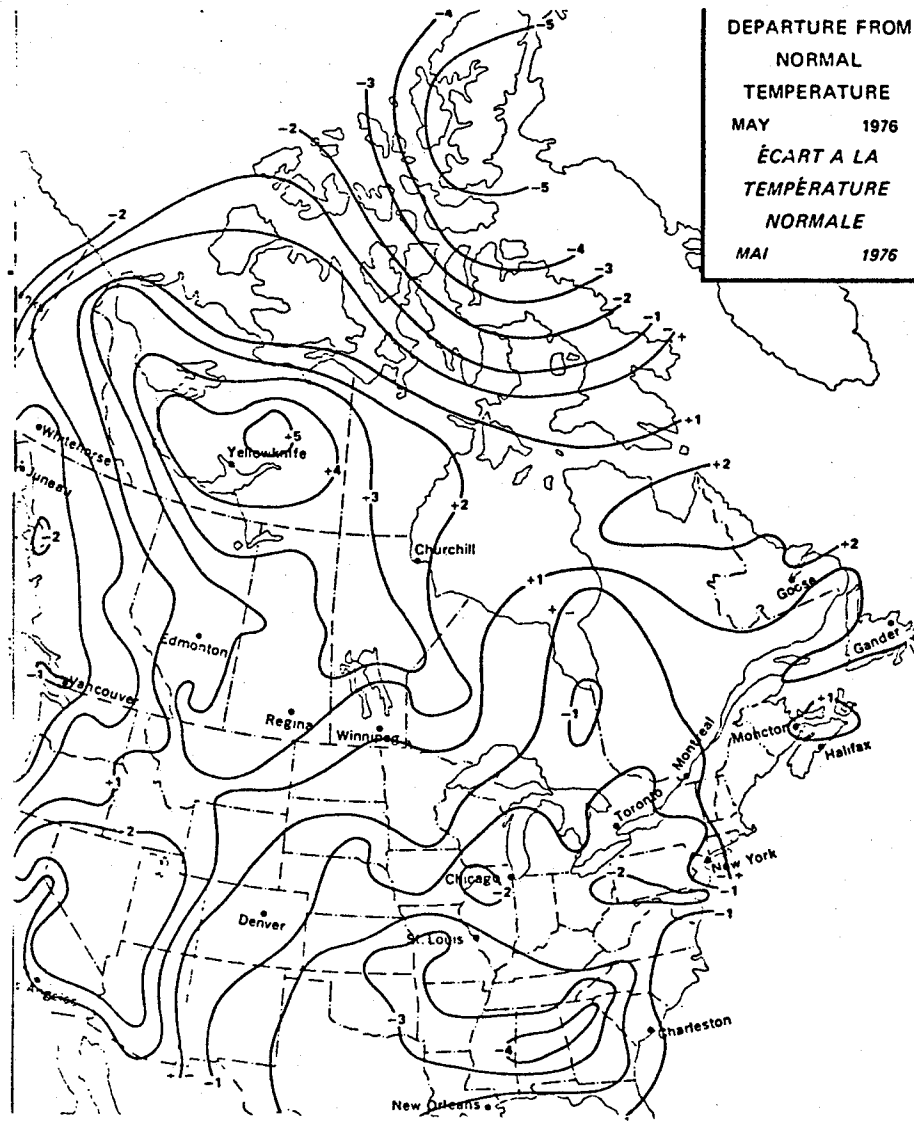
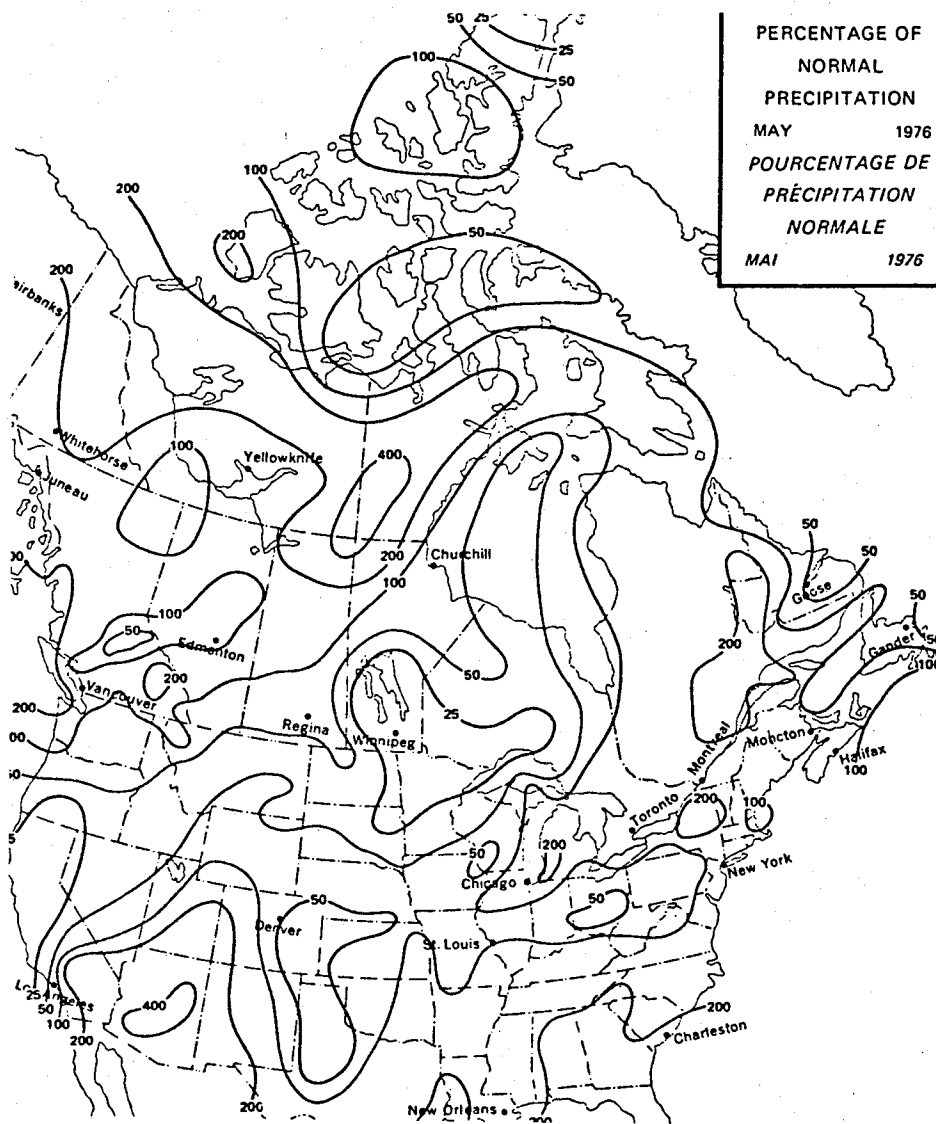
SOURCE : CANADA
 DEPARTMENT OF THE ENVIRONMENT
 ATMOSPHERIC ENVIRONMENT SERVICE
 CANADIAN WEATHER REVIEW, Vol. 14, 1976, No. 3

MAP 9.4.4 : PRECIPITATION AND TEMPERATURE ABNORMALITIES FOR APRIL, 1976



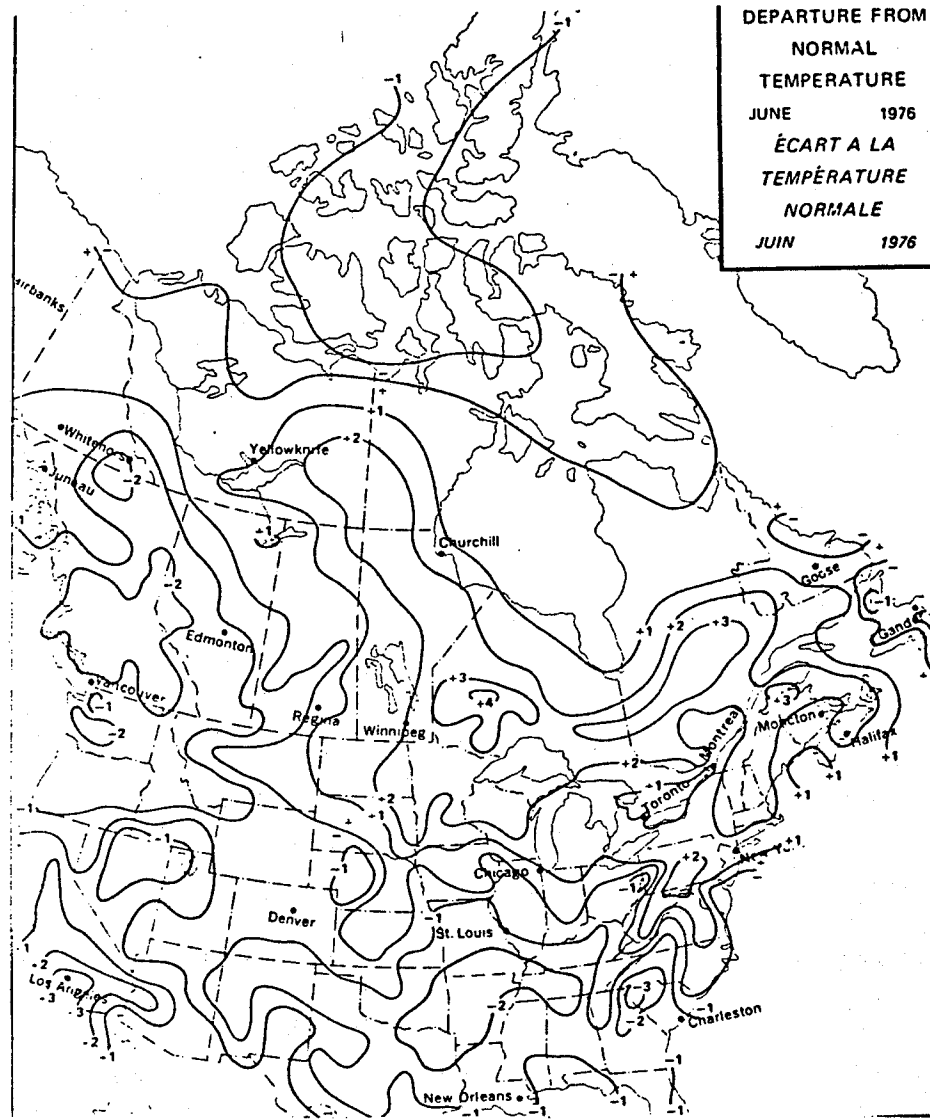
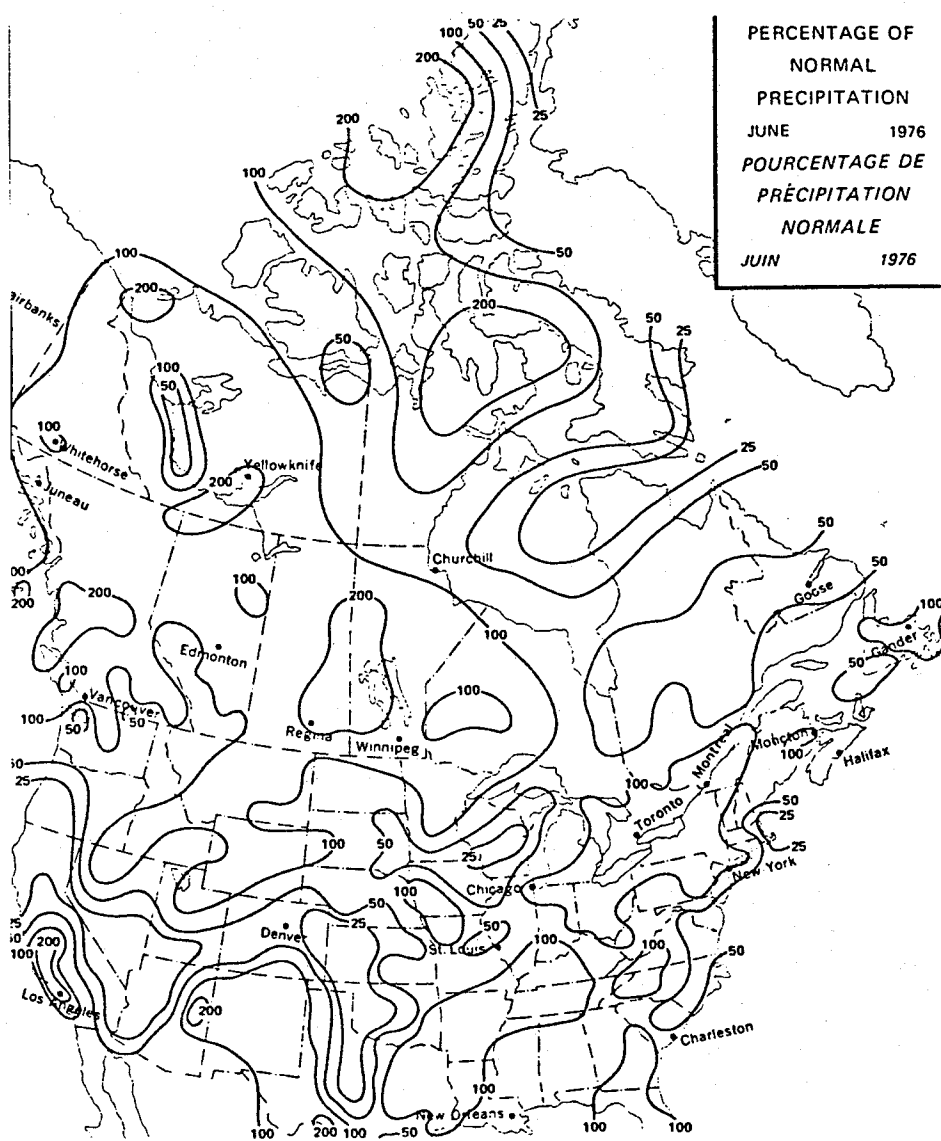
SOURCE : CANADA
 DEPARTMENT OF THE ENVIRONMENT
 ATMOSPHERIC ENVIRONMENT SERVICE
 CANADIAN WEATHER REVIEW, Vol. 14, 1976, No. 4

MAP 9.4.5 : PRECIPITATION AND TEMPERATURE ABNORMALITIES FOR MAY, 1976



SOURCE : CANADA
DEPARTMENT OF THE ENVIRONMENT
ATMOSPHERIC ENVIRONMENT SERVICE
CANADIAN WEATHER REVIEW, Vol. 14, 1976, No. 5

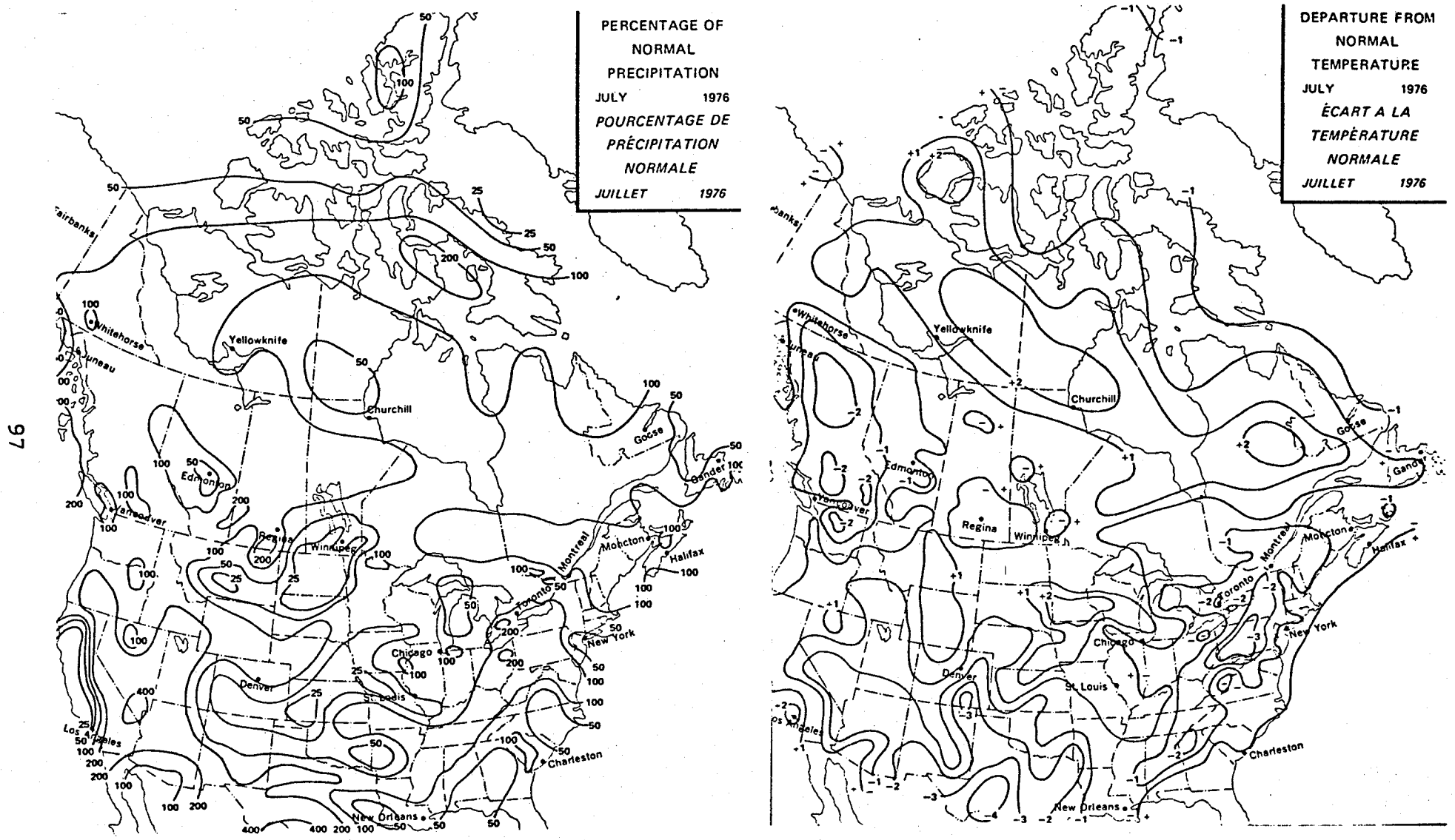
MAP 9.4.6 : PRECIPITATION AND TEMPERATURE ABNORMALITIES FOR JUNE, 1976



96

SOURCE : CANADA
 DEPARTMENT OF THE ENVIRONMENT
 ATMOSPHERIC ENVIRONMENT SERVICE
 CANADIAN WEATHER REVIEW, Vol. 14, 1976, No. 6

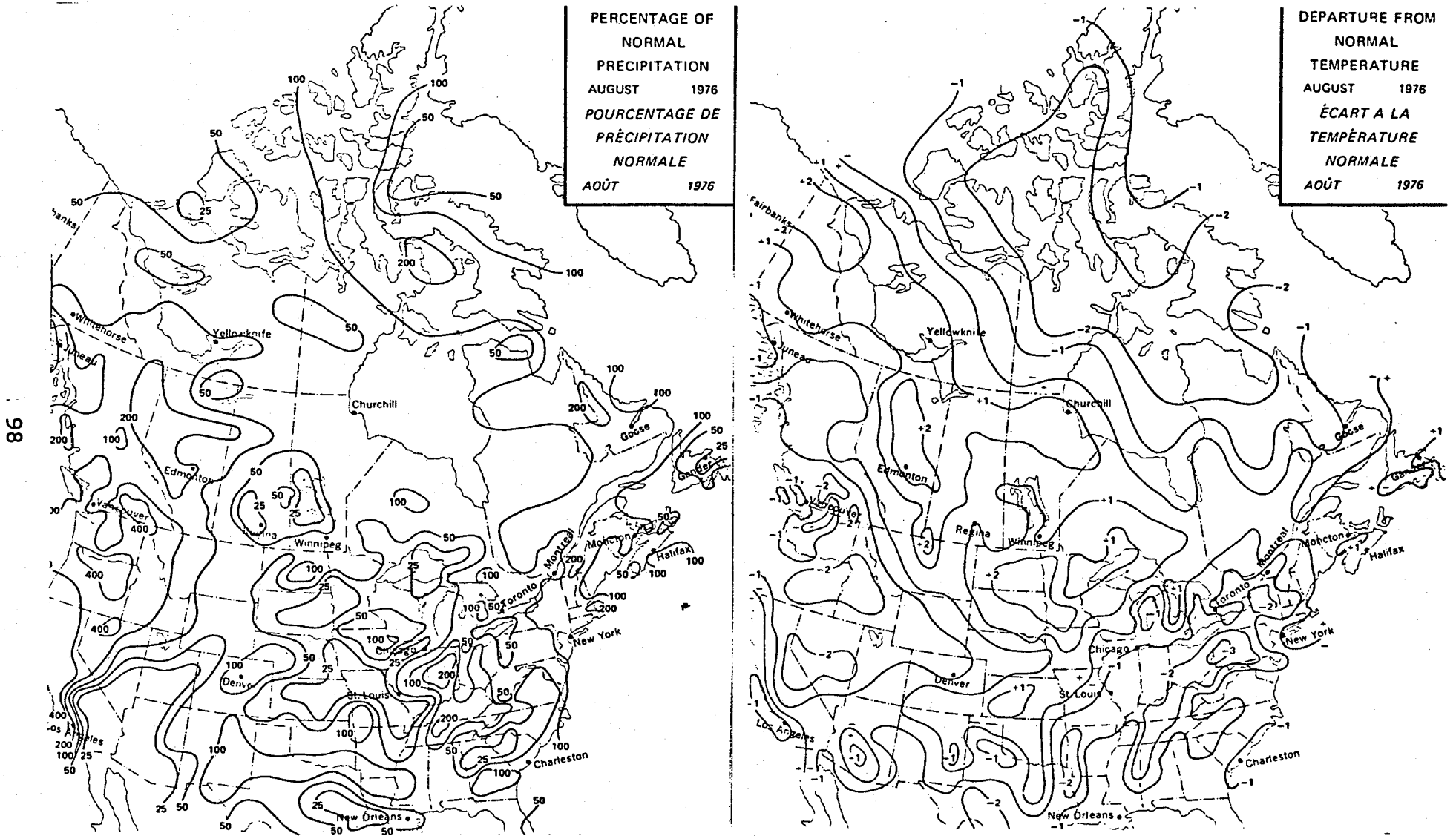
MAP 9.4.7 : PRECIPITATION AND TEMPERATURE ABNORMALITIES FOR JULY, 1976



97

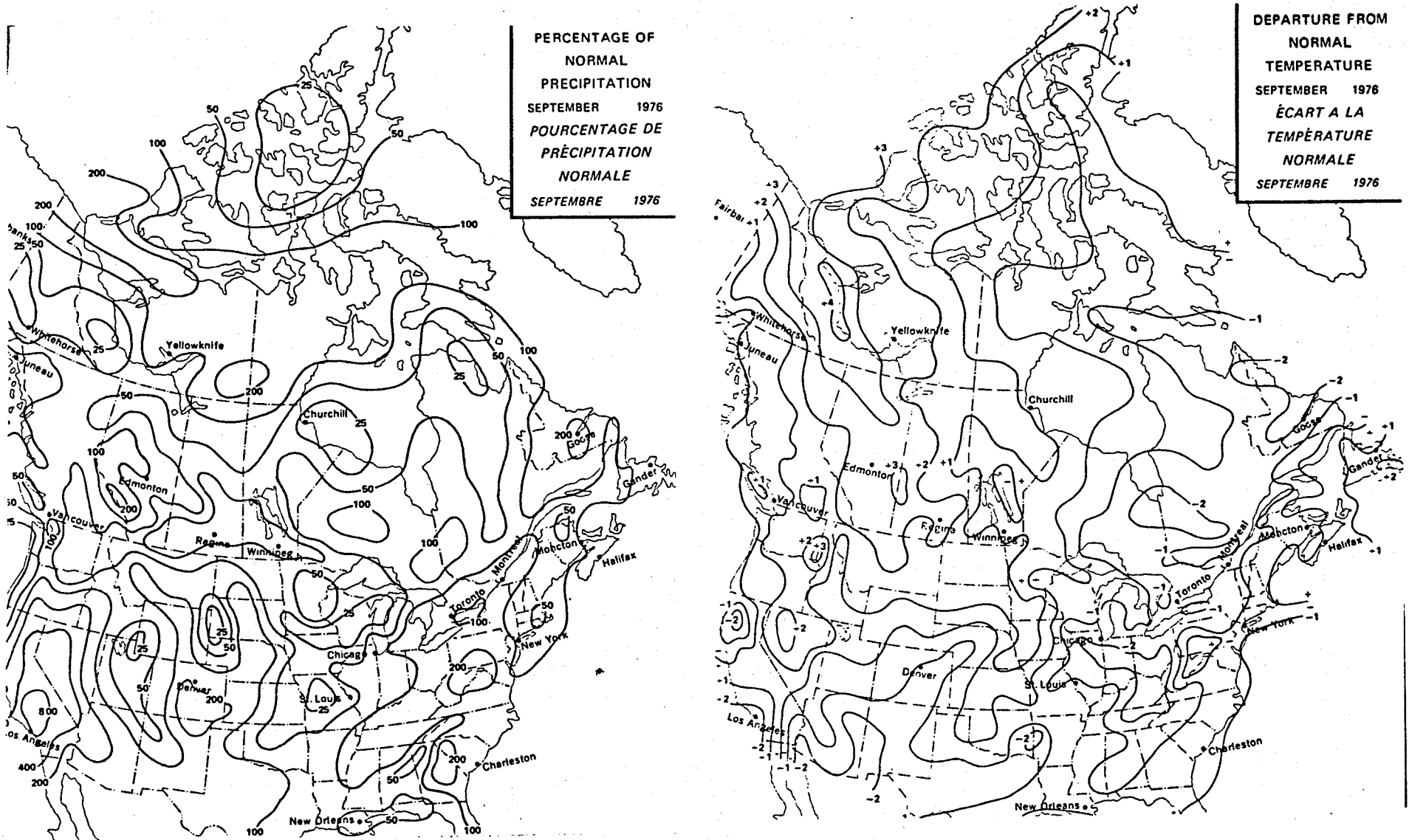
SOURCE : CANADA
 DEPARTMENT OF THE ENVIRONMENT
 ATMOSPHERIC ENVIRONMENT SERVICE
 CANADIAN WEATHER REVIEW, Vol. 14, 1976, No. 7

MAP 9.4.8 : PRECIPITATION AND TEMPERATURE ABNORMALITIES FOR AUGUST, 1976



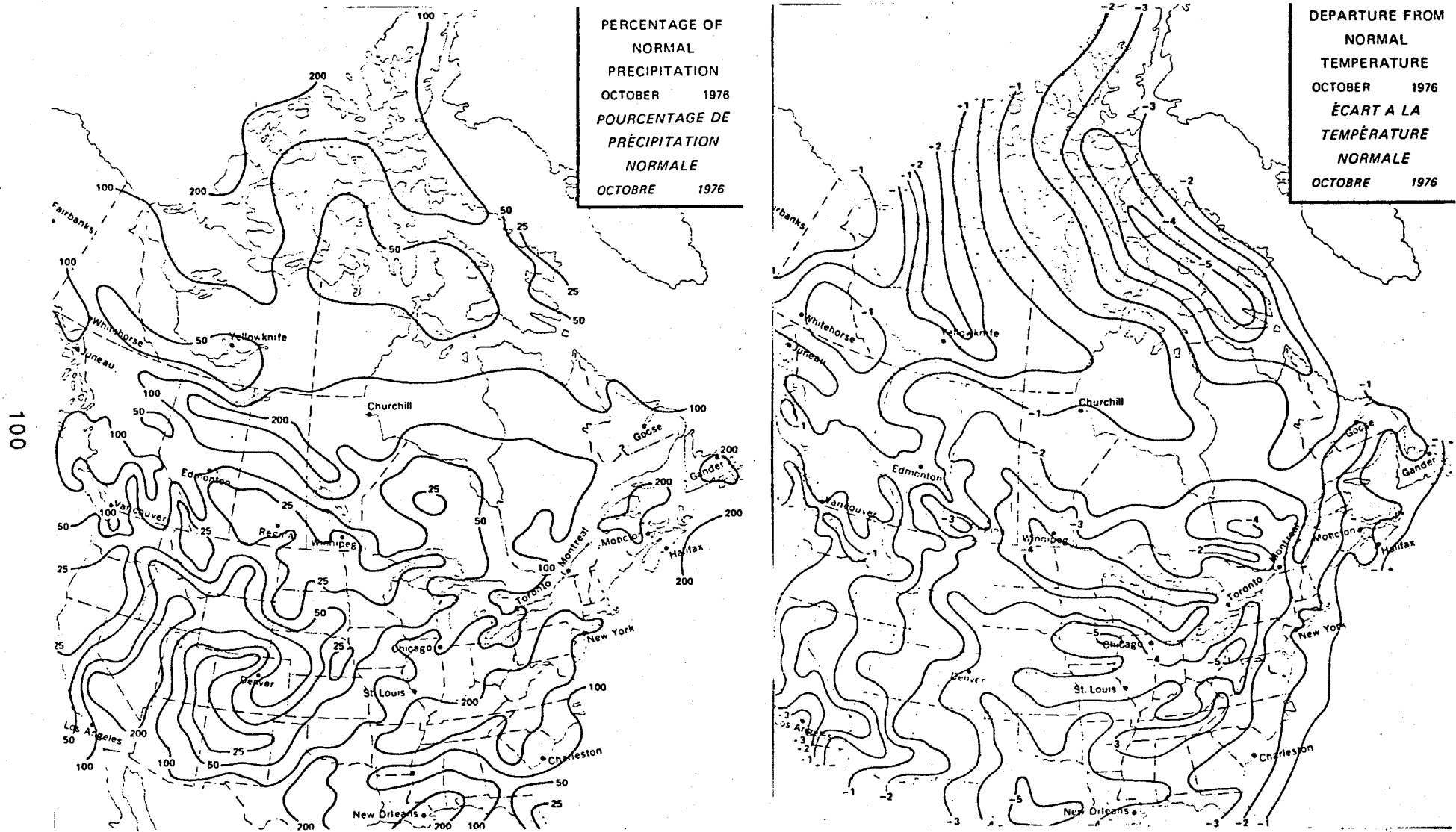
SOURCE : CANADA
 DEPARTMENT OF THE ENVIRONMENT
 ATMOSPHERIC ENVIRONMENT SERVICE
 CANADIAN WEATHER REVIEW, Vol. 14, 1976, No. 8

MAP 9.4.9 : PRECIPITATION AND TEMPERATURE ABNORMALITIES FOR SEPTEMBER, 1976



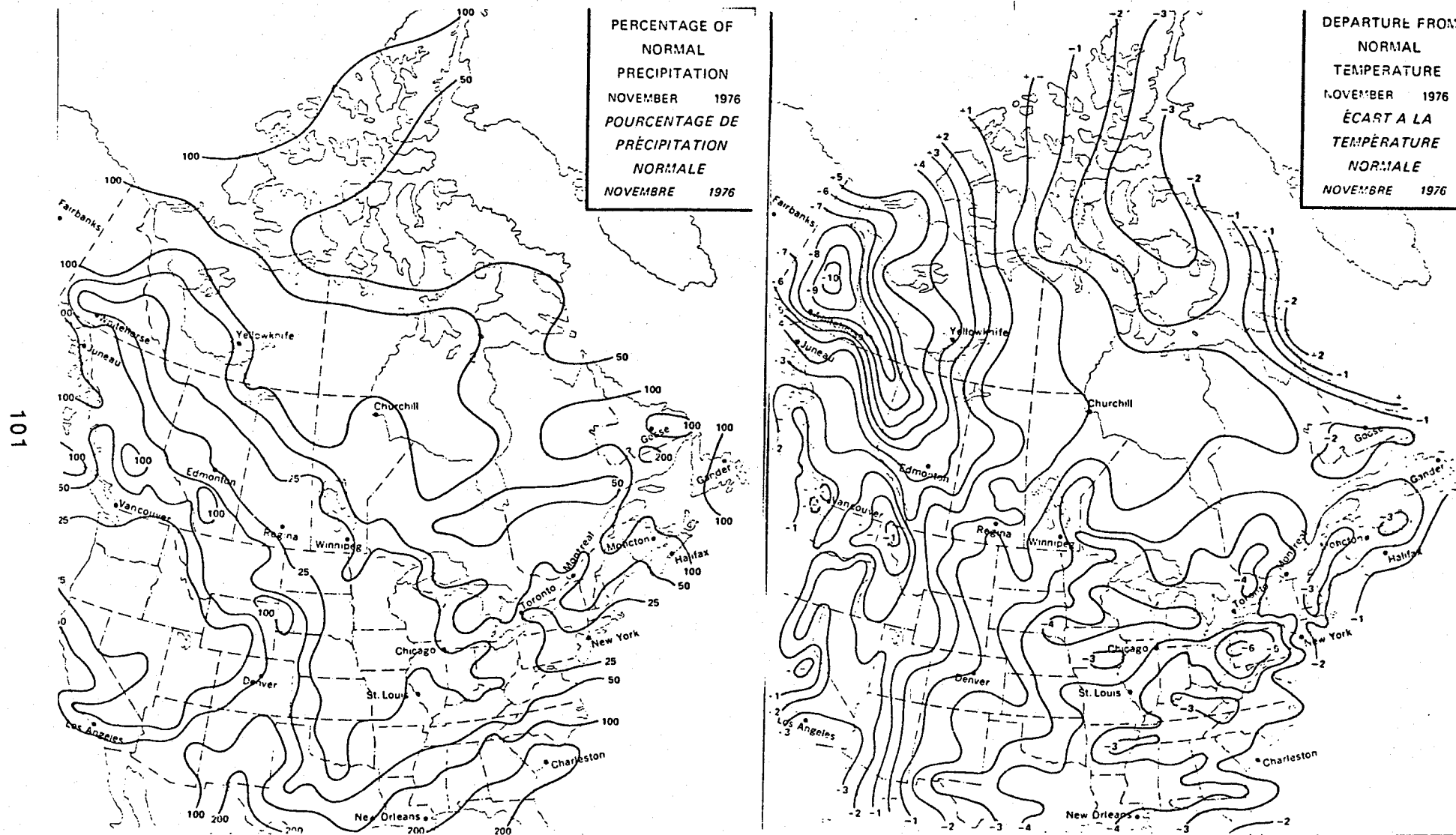
SOURCE : CANADA
DEPARTMENT OF THE ENVIRONMENT
ATMOSPHERIC ENVIRONMENT SERVICE
CANADIAN WEATHER REVIEW, Vol. 14, 1976, No. 9

MAP 9.4.10 : PRECIPITATION AND TEMPERATURE ABNORMALITIES FOR OCTOBER, 1976



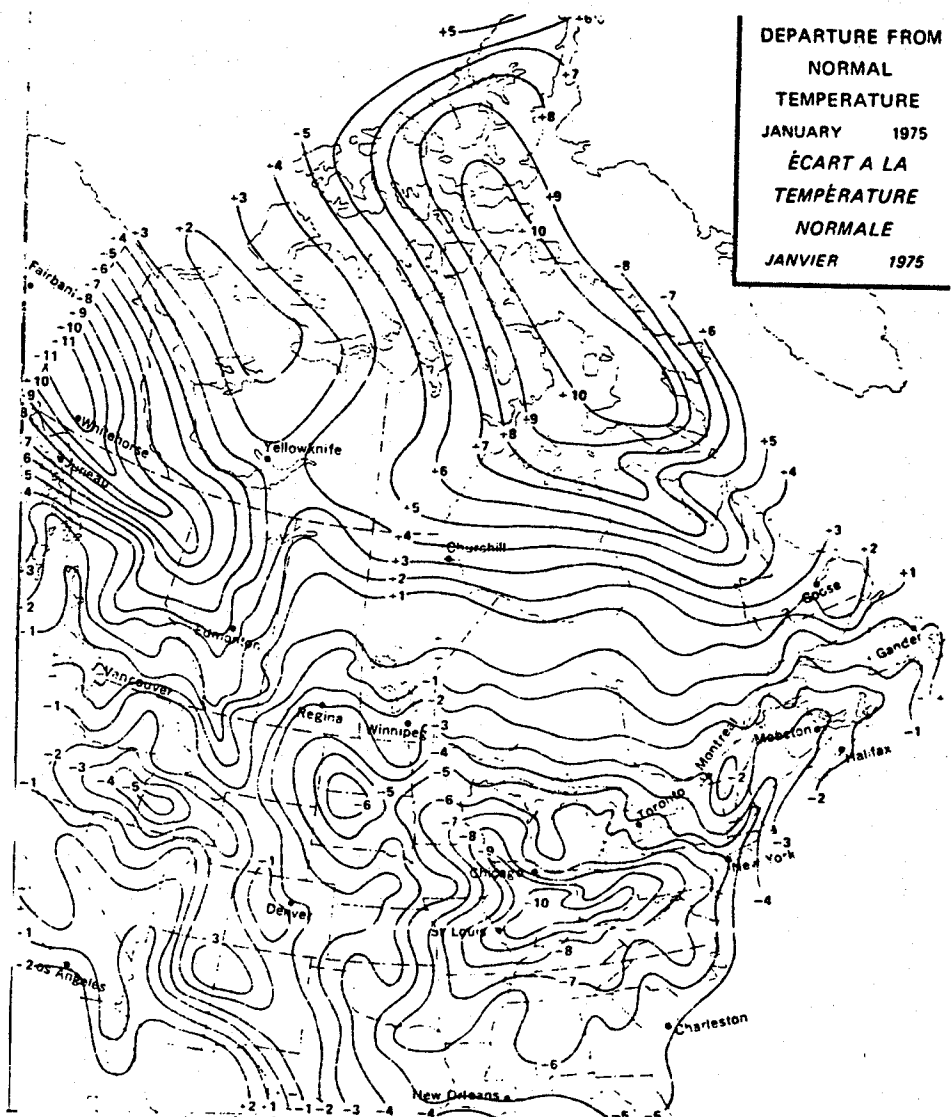
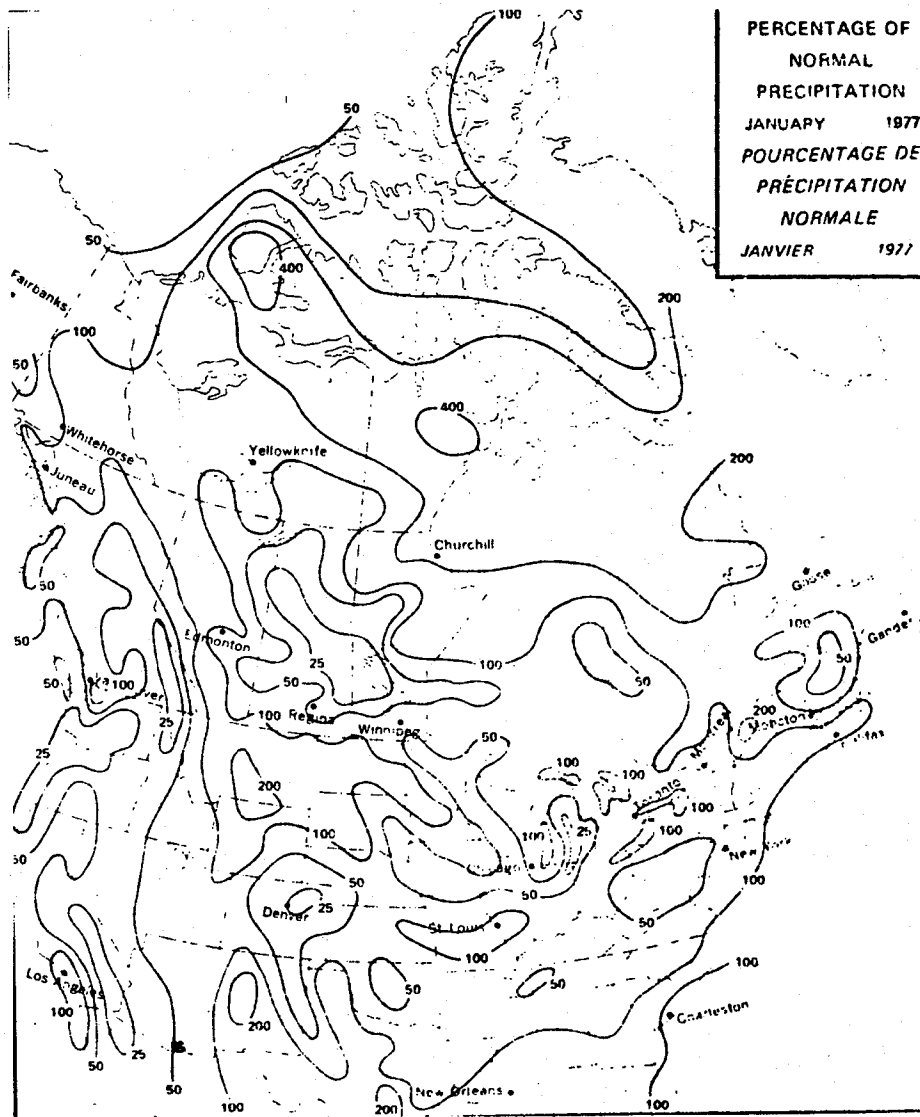
SOURCE : CANADA
 DEPARTMENT OF THE ENVIRONMENT
 ATMOSPHERIC ENVIRONMENT SERVICE
 CANADIAN WEATHER SERVICE, Vol. 14, 1976, No. 10

MAP 9.4.II : PRECIPITATION AND TEMPERATURE ABNORMALITIES FOR NOVEMBER, 1976



SOURCE : CANADA
 DEPARTMENT OF THE ENVIRONMENT
 ATMOSPHERIC ENVIRONMENT SERVICE
 CANADIAN WEATHER REVIEW, Vol. 14, 1976, No. II

MAP 9.4.I3 : PRECIPITATION AND TEMPERATURE ABNORMALITIES FOR JANUARY, 1977

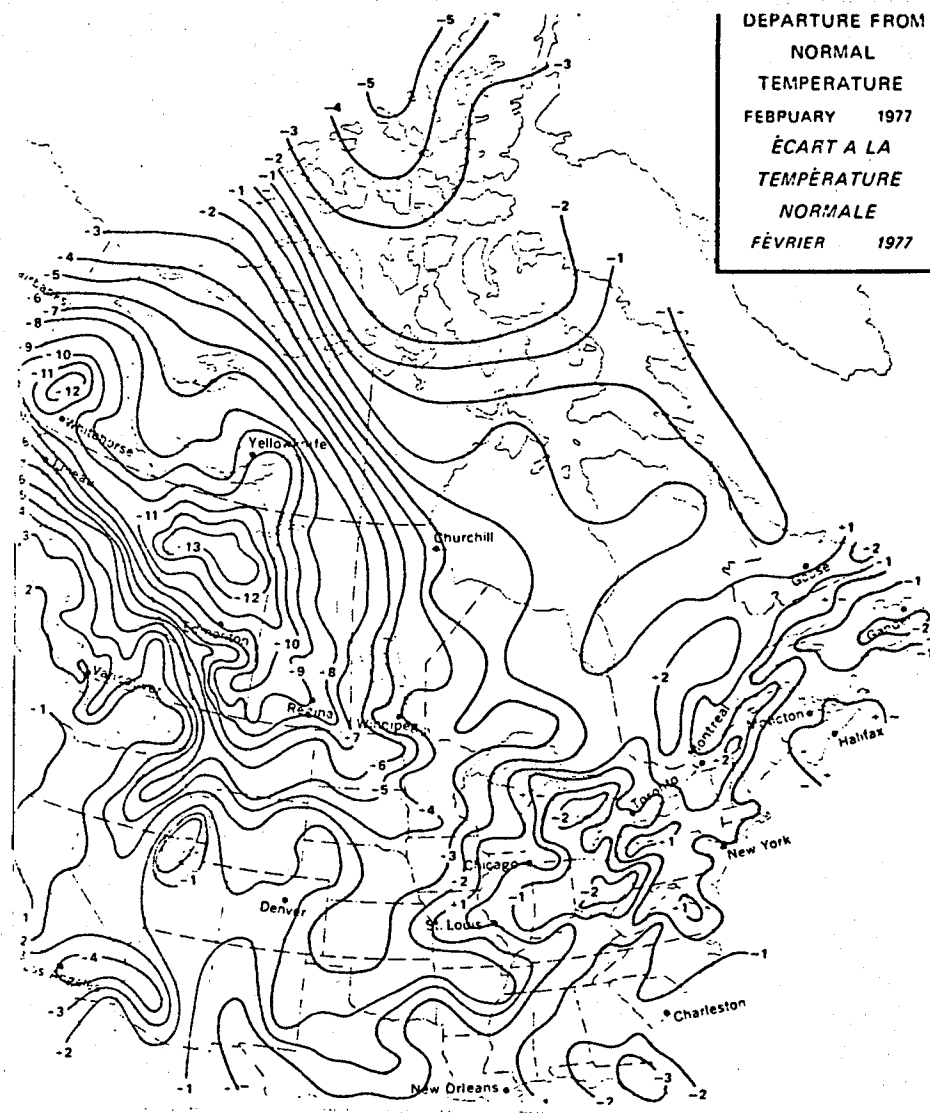
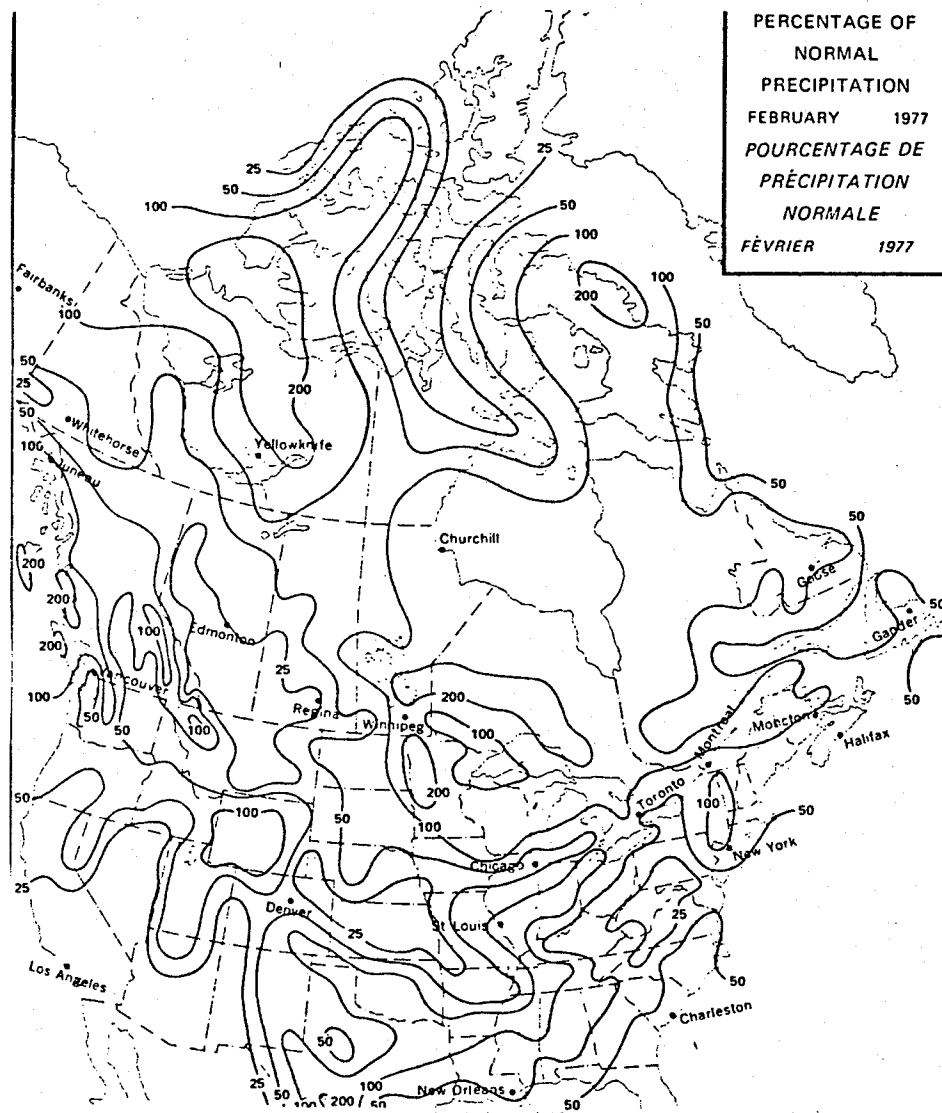


103

SOURCE : CANADA
 DEPARTMENT OF FISHERIES AND ENVIRONMENT
 ATMOSPHERIC ENVIRONMENT SERVICE
 CANADIAN WEATHER REVIEW, Vol. 15, 1977, No. 1

MAP 9.4.14 : PRECIPITATION AND TEMPERATURE ABNORMALITIES FOR FEBRUARY, 1977

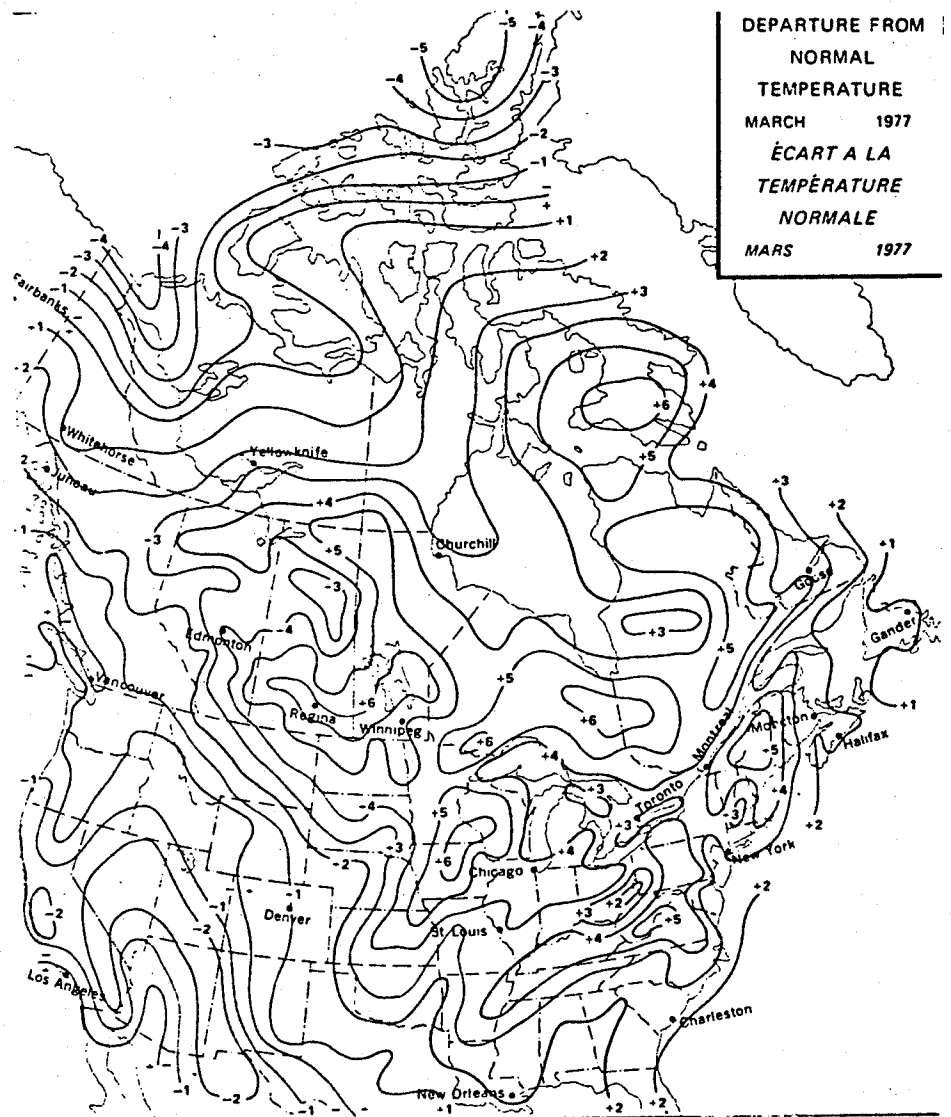
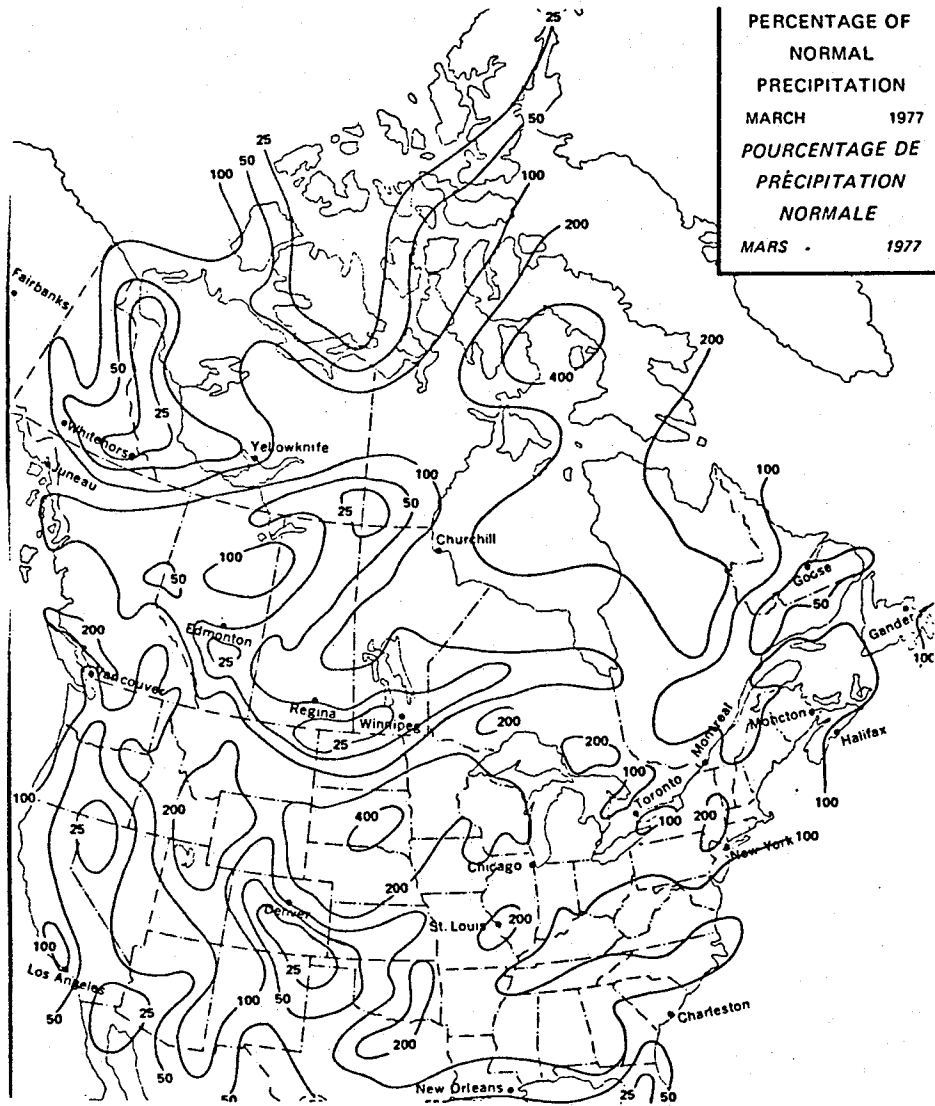
104



SOURCE : CANADA
 DEPARTMENT OF FISHERIES AND ENVIRONMENT
 ATMOSPHERIC ENVIRONMENT SERVICE
 CANADIAN WEATHER REVIEW, Vol. 15, 1977, No. 2

MAP 9.4.15 : PRECIPITATION AND TEMPERATURE ABNORMALITIES FOR MARCH, 1977

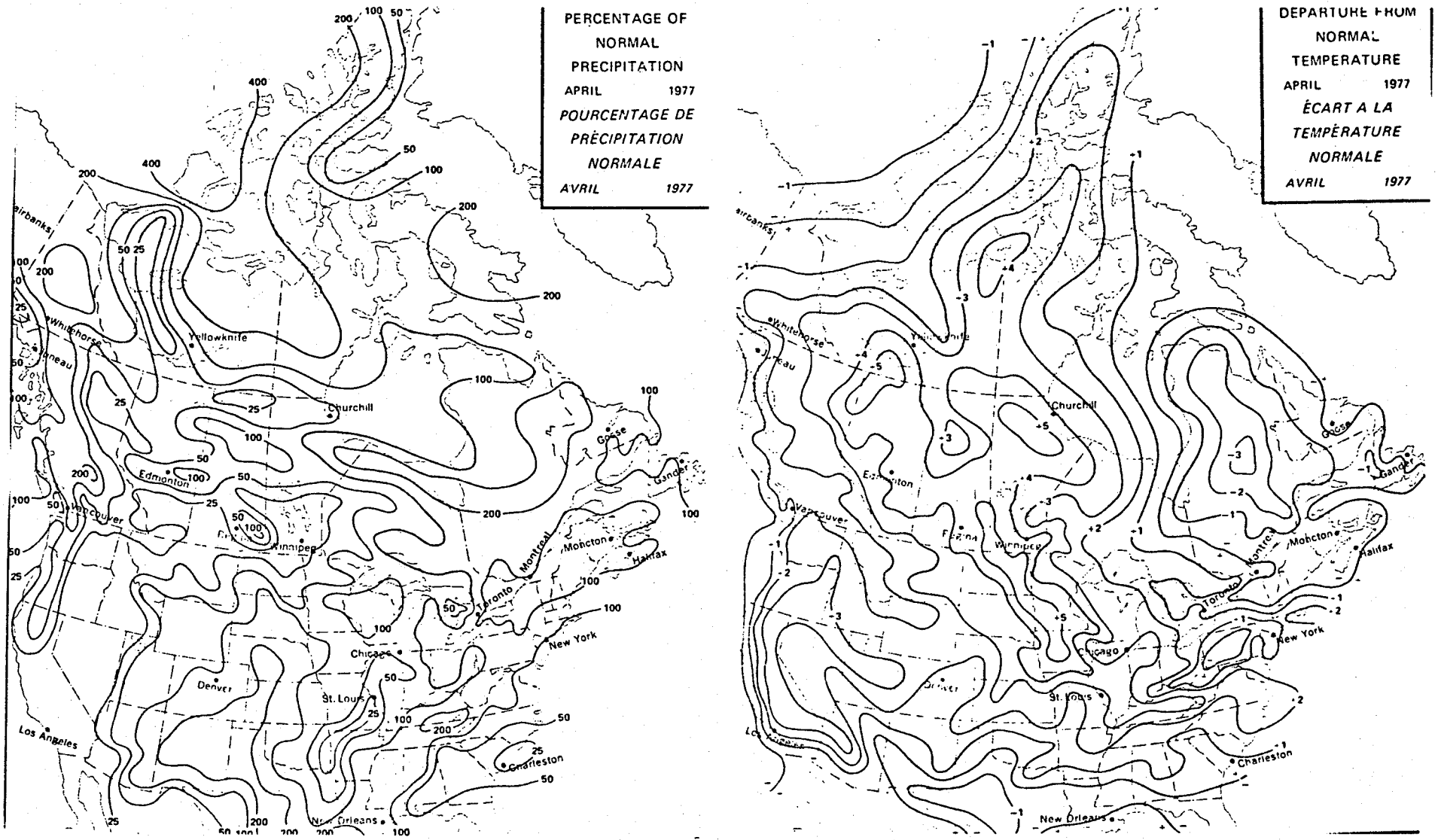
105



SOURCE : CANADA
DEPARTMENT OF FISHERIES AND ENVIRONMENT
ATMOSPHERIC ENVIRONMENT SERVICE
CANADIAN WEATHER REVIEW, Vol. 15, 1977, No. 3

MAP 9.4.I6 : PRECIPITATION AND TEMPERATURE ABNORMALITIES FOR APRIL, 1977

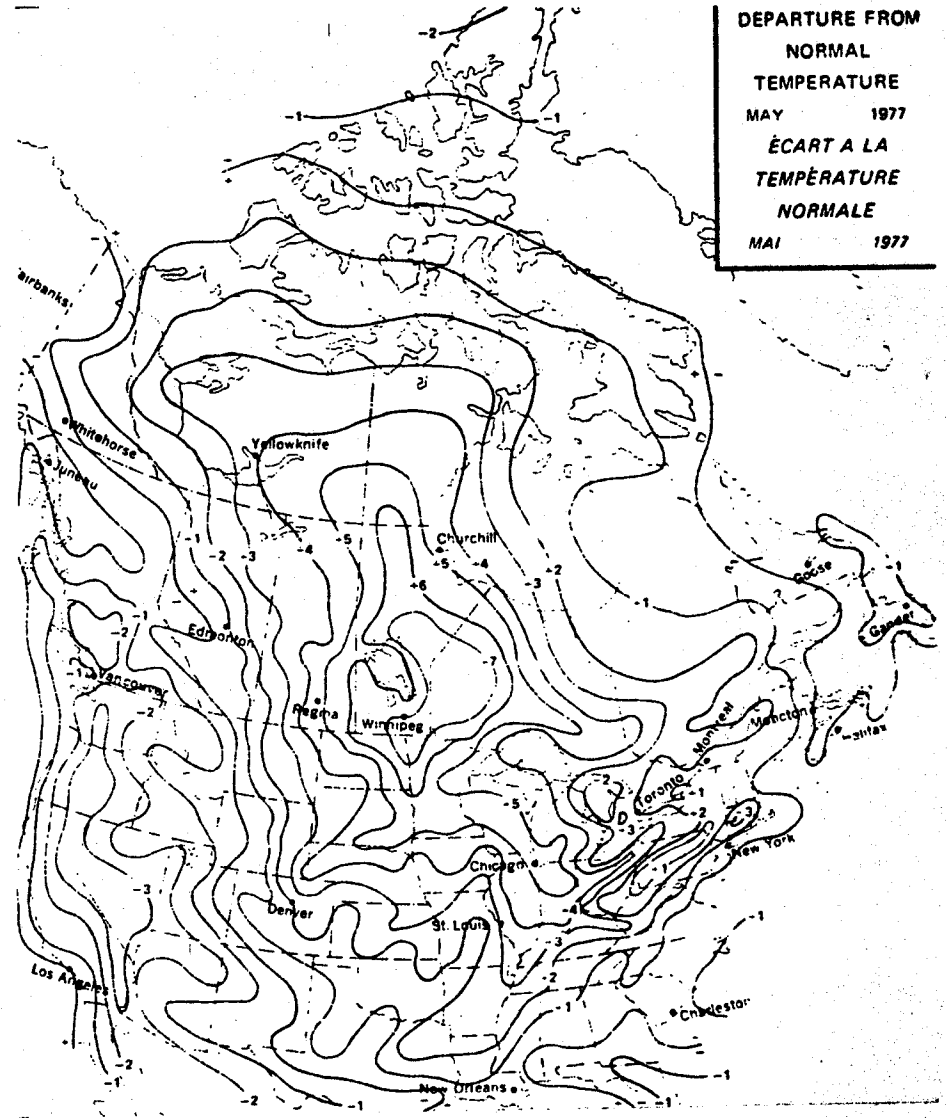
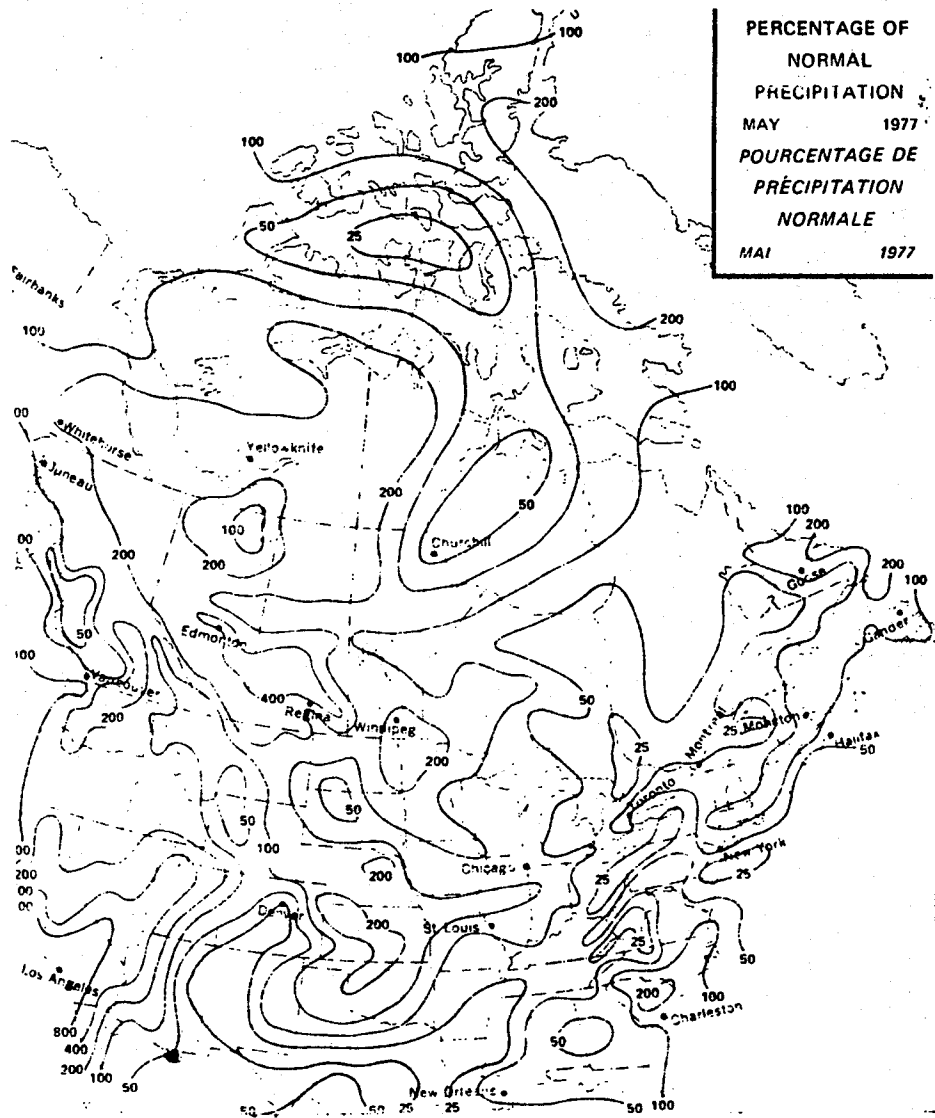
106



SOURCE : CANADA
DEPARTMENT OF FISHERIES AND ENVIRONMENT
ATMOSPHERIC ENVIRONMENT SERVICE
CANADIAN WEATHER REVIEW, Vol. 15, 1977, No. 4

MAP 9.4.17 : PRECIPITATION AND TEMPERATURE ABNORMALITIES FOR MAY, 1977

107



SOURCE : CANADA
DEPARTMENT OF FISHERIES AND ENVIRONMENT
ATMOSPHERIC ENVIRONMENT SERVICE
CANADIAN WEATHER REVIEW, Vol. 15, 1977, No. 5

LIST OF REFERENCES

- Anderson, R., Bouville, B.W. and McClellan, D.E., 1955: An Operational Frontal Contour-Analysis Model. Quar. Jour. Roy. Met. Soc., 81, 588-599
- Barry, R.G., 1967: Seasonal Location of the Arctic Front Over North America. Geog. Bull., 9, 79-95.
- Bell, W.C., 1974: An Analysis of Temperature, Lapse Rate and Wind in the Lower 810' Near Winnipeg. Ph.D. Theses. University of Edinburgh, 2 vols, 500pp.
- Bryson, R.A. and Hare, F.K., 1974: Climates of North America. IN World Survey of Climatology, 2, New York, Elsevier Scientific Publishing Co., 21-49.
- Crocker, A.M., Godson, W.L. and Penner, C.M., 1947: Frontal Contour Charts. Jour. of Meteor., 4, 95-99.
- Fraser, H.M., 1977: The Dry Fall of 1976 and Its Implications. Environment Canada, Atmospheric Environment Service, Internal Report, 22pp..
- _____ : The Continuing Drought of 1976-77. Environment Canada, Atmospheric Environment Service, Internal Report, 18pp..
- Krebs, J.S. and Barry, R.C., 1970: The Arctic Front and the Tundra-Taiga Boundary in Eurasia. Geog. Rev., 60, 548-554.
- Larsen, J.A., 1971: Vegetational Relationships With Air Mass Frequencies: Boreal Forest and Tundra. Arctic, 24, 177-194.
- LaBelle, T.J., Brown, R.T and Hasinoff, M.D., 1965: Climate of Winnipeg, Circular No. 4437, Department of Transport, Meteorological Branch, Toronto, 82pp.

- Longley, R.W., 1972:The Climate of the Prairie Provinces.
Climatological Studies No. 13, Department of
Transport, Meteorological Branch, Environment
Canada, 81pp.
- Lowe, A.B. and McKay, G.A., 1962:Tornado Composite Charts
for the Canadian Prairies. Jour. of Appl.
Met., 1, 157-162.
- McKay, G.A. and Lowe, A.B., 1960:The Tornado in Western
Canada. Bull. Amer. Met. Soc., 41, 1-8.
- Namias, J., 1955:Some Meteorological Aspects of Drought.
Mon. Weather Rev., 83, 199-205.
- Penner, C.M., 1955:A Three-Front Model for Synoptic
Analysis. Quart. Jour. Roy. Met.Soc., 81, 89-91.
- Sands, R.D., 1966:A Feature-of-Circulation Approach to
Synoptic Climatology Applied to Western United States.
Denver, University of Denver.
- Thomas, M.K., 1975:Recent Climatic Fluctuations in Canada.
Climatological Studies No.28, Environment
Canada, Ottawa.
- Weir, T.R., 1960:Economic Atlas of Manitoba. Department of
Industry and Commerce, Province of Manitoba.

CHAPTER FIVE

Methods of Investigation

5.1 Introduction

With a population of 586, 486 or 55% that of the province (M.H.S.C., 1977), Winnipeg exists as an island of urbanization in a rural setting. The nearest centers with populations greater than 5000, as defined by Census Canada are Portage la Prairie, 83km. WNW.; Selkirk, 35km. NNE., and Steinback 64km. SE. of the city. Of the above, only Selkirk has heavy industry associated with its economy. Winds from the north-northeast, the main anthropogenic heat and moisture carriers from Selkirk into the research area, are infrequent, averaging an occurrence frequency of 0.67 annually out of a cumulative frequency of 100. Those that do penetrate into the city have mean speeds of 19km./hr. The latter speeds encourage considerable mixing within surrounding air. The city's isolation thus indicates that anthropogenic heat, moisture, and pollutant production must be internal with little or no external influence.

Due to the lack of topographic obstacles, Winnipeg has expanded horizontally rather than vertically, covering a

land area of 571km.². Of the latter figure, 68% is either undeveloped, vacant or under crop;16% is residential;5% is devoted to parks, schools, cemeteries, etc.;4% is under industrial land use classifications;5% is owned by public utilities;2% is commercial , and 1% is devoted to churches, hospitals, and other public buildings (L. Loreth,Department of Environmental Planning,The City of Winnipeg, personal communication;The City of Winnipeg,1977). Spacing between buildings can be classified as "tight" within the C.B.D.. Multiple reflection will be greatest in this area. Maximum heating through direct or indirect absorption of solar radiation will nevertheless occur at ground level throughout most of the traversed research area rather than aloft in areas of packed tall buildings and at ground levels in regions outside these areas. If these factors are not taken into consideration, misinterpretation of urban-rural temperature differences is quite possible (Ludwig, 1968).

Vegetation growth within the research area is profuse. Elm trees number 273,000;poplars 819,000 (G.J. Kuta,Forestry,Regional Parks & Operations,The City of Winnipeg, personal communication). These figures do not include 144km of natural river frontage. Tree density per square mile is greater in the research area than in Ottawa, Toronto, London, Windsor, and Saute Ste. Marie, to mention only a few (G.J. Kuta,Forestry,Regional Parks &

Operations, The City of Winnipeg, personal communication.). Transpiration therefore plays an important part in the formation and in the maintaining of the research area's humidity island(s) within the temperature range -1.4°C . to 40°C ..

The city's ideal site in the centre of an "infinite" plain well removed from lake and valley effects, and an immense vegetative ecotone combined with the previously discussed climatic conditions are unique characteristics not noted in any of the relatively few comparative urban-rural heat island-moisture studies. The City of Winnipeg is therefore an ideal research zone.

5.2 Choice of Route

5.2.1 Introduction

Comparability of analyzed data and the power restraints placed upon the batteries by the data acquisition equipment governed the final selection of the itinerary to be used for this study.

The route, totalling 86.3km., is almost exactly the same as that chosen by Bell during his 1972-74 studies of the Winnipeg urban climate. All possible areas associated with varied urban-rural morphologies residential, commercial, industrial, recreational, agricultural, and natural land, within all the eight major compass directions are included in the itinerary. This ensured that data

gathered would be representative of those areas within, through, and outside of the urban heat dome or the boundaries of the city's heat plume. The traverse commences and terminates at the same location and crosses itself at several points thus providing a means of checking temperature and dewpoint variations with time. This is fundamental for the reduction of readings to a constant time.

Visibility rather than equal distance between points was the main criteria for choosing fixed point locations at which measurements would be recorded. Preliminary traverses undertaken in November 1975 proved that equidistant points were often obscure points almost impossible to recognize after dark. Street intersections and illuminated sign posts were the major fixed point reference locations. In total, the latter numbered 127.

Map 5.2.1 shows the itinerary with reference point locations.

Map in pocket at back of thesis.

5.2.2 Power Restraints as a Limiting Factor

The power requirements of the data acquisition equipment, 115VAC($\pm 10\%$)-50/60cps-100VAm_{ax}, were supplied by a 12volt, 90 plate car battery which has a maximum life of 4 hours. The route, therefore, had to be short enough so that no errors result from an inadequate energy supply. Unexplainable extreme variations in the dewpoint trend on the stripchart, generally in the form of arcs of increasing amplitude with rapid drop-offs after each cycle, constituted error. Preliminary runs showed that traverses of 3-3.5 hours duration registered no such occurrence. Three hours also corresponded to the maximum amount of driving undertaken prior to engine overheating, therefore, a 3 hour limit was placed on each traverse.

Traverses commenced at 0900hrs., 1300hrs., 1700hrs., and 2100hrs. C.S.T. on randomly selected days. Average car speed was 36km./hr.. Approximately 80% of the time was devoted to continuous cruising while 20% was taken up in a stop-go flow. The latter flow type occurred in the C.B.D. and at major intersections.

Table 5.2.2 lists the location of fixed points on the itinerary, the difference in kilometers between adjacent points and the time required for passage between two adjacent points. The table is located at the end of the chapter before the List of References.

5.2.3 Control Site Location

Unlike Goldreich(1970), Conrads et al.(1971) and Lyons et al.(1975), the establishment of control sites along the itinerary could not be undertaken. Companies which maintained automatic temperature and relative humidity monitoring devices showed little interest in the project while those which desired to co-operate, notably the ESSO refinery in East St. Paul, ceased to function at the commencement of the study. Others would unfortunately take readings only when adjustments of their air-conditioning systems demanded them or when requested by me at a particular time and day.

The first order meteorological station at the Winnipeg International Airport would not be designated a control site for this study because the representativeness of the observation site with its surroundings has not yet been adequately examined. Simultaneous monitoring of temperature and other parameters at various radii from the observation site, as described by Hoehme(1971) would aid in determining the diurnal, seasonal and annual variations in micro- and mesoclimatic influencing parameters, but it was beyond the economical feasibility of this research project to initiate such an analysis.

5.3 Instrumentation

5.3.1 Introduction

A Cambridge Systems Model 110S-M Automatic Meteorological Temperature and Dew Point Measuring Hygrometer was the only data acquisition instrument employed during this study. Its accuracy of 0.28°C . within the operating range of -62.2°C . to 48.9°C . and its precision of 0.05°C . between -50.0°C . and 40.0°C . ensures that temperature and dewpoint data will be well within the World Meteorological Organization accuracy requirements of $\pm 1^{\circ}\text{C}$. and $\pm 5^{\circ}\text{C}$. for surface observations of temperature and dewpoint respectively. Response and cooling rates for both parameters are $2.0^{\circ}\text{C}/\text{sec}$.

A photoresistive, condensate-detecting optical system automatically maintains a Peltier-cooled mirror at true dewpoint. Both the mirror temperature and the ambient air temperature are determined with 3 wire platinum resistance temperature sensors. The former is embedded in the mirror while the latter is mounted in a thermally shielded and aspirated thermometer well. The resistance changes of both thermometer elements are converted to millivolt output by means of zener-regulated bridge circuits located in the control unit. Output is linear, following the Callendar-van Dusen equation for platinum. The three r's of the equation are determined by measuring resistivity of

the wire at the temperatures 0°C., 100°C. and -78.51°C..
The lattermost value is the sublimation point of CO₂.

Errors arising from solar heating at all radiation levels have been eliminated by enclosing the independent sensors in a double-walled, thermally insulated, aspirator located within a transmitter unit finished in tough baked on white enamel. The control unit containing the transducer amplifier and signal conditioning equipment is similarly finished. Exposed hardware is aluminum or stainless steel so as to minimize corrosion.

The system's built in automatic test cycle and manual initiated test cycle permits the operator to check whether or not the thermoelectrically cooled detecting dewpoint mirror is at dew (frost) point at all times. During the cycles, the mirror is heated above the ambient temperature (maximum heating is 50°C. under automatic control) causing the dew layer to evaporate, thereby cleaning the mirror. At the end of the balancing cycle (about 15 minutes duration automatically), the mirror supercools so that a new dew layer can form and then returns to the true ambient air temperature's dew point. A mid-scale indication on the control condition meter located on the control unit indicates that the system is properly balanced.

Resistance voltage dividers connected the 110S-M to a 2 pen Hewlett-Packard Strip-chart Recorder with event

marker. Both temperature and dewpoint sensors were zeroed prior to traverse commencement. After zeroing, the base temperature was registered at 50mv while the continuous offsets during the entire traverse were registered at 20mv. By closing an electrical circuit, the event marker marked the location of each itinerary point on the chart. All chart speeds were one inch per minute. Car vibrations did not influence recordings.

The 110S-M control unit, the energy supply, the inverter, and the strip-chart recorder were sheltered within the traverse vehicle.

5.3.2 Sensor Lag Response Estimation

The response lag between the temperature and dewpoint sensors was monitored on a monthly basis during the research period. In order to facilitate the need for a great quantity of pressurized steam, defroster tubing of diameter 1.75 inches was clamped (gear type) to the spout of an electric steam kettle. A Peterson grip-clamp secured the opposite end until testing was to commence. Testing took place in the basement of the researcher's home, as temperature and relative humidity remained constant at 20°C. and 70% respectively. The 110S-M was allowed to run for 30 minutes prior to testing. The Hewlett-Packard strip-chart, to which the dewpointer was attached, was set at 20mv at a speed of 1 inch per minute after zeroing. The

chart speed was altered to 1"/sec when measurement was to commence.

When the steam pressure was great enough to begin to deform the defroster tubing, the kettle was brought to within 15cm. of the transmitter air intake. The grip-clamp was released for 30 seconds. The process was repeated a number of times. Response lag between sensors was noted and averages were calculated.

Sensor lag over the two year research period was minimal ranging from 0.013"/min.-0.12"/min. at 20mv settings. In other words, there was an overall 8sec difference in response rates. This corresponds to 80m. on the ground at vehicle speed. Therefore, the temperature and dewpoint measurements taken simultaneously at each specific location are representative of that specific location.

5.3.3 Principle of Operation of Model 110S-M

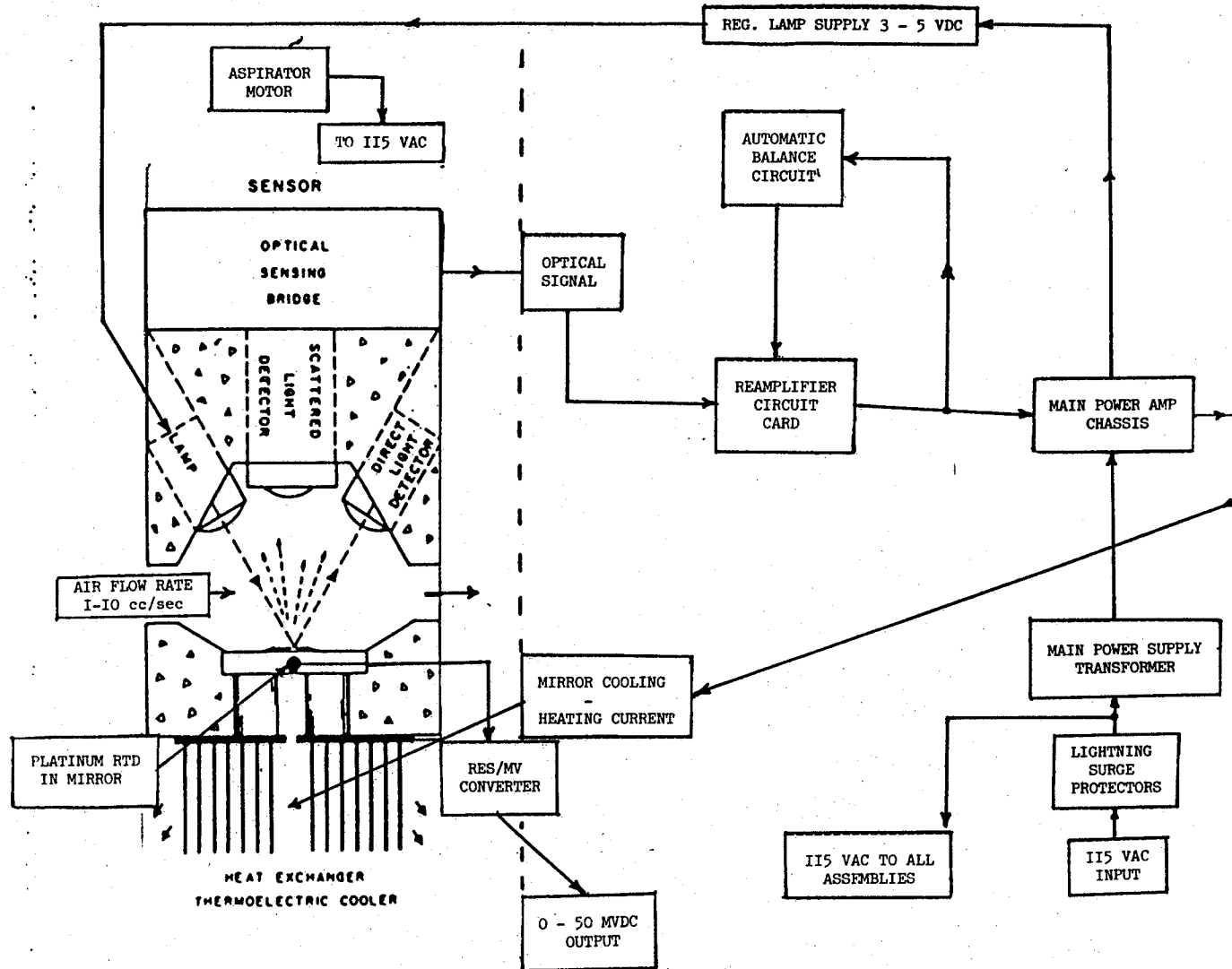
The basic concept of the Peltier-cooled¹ dewpoint hygrometer is shown in Figure 5.3.3.1. It must be noted that the sensor mirror is thermally bonded to, but electrically insulated from the thermoelectric cooling

¹ In the Peltier effect when a direct electrical current flows through a circuit made of 2 different conductors or semi-conductors, one junction between the two materials is cooled while the other is heated, depending on the direction of the current. The degree of cooling depends upon the thermal conductivity and resistivity of the conductor or semiconductor used.

module². Air flow across the plane of the rhodium-plated mirror and temperature thermometer well is regulated by a pump at a rate of 1-10cc/sec (0.2-2cm/sec). Changes in flow rates over this range do not effect the measurement. (Model 110S-M Instruction Manual). Heat rejected by the hot side of the thermoelectric module is displaced by a blower away from the mirror. The system operates as follows.

² A module is composed of several thermoelectric couples arranged either parallelly to provide increased heat-pumping capacity or connected electrically in series to increase the overall impedance level. In the 110S-M, each thermocouple is composed of 2 rods of semiconducting bismuth telluride, one classified p-type (given an excess of positive charge), the other n-type (given an excess of negative charge), bounded by a flat copper bar to produce a heat transfer surface as well as an electrical conducting medium.

FIGURE 5.3.3.I : GENERAL BLOCK DIAGRAM OF THE AUTOMATIC METEOROLOGICAL TEMPERATURE AND DEW POINT MODEL IIOS - M MEASURING SYSTEM



122

SOURCE : INSTRUCTION MANUAL, MODEL IIOS - M AUTOMATIC METEOROLOGICAL TEMPERATURE AND DEW POINT MEASURING SYSTEM
CAMBRIDGE SYSTEMS INC.
NEWTON, MASSACHUSETTS
UNITED STATES OF AMERICA

An incandescent light source illuminates the mirror surface while separate cadmium sulfide photoresistors compare the direct reflected light of the scattered light when dew forms. If the optical sensing bridge is unbalanced, sufficient signal from the bridge is supplied to an amplifier which converts the signals to pulses for operating silicon controlled rectifiers. The latter controls DC power supply output and hence regulates the cooling current delivered to the thermoelectric module. As the mirror cools to the new dew point, formation of dew on the mirror causes attenuation of the directly reflected light beam and an increase in the light received by the scattered photoresistor. This forces the bridge towards the balance point, proportionally decreasing the current supplied to the cooler, until a stable current is attained, whereby a thin dew film is maintained on the mirror surface. The instrument tracks changes in dewpoint by increasing or decreasing the DC current about the stable point in proportion to the thickness of the dew deposit on the mirror. Should a lower dewpoint sample be encountered, the thinning dew formation on the mirror causes an increase in the cooling current and a lowering of the mirror temperature to the new dewpoint. In the like fashion, should the dew layer tend to thicken due to a higher dew point sample, decreasing current results in the mirror heating to a higher dewpoint. True proportional

control of the dewpoint mirror is obtained at all times in this fashion.

5.3.4 Maintenance of Equipment

Due to the drought conditions which prevailed during the data acquisition period, weekly removal of particulate matter from the mirror was necessary as individual particles can act as nuclei in dew-frost formation thus contributing to higher dew-frost point measurements. Distilled water and Q-tips were the general materials used. To insure correct sampling flow, the small slit at the dew point sensor wall which controls the air flow rate was also cleaned.

Prior to the commencement of each traverse, the dew pointer was placed on automatic balance and allowed to operate outdoors for half an hour so that a new thin evaporation film could form. After the initial film has formed, deposition of additional film has only a slight effect (Model 110S-M Instruction Manual). During winter traverses, the warming period was extended. Traverses did not commence until stabilization was achieved.

5.4 Error Minimization

The transmitter containing the aspirated thermometer and dew point transducers was screwed onto a horizontal, square 15.2cm., metal base, which in turn was bolted to the arms of an extended trailer mirror. When mounted over the right

front bumper of the traverse vehicle, the base of the transmitter was approximately 1.25m. from the road surface; 11.5cm. from the side edge of the bumper, and 25.3cm. from the car hood. Being 25cm. above the horizontal car hood level also, one can be assured that engine heat influence was non-existent.

To minimize exhaust influences, the vehicle's dual exhaust system was altered to a driver side single. At least two car lengths were maintained from preceding vehicles (doubled in cases of buses), so that exhaust from them would minimize interference.

5.5 Data Conversion

Conversion of temperature and dew point millivolt strip chart data to degree Celsius data was mechanized using a Hewlett-Packard Programmable Calculator and Digitizer. Constants for the 110S-M linear equation for platinum were computed by Bell. The linear equation employed was:

$$T^{\circ}\text{F} = -81.122 + 4.0075(\text{mv}) + 0.000001(\text{mv}^2)$$

where

$T^{\circ}\text{F}$ = temperature in $^{\circ}\text{F}$.

mv = millivolt output(base±offset)

For reasons previously discussed, reduction of traverse data to the commencement time of each traverse was based

upon the overall temperature and dew point temperature change during the traverse, as registered on the strip-chart, rather than adding or subtracting interpolated estimates based upon hourly readings taken at the airport. It was assumed that the general temperature and dewpoint change on the strip-chart was linear³. The conversion formula is:

$$T_{i, c} = T_{i, t} - (K_{t, i} \cdot T_e)$$

where

- $T_{i, c}$ = the temperature or dew point temperature at the location, i , at the constant time, c , to which the whole traverse is reduced.
- $T_{i, t}$ = the measured temperature or dew point temperature at the location, i , at the time, t , as calculated from the strip chart.
- $K_{t, i}$ = cumulative time in seconds required for the research vehicle to proceed from the starting location to adjacent locations.
- T_e = overall temperature or dewpoint temperature change in a traverse as determined by summing the individual linear interpolations between full-hour traverse values ($c+1-c$, $c+2-c+1$, $c+3-c+2$) and dividing that sum by the overall traverse duration time in seconds.

Following standardization, the following parameters were computed using formulae referenced in the Smithsonian Meteorological Tables(1968),page 350.

³ In the case of dew points, conversion from the dew point value to its associated vapor pressure and vice versa, after averaging, was required.

$$e_w = \text{EXP } 2.302585 - 7.90298(T_s/T - 1) + 5.02808 \log_{10} (T_s/T)$$

$$- 1.3816 * 10^{-7} (10^{11.344(1-T/T_s)} - 1)$$

$$+ 8.1328 * 10^{-3} (10^{-3.49149(T_s/T - 1)} - 1) + \log_{10} \frac{e_{ws}}{e}$$

$$e_i = \text{EXP } 2.302586 - 9.09718(T_o/T - 1) - 3.56654 \log_{10} (T_o/T)$$

$$+ 0.876793(1 - T/T_o) + \log_{10} \frac{e_{io}}{e}$$

where

e_w = saturation vapor pressure over a plane of pure ordinary liquid water.

e_i = saturation vapor pressure over a plane of pure ordinary water ice.

T = absolute thermodynamic temperature ($^{\circ}\text{K}.$)

T_s = steam point temperature ($373.15^{\circ}\text{K}.$)

T_o = ice point temperature ($273.15^{\circ}\text{K}.$)

e_{ws} = saturation pressure of pure ordinary liquid water at steam-point temperature at one standard atmosphere ($1013.246\text{mb}.$)

e_{is} = saturation pressure of pure ordinary water ice at ice-point temperature at 0.0060273 standard atmosphere ($6.1071\text{mb}.$)

Saturation deficit (SATD), relative humidity (U), mixing ratio (r), and absolute humidity (dv) were computed for each location, i, as

follows:

$$\text{satd} = e_w(T) - e_w(T_d)$$

$$U = (e_w(T_d)/e_w(T))*100$$

$$r = (((0.62197*e_w(T_d))/(p-e_w(T_d)))*1000.)$$

$$dv = (217.*e_w(T_d))/T^{\circ}\text{K}.$$

where

$e_w(T)$ = saturation vapor pressure over a plane surface of pure liquid water at the ambient air temperature in $^{\circ}\text{K}$.

$e_w(T_d)$ = saturation vapor pressure over a plane surface of pure ordinary liquid water at the ambient air temperature's dew point in $^{\circ}\text{K}$.

p = station pressure in mb.

The subscript for saturation pressure of pure ordinary liquid water is replaced by that over a plane of pure water ice if the temperature is less than 0.0°C .

In all, 257, 048 values to the 3rd decimal place were calculated. The data were edited several times and then put on tape. The entire process of editing took a considerable amount of computer time and over half a year of full time work.

Regular hourly synoptic observations for traverse days were obtained from the Airport and merged with the computed data. Air mass classification was based upon Penner(1955) and checked against streamline flow methods used by Bell(1974). Both methods yielded the same results. The data base was labelled according to air mass and season criteria. Further stratification into wind direction quadrants followed. Several statistical methods were used in the analyses of the readings, the results of which are presented from Chapter 8 onwards.

TABLE 5.2.2

POINT LOCATION, DISTANCE AND TIME INFORMATION

<u>POINT</u>	<u>LOCATION</u>	<u>D</u> (km)	<u>T</u> (sec)
1	Home Driveway	0.00	0.0
2	Driveway-Kennedy	0.03	3.2
3	Kennedy-Sargent	0.13	12.8
4	Sargent-Balmoral	0.10	9.6
5	Balmoral-Ellice	0.35	35.2
6	Colony-Portage	0.29	28.8
7	Portage-Sherbrook	0.60	59.2
8	Portage-Maryland	0.01	9.6
9	Portage-Arlington	0.68	67.2
10	Portage-Sherburn	0.48	48.0
11	Portage-Wall	0.24	24.0
12	Portage-Valour Rd.	0.24	24.0
13	Portage-Tylehurst	0.81	80.0
14	Portage-onto Cloverleaf	0.63	62.4
15	Cloverleaf-Century	0.48	48.0
16	Century-mid Bridge	0.45	44.8
17	Kenaston-Academy	0.32	32.0
18	Academy-Wellington	0.28	25.6
19	Wellington-Chataway	0.68	67.2
20	Wellington-Park Bd.	0.50	49.6
21	Wellington-Conservatory Rd.	0.77	96.0
22	Conservatory Rd.-Corydon	0.48	48.0
23	Corydon-Zoo Entrance	0.56	56.0
24	Roblin-Waxford	1.61	160.0
25	Roblin-Alcrest	0.48	48.0
26	Roblin-Batchelor	0.97	96.0
27	Roblin-Grant	0.81	80.0
28	Roblin-Pepper Loaf Cr.	1.29	128.3
29	Roblin-Community Rd.	0.64	64.0
30	Roblin-Dale	0.97	96.0
31	Roblin-Hwy. 101	0.74	73.6
32	Hwy. 101-mid Bridge	0.48	48.0
33	Hwy. 101-mid Portage Overpass	1.24	123.3
34	Hwy. 101-Downs Entrance	1.29	128.3
35	Hwy. 101-Saskatchewan	0.74	73.6
36	Hwy. 101-on to Hwy. 221	6.28	624.2
37	Cloverleaf-Hwy. 221	0.48	48.0
38	Hwy. 221-Grain Elevator	2.41	240.0
39	Hwy. 221-Sturgeon Rd.	0.97	96.0
40	Hwy. 221-Hwy. 7	0.97	96.0

TABLE 5.2.2 (CON'T)

POINT LOCATION, DISTANCE AND TIME INFORMATION

<u>POINT</u>	<u>LOCATION</u>	<u>D</u> (km)	<u>T</u> (sec)
41	Inkster-Drainage Ditch	2.41	240.0
42	Inkster-King Edward	0.71	169.7
43	Inkster-Keewatin	0.84	83.2
44	Keewatin-Church	0.55	54.4
45	Keewatin-Tyndall	0.58	57.6
46	Keewatin-Selkirk	0.48	48.0
47	Keewatin-Logan	1.03	102.4
48	Keewatin-Notre Dame	0.60	59.2
49	Notre Dame-Dublin	0.87	86.4
50	Notre Dame-Wall	0.68	67.2
51	Notre Dame-Sherburn	0.53	52.8
52	Notre Dame-Arlington	0.50	49.6
53	Notre Dame-Maryland	0.64	64.0
54	Cumberland-Sherbrook	0.16	16.0
55	Cumberland-Balmoral	0.48	48.0
56	Balmoral-Sargent	0.19	19.2
57	Balmoral-Ellice	0.35	35.2
58	Colony-Portage	0.29	28.8
59	Memorial-St.Mary	0.21	20.8
60	Memorial-York	0.16	16.0
61	York-Vaughan	0.10	9.6
62	Vaughan-St. Mary	0.16	16.0
63	Vaughan-Portage	0.26	25.6
64	Portage-Edmonton	0.10	9.6
65	Portage-Donald	0.29	28.8
66	Portage-Smith	0.10	9.6
67	Portage-Fort	0.19	19.2
68	Portage-Main	0.10	9.6
69	Portage-Westbrook	0.37	36.8
70	Westbrook-Water	0.15	14.4
71	Water-mid Bridge	0.63	62.4
72	Provencher-Alneau	1.03	102.4
73	Provencher-Des Meurons	0.60	59.2
74	Provencher-mid Bridge	0.23	22.4
75	Provencher-Archibald	0.39	38.4
76	Archibald-Plinquet	0.42	41.6
77	Plinquet-Dawson Rd.	0.32	32.1
78	Dawson Rd.-Dugald Rd.	1.16	115.3
79	Dawson Rd.-Maion	0.58	57.6
80	Dawson Rd.-Hwy. 59	0.97	96.0
81	Hwy. 59-Maginot	0.45	44.8

TABLE 5.2.2 (CON'T)

POINT LOCATION, DISTANCE AND TIME INFORMATION

<u>POINT</u>	<u>LOCATION</u>	<u>D</u> (km)	<u>T</u> (sec)
82	Hwy.59-Botournay	1.13	112.3
83	Hwy.59-Cottonwood	0.97	96.0
84	Hwy.59-Paterson	0.81	8.1
85	Paterson-Lochmore	0.39	38.9
86	Paterson-Westmount	0.16	16.0
87	Westmount-Hwy. 1	0.27	27.2
88	Hwy. 1-Lakewood	0.93	92.8
89	Hwy. 1-Archibald	0.68	67.2
90	Hwy. 1-mid Bridge	0.81	80.0
91	Hwy. 1-St. Anne's Rd.	0.90	89.6
92	Hwy. 1-St. Mary's Rd.	0.66	65.6
93	St. Mary's Rd.-Glenview	0.32	32.0
94	St. Mary's Rd.-Poplarwood	0.48	48.0
95	St. Mary's Rd.-Dunkirk	0.71	70.4
96	St. Mary's Rd.-Bay Avalon	0.97	96.0
97	St. Mary's Rd.-Woodlawn	0.64	64.0
98	St. Mary's Rd.-Riverside	0.97	96.0
99	St. Mary's Rd.-Hwy. Exit Sign	2.15	214.4
100	St. Mary's Rd.-Hwy. 101	0.81	80.0
101	Hwy. 101-mid Bridge	1.61	160.0
102	Hwy. 101-on Cloverleaf	1.61	160.0
103	Cloverleaf-Pembina	0.16	16.0
104	Pembina-Killarney	1.29	128.3
105	Pembina-Matherson	0.97	96.0
106	Pembina-Markham Rd.	1.29	128.3
107	Pembina-University Cres.	1.13	112.3
108	Pembina-Chevrier	1.45	144.2
109	Pembina-McGillivray Bd.	1.00	99.2
110	Pembina-Point Rd.	0.64	64.0
111	Pembina-Underpass	0.90	89.6
112	Pembina-Stafford	0.48	48.0
113	Pembina- Grant	1.0	99.2
114	Pembina-Corydon	1.22	121.3
115	Donald-Stradbroom	0.74	73.6
116	Donald-mid Bridge	0.50	49.6
117	Smith-York	1.03	102.4
118	Smith-St.Mary	0.19	19.2
119	Smith-Portage	0.37	36.8
120	Smith-Ellice	0.10	9.6
121	Smith-Notre Dame	0.06	6.4
122	Notre Dame-Edmonton	0.55	54.4

TABLE 5.2.2 (CON'T)

POINT LOCATION, DISTANCE AND TIME INFORMATION

<u>POINT</u>	<u>LOCATION</u>	$\frac{D}{(km)}$	$\frac{T}{(sec)}$
123	Notre Dame-Balmoral	0.21	20.8
124	Balmoral-Cumberland	0.10	9.6
125	Cumberland-Kennedy	0.06	6.4
126	Kennedy-Home Driveway	0.02	1.6
127	Home Driveway	0.03	3.2

LIST OF REFERENCES

- Bell, W.C., 1974:An Analysis of Temperature, Lapse Rate, and Wind in the Lower 810' Near Winnipeg. Ph.D. Thesis, University of Edinburgh, 171pp.
- City of Winnipeg. The Convention City, 1977. Winnipeg, Manitoba:Hignell Printing Ltd., 1977.
- Conrads, L.A. and van der Hage, J.C.H., 1971:A New Method of Air Temperature Measurement in Urban Climatological Studies. Atmos. Environ., 5, 629-635.
- Goldreich, J., 1970:Computation of the Magnitude of Johannesburg's Heat Island. Notos, 19, 95-106.
- Hoehme, W.E., 1972:Standardizing Functional Tests. In Proceedings of the Second Symposium on Meteorological Observation and Instrumentation of the Americal Meteorological Society in Co-operation with the American Institute of Aeronautics and Astronautics Inc. and the W.M.O., 27-30 March, San Diego, California, 161-165.
- Ludwig, F.L., 1968:Urban Temperature Fields. In Urban Climates, Technical Note No. 108, World Meteorological Organization, Geneva,
- Lyons, T.J. and Cutten, D.R., 1975:Atmospheric Pollutant and Temperature Traverses in an Urban Area. Atmos. Environ., 9.731-737.
- Annual Statistics-1977. Manitoba Health Service Commission, Department of Health and Welfare, Government of Manitoba.
- Penner, C.M., 1955:A Three-Front Model for Synoptic Analysis. Quart. Jour. Roy. Met. Soc., 81, 89-91.
- Smithsonian Meteorological Tables, 1968. (Sixth Revised Edition). Smithsonian Miscellaneous

Collections, 114, Smithsonian
Press, Washington, D.C.

Institute

CHAPTER SIX

Classification of Winnipeg's Dew Point Regimes

6.1 Introduction

Average hourly temperature and dew point temperature data per month from the 1953-1975 records for Winnipeg were subjected to the climatic parameter formulas mentioned in the previous chapter. Tables 6.1.1-6.1.12 list the hourly, daily annual, and monthly annual averages, while Figures 6.1.1-6.1.12 translate these values into graph form for rapid interpretation.

6.2 Classification

The months January-April and October-December have Type I (humid) dew point regimes. Dew point trends vary almost directly with those of temperature. Lowest average values of both parameters, temperature and dew point, occur in the morning prior to sunrise (0700-0900hrs.) while the highest occur in the afternoon during the hours 1500-1700. Trend parallelism is greatest in winter, least during March, April, and November. March registers the greatest monthly average dew point maximum - minimum change during the year with 5.4°C.; the time when Eastern Arctic air masses are pinching out Pacific air masses as true mT air flows northward. All the above air masses are being modified moisture wise through snow melt. November, the month with the longest dry spell duration and a relatively large

irregular precipitation pattern, has the least maximum-minimum dew point change at 1.9°C .. Dry Pacific air masses dominate the research area during this period. Rate of increase in dew point temperature from minimum to maximum is at its lowest in April with $0.21^{\circ}\text{C}/\text{hr}$.. April's decreasing rate (maximum to minimum) is second only to November's $0.12^{\circ}\text{C}/\text{hr}$., registering 0.17°C .. Both April and November have dew point trends showing transition from Type I to Type II (modified humid).

The remaining months of the year, May-September, have Type II dew point regimes. The primary minimum occurs in the morning at the time of the minimum temperature while a secondary minimum occurs during the day between 1100-2100hrs. July has the highest average dew point of the year, 14.1°C ., while the minimum for Type II, 1.9°C ., occurs in May. The former also registers the greatest annual hourly and monthly mixing ratios. Modified Pacific air masses, CR and Nr with mT, as well as mT air, make up 78% of July's air masses. July also has its primary maxima dew point occurring in the evening. The latter characteristic can only be found in the more humid eastern areas of Canada and the United States, where mT air masses in pure form dominate (Dodd, 1964).

Dew point variation in the Type II regime, unlike Type I, is quite minute with a minimum of 1.25°C . being recorded

in May; a maximum of 1.92°C. in July. August followed by September have the largest dew point dip between dew point maxima; 0.88°C. and 0.86°C respectively.

Figure 6.1.13 shows that Winnipeg's annual dew point regime is of Type I. This indicates that the incoming radiant energy during the day is not sufficient to cause a day time decrease in dew point due to turbulent mass exchange especially during low sun months.

6.3 Dew Point Regimes During the Study Period

The more than twice the normal rainfall of June, 1976, was sufficient to alter the normal dew point regime from Type II to Type I (oceanic). A ready availability of water at the surface for evaporation into the air during the day continued till September giving Winnipeg insular or coastal dew point regimes. The intensification of the drought during September and further plus the lack of intense insolation, allowed Type I (humid) regimes to be established after August.

It may be noted that during the drought period, the average monthly and hourly dew points averages did not register a Type III (dry) regime. The lowest dew point on record occurred in October and was of Type I (humid).

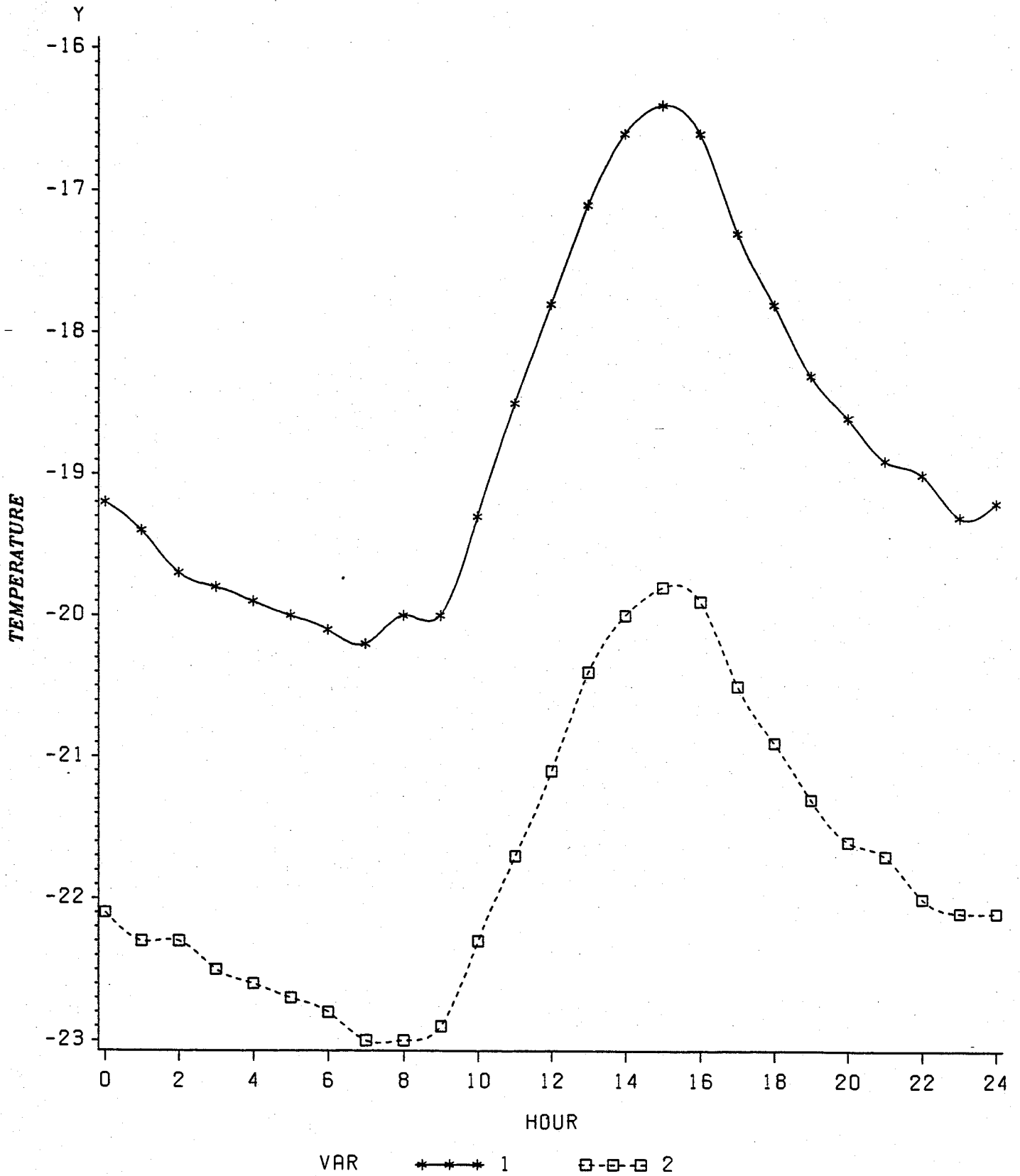
TABLE 6.1.1

HOURLY AND MONTHLY PARAMETER MEANS FOR JANUARY

<u>HOURLY</u> (CST)	<u>T</u> (°C)	<u>SD</u> (°C)	<u>TD</u> (°C)	<u>SD</u> (°C)	<u>SATD</u> (mb)	<u>U</u> (%)	<u>R</u> (g/kg)	<u>DV</u> (g/m ³)
0000	- 19.2	5.8	- 22.1	6.0	0.265	76.1	0.532	0.722
0100	- 19.4	5.8	- 22.3	6.0	0.262	76.0	0.522	0.709
0200	- 19.7	5.7	- 22.3	6.1	0.236	77.8	0.520	0.707
0300	- 19.8	5.8	- 22.5	6.1	0.244	76.9	0.512	0.696
0400	- 19.9	5.7	- 22.6	6.1	0.240	77.0	0.506	0.688
0500	- 20.0	5.7	- 22.7	6.0	0.239	76.9	0.500	0.681
0600	- 20.1	5.9	- 22.8	6.0	0.235	77.0	0.494	0.674
0700	- 20.2	5.9	- 23.0	6.1	0.240	76.3	0.488	0.665
0800	- 20.2	6.0	- 23.0	6.1	0.239	76.3	0.485	0.661
0900	- 20.0	6.0	- 22.9	6.2	0.251	75.6	0.490	0.668
1000	- 19.3	6.0	- 22.3	6.2	0.280	74.7	0.520	0.706
1100	- 18.5	6.0	- 21.7	6.2	0.312	73.8	0.553	0.749
1200	- 17.8	6.0	- 21.1	6.2	0.342	73.0	0.582	0.786
1300	- 17.1	6.1	- 20.4	6.2	0.373	72.7	0.624	0.840
1400	- 16.6	6.1	- 20.0	6.2	0.396	72.2	0.647	0.869
1500	- 16.4	6.0	- 19.8	6.3	0.403	72.3	0.661	0.888
1600	- 16.6	6.0	- 19.9	6.2	0.389	72.8	0.653	0.878
1700	- 17.3	6.0	- 20.5	6.3	0.350	73.8	0.621	0.836
1800	- 17.8	6.0	- 20.9	6.4	0.327	74.3	0.596	0.804
1900	- 18.3	5.8	- 21.3	6.2	0.305	74.9	0.573	0.776
2000	- 18.6	5.8	- 21.6	6.2	0.293	75.2	0.558	0.756
2100	- 18.9	5.8	- 21.7	6.0	0.277	76.0	0.550	0.746
2200	- 19.0	5.9	- 22.0	6.1	0.279	75.3	0.537	0.728
2300	- 19.3	5.9	- 22.1	6.1	0.268	75.8	0.528	0.718
AVER	- 18.7	5.9	- 21.8	6.2	0.295	74.7	0.547	0.741

FIGURE 6.1.1

HOURLY TEMPERATURE AND DEW POINT
MEANS FOR JANUARY



VAR1=TEMPERATURE
VAR2=DEW POINT

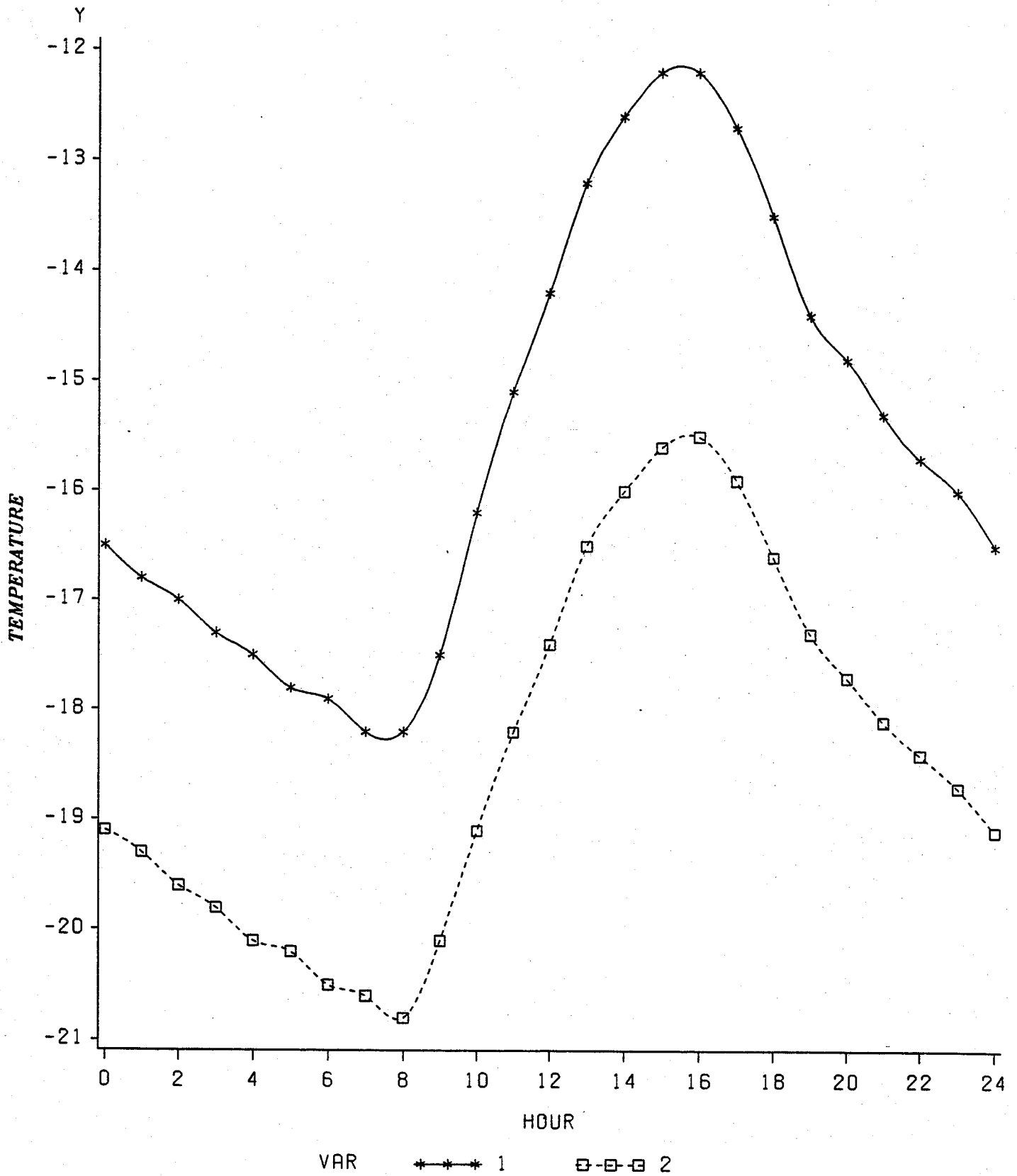
TABLE 6.1.2

HOURLY AND MONTHLY PARAMETER MEANS FOR FEBRUARY

<u>HOURLY</u> (CST)	<u>T</u> (°C)	<u>SD</u> (°C)	<u>TD</u> (°C)	<u>SD</u> (°C)	<u>SATD</u> (mb)	<u>U</u> (%)	<u>R</u> (g/kg)	<u>DV</u> (g/m ³)
0000	- 16.5	5.9	- 19.1	6.4	0.310	78.3	0.706	0.948
0100	- 16.8	5.9	- 19.3	6.5	0.303	78.4	0.693	0.932
0200	- 17.0	5.8	- 19.6	6.4	0.295	78.5	0.677	0.911
0300	- 17.3	5.8	- 19.8	6.4	0.283	78.8	0.661	0.891
0400	- 17.5	5.7	- 20.1	6.3	0.278	78.7	0.646	0.871
0500	- 17.8	5.7	- 20.2	6.3	0.269	79.0	0.635	0.857
0600	- 17.9	5.7	- 20.5	6.3	0.270	78.5	0.621	0.838
0700	- 18.2	5.7	- 20.6	6.3	0.259	78.9	0.611	0.826
0800	- 18.2	5.7	- 20.8	6.3	0.269	78.1	0.603	0.815
0900	- 17.5	5.7	- 20.1	6.3	0.296	77.5	0.641	0.865
1000	- 16.2	5.6	- 19.1	6.2	0.344	76.7	0.711	0.954
1100	- 15.1	5.6	- 18.2	6.1	0.404	75.3	0.774	1.034
1200	- 14.2	5.6	- 17.4	6.1	0.455	74.4	0.833	1.109
1300	- 13.2	5.6	- 16.5	6.0	0.510	73.8	0.908	1.203
1400	- 12.6	5.5	- 16.0	5.9	0.565	72.7	0.945	1.249
1500	- 12.2	5.6	- 15.6	5.9	0.570	73.3	0.988	1.304
1600	- 12.2	5.5	- 15.5	5.9	0.568	73.5	0.991	1.308
1700	- 12.7	5.6	- 15.9	6.0	0.525	74.3	0.954	1.262
1800	- 13.5	5.7	- 16.6	6.1	0.472	75.1	0.897	1.191
1900	- 14.4	5.7	- 17.3	6.2	0.408	76.6	0.841	1.120
2000	- 14.8	5.7	- 17.7	6.2	0.389	76.8	0.811	1.082
2100	- 15.3	5.8	- 18.1	6.3	0.370	77.0	0.781	1.043
2200	- 15.7	5.8	- 18.4	6.5	0.341	77.9	0.757	1.013
2300	- 16.0	5.8	- 18.7	6.3	0.340	77.5	0.738	0.989
AVER	- 15.5	5.7	- 18.4	6.2	0.367	76.6	0.759	1.015

FIGURE 6.1.2

HOURLY TEMPERATURE AND DEW POINT
MEANS FOR FEBRUARY



VAR1=TEMPERATURE
VAR2=DEW POINT

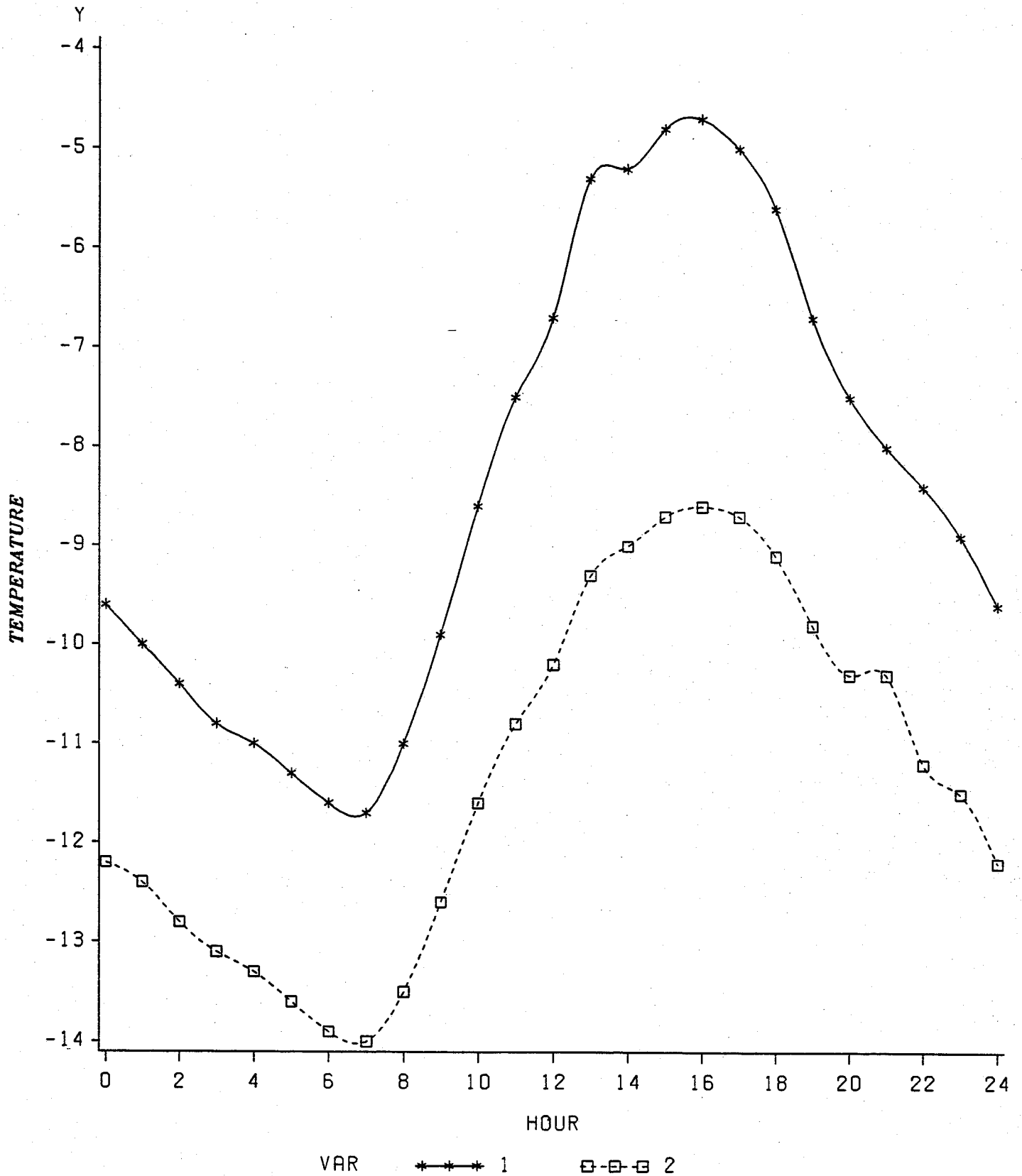
TABLE 6.1.3

HOURLY AND MONTHLY PARAMETER MEANS FOR MARCH

<u>HOUR</u> (CST)	<u>T</u> (°C)	<u>SD</u> (°C)	<u>TD</u> (°C)	<u>SD</u> (°C)	<u>SATD</u> (mb)	<u>U</u> (%)	<u>R</u> (g/kg)	<u>DV</u> (g/m ³)
0000	- 9.6	6.8	- 12.2	5.8	0.562	79.2	1.349	1.760
0100	- 10.0	6.9	- 12.4	5.9	0.510	80.4	1.317	1.721
0200	- 10.4	7.0	- 12.8	6.0	0.488	80.6	1.279	1.674
0300	- 10.8	7.0	- 13.1	6.2	0.464	80.9	1.240	1.626
0400	- 11.0	7.0	- 13.3	6.3	0.446	81.2	1.214	1.594
0500	- 11.3	7.0	- 13.6	6.4	0.428	81.4	1.184	1.555
0600	- 11.6	7.1	- 13.9	6.4	0.427	81.1	1.156	1.520
0700	- 11.7	7.2	- 14.0	6.5	0.428	80.9	1.141	1.501
0800	- 11.0	7.1	- 13.5	6.3	0.478	79.9	1.195	1.568
0900	- 9.9	6.9	- 12.6	6.2	0.574	78.2	1.294	1.691
1000	- 8.6	7.0	- 11.6	5.9	0.688	76.5	1.415	1.840
1100	- 7.5	7.7	- 10.8	5.6	0.804	75.1	1.529	1.979
1200	- 6.7	6.7	- 10.2	5.2	0.925	73.4	1.615	2.083
1300	- 5.3	6.6	- 9.3	5.0	1.173	70.1	1.738	2.230
1400	- 5.2	6.0	- 9.0	4.8	1.100	72.1	1.799	2.308
1500	- 4.8	6.6	- 8.7	4.7	1.166	71.4	1.838	2.354
1600	- 4.7	6.6	- 8.6	4.6	1.161	71.7	1.859	2.380
1700	- 5.0	6.6	- 8.7	4.7	1.102	72.6	1.846	2.365
1800	- 5.6	6.7	- 9.1	5.0	1.014	73.5	1.776	2.280
1900	- 6.7	6.7	- 9.8	5.2	0.830	76.1	1.667	2.151
2000	- 7.5	6.7	- 10.3	5.4	0.723	77.7	1.593	2.062
2100	- 8.0	6.7	- 10.8	5.4	0.670	78.4	1.532	1.986
2200	- 8.4	6.7	- 11.2	5.5	0.641	78.5	1.478	1.920
2300	- 8.9	6.8	- 11.5	5.7	0.597	79.1	1.428	1.859
AVER	- 8.3	6.8	- 11.3	5.6	0.695	76.9	1.461	1.897

FIGURE 6.1.3

HOURLY TEMPERATURE AND DEW POINT
MEANS FOR MARCH



VAR1=TEMPERATURE
VAR2=DEW POINT

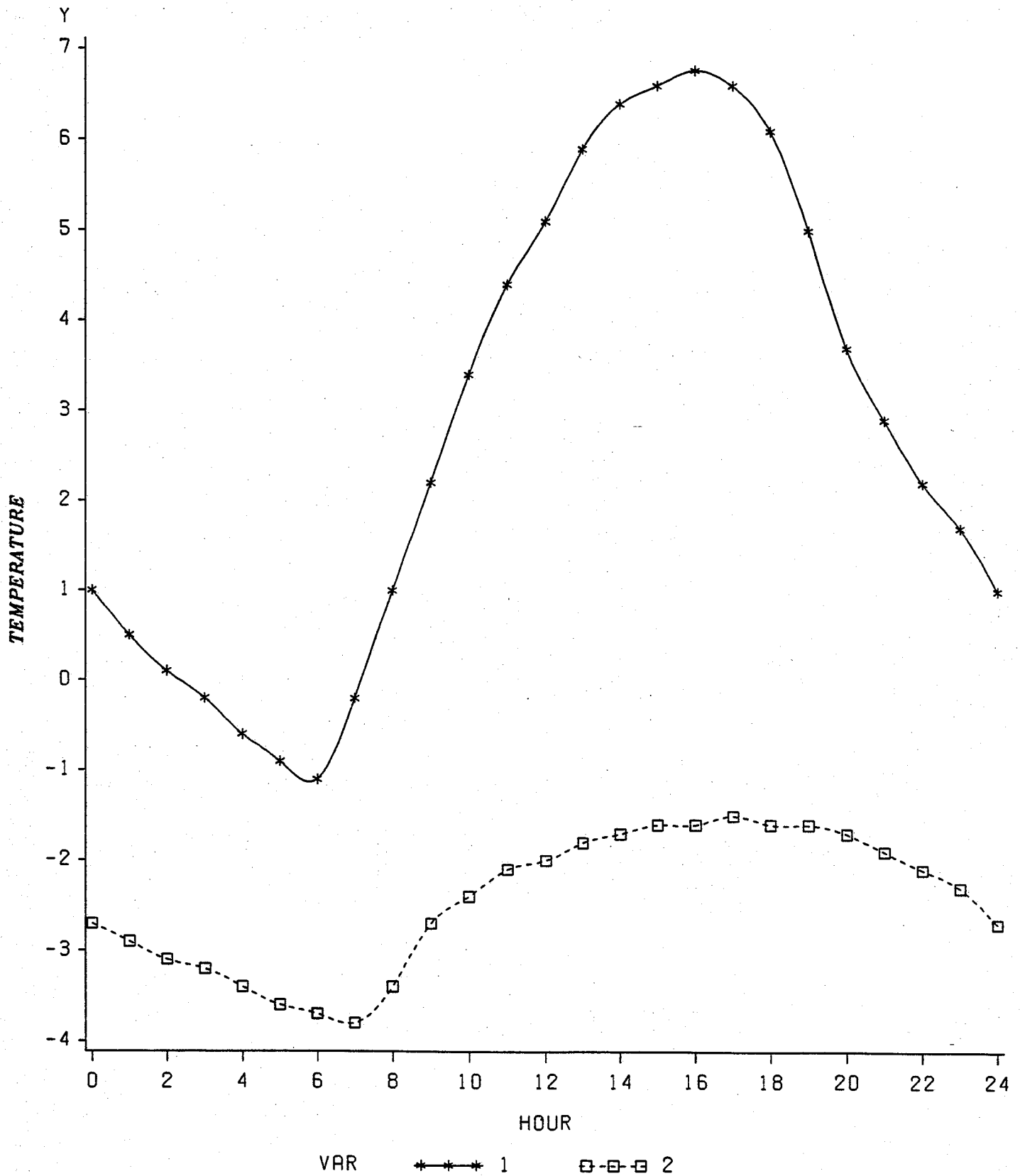
TABLE 6.1.4

HOURLY AND MONTHLY PARAMETER MEANS FOR APRIL

<u>HOURLY</u> (CST)	<u>T</u> (°C)	<u>SD</u> (°C)	<u>TD</u> (°C)	<u>SD</u> (°C)	<u>SATD</u> (mb)	<u>U</u> (%)	<u>R</u> (g/kg)	<u>DV</u> (g/m ³)
0000	1.0	3.5	- 2.7	2.9	1.650	74.8	3.101	4.836
0100	0.5	3.5	- 2.9	3.0	1.523	76.0	3.051	4.767
0200	0.1	3.4	- 3.1	3.1	1.410	77.1	3.000	4.694
0300	- 0.2	3.4	- 3.2	3.2	1.332	77.8	2.957	3.710
0400	- 0.6	3.3	- 3.4	3.2	1.219	79.0	2.905	3.650
0500	- 0.9	3.3	- 3.6	3.3	1.172	79.4	2.856	3.592
0600	- 1.1	3.2	- 3.7	3.2	1.112	80.2	2.844	3.579
0700	- 0.2	3.3	- 3.8	3.2	1.540	74.3	2.825	3.544
0800	1.0	3.6	- 3.4	3.1	1.984	69.9	2.912	4.542
0900	2.2	4.0	- 2.7	3.0	2.282	68.1	3.093	4.801
1000	3.4	4.3	- 2.4	3.0	2.784	64.5	3.185	4.923
1100	4.4	4.5	- 2.1	3.0	3.264	61.0	3.242	4.992
1200	5.1	4.6	- 2.0	3.1	3.614	58.8	3.275	5.030
1300	5.9	4.7	- 1.8	3.0	3.985	57.0	3.350	5.131
1400	6.4	4.8	- 1.7	3.0	4.280	55.3	3.361	5.139
1500	6.6	4.9	- 1.6	3.2	4.424	54.7	3.384	5.168
1600	6.7	4.9	- 1.6	3.2	4.424	54.5	3.396	5.180
1700	6.6	4.9	- 1.5	3.1	4.337	55.4	3.418	5.221
1800	6.1	4.8	- 1.6	3.2	4.085	56.7	3.390	5.186
1900	5.0	4.5	- 1.6	3.2	3.329	61.7	3.398	5.221
2000	3.7	4.2	- 1.7	3.2	2.675	66.5	3.361	5.188
2100	2.9	4.2	- 1.9	3.2	2.302	69.5	3.319	5.138
2200	2.2	3.8	- 2.1	3.1	2.026	71.7	3.256	5.053
2300	1.7	3.7	- 2.3	3.1	1.830	73.4	3.202	4.980
AVER	2.9	4.1	- 2.4	3.1	2.509	66.6	3.164	4.900

FIGURE 6.1.4

HOURLY TEMPERATURE AND DEW POINT
MEANS FOR APRIL



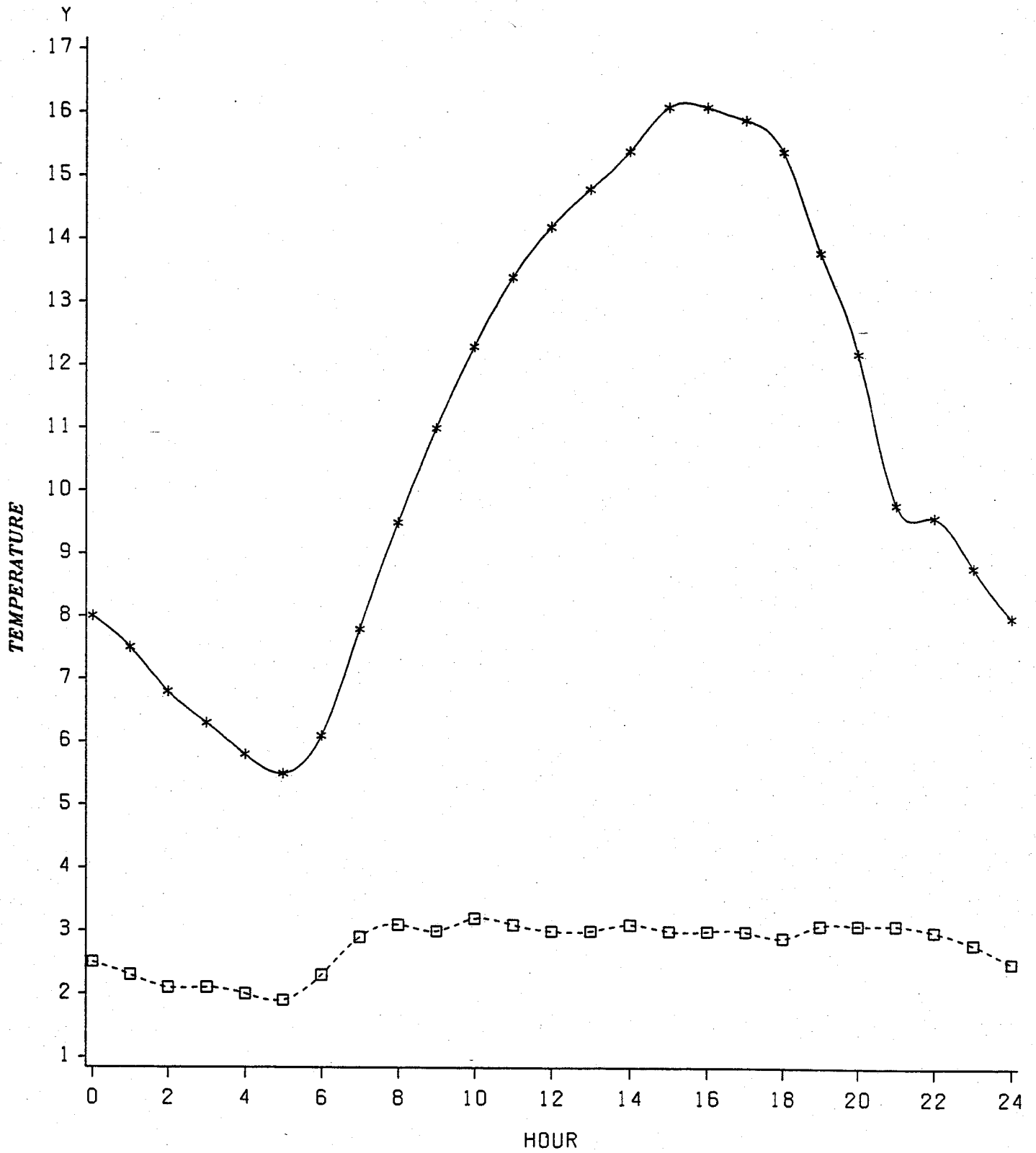
VAR1=TEMPERATURE
VAR2=DEW POINT

TABLE 6.1.5

HOURLY AND MONTHLY PARAMETER MEANS FOR MAY

<u>HOURLY</u> (CST)	<u>T</u> (°C)	<u>SD</u> (°C)	<u>TD</u> (°C)	<u>SD</u> (°C)	<u>SATD</u> (mb)	<u>U</u> (%)	<u>R</u> (g/kg)	<u>DV</u> (g/m ³)
0000	8.0	2.7	2.5	3.2	3.453	67.9	4.637	5.625
0100	7.5	2.7	2.3	3.2	3.156	69.5	4.574	5.560
0200	6.8	2.8	2.1	3.2	2.742	72.2	4.528	5.519
0300	6.3	2.6	2.1	3.3	2.434	74.6	4.512	5.509
0400	5.8	2.6	2.0	3.2	2.197	76.2	4.476	5.475
0500	5.5	2.7	1.9	3.1	1.997	77.9	4.466	5.470
0600	6.1	2.6	2.3	3.0	2.194	76.6	4.577	5.592
0700	7.8	2.6	2.9	3.0	3.089	70.9	4.782	5.804
0800	9.5	3.2	3.1	3.1	4.198	64.6	4.864	5.869
0900	11.0	3.2	3.0	3.2	5.550	57.8	4.826	5.792
1000	12.3	3.5	3.2	3.2	6.628	53.7	4.885	5.836
1100	13.4	3.7	3.1	3.3	7.684	49.9	4.861	5.785
1200	14.2	3.8	3.0	3.4	8.588	46.8	4.806	5.704
1300	14.8	3.9	3.0	3.2	9.319	44.8	4.802	5.687
1400	15.4	3.9	3.1	3.3	9.829	43.6	4.843	5.725
1500	16.1	3.9	3.0	3.3	10.645	41.6	4.833	5.700
1600	16.1	3.8	3.0	3.2	10.717	41.4	4.809	5.670
1700	15.9	3.7	3.0	3.1	10.444	42.0	4.806	5.671
1800	15.4	3.7	2.9	3.0	9.998	42.9	4.771	5.639
1900	13.8	3.5	3.1	2.9	8.131	48.3	4.840	5.753
2000	12.2	3.4	3.1	3.0	6.576	53.8	4.864	5.813
2100	9.8	3.1	3.1	3.2	4.455	63.2	4.864	5.863
2200	9.6	3.0	3.0	3.0	4.412	63.1	4.809	5.800
2300	8.8	3.1	2.8	3.0	3.817	66.2	4.758	5.756
AVER	10.9	3.2	2.8	3.1	5.588	57.2	4.741	5.692

FIGURE 6.1.5
HOURLY TEMPERATURE AND DEW POINT
MEANS FOR MAY



VAR *-*-* 1 □-□-□ 2

VAR1=TEMPERATURE
VAR2=DEW POINT

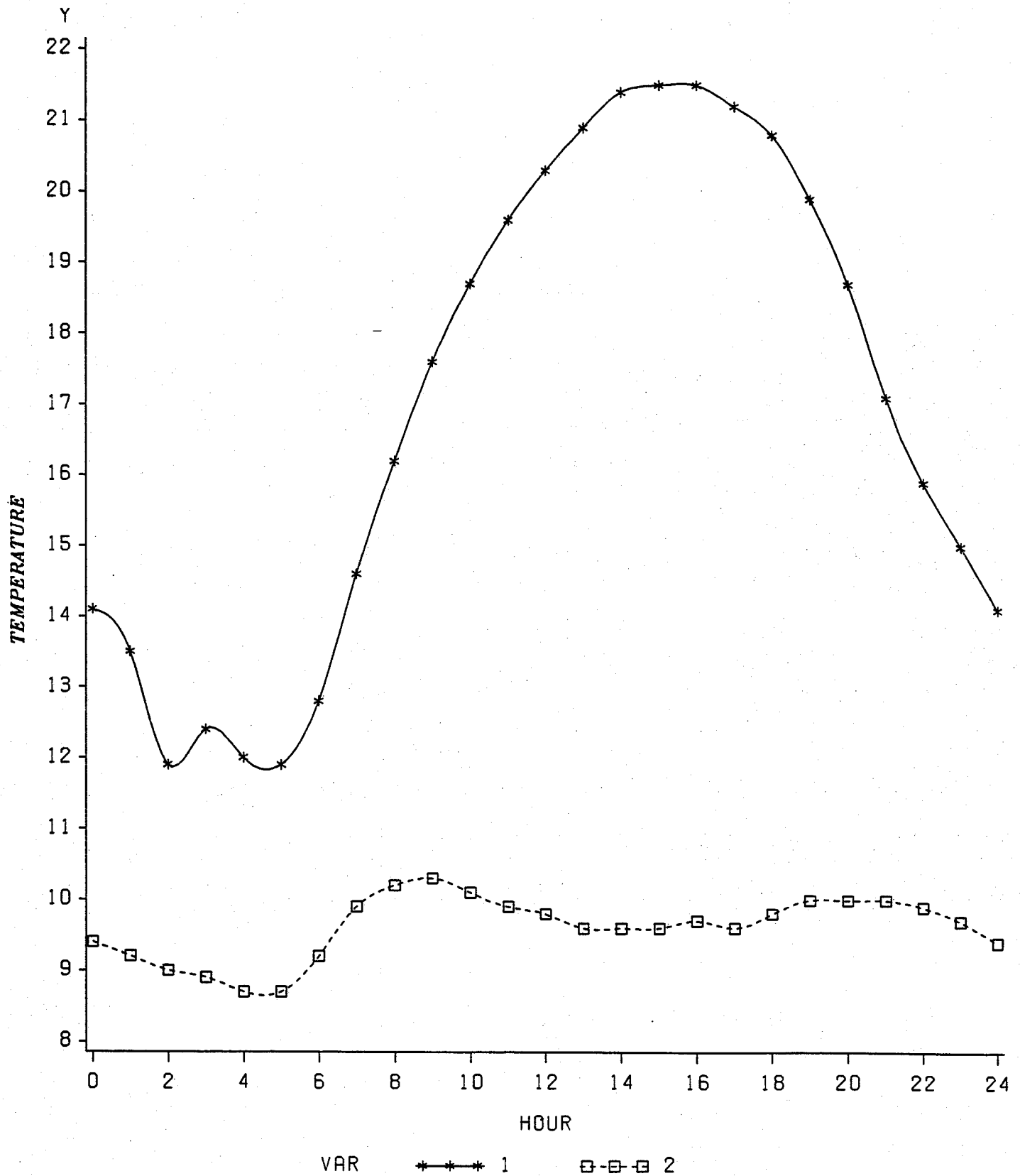
TABLE 6.1.6

HOURLY AND MONTHLY PARAMETER MEANS FOR JUNE

<u>HOURLY</u> (CST)	<u>T</u> (°C)	<u>SD</u> (°C)	<u>TD</u> (°C)	<u>SD</u> (°C)	<u>SATD</u> (mb)	<u>U</u> (%)	<u>R</u> (g/kg)	<u>DV</u> (g/m ³)
0000	14.1	3.3	9.4	3.7	4.374	72.9	7.524	8.872
0100	13.5	3.1	9.2	3.8	3.764	75.6	7.468	8.828
0200	11.9	3.1	9.0	3.7	2.432	82.5	7.346	8.734
0300	12.4	3.1	8.9	3.6	2.962	79.3	7.286	8.649
0400	12.0	3.2	8.7	3.6	2.723	80.5	7.212	8.573
0500	11.9	3.2	8.7	3.6	2.622	81.1	7.212	8.577
0600	12.8	3.1	9.2	3.5	3.083	79.1	7.468	8.849
0700	14.6	3.7	9.9	3.4	4.440	73.3	7.811	9.191
0800	16.2	3.0	10.2	3.6	5.953	67.6	7.966	9.321
0900	17.6	3.3	10.3	3.6	7.590	62.2	8.004	9.320
1000	18.7	3.3	10.1	3.8	9.246	57.2	7.923	9.190
1100	19.6	3.5	9.9	3.9	10.690	53.2	7.795	9.015
1200	20.3	3.6	9.8	4.0	11.763	50.7	7.737	8.928
1300	20.9	3.8	9.6	4.1	12.774	48.4	7.664	8.827
1400	21.4	3.8	9.6	4.2	13.435	47.1	7.674	8.825
1500	21.5	3.8	9.6	4.3	13.678	46.7	7.669	8.815
1600	21.5	3.8	9.7	4.3	13.560	46.9	7.685	8.834
1700	21.2	3.8	9.6	4.3	13.211	47.5	7.669	8.824
1800	20.8	3.7	9.8	4.1	12.532	49.1	7.732	8.907
1900	19.9	3.4	10.0	4.1	11.038	52.6	7.848	9.067
2000	18.7	3.3	10.0	3.9	9.210	57.2	7.885	9.149
2100	17.1	3.3	10.0	3.9	7.271	62.8	7.853	9.161
2200	15.9	3.3	9.9	3.7	5.864	67.5	7.790	9.127
2300	15.0	3.3	9.7	3.7	5.042	70.4	7.695	9.044
AVER	17.1	3.4	9.6	3.8	7.485	61.5	7.658	8.938

FIGURE 6.1.6

HOURLY TEMPERATURE AND DEW POINT
MEANS FOR JUNE



VAR1=TEMPERATURE
VAR2=DEW POINT

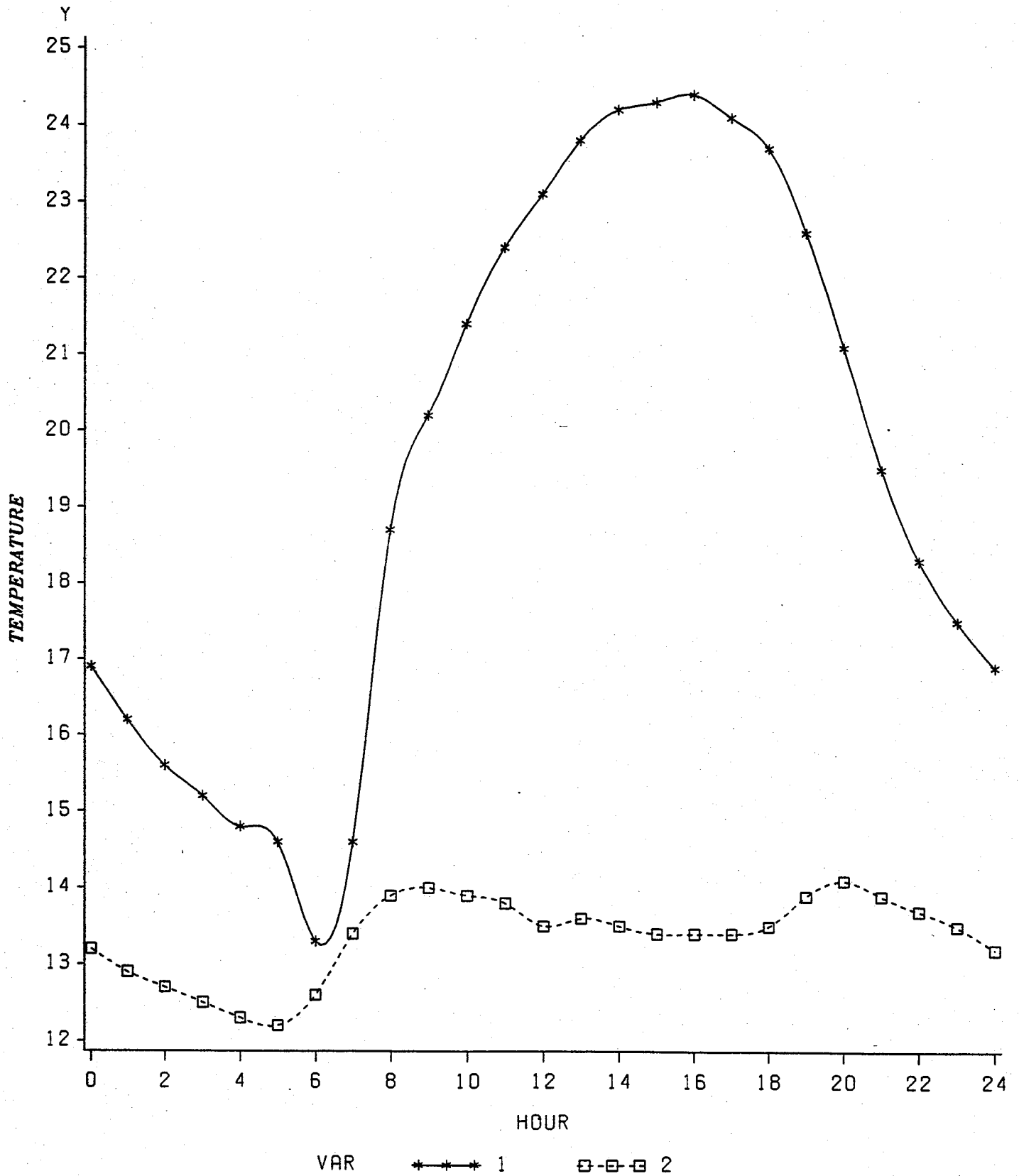
TABLE 6.1.7

HOURLY AND MONTHLY PARAMETER MEANS FOR JULY

<u>HOURLY</u> (CST)	<u>T</u> (°C)	<u>SD</u> (°C)	<u>TD</u> (°C)	<u>SD</u> (°C)	<u>SATD</u> (mb)	<u>U</u> (%)	<u>R</u> (g/kg)	<u>DV</u> (g/m ³)
0000	16.9	3.0	13.2	2.6	4.047	78.9	9.708	11.324
0100	16.2	2.9	12.9	2.7	3.467	81.1	9.542	11.160
0200	15.6	2.8	12.7	2.6	3.129	82.4	9.378	10.991
0300	15.2	2.8	12.5	2.6	2.816	83.7	9.260	10.871
0400	14.8	2.7	12.3	2.7	2.555	84.8	9.137	10.745
0500	14.6	2.6	12.2	2.6	2.444	85.3	9.077	10.681
0600	13.3	3.5	12.6	2.4	0.761	95.0	9.316	11.007
0700	14.9	2.6	13.4	2.4	1.537	90.9	9.864	11.582
0800	18.7	2.7	13.9	2.3	5.673	73.6	10.169	11.779
0900	20.2	2.8	14.0	2.4	7.689	67.6	10.283	11.846
1000	21.4	2.9	13.9	2.6	9.521	62.5	10.202	11.709
1100	22.4	2.9	13.8	2.8	11.337	58.2	10.115	11.569
1200	23.1	3.0	13.5	3.0	12.698	55.0	9.949	11.357
1300	23.8	3.0	13.6	3.0	13.884	52.8	9.969	11.352
1400	24.2	3.0	13.5	3.0	14.733	51.2	9.929	11.292
1500	24.3	3.1	13.4	3.0	14.995	50.7	9.877	11.229
1600	24.4	3.0	13.4	3.1	14.858	50.9	9.861	11.214
1700	24.1	3.1	13.4	3.0	14.719	51.0	9.844	11.199
1800	23.7	3.0	13.5	3.0	13.826	52.8	9.903	11.282
1900	22.6	3.1	13.9	2.9	11.559	57.8	10.175	11.630
2000	21.1	3.1	14.1	2.8	8.938	64.2	10.310	11.842
2100	19.5	3.1	13.9	2.7	6.761	70.1	10.195	11.776
2200	18.3	3.2	13.7	2.7	5.403	74.3	10.048	11.655
2300	17.5	3.1	13.5	2.7	4.539	77.3	9.897	11.516
AVER	19.6	3.0	13.4	2.7	7.489	67.2	9.831	11.358

FIGURE 6.1.7

HOURLY TEMPERATURE AND DEW POINT
MEANS FOR JULY



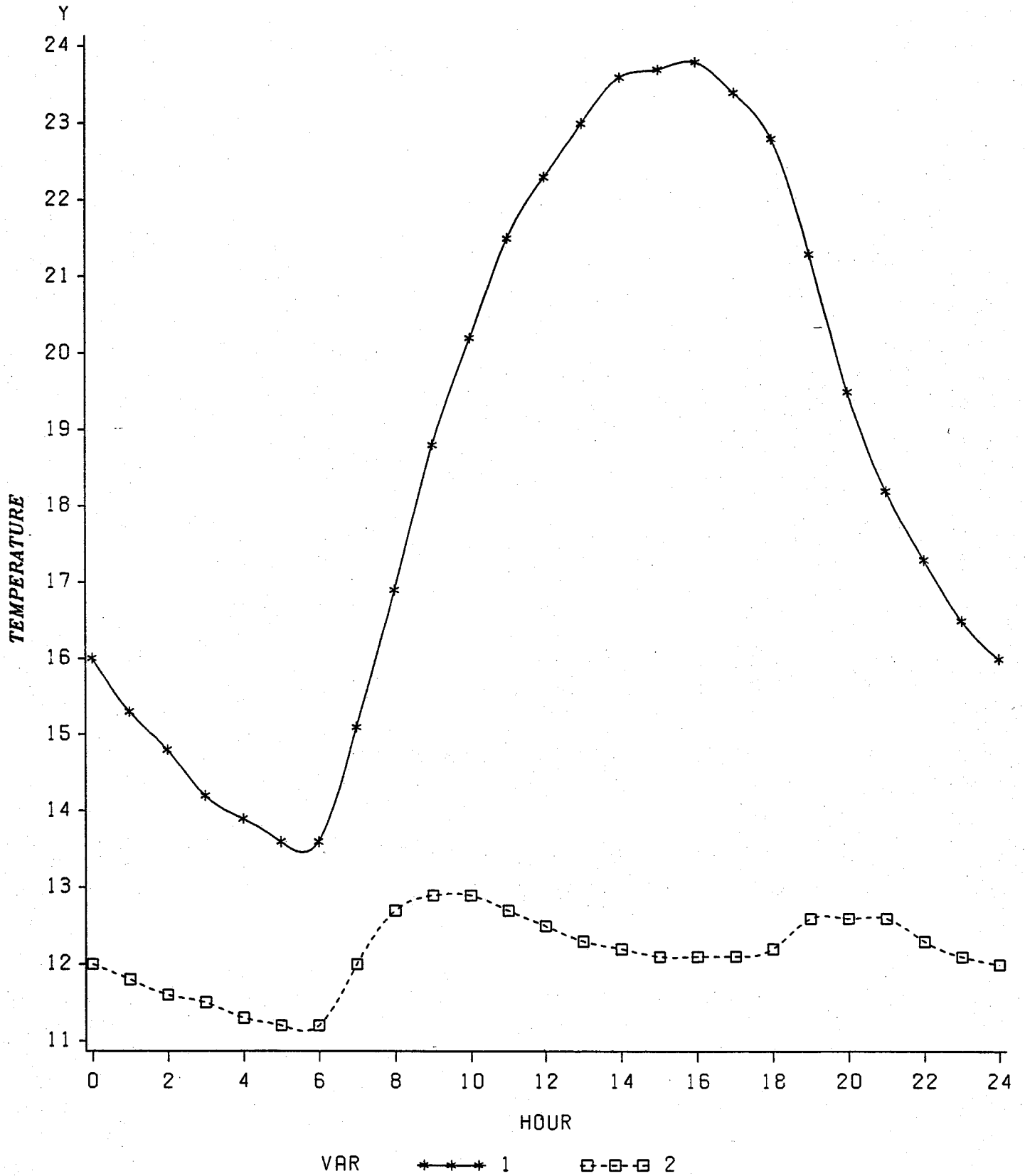
VAR1=TEMPERATURE
VAR2=DEW POINT

TABLE 6.1.8

MEAN HOURLY AND MONTHLY AVERAGES FOR AUGUST

<u>HOUR</u> (CST)	<u>T</u> (°C)	<u>SD</u> (°C)	<u>TD</u> (°C)	<u>SD</u> (°C)	<u>SATD</u> (mb)	<u>U</u> (%)	<u>R</u> (g/kg)	<u>DV</u> (g/m ³)
0000	16.0	2.5	12.0	2.1	4.155	77.1	8.949	10.485
0100	15.3	2.4	11.8	2.2	3.555	79.6	8.866	10.411
0200	14.8	2.4	11.6	2.2	3.130	81.4	8.742	10.288
0300	14.1	2.2	11.5	2.2	2.567	84.1	8.666	10.223
0400	13.9	2.2	11.3	2.2	2.557	83.9	8.544	10.088
0500	13.6	2.2	11.2	2.2	2.265	85.4	8.481	10.028
0600	13.6	2.2	11.2	2.2	2.215	85.7	8.527	10.080
0700	15.1	2.3	12.0	2.2	3.094	81.9	8.985	10.559
0800	16.9	2.4	12.7	2.1	4.654	75.9	9.384	10.949
0900	18.8	2.5	12.9	2.0	6.713	69.0	9.560	11.083
1000	20.2	2.9	12.9	2.0	8.846	62.7	9.528	10.991
1100	21.5	3.1	12.7	2.1	10.897	57.4	9.396	10.796
1200	22.3	3.2	12.5	2.3	12.428	53.9	9.296	10.653
1300	23.0	3.4	12.3	2.3	13.837	50.9	9.173	10.487
1400	23.6	3.6	12.2	2.4	14.802	49.0	9.118	10.407
1500	23.7	3.6	12.1	2.4	15.143	48.3	9.045	10.320
1600	23.8	3.5	12.1	2.4	15.313	47.9	9.015	10.284
1700	23.4	3.4	12.1	2.5	14.644	49.1	9.051	10.337
1800	22.8	3.3	12.2	2.6	13.464	51.4	9.118	10.434
1900	21.3	3.0	12.6	2.4	10.715	57.7	9.352	10.752
2000	19.5	3.0	12.6	2.3	8.071	64.4	9.359	10.824
2100	18.2	2.8	12.6	2.3	6.330	69.7	9.315	10.824
2200	17.3	2.6	12.3	2.2	5.360	72.8	9.173	10.696
2300	16.5	2.6	12.1	2.3	4.640	75.3	9.039	10.570
AVER	18.7	2.8	12.1	2.3	7.408	65.6	9.064	10.517

FIGURE 6.1.8
HOURLY TEMPERATURE AND DEW POINT
MEANS FOR AUGUST



VAR1=TEMPERATURE
VAR2=DEW POINT

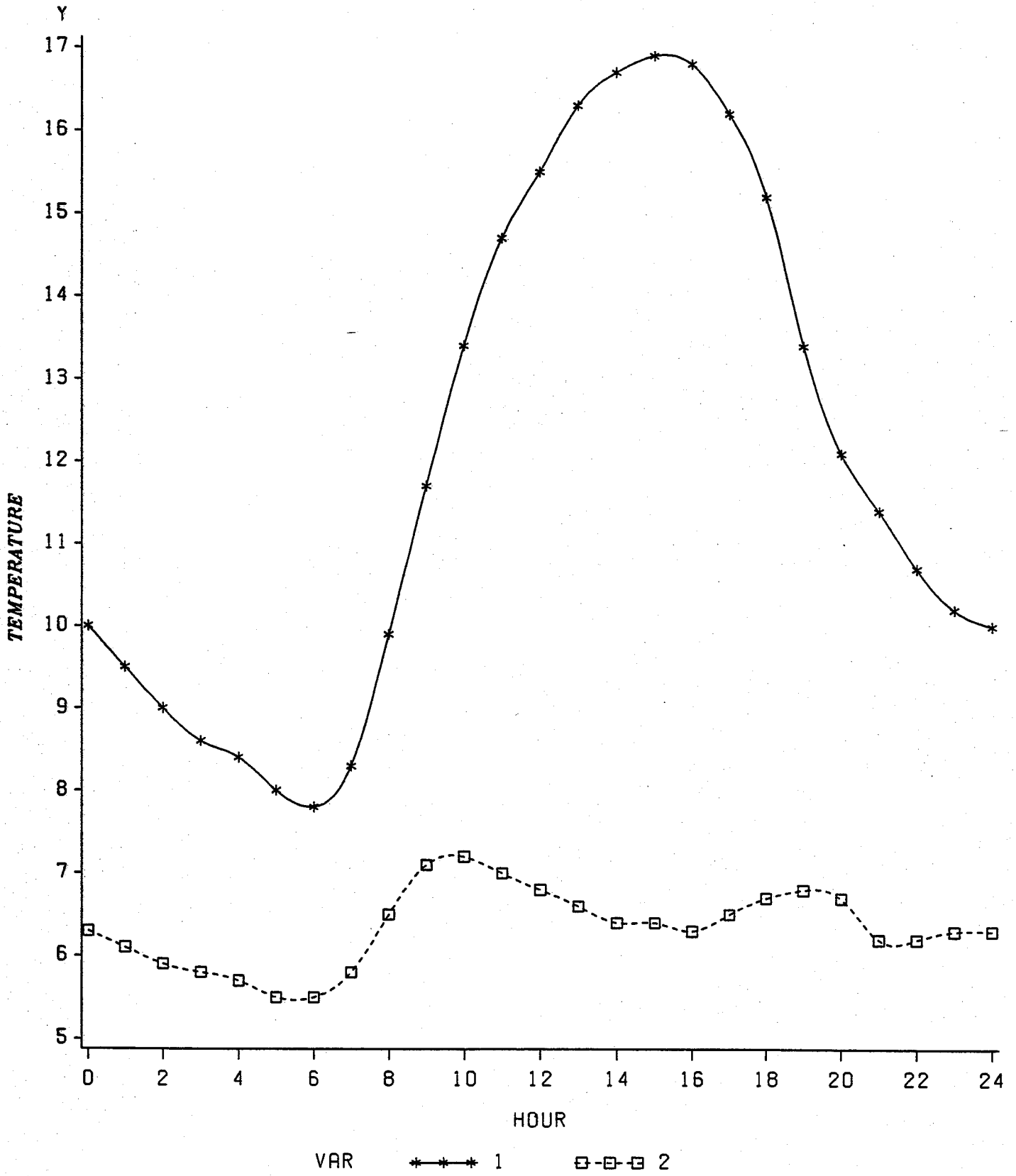
TABLE 6.1.9

MEAN HOURLY AND MONTHLY AVERAGES FOR SEPTEMBER

<u>HOUR</u> (CST)	<u>T</u> (°C)	<u>SD</u> (°C)	<u>TD</u> (°C)	<u>SD</u> (°C)	<u>SATD</u> (mb)	<u>U</u> (%)	<u>R</u> (g/kg)	<u>DV</u> (g/m ³)
0000	10.0	2.7	6.3	2.6	2.704	78.0	6.099	7.332
0100	9.5	2.7	6.1	2.5	2.443	79.4	6.006	7.234
0200	9.0	2.6	5.9	2.5	2.193	80.9	5.919	7.142
0300	8.6	2.6	5.8	2.6	2.012	82.0	5.853	7.073
0400	8.4	2.7	5.7	2.5	1.853	83.1	5.824	7.045
0500	8.0	2.7	5.5	2.5	1.704	84.2	5.763	6.980
0600	7.8	2.6	5.5	2.6	1.550	85.4	5.759	6.981
0700	8.3	2.5	5.8	2.5	1.721	84.2	5.861	7.092
0800	9.9	2.6	6.5	2.6	2.482	79.6	6.167	7.417
0900	11.7	2.6	7.1	2.7	3.669	73.3	6.412	7.659
1000	13.4	2.9	7.2	2.8	5.187	66.2	6.465	7.677
1100	14.7	3.2	7.0	2.9	6.676	60.1	6.403	7.568
1200	15.5	3.4	6.8	3.1	7.752	56.0	6.293	7.418
1300	16.3	3.5	6.6	3.0	8.813	52.5	6.197	7.287
1400	16.7	3.6	6.4	3.1	9.414	50.6	6.141	7.211
1500	16.9	3.6	6.4	3.0	9.619	49.9	6.112	7.173
1600	16.8	3.7	6.3	3.1	9.518	50.1	6.090	7.151
1700	16.2	3.7	6.5	3.0	8.744	52.5	6.159	7.244
1800	15.2	3.6	6.7	3.0	7.509	56.6	6.240	7.365
1900	13.4	3.4	6.8	2.8	5.458	64.4	6.284	7.464
2000	12.1	3.1	6.7	2.8	4.349	69.2	6.240	7.446
2100	11.4	3.1	6.2	2.7	3.979	70.4	6.027	7.212
2200	10.7	2.9	6.2	2.6	3.374	73.7	6.040	7.244
2300	10.2	2.9	6.3	2.5	2.890	76.7	6.069	7.292
AVER	12.0	3.1	6.3	2.7	4.430	68.4	6.099	7.281

FIGURE 6.1.9

HOURLY TEMPERATURE AND DEW POINT
MEANS FOR SEPTEMBER



VAR1=TEMPERATURE
VAR2=DEW POINT

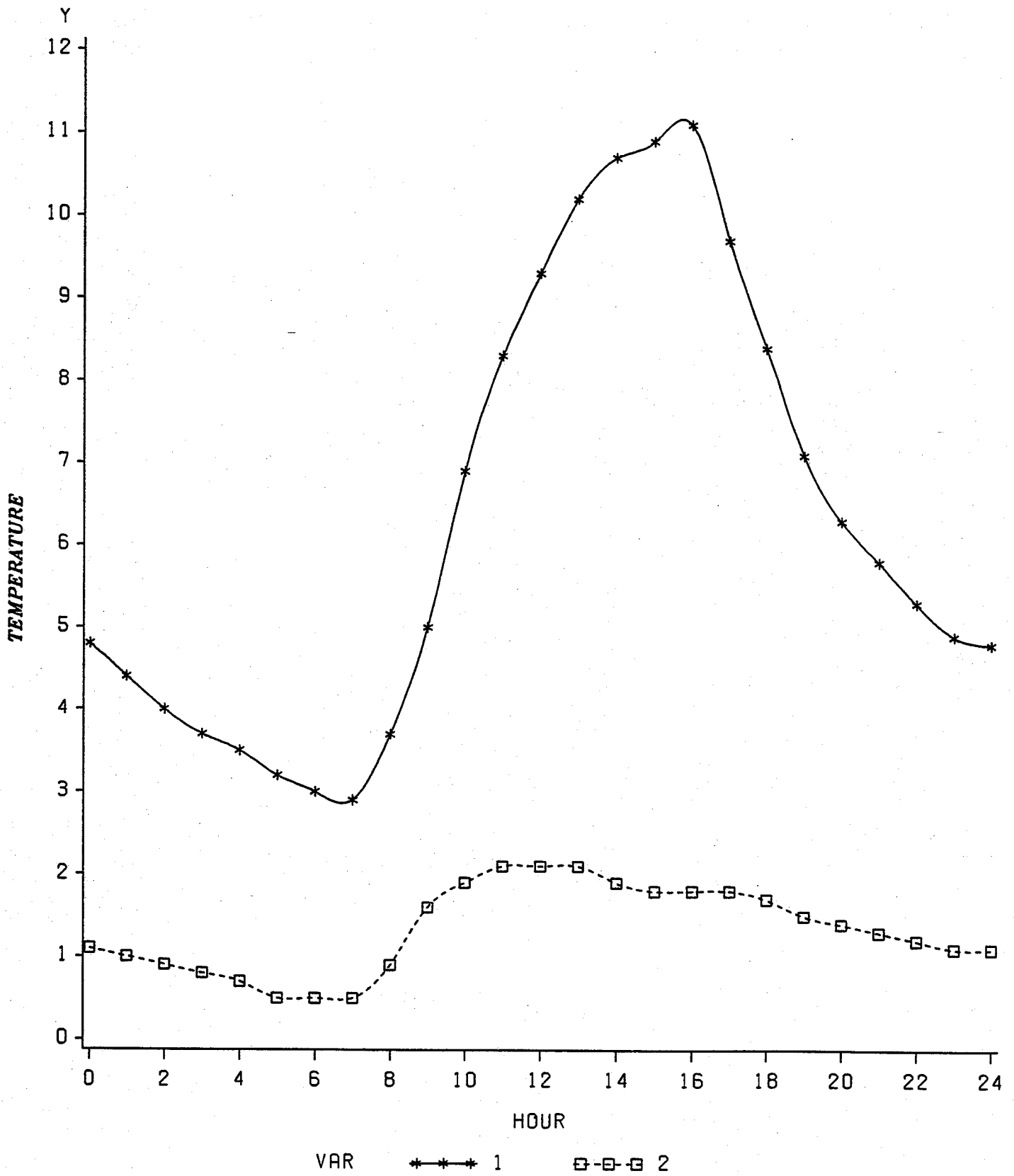
TABLE 6.1.10

MEAN HOURLY AND MONTHLY AVERAGES FOR OCTOBER

<u>HOURLY</u> (CST)	<u>T</u> (°C)	<u>SD</u> (°C)	<u>TD</u> (°C)	<u>SD</u> (°C)	<u>SATD</u> (mb)	<u>U</u> (%)	<u>R</u> (g/kg)	<u>DV</u> (g/m ³)
0000	4.8	3.8	1.1	3.1	1.945	77.3	4.209	5.171
0100	4.4	3.6	1.0	3.0	1.782	78.6	4.170	5.130
0200	4.0	3.6	0.9	3.2	1.632	80.0	4.140	5.099
0300	3.7	3.4	0.8	3.1	1.510	81.1	4.113	5.071
0400	3.5	3.2	0.7	3.0	1.425	81.9	4.074	5.029
0500	3.2	3.1	0.5	3.0	1.341	82.6	4.030	4.979
0600	3.0	3.1	0.5	2.9	1.272	83.3	4.015	4.965
0700	2.9	3.0	0.5	2.9	1.213	83.9	4.015	4.967
0800	3.7	3.2	0.9	3.0	1.432	82.0	4.152	5.120
0900	5.0	3.6	1.6	3.2	1.865	78.6	4.361	5.351
1000	6.9	4.1	1.9	3.3	2.933	70.5	4.466	5.442
1100	8.3	4.6	2.1	3.4	3.809	65.2	4.531	5.493
1200	9.3	5.0	2.1	3.3	4.611	60.7	4.528	5.469
1300	10.2	5.2	2.1	3.2	5.359	57.0	4.511	5.432
1400	10.7	5.4	1.9	3.3	5.868	54.4	4.450	5.350
1500	10.9	5.5	1.8	3.3	6.078	53.3	4.415	5.305
1600	11.1	5.4	1.8	3.4	6.276	52.5	4.406	5.289
1700	9.7	5.1	1.8	3.4	5.050	58.0	4.431	5.346
1800	8.4	5.0	1.7	3.4	4.072	62.9	4.396	5.329
1900	7.1	4.6	1.5	3.4	3.228	67.9	4.339	5.285
2000	6.3	4.3	1.4	3.3	2.820	70.5	4.289	5.238
2100	5.8	4.1	1.3	3.1	2.516	72.7	4.268	5.222
2200	5.3	3.9	1.2	3.1	2.265	74.6	4.231	5.186
2300	4.9	3.7	1.1	3.1	2.059	76.2	4.194	5.149
AVER	6.4	4.2	1.3	3.2	2.866	70.1	4.277	5.223

FIGURE 6.1.10

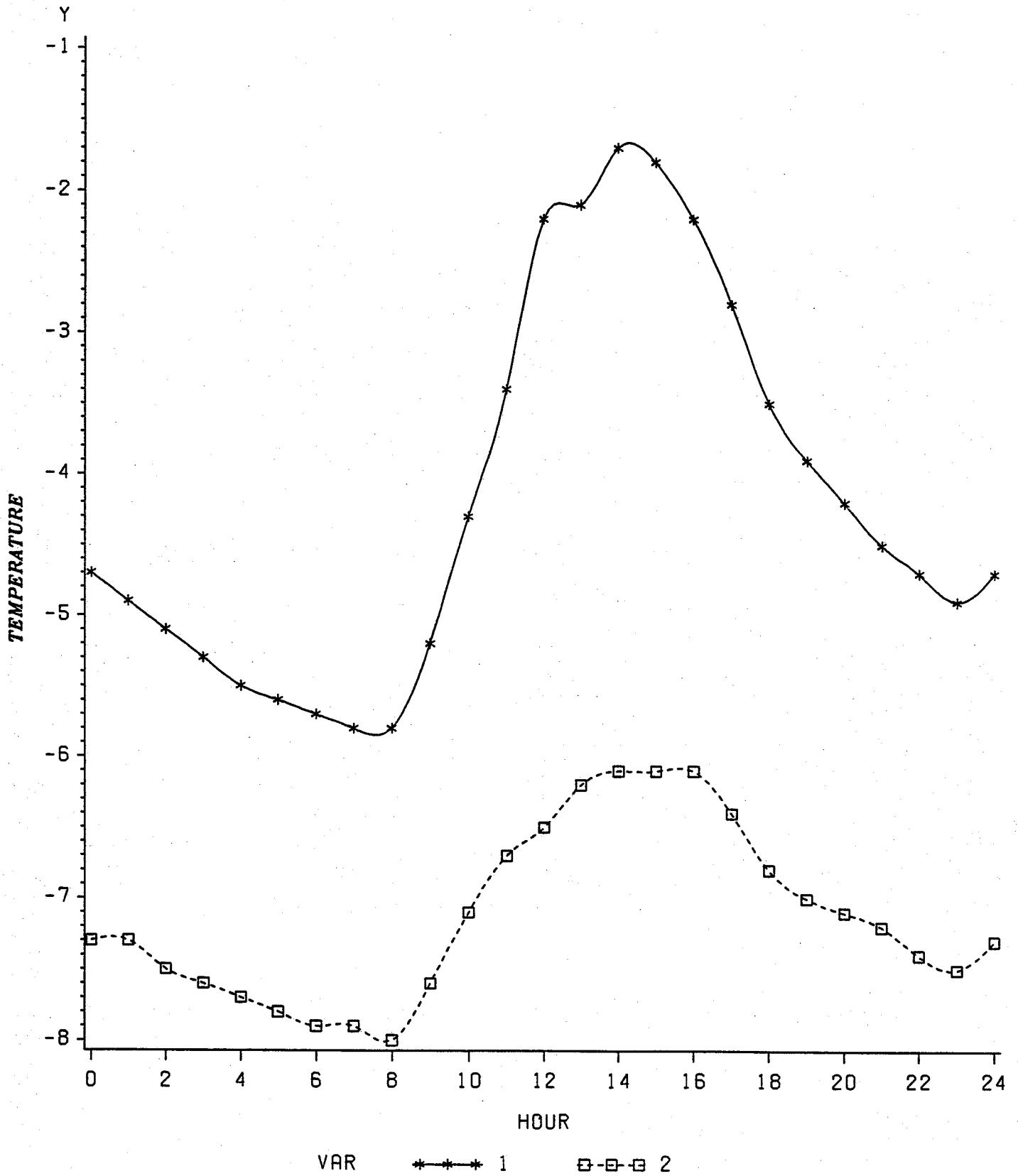
HOURLY TEMPERATURE AND DEW POINT
MEANS FOR OCTOBER



VAR1=TEMPERATURE
VAR2=DEW POINT

FIGURE 6.1.11

HOURLY TEMPERATURE AND DEW POINT
MEANS FOR NOVEMBER



VAR1=TEMPERATURE
VAR2=DEW POINT

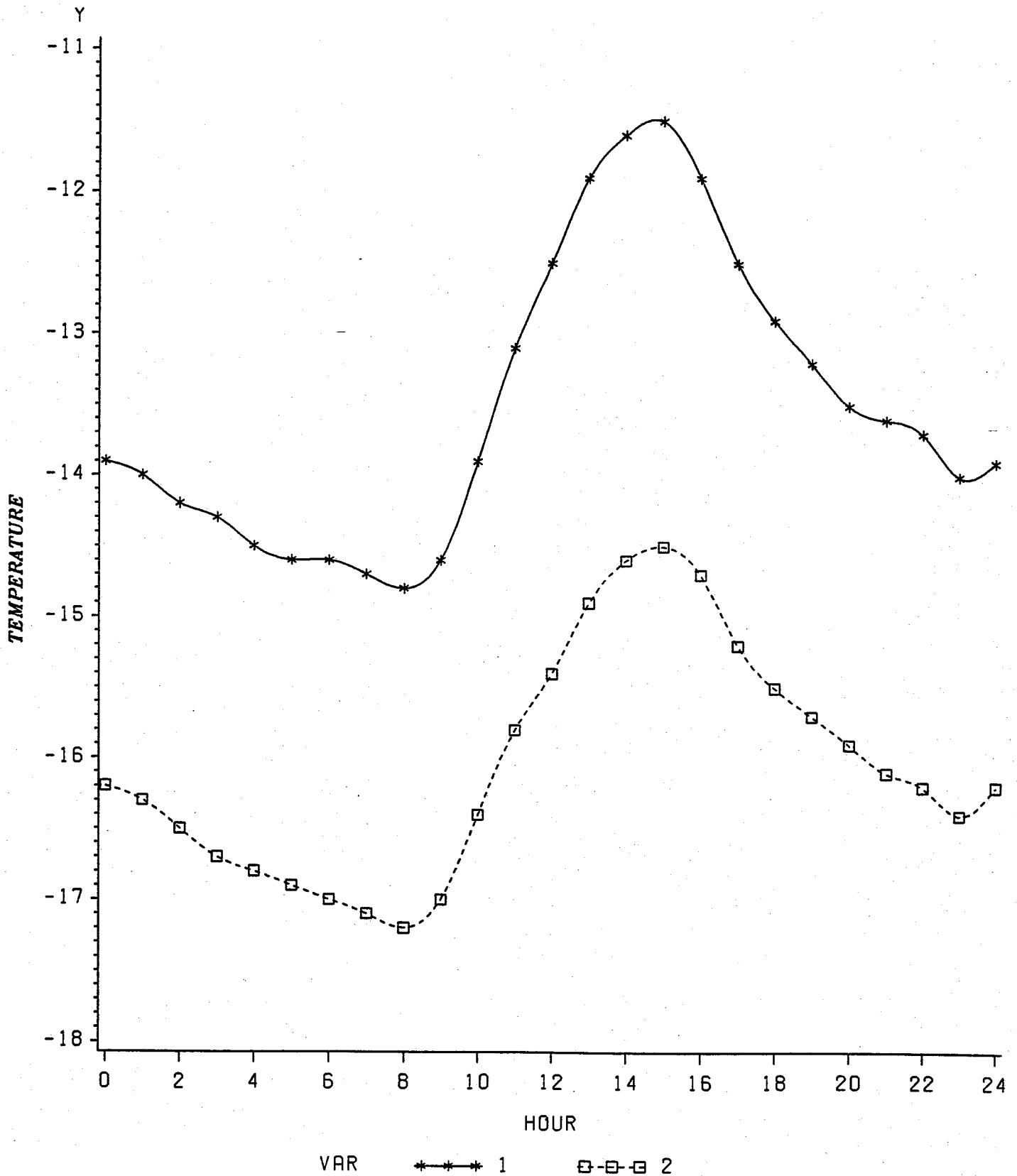
TABLE 6.1.12

MEAN HOURLY AND MONTHLY AVERAGES FOR DECEMBER

<u>HOUR</u> (CST)	<u>T</u> (°C)	<u>SD</u> (°C)	<u>TD</u> (°C)	<u>SD</u> (°C)	<u>SATD</u> (mb)	<u>U</u> (%)	<u>R</u> (g/kg)	<u>DV</u> (g/m ³)
0000	- 13.9	6.3	- 16.2	4.1	0.353	80.7	0.931	1.236
0100	- 14.0	6.3	- 16.3	4.2	0.349	80.7	0.923	1.224
0200	- 14.2	6.4	- 16.5	4.1	0.337	81.1	0.910	1.209
0300	- 14.3	6.4	- 16.7	4.2	0.344	80.4	0.893	1.187
0400	- 14.5	6.4	- 16.8	4.1	0.330	80.9	0.884	1.177
0500	- 14.6	6.5	- 16.9	4.2	0.326	81.0	0.876	1.166
0600	- 14.6	6.5	- 17.0	4.1	0.332	80.5	0.867	1.154
0700	- 14.7	6.5	- 17.1	4.1	0.332	80.4	0.857	1.142
0800	- 14.8	6.5	- 17.2	4.1	0.327	80.5	0.852	1.135
0900	- 14.6	6.6	- 17.0	4.1	0.341	80.1	0.865	1.151
1000	- 13.9	6.6	- 16.4	4.1	0.379	79.3	0.916	1.151
1100	- 13.1	6.6	- 15.8	4.2	0.429	78.2	0.969	1.282
1200	- 12.5	6.5	- 15.4	4.2	0.472	77.2	1.007	1.329
1300	- 11.9	6.3	- 14.9	4.1	0.517	76.4	1.053	1.387
1400	- 11.6	6.2	- 14.6	4.1	0.541	76.0	1.080	1.420
1500	- 11.5	6.1	- 14.5	4.1	0.536	76.4	1.091	1.435
1600	- 11.9	6.1	- 14.7	4.1	0.493	77.4	1.050	1.389
1700	- 12.5	6.1	- 15.2	4.2	0.451	78.2	1.020	1.346
1800	- 12.9	6.1	- 15.5	4.2	0.420	79.0	0.996	1.316
1900	- 13.2	6.1	- 15.7	4.2	0.403	79.3	0.975	1.291
2000	- 13.5	6.1	- 15.9	4.1	0.390	79.5	0.955	1.265
2100	- 13.6	6.1	- 16.1	4.1	0.381	79.6	0.941	1.247
2200	- 13.7	6.1	- 16.2	4.1	0.378	79.6	0.932	1.236
2300	- 14.0	6.0	- 16.4	4.1	0.365	80.0	0.917	1.218
AVER	- 13.5	6.3	- 16.0	4.1	0.392	79.3	0.947	1.255

FIGURE 6.1.12

HOURLY TEMPERATURE AND DEW POINT
MEANS FOR DECEMBER



VAR1=TEMPERATURE
VAR2=DEW POINT

LIST OF REFERENCES

Dodd, Arthur van Zandt, 1964:Water Vapor Near the Ground in the Continuous United States. Ph.D. Thesis, Pennsylvania State University, 199pp.

CHAPTER 7

ANALYSIS PROCEDURE

7.1 Introduction

With reference to the Literature Review, Chapter 3, the following two facts become quite evident:

- (1) few intensive studies have been made of the influences of urbanization on humidity distributions in towns or on the difference between urban and rural areas.
- (2) what observational evidence there is, is not completely conclusive.

Incongruent conclusions have arisen because emphasis throughout the majority of urban climatic studies has been placed upon the descriptive analysis of case studies rather than upon their validity. Intuitive reasoning was the basis for rejecting individual observations which did not fit the general situation. A coherent pattern was thus constructed out of, in many cases, incomplete, biased and somewhat discordant data.

Since objective analysis is an absolute necessity to check upon the validity of data, this chapter will be devoted to the discussion of such topics as classification procedures, tests of normality, and statistical applications. Emphasis throughout will be directed to their applied usage in this study.

7.2 Classification

7.2.1 Introduction

Classification is essentially the identification of groups of similar objects within the set of objects under study. It is necessary so that generalizations concerning within and between group similarities and differences can be made. Such generalizations can be purely descriptive or they can form the basis of a hypothesis which can then be tested by the use of various statistics, both parametric and nonparametric.

Two approaches to classification are possible. The identification of groupings is termed classification proper and includes clustering methods and ordination. The object of the former exploratory method is to sort or separate a sample of cases using the information for each case given by the p variables into constituent groups such that the degree of association is high between members of the same group and low between members of a different group. Groups may be disjoint or overlapping. Its use is appropriate to those studies where little or nothing is known about the category structure of the data or whenever the input data matrix under examination is of such a dimension that manual sorting using various combination theories become increasingly prone to error.

The second approach to classification is termed discrimination. It is the assessment of the degree of separateness of groups of individuals which are postulated either by a classification or by a priori information. This statistic provides information regarding what variables are most effective in distinguishing between the groups under examination; how best to combine the measurements, and how successfully the distinction can be made. Discriminant function analysis reduces the variables to a single one which is compounded of the original number.

Both these modern statistics are complementary. They have been used for a diversity of subjects including meteorology and climatology. For examples of the use of cluster analysis in the latter two fields see Bell(1974), Perry(1968) and Gregory(1964). Discriminant applications in the same fields are detailed by Miller(1962), Brinkmann(1970), and Suzuki(1969).

7.2.2 Cluster Analysis

One of the most primitive and common pursuits of man is the act of sorting similar objects, things or variables into categories. Individual uniqueness must be overshadowed by mutually exclusive group traits. In this manner, it is easier to consider and understand relations in large collections. Hence, efficiency of management is often increased.

In the early 1960's, D. Wishart (1978) consolidated the various dissimilar cluster analysis methods and their particular applications in the form of a computer statistical package and accompanying reference manual. Clustan-1C2, the latest revised edition, is now the most frequently used classification package in modern research (Van Ryzin, 1977). The above is also the cluster analysis package used in this project.

A Clustan-1C2 job usually commences with procedures File and Correl. The former reads the data deck from cards, disk or tape and creates the clustan data file on disk. Other functions include data standardization¹ and the computation of various statistics such as principal component correlations. All the raw input and computed results are stored in the data file.

Procedure population constraints are also defined in procedure File. In general, the population size N is set at a maximum of 999 cases, each with no greater than 200 continuous variables, MN. Because of the latter

¹ When columns correspond to variables and the rows correspond to individuals, the data is classified as continuous and should therefore be standardized. If not, similarity coefficients will be biased towards those variables with large variances.

To obtain standard-scores, the variable mean is subtracted from each member and divided by the variable standard deviation. For example, the standard-scores of the following wind velocities, 1, 2, 7, 9, and 12 with mean 6.2 km per hour and standard deviation 4.6583 are -1.116, -0.902, 0.172, 0.601 and 1.245 respectively.

restriction, the total temperature and mixing ratio observations from each of the 127 fixed point locations per traverse could not be used. Consequently, this necessitated averaging those observations recorded at consecutive fixed point locations which had the least strip chart variability. This procedure reduced MN from 254 to 194 variables, or in other words, from 127 fixed locations per traverse to 97. To these variables the climatic parameters opacity, pressure, wind speed and wind direction were added. Respective units for each are tenths, millibars, km per hour and 360 degrees. The final edited cluster data field thus consisted of a 253 X 198 matrix.

For principal components analysis and correlations, MN was not to exceed 80. The constraint limited the optimum use of Clustan-1C2 both in terms of analysis and graphical display. The recommended analysis for large populations (see Wishart(1978),page 9) therefore had to be replaced by Ward's Algorithm: a fusion procedure for forming heirarchical groups of mutually exclusive subsets,each of which has members that are maximally similar with respect to specified characteristics. Moreover, graphical procedures such as Scatter, which plot scatter and cluster diagrams to scale, had to be replaced by the dendrogram plotting Procedure Tree. The full dendrogram produced by procedure Tree for each 252 cluster job submission was approximately 52 inches long and about 44 inches wide. To ensure

comprehensible result analysis, Xerox reduction of the original was limited to 0.5. The latter sizes were well beyond thesis figure measurement restrictions.

Procedure Correl computes and stores on the data file the similarity matrix and k-linkage lists from all or part of either the raw or standardized data. The results are essential for the successful execution of procedure Hierarchy.

The similarity matrix is a triangular array of $N(N-1)/2$ coefficients of average distance, error sums of squares, variance or information gain such that each element measures the similarity between two individuals. For each cluster analysis submitted, the maximum number of coefficients that could be computed on the data field was $253(252)/2$ or 31878.

The k-linkage lists are the lists of $5000/N$ nearest neighbors for all N individuals from which the similarity coefficient is calculated. For this study, the maximum number, KMAX was $5000/253$ or 19. If an excessive value is specified, the program adjusts KMAX to the maximum permissible value.

Procedure Correl also provides variable masking facilities. When a variable is masked, that variable is not included in the calculation of a similarity

coefficient. For example, to examine what effect the climatic variable wind direction would have on the clustering of data, MSKN, the number of continuous variables to be masked was set to one while the following partial-mask card was coded 0198: the variable's location in the MN field. The main reason for using this facility was that wind direction is the only variable in the data which has the circumference of a circle as a reference. The Euclidean metric from any fixed point on the circumference to any symmetric circumference point is therefore equal. For instance, D^2 from 358° to 002° is smaller than from 353° to 358° , yet the error sum of squares for the latter is less than that for the former. By Ward's algorithm, 353° would be clustered with 358° even though this clustering would be false.

The number of combinations of the 4 distinct climatic variables, taken r at a time was $4C1$, $4C2$, $4C3$ and $4C4$ where $nCr = n!/r!(n-r)!$. Thus a total of 15 cluster analyses were run on the 253 X 198 traverse data matrix. Fifteen additional cluster analyses were generated using the 129 X 94 estimated Winnipeg radiosonde data matrix.

In Clustan-1C2, eight hierarchic combinatorial transformations of the similarity matrix are defined in procedure Hierarchy. Ward's algorithm is coded 6 and is possibly the best of the eight options (Wishart, 1978).

Ward(1963) proposed that at any stage of an analysis the loss of information which results from the grouping of individuals into clusters can be measured by the total sum of squared deviations of every point from the mean of the cluster to which it belongs. At each step in the analysis, union of every possible pair of clusters is considered. The two clusters whose fusion results in the minimum increase in the error sum of squares are combined. The process continues until all k clusters are combined to a single cluster which is characterized by the largest error sum of squares.

The error sum of squares is given by the functional relation,

$$ESS = \Sigma(X_i^2) - ((\Sigma X_i)^2/n)$$

where X_i is the score of the i th individual in a sample of size n .

The minimum number of clusters which are of interest, K_A is usually set at one while the maximum number is set to the number of cases in the data matrix minus one.

To illustrate the procedure, let us consider a small problem in which five individual wind velocities are to be grouped. The non - standardized values are 1, 2, 7, 9, and 12.

In step 1 there are 10 possible combinations. They are (1,2), (1,7), (1,9), (1,12), (2,7), (2,9), (2,12), (7,9), (7,12), and (9,12). The first task is to calculate the sum of squares (ss) for each of the above combinations. For example, the sum of squares for group (1,2) is $(1 - 1.5)^2 + (2 - 1.5)^2 = 0.5$ where 1.5 is the mean for the group, $(1 + 2)/2 = 1.5$. The results for the above combinations are 0.5, 18, 32, 60.5, 12.5, 24.5, 50.0, 2.0, 12.5 and 4.5. The lowest sum of squares is 0.5 for group (1,2). Labelling this group A(1,2), the original 5 combinations have been reduced to four. That is, A(1,2), 7, 9, and 12.

In the second cluster stage, there are 6 possible pairings. They are, (A(1,2)~7), (A(1,2)~9), (A(1,2)~12), (7,9), (7,12) and (9,12). As the sum of squares for the latter 3 have already been determined, all that is required are the values for the formost A combinations. The sum of squares for (A(1,2)~7) is determined from the equation

$$(1 - 3.3)^2 + (2 - 3.3)^2 + (7 - 3.3)^2 = 20.89$$

where the mean for the group is $(1 + 2 + 7)/3 = 3.3$. The resultant values for step 2 are 20.89, 38.0, 74.0, 2.0, 12.5 and 4.5 respectively. The lowest sum of squares is 2.0 for group (7,9). Labelling this group B(7,9), the original 5 groups have now been reduced to three. That is, A(1,2), B(7,9) and 12.

There are three possible combinations in the third step. They are, $(A(1,2) \sim B(7,9))$, $(A(1,2) \sim 12)$ and $(B(7,9) \sim 12)$. Repeating the same processes as above, the lowest sum of squares calculated is 12.67 for group $(B(7,9) \sim 12)$.

The concluding step is the union of all the original groups. Here the sum of squares is the total sum of squares, the value being 86.80.

In summation, there were 4 steps. The first clustering has a sum of squares of 0.5 whilst the final had 86.80. The change in error term at each union is shown is termed d_1 . A sharp value increase suggests that much of the classification system's accuracy has been lost by reducing the number of groups by one at this stage.

Because Clustan-1C2 requires the distance metric for the calculation of Ward's algorithm, the printed output coefficient value d_1 is twice the increase caused by fusion. The total error sum of squares for any grouping is obtained on division by two of the cumulative ESS which precede that grouping in the printout.

Several data matrices were subjected to both the recommended Clustan-1C2 analysis for large populations and the Ward's algorithm version discussed above in order to test the effectiveness of both methods. A system abend message was generated for the former mode for each run.

Boosting CPU and I/O to the maximum allowed non-prime amount did not correct the situation. Ward's method was the only workable method. On the average, each job submitted generated 46,000 lines and required 856 I/O, 610K of region and 20M CPU. Total cost per run was approximately 350.00 units.

In all, 30 cluster analysis jobs were submitted. The results of the analyses and the dendrogram selected for subsequent statistical analysis are discussed in Section 8.2.

7.2.3 Canonical Discriminant Analysis

Discriminant function analysis assumes that each of the samples is drawn from a separate population which may differ in their means but do not differ in their dispersions. By assuming that the distribution of members of a population about the population mean is multivariate normal, an ellipsoidal surface whose centre is the population mean is obtained by joining together areas of equal density. Thus every sample may be represented as an ellipse if there are two test axes or an ellipsoid if there are more than two test axis. The ellipsoids or ellipses may be of the same shape, size or lie in the same orientation in the test space.

If there are no correlations among the tests, the ellipsoids may be reduced to spheres by standardizing the

variables. This involves division by the within group dispersion matrix. The canonical analysis of discriminance is a transformation of the original test space which reduces the within sample ellipsoids to spheres. The radius of the sphere, which is the standard deviation within samples, is set to unity. Each variable provides maximal separation between the groups whilst being orthogonal to previous variates. If there are k groups, there are therefore k^2 discriminant functions per canonical variates.

The canonical discriminant analysis yields values for the coefficients or weights W_{ij} for each discriminating variable i on each discriminant function j for each canonical variate. By multiplying each weight by the standard deviation of the variable, the degree of contribution per variable to the discriminant function is calculated. The sign denotes whether the variable is making a positive or negative contribution. Graphical display of discriminant function means illustrates the discriminating power of each function. The greater the distance between groups on each function, the more significant the function is in discriminating between the groups.

² The stepwise method was selected for the SPSS canonical discrimination analysis. In this method, the independent non-correlated variables, hour, temperature, mixing ratio, opacity, pressure, wind speed and wind direction are

Canonical discrimination analysis is supported by SPSS²
For stepwise computation formulae and further discussion see
Mather(1976),Lachenbruch(1975) and Bennett et al.,(1978).

entered into the analysis only if a predetermined tolerance
level is met. The climatic variables listed above are the
same as those used in the cluster analysis.

7.2.4 Conclusion

The fundamental purpose of all systems of classification is to obtain the least variability within the groups and the maximum differences between the groups. Cluster analysis is useful in the analysis of the relationship between a set of variables. The variables are in fact the results of several measures taken on a single group of objects or locations. In discrimination several groups of objects or locations are measured on the same set of variables. The principle question to be answered is can the groups be differentiated on the bases of the measurements obtained from the set of variables?

Although both these statistics are complementary, the usage of canonical discrimination in this study is questionable. Exploratory analysis of the input data matrix indicated that both temperature and mixing ratio vary polynomially and in the majority of cases, the other climatic parameters have non normal distributions. The critical assumptions for a canonical analysis, therefore can not be assumed. Hence, only cluster analysis will be used. It will agglomerate similar groups from an input data matrix of 253 X 198.

7.3 Tests of Normality

Since many of the standard statistical techniques are based on the assumption of normality, methods for judging the

normality of a set of data are of interest (Snedecor et al.,1976). If a population is characterized by a significant departure from normality, careful consideration must be given towards the statistical inference techniques chosen in order to prevent erroneous conclusions. For instance,theoretical investigations have shown that nonparametric procedures are only slightly less efficient than their normal theory competitors when the underlying populations are normal,though they can be mildly and widely more efficient than these competitors when the underlying populations are not normal (Hollander et al.,1973).

To check on the assumption of normality itself,the multinomial non-specific Chi-square Goodness-of-Fit test can be applied.³ For data that falls into categories,this test examines whether a significant difference exists between the observed number of cases in each category and the expected number on the assumption of normality. The test criterion is $\chi^2 = \sum (Y_i - \text{EXPECTED } E_i)^2 / \text{EXPECTED } E_i$ summed over the classes. If the data actually comes from a normal distribution,the right hand quantity follows approximately the theoretical Chi-square distribution with k-3 degrees of

³ Chi-square is non-specific as the test criterion is directed against no particular type of departure from normality. Two alternative tests that are designed to detect particular types of departure are the sample estimates of the coefficients of skewness and kurtosis,denoted g1 and g2 respectively. For further discussion and derivation formulae see Snedecor et al.,(1976).

freedom where k is the number of classes used in the computing of the test criterion. If the data comes from some other distribution, the observed Y_i will tend to agree poorly with the values E_i that are expected on the assumption of normality and the computed X^2 becomes large. The null hypothesis H_0 , that there is no difference between the expected and observed frequencies, is thus rejected.

For an example, suppose we want to test at the one percent level, the hypothesis that the 381 temperature measurements of Table 7.3.2⁴ come from some normal population.

⁴ The data was collected on traverses conducted on November 30, 1976 at 0900 hours and on December 6, 1976 at 1700 and 2100 hours. Respective traverse codes are 203, 208 and 209.

Continental Arctic air masses engulfed the research area during these itineraries. Inversions were present. The change in pseudo-equivalent potential temperature between the surface and the 950mb level with respective change in geopotential meter height, dQ_{se}/dz , varied from 0.0046 to 0.0130. Wind velocities were relatively constant at 11.1km per hour while wind direction altered from 180° to 210° degrees. Traverse 203 recorded the greatest temperature range, 9.8°C., whilst the least, 2.9°C. was measured during traverse 208.

Ward's hierarchic algorithm fused traverses 208 and 209 during cycle 6 at error coefficient change 0.003. Traverse 203 was added during cycle 43. The d_1 increased to 0.019 which is still quite negligible when one considers that the total error sum of squares for 253 fusions was 150.13.

TABLE 7.3.1

TEMPERATURES RECORDED AT 127 LOCATIONS DURING 3 CA TRAVERSES

<u>POINT</u>	<u>203</u>	<u>208</u>	<u>209</u>
1	-15.53	-20.27	-19.43
2	-18.29	-19.91	-20.50
3	-20.20	-20.62	-21.38
4	-18.89	-19.53	-19.65
5	-18.29	-20.11	-20.41
6	-18.68	-19.78	-19.82
7	-19.31	-20.04	-21.66
8	-19.58	-20.06	-21.24
9	-19.22	-19.97	-21.70
10	-19.76	-19.69	-21.05
11	-21.35	-19.96	-22.01
12	-20.35	-19.60	-21.64
13	-20.56	-20.48	-23.07
14	-20.83	-20.56	-23.08
15	-21.31	-22.04	-24.01
16	-21.14	-20.74	-23.05
17	-20.41	-20.07	-22.10
18	-26.98	-22.03	-24.13
19	-27.15	-22.20	-25.03
20	-27.25	-22.46	-26.16
21	-27.41	-24.05	-27.09
22	-27.06	-22.84	-25.42
23	-27.11	-23.94	-25.96
24	-26.51	-22.14	-24.54
25	-26.56	-22.31	-24.61
26	-26.27	-22.93	-24.64
27	-26.22	-22.43	-24.51
28	-26.22	-22.90	-24.98
29	-26.08	-23.96	-25.65
30	-26.91	-21.99	-24.35
31	-26.94	-23.27	-24.80
32	-26.29	-23.26	-24.38
33	-26.02	-22.93	-23.91
34	-25.62	-22.70	-23.71
35	-26.01	-23.04	-24.07
36	-24.83	-23.85	-24.86
37	-24.47	-26.07	-25.75
38	-23.63	-26.35	-25.53
39	-23.21	-25.45	-26.82
40	-23.14	-27.31	-25.88

TABLE 7.3.1 (CON'T)

TEMPERATURES RECORDED AT 127 LOCATIONS DURING 3 cA TRAVERSES

<u>POINT</u>	<u>203</u>	<u>208</u>	<u>209</u>
41	-22.08	-26.07	-25.97
42	-22.18	-22.98	-22.36
43	-21.90	-23.01	-23.09
44	-21.69	-22.47	-22.15
45	-21.29	-21.79	-21.14
46	-20.99	-21.92	-21.25
47	-19.85	-20.57	-20.30
48	-19.23	-20.97	-20.31
49	-19.97	-21.08	-21.17
50	-19.83	-21.20	-20.96
51	-19.48	-21.29	-20.39
52	-19.41	-21.09	-19.84
53	-18.25	-20.64	-18.96
54	-19.04	-20.86	-19.62
55	-16.93	-20.30	-19.34
56	-18.89	-19.53	-19.65
57	-18.29	-20.11	-20.41
58	-18.68	-19.78	-19.82
59	-18.10	-20.63	-19.47
60	-18.55	-20.27	-19.82
61	-18.99	-21.21	-19.73
62	-19.13	-21.07	-19.60
63	-18.11	-20.14	-18.17
64	-18.52	-20.18	-18.79
65	-18.22	-19.43	-17.68
66	-18.09	-19.65	-17.80
67	-17.62	-18.58	-16.47
68	-17.49	-19.43	-16.87
69	-17.60	-19.56	-18.25
70	-17.91	-19.96	-18.38
71	-16.74	-21.26	-19.85
72	-17.24	-19.74	-19.98
73	-17.32	-21.39	-19.84
74	-17.42	-21.57	-20.20
75	-17.66	-21.30	-19.93
76	-16.99	-20.00	-20.55
77	-17.63	-21.35	-20.19
78	-17.91	-21.89	-20.94
79	-17.72	-22.56	-22.77
80	-18.66	-23.49	-23.21

TABLE 7.3.1 (CON'T)

TEMPERATURES RECORDED AT 127 LOCATIONS DURING 3 CA TRAVERSES

<u>POINT</u>	<u>203</u>	<u>208</u>	<u>209</u>
81	-18.46	-22.65	-22.50
82	-19.46	-23.54	-23.03
83	-19.51	-24.03	-24.85
84	-19.55	-24.12	-24.27
85	-19.49	-23.76	-23.29
86	-19.75	-23.76	-23.33
87	-19.41	-24.25	-23.87
88	-18.83	-23.32	-23.06
89	-18.02	-22.52	-23.24
90	-18.95	-23.68	-24.17
91	-18.91	-20.65	-22.03
92	-28.94	-21.94	-21.98
93	-19.13	-22.12	-21.22
94	-19.42	-21.77	-22.24
95	-19.59	-21.72	-22.38
96	-19.73	-23.01	-25.31
97	-19.67	-22.53	-24.51
98	-20.12	-23.73	-27.40
99	-20.46	-24.04	-26.15
100	-20.90	-23.91	-27.17
101	-21.61	-23.11	-24.00
102	-21.69	-23.33	-24.40
103	-21.61	-23.42	-24.22
104	-19.53	-23.34	-22.25
105	-20.08	-24.90	-23.50
106	-20.06	-23.38	-22.78
107	-18.87	-22.76	-22.51
108	-17.92	-23.43	-21.88
109	-16.95	-23.21	-21.88
110	-15.87	-21.61	-21.21
111	-16.89	-22.28	-21.74
112	-17.14	-21.48	-22.23
113	-17.43	-20.93	-21.64
114	-17.58	-20.71	-20.66
115	-17.12	-20.46	-21.46
116	-17.84	-20.64	-20.20
117	-17.28	-20.25	-19.31
118	-17.04	-20.13	-19.17
119	-18.09	-19.65	-17.80
120	-17.87	-20.15	-18.86

TABLE 7.3.1 (CON'T)

TEMPERATURES RECORDED AT 127 LOCATIONS DURING 3 CA TRAVERSES

<u>POINT</u>	<u>203</u>	<u>208</u>	<u>209</u>
121	-17.37	-20.30	-18.46
122	-17.67	-20.59	-19.43
123	-17.11	-20.78	-19.34
124	-16.93	-20.30	-19.34
125	-16.91	-20.45	-19.74
126	-17.60	-20.40	-19.65
127	-15.53	-20.27	-19.43

We first sort the data into non overlapping categories and note the observed frequencies Y_i per class. Table 7.3.2 shows the results for our 381 sample.

TABLE 7.3.2

FREQUENCY DISTRIBUTION OF TABLE 7.3.1 DATA

<u>CLASS</u>	<u>MEASUREMENTS</u>	<u>Y_i</u>
1	-27.55 to -26.00	26
2	-26.00 to -24.45	24
3	-24.45 to -22.90	59
4	-22.90 to -20.35	112
5	-20.35 to -18.80	101
6	-18.80 to -17.25	42
7	-17.25 to -15.70	15
8	-15.70 to -14.15	2
	TOTAL	<u>381</u>

Next, standardize the class boundaries in order to compute what probability a normal distributed random variable with mean -21.31 and standard deviation 2.502 has of falling in

each of the eight classes represented in Table 7.3.2. For example, the probability that the standardized variable $(X - 20.31)/2.502$ falls between $(-24.45 + 20.31)/2.502$ or -1.655 and $(-22.90 + 20.31)/2.502$ or -1.036 is calculated by subtracting the tabulated area under the standard normal curve from -1.655 to -1.036 . The result is $0.45104 - 0.35083$ or 0.10921 .

Now we chi-square the observed frequencies in Table 7.3.2 against the above probabilities. Since the probability of class 3 is 0.10921 and the total number of observations is 381 , the average expectation is 381×0.10921 or 41.61 observations to fall in class 3. Table 7.3.3 shows the remaining calculations.

TABLE 7.3.3

TEST OF NORMALITY FOR DATA OF TABLE 7.3.1

CLASS	PROBABILITY	E _i	Y _i	Y _i -E _i	(Y _i -E _i) ² /E _i
1	0.00644	2.45	26	23.55	226.37
2	0.03751	14.29	24	9.71	6.60
3	0.10921	41.61	59	17.39	7.27
4	0.34285	130.63	112	-18.63	2.66
5	0.23373	89.05	101	11.95	1.60
6	0.16302	62.11	42	-20.11	6.51
7	0.07835	29.85	15	-14.85	7.39
8	0.02889	11.01	2	-9.01	7.39
-	<u>1.00000</u>	<u>381.00</u>	<u>381</u>	<u>0.00</u>	<u>265.77</u>

The degrees of freedom for chi-squared is determined by the following equation

$$\text{d.f.} = (\text{No. of classes}) - (\text{No. of estimated parameters}) - 1$$

In this example, the number of classes is 8 and two parameters, the mean and standard deviation, were estimated in fitting the distribution. The one percent point on a chi-square distribution with 5 degrees of freedom is 15.09. The calculated value, 265.77, is greater than this, therefore, the data does not fit a normal distribution well. Hence, further analysis of Table 7.3.1 would require the use of nonparametric statistics.

Although the goodness-of-fit test is supported by SPSS, excessive modification of the test data is required prior to the submission of a job specifying this task. Data must be manually categorized; the expected frequencies must be computed, and each category must be recoded. Furthermore, small expectations are not allowed. Hence, this statistic will only be calculated for major cluster and sub-cluster group data.

7.4 Statistic Applications

7.4.1 Introduction

The precise classification of a particular test as parametric, nonparametric or distribution-free is unimportant. Far more important to the researcher is the

selection of a test for which the power of rejection is maximized when the hypothesis tested is false. If the data adhere to the assumptions required for a classical normally based statistic, the statistic should be used since it is optimum when justified. Only when the assumptions for the classical tests cannot be satisfied, should one seek out substitute tests (Marascuilo et al., 1977).

In exploratory research, such as this thesis, when the investigator does not know much about the type of distribution being sampled, distribution free or non-parametric statistics⁵ should first be applied (Snedecor et al., 1976). Otherwise, erroneous conclusions could be formulated from results generated by statistical application.

Furthermore, prior to the application of a particular statistic or group of statistics, the investigator must understand the fundamental objectives and limitations of the statistic. One can not assume, for example, that an insignificant increase in the change of the error term between Ward's hierarchical fusions is a definite indication

⁵ A statistical test is distribution free if the sampling distribution of the statistic on which the test is based is completely independent of the parent distribution of the variable. If a statistical test does not test a hypothesis characterizing one of the parameters of the parent variable of interest, it is termed nonparametric. Both types of tests are procedures in nonparametric inference. Their main advantage over their competitors is that they are more efficient when the underlying populations are not normal.

of normality. In fact, from the example in Section 7.3, we see that the two have nothing in common. That is, although the objective function calculated for the fusions of traverses 203, 208 and 209 was 0.009, the 381 temperatures generated a chi-square well above the critical one percent level for five degrees of freedom.

Investigations are often designed to discover and evaluate differences between effects rather than the effects themselves. With 253 traverses randomly conducted over a two year period under all weather conditions within a well defined urban-rural complex, 32131 cases of point data was acquired which had to be analyzed. As there were 127 fixed point measurements per traverse, each with a temperature and mixing ratio measure, it is desirable to learn whether or not both variables depend upon the location at which they were recorded. Moreover, do such climatic parameters as wind speed, wind direction, opacity and pressure influence the temporal and spatial variability of temperature and mixing ratio? Is atmospheric stability the key factor?

The analysis of variance is the first step in answering these queries. For instance, with respect to Table 7.3.1 data, the null hypothesis formulated could be, are the traverse temperatures for each location random samples from populations with the same mean. In other words,

$$H_0: \mu_1 = \mu_2 = \dots = \mu_{126} = \mu_{127}$$

If the null hypothesis is rejected, the second step is to examine the class means in order to see which differences among them appear to be real. The results of the analysis will reveal which cluster of point locations form the urban heat island, which cluster of point locations are urban rural transitional and which cluster of point locations are rural. When urban and rural location variables vary greatly, both their respective clusters will have significant alphas.

As both parametric and nonparametric statistics can be employed in the above analytic steps, each type shall be discussed in the forthcoming sections. Each test will be applied to the data of Table 7.3.1 in order to indicate the degree conclusions are altered when statistics are applied with erroneous assumptions.

7.4.2 The Kruskal-Wallis One-way Nonparametric Anova Test

The Kruskal-Wallis test does not require the assumptions of normality of the population distribution. All that is assumed is:

- (1) all samples are random samples from their respective populations.
- (2) there is a mutual independence among the various samples.
- (3) all random variables are continuous.
- (4) either the k population distribution functions are identical or some of the populations tend to yield larger values than other populations.

The null hypothesis to be tested is that the means of the k populations sampled are identical. The alternative is that they are not identical in at least one of the populations. To perform the test, the scores from all the k samples combined are ranked from the lowest to the highest with the highest score in the total number of observations being given the highest rank N . The sum of the ranks for the observations of each sample is then computed, and is designated R_i for $k = 1, 2, \dots, k$. The test statistic H is defined as:

$$H = 12/N(N+1) \left\{ \sum_{i=1}^k R_i^2/n_i - 3(N+1) \right\}$$

and is distributed approximately as chi-square with $k-1$ degrees of freedom. By comparing the value of H with the critical X^2 value at a given level of significance, $H_0: (\mu_1 = \mu_2 = \dots = \mu_{126} = \mu_{127})$ is tested.

Take for example the temperature data of the first five locations of Table 7.3.1. If we assign ranks to these 15 observations according to size, the results are

	TEMPERATURES	:	RANKS
Location 1:	-15.53 -20.27 -19.43	:	1.0 11.0 5.0
Location 2:	-18.29 -19.91 -20.50	:	2.5 8.0 13.0
Location 3:	-20.20 -20.62 -21.38	:	10.0 14.0 15.0
Location 4:	-18.89 -19.53 -19.65	:	4.0 6.0 7.0
Location 5:	-18.29 -20.11 -20.41	:	2.5 9.0 12.0

Summing the ranks for each we get $R_1=17$, $R_2=23.5$, $R_3=39$, $R_4=17$ and $R_5=23.5$. The computed H value is therefore

$$H = \frac{12}{15(15+1)} \{ [(17)^2 + (23.5)^2 + (39)^2 + (17)^2 + (23.5)^2 / 3] - 3(15+1) \} \\ = 5.3917$$

The critical alpha for chi-square 0.05 at $k-1$ or 2 degrees of freedom is 5.99. Thus, the null hypothesis that $\mu_1 = \dots = \mu_5$ is valid.

The degrees of freedom $k-1$ remain constant in this research undertaking. The respective rejection regions for $H \geq \chi^2_{0.05, 126}$ and $H \geq \chi^2_{0.01, 126}$ are 153.20 and 165.85.

The calculated H value for Table 7.3.1 data is 250.42. The null hypothesis is rejected. The means are unequal. It can hence be stated that a heat island was well formed during traverses 203, 208 and 209. The objective now is to locate the spatial distribution of location temperature means that are statistically significant from certain locations.

7.4.3 The One-way Analysis of Variance

A oneway ANOVA will now be performed on the temperature data of Table 7.3.1 in order to examine the possible effects a parametric statistic would have on a nonparametric data set. Will the conclusions drawn about the null hypothesis be similar to those made in the previous section?

The analysis of variance is an arithmetic device for partitioning the total variation in a set of data according

to the various sources of variation that are present. The technique performs two functions. In complex classifications it is the only simple and reliable parametric method of determining the appropriate pooled error variance. It also provides a new statistic, the variance ratio F . The F test is a single test determining whether sample differences signify differences among the populations or are merely the chance variations to be expected among random samples from the same population. The null hypothesis to be accepted or rejected is similar to that in the previous section. F is defined as:

$$F = \frac{\text{Treatment Mean Square}}{\text{Error Mean Square}}$$

To apply the test, the following assumptions must first be assumed:

- (1) the population of scores is normally distributed with mean μ and a variance σ^2 .
- (2) the variance is the same for all populations and all the scores are independent of each other.
- (3) each score is sampled randomly and independently from a normal distributed population having a mean μ_i and variance σ^2 .

None of the above assumptions however are ever fully satisfied by real data. When assumption two is violated, the obtained significance is usually higher than it should be (Scheffe, 1959). Tests for equality of variance such as Bartlett's have been used in research as a

prerequisite for the calculating of the F ratio but as they in turn are also sensitive to non-normality in the data, particularly to kurtosis, incorrect conclusions are quite probable (Snedecor et al., 1976). With respect to the first assumption, only kurtosis can have any appreciable effect on the F statistic (Scheffe, 1959). The effect in turn is limited to the mean square within groups, for the variance for this grouping depends on the kurtosis of the population. If the sample size is fairly large as in this study, the effects of nonzero kurtosis can be ignored (Lindman, 1974).

The degrees of freedom for among groups or treatments will remain constant at $k-1$ or 126 for each submitted job. The rejections for F vary with alpha and $k(n-1)$ degrees of freedom.

The following example illustrates the stepwise procedure of constructing the analysis of variance table. The formulae are of the conservative, non-calculator type. The data base is the temperature field of Table 7.3.1.

The overall mean of the 381 cases is -21.33 and is represented by $(\bar{X}..)$ in the following formulae. The mean of each of the 127 groups is represented as X (subscript i).

STEP 1: THE TOTAL SUMS OF SQUARES IS:

$$\begin{aligned}
 \sum_{ij} (x_{ij} - \bar{x}_{..})^2 &= (-15.53_1 - (-21.33))^2 + (-20.27_1 - (-21.33))^2 + \\
 &= (-19.43_1 - (-21.33))^2 + \dots + \\
 &= (-15.53_{127} - (-21.33))^2 + \dots + \\
 &= (-19.42_{127} - (-21.33))^2 \\
 &= 2637.8638
 \end{aligned}$$

STEP 2: THE AMONG - GROUPS SUMS OF SQUARES (ERROR) IS:

$$\begin{aligned}
 n \sum_i (x_i - \bar{x}_{..})^2 &= 3 [(-18.41_1 - (-21.33))^2 + \dots + \\
 &= (-18.41_{127} - (-21.33))^2] \\
 &= 841.86
 \end{aligned}$$

STEP 31 WITHIN GROUPS SUMS OF SQUARES IS:

$$= \text{TOTAL SUMS OF SQUARES} - \text{ERROR}$$

The analysis of variance develops from the fact that three different estimates of the population variance can be estimated from data. Since it has been assumed that all 381 observations come from the same population, the total sum of squares of deviations for the 381 observations is 2637.8638. The sum of squares has 380 degrees of freedom. The mean square, $2637.8638/380$ or 6.9417, is the first estimate of the population variance.

The second estimate is the pooled σ^2 and is obtained by dividing the sum of squares within temperatures, 841.86, by its degrees of freedom, 254. The result is 3.3144. The within source of variation is also known as error variation.

The third estimate is calculated between treatment temperatures or $2637.8638 - 841.8600 = 1796.0038$. The mean square being $1796.0038/126$ or 14.2540 . Table 7.4.3.1 summarizes the above results.

TABLE 7.4.3.1

ANALYSIS OF VARIANCE OF TABLE 7.3.1 DATA

VARIATION SOURCE	df	SUMS OF SQUARES	U SQUARE
TREATMENTS	$k-1 = 126$	1796.0038	14.2540
ERROR	$k(n-1) = 254$	841.8600	3.3144
TOTAL	$kn-1 = 380$	<u>2637.8638</u>	

The calculated F ratio is $14.8476/3.3132$ or 4.4813 which is significant at all alpha levels. The null hypothesis is therefore rejected.

The question now posed is why does the ANOVA test reject the null hypothesis when administered on a data set that has a non normal distribution? The answer lies in the data. That is, the prevailing climatic parameters during the days traverses 203, 208 and 209 were conducted were such as to optimize heat island development.

The example chosen is unique. As will be shown latter, a significant H value does not connotate a significant F ratio.

For the required ANOVA formulae, see Huntsberger et al., (1973).

7.4.4 Kruskal-Wallis Multiple Comparison Rank Sums

If the Kruskal-Wallis H statistic is sufficiently large to reject the null hypothesis for any alpha level greater or equal to 0.05, we can conclude that the k populations are not all the same. The question now posed is which populations differ from which others. When the location model is assumed, this question reduces specifically to which populations have different medians. Since the goal is simultaneous statistical inference, a special technique known as multiple comparisons should be used (Hollander et al., 1973).

Although several nonparametric methods of simultaneous multiple comparisons between the location of all pairs of two of the k populations have been formulated, the procedure described here is attributed to Dunn (1964). As there are 8001 possible example combinations to be tested for significance, the following procedure would be used. Arrange the population means from maximum to minimum value or vice versa as in SPSS, keeping track of each mean's representative location simultaneously. It can then be stated that population means ($R_{i,max.}$) and ($R_{j,min.}$) seem to be different if the following inequality is satisfied:

$$|\bar{R}_i - \bar{R}_j| \geq z_{1-(\alpha/2)} \sqrt{S^2 \frac{N-1-H}{N-k} \left(\frac{1}{n_i} - \frac{1}{n_j} \right)}$$

where

- H = Kruskal-Wallis H Statistic
k = the number of sample populations
N = the total number of observations
 \bar{R}_i = R_i/n denote the mean of the ranks corresponding to the i th maximum sample.
 \bar{R}_j = R_j/n denote the mean of the ranks corresponding to the j th minimum sample.
 $z_{1-(\alpha/2)}$ = the critical z value or the quantile point of the standard normal distribution that corresponds to a right-tail probability of $1-(\alpha/2)$ with $N-k$ degrees of freedom.
 S^2 = $N(N+1)/12$

For further explanation of the above statistic see Conover(1971), page 230. If the above inequality is satisfied, the next pair of means to be analyzed would be $(R_{i,max.})-1$ and $(R_{j,min.})+1$. The process repeats itself until the inequality can not be maintained at 95 percent of the standard normal distribution. The maximum $z_{1-(\alpha/2)}$ percentile is 99.99995. For this study, eight $\alpha/2$ groups were calculated.

With reference to the temperature data of Table 7.3.1, the H value calculated was 259.42 which clearly leads to the rejection of the null hypothesis. Because of this rejection, the multiple comparison procedure may be used. With S^2 equal to $381(382)/12$ or 12128.50; k constant at 127

and both n_i and n_j equal to 3, the right side of the above equation reduces to

$$|\bar{R}_i - \bar{R}_j| = z_{1-(\alpha/2)} (64.2259)$$

The critical inequalities required for significant mean rank differences at various percentiles of the standard normal distribution for this example are listed in Table 7.4.4.1. For a complete z value table see Table 9, Pearson et al., 1966. The mean ranks per location and their group memberships are listed in Table 7.4.4.2.

TABLE 7.4.4.1

CRITICAL INEQUALITIES OF MULTIPLE COMPARISON OF TABLE 7.3.1 DATA

$\alpha/2$	z	INEQUALITY
0.050	1.960	125.88
0.025	2.326	149.39
0.010	2.576	165.45
0.005	3.090	198.46
0.001	3.291	211.37
0.0005	3.891	249.90
0.00005	4.417	283.69
0.000005	5.327	342.13

TABLE 7.4.4.2

MULTIPLE COMPARISONS OF TABLE 7.3.1 TEMPERATURE DATA

LOC	MEAN	ALPHA	LOC	MEAN	ALPHA	LOC	MEAN	ALPHA
67	352.67	0.00005	115	248.50		97	145.50	
68	342.67	0.00005	52	246.33		87	141.17	
65	327.00	0.00005	10	240.33		89	141.00	
69	324.17	0.00005	110	239.50		96	136.67	
66	321.00	0.00005	48	239.00		44	136.50	
119	321.00	0.00005	113	236.83		84	132.00	0.050
70	308.33	0.00005	9	236.17		83	130.67	0.050
121	305.00	0.00005	7	235.50		15	124.00	0.050
118	304.67	0.00005	8	233.83		42	121.00	0.050
63	304.00	0.00005	47	228.67		105	120.33	0.050
1	300.83	0.001	78	227.83		43	115.83	0.025
127	300.83	0.001	51	227.17		101	107.33	0.025
120	300.23	0.001	112	220.56		98	105.00	0.010
55	299.33	0.001	12	219.33		103	99.67	0.010
124	299.33	0.001	91	218.50		99	99.17	0.010
117	299.17	0.001	111	218.00		102	97.33	0.010
64	294.33	0.001	50	209.67		100	89.17	0.010
72	292.83	0.001	93	206.83		34	74.00	0.005
56	291.83	0.001	49	204.83		18	69.17	0.001
4	291.83	0.001	109	204.17		30	69.00	0.001
123	288.67	0.001	3	201.33		33	67.00	0.001
125	285.17	0.001	92	200.33		24	65.33	0.001
126	284.67	0.001	17	198.67		27	63.67	0.001
124	284.00	0.005	79	192.67		41	63.17	0.001
53	283.00	0.010	94	192.33		35	63.00	0.001
58	281.67	0.010	108	190.83		25	62.00	0.001
6	281.67	0.010	70	187.83		19	58.33	0.001
59	277.67	0.010	11	186.67		26	56.83	0.001
60	271.33	0.010	95	185.67		28	55.83	0.001
71	268.50	0.025	89	183.67		32	53.00	0.001
2	265.33	0.025	107	183.33		22	51.67	0.001
5	263.17	0.050	13	173.17		36	51.67	0.0005
57	263.17	0.050	46	169.50		20	49.00	0.0005
73	261.83	0.050	88	169.00		31	48.00	0.0005
54	260.57	0.050	45	168.33		39	47.00	0.0005
116	260.50	0.050	14	167.50		40	42.67	0.0005
75	258.67		80	165.67		38	42.33	0.0005
62	257.67		104	165.67		29	40.33	0.00005
76	256.17		16	160.50		37	35.17	0.00005
61	252.67		82	157.33		23	34.33	0.00005
77	252.17		85	149.50		21	23.33	0.00005
114	252.00		90	148.67				
74	251.67		106	146.17				

The difference in the extreme rand means, $352.67 - 23.33 = 329.34$, is greater than the critical inequality of 283.69 though less than the critical inequality of 342.13. Hence, the difference is significant at an alpha of 0.00005. Comparisons (68,23), (65,37) and (69,29) also yield significant inequalities at this alpha level. Thus, there are eight maximum-minimum alpha and eight minimum-maximum alpha clusters.

This procedure shows that whereas there is only a single urban heat island nucleus centred on Portage Avenue between Donald and Westbrook, two distinct rural cold nuclei exist. One is located within the Assiniboine Park complex, points 21 and 23, while the other is situated approximately 16.6 km. northeast of point 67 at the Perimeter-Highway 221 Cloverleaf intersections. A third cold sink nucleus is present at the junction of St. Mary's Road and Highway 101; point 101. The inequality, however, is only significant at an alpha of 0.025. Respective temperature deviations per kilometer from nuclei locations 67, 101, 37 and 21 to the airport meteorological monitoring site with respect to direction, are 3.06°C . at 275° , 0.51°C . at 323° , 0.08°C . at 140° and -0.42°C . at 339° .

Fifty-five of the remaining comparisons have insignificant inequalities and hence can be classified as transitional.

7.4.5 Bonferroni Multiple Comparisons Method

There are several parametric alternatives to the nonparametric Kruskal-Wallis Multiple Comparisons Rank Sums statistic. However, because of the great number of possible comparisons, 8001 alone in the above data example, a sequential test is required.

Bonferroni t statistics was chosen as it is conservative and uses a single range for testing all $k(k-1)/2$ planned comparisons. The procedure has the property that if alpha E is defined as:

$$Ae = \frac{\alpha}{k(k-1)/2}$$

and is taken to be the level of significance for a t test, then the probability of making a type 1 error in testing all $k(k-1)/2$ possible differences will be at most alpha (Winer, 1971). Winer(1971) redefines the above alpha as a per experiment level of significance. It is the number of type 1 errors with respect to tests on sample differences divided by the number of experiments.

However, it should be noted that the Bonferroni t method, as do most multiple comparison techniques, therefore require a higher significance level as the number of comparisons k

increase. The significance level thus required for the data of Table 7.3.5 would be $0.05/(127(126)/2)$ or 0.0000063. To obtain such an untabled percentile, linear interpolation off z distribution graphs would be required. Moreover, the significance level corresponding to the lowest alpha value for the previous Kruskal-Wallis statistic would be $0.000005/8001$ or 0.00000000062. Thus, statistics have to be calculated in order to analyze the data statistically a futile exercise.

Nevertheless, the critical distance, d , that a comparison must exceed in order to be declared significant is given by:

$$d = t_{1-(\alpha/2); N-k} \sqrt{\text{mes} \left| \frac{1}{n_i} - \frac{1}{n_j} \right|}$$

where MES is the mean error square. The other symbols carry the same meanings as previously defined.

The critical distance so computed is more conservative than Tukey's HSD test though more liberal than Scheffe's S Method (see Kirk, 1968). For further discussion refer to Neter et al., 1974; Sarhan et al., 1962 and Wike, 1971.

7.4.6 Conclusion

In statistical analysis, tests of normality such as the chi-squared goodness-of-fit statistic, determine whether or not parametric or nonparametric statistics should be

employed. If the null hypothesis that there is no difference between the expected and observed frequencies is accepted, the former statistic type should be used. If H_0 is rejected, the latter should be implemented. As most of the statistics described in this section are supported by SPSS, SAS and other computer statistical packages, minimal computational error can be expected. However, the major drawback is that the various options available per statistic are limited. For example, alpha values are rarely lower than 0.0001. Therefore, a minimal amount of computation is required.

7.5 Summary

Unlike the majority of urban climatic studies, emphasis shall not be placed upon the descriptive analysis of space studies but upon the validity of a group of data being analyzed. Cluster analysis will be employed to identify the number, nature and composition of relatively homogeneous groups which together make up the data set under scrutiny. As virtually no information is known about the population from which the samples are taken, nonparametric statistics only shall be implemented. With the assumption of non normality, tests of normality need not be performed on the data. This is an important decision, for although the goodness-of-fit test is supported by SPSS, excessive modification of the test data is required prior to the submission of a job specifying this task. Data must be

manually categorized, the expected frequencies must be computed, and each category must be recorded in the data field. Furthermore, small expectations are not allowed. Hence, this statistic would consume a great deal of time and be subjected to varying degrees of computational error.

The parametric ANOVA will be calculated, though used only as a descriptive statistic. The F ratio will be compared with the H value in order to point out that significant H value data does not necessarily have corresponding significant F ratios. The main clusters will then be subjected to non-parametric statistical tests. If the nonparametric ANOVA statistics indicate insignificance, sub-clusters will be analyzed. If the null hypothesis is again accepted by the above tests, analyses shall cease. If rejected, analysis will parallel the discussion in the chapter.

LIST OF REFERENCES

- Anderberg, M.R., 1973: Cluster Analysis for Applications. Academic Press, New York, 359pp.
- Bell, W.C., 1974: An Analysis of Temperature, Lapse Rate, and Wind in the Lower 810' Near Winnipeg. PhD. Thesis, University of Edinburgh, 171pp.
- Brinkmann, W.A.R., 1970: The Chinook at Calgary (Canada). Arch. Met. Geophys. Brokl. B., 18, 269-298.
- Fisher, R.A., 1935: The Design of Experiments. Edinburgh, Oliver & Boyd., 150pp.
- Gregory, S., 1964: Climate. In The British Isles A Systematic Geography. Edited by J. W. Watson and J. B. Sissons. Nelson, London, 53-73.
- Hollander, M. and Wolfe, D.A., 1973: Nonparametric Statistical Methods. New York, John Wiley and Sons, 245pp.
- Hope, K., 1968: Methods of Multivariate Analysis. London, University of London Press Ltd., 288pp.
- Huntsberger, D.V., and Billingsley, P., 1975: Elements of Statistical Inference. Boston, Allyn & Bacon, Inc., 349pp.
- James, R.W., 1970: Statistical Inference and Synoptics. Meteorol. Rdsch., 1, 10-14.
- Kirk, R.E., 1968: Experimental Design Procedures for the Behavior Sciences. Belmont, California Brooks/Cole Publishing Co., 577pp.
- Lachenbruch, P.A., 1975: Discriminant Analysis. New York, Hafner Press, 125pp.

- Lindman, H.R., 1974: Analysis of Variance in Complex Experimental Designs. San Francisco, W.H. Freeman & Co., 352pp.
- Marascuilo, L.A. and McSweeney, M., 1977: Nonparametric and Distribution-Free Methods for the Social Sciences. Monterey, California, Brooks/Cole Publishing Co., 556pp.
- Mather, P.M., 1976: Computational Methods of Multivariate Analysis in Physical Geography. London, John Wiley & Sons, 532pp.
- Miller, R.G., 1962: Statistical Prediction by Discriminant Analysis. Met. Monogr. Amer. Met. Soc., 4(25), 54pp.
- Neter, J. and Wasserman, W., 1974: Applied Linear Statistical Models. Homewood, Illinois Richard D Irwin, Inc., 842pp.
- Pearson, E.S. and Hartley, H.D., 1966: Biometrika Tables For Statisticians Volume 1 London, University of Cambridge Press, 264pp.
- Perry, A.H., 1968: The Regional Variation of Climatological Characteristics with Synoptic Indices. Weather, 23, 325-330.
- Sarhan, A.E. and Greenberg, B.G., 1962: Contributions to Order Statistics. New York, John Wiley & Sons Inc., 482pp.
- Scheffe, H., 1959: The Analysis of Variance. New York, Wiley & Sons Inc., 190pp.
- Snedecor, G.W. and Cochran, W.G., 1976: Statistical Methods. Ames, Iowa; Iowa State University Press, 593pp.
- Suzuki, E., 1969: A Discrimination Theory Based on Categorical Variables and Its' Application to Meteorological Variables. Jour. Met. Soc. Japan., Ser. 2, 47, 147-158.

Tryon, R.C. and Barley, D.E., 1970: Cluster Analysis. New York, McGraw-Hill, 348pp.

Wike, E.L., 1971: Data Analysis A Statistical Primer for Psychological Students. Chicago, Aldine/Atherton, 200pp.

Winer, B.J., 1971: Statistical Principles in Experimental Design. New York, McGraw-Hill Book Co., 907pp.

Wishart, D., 1978: Clustan-User Manual Third Edition. Edinburgh, Edinburgh Press, 198pp.

CHAPTER 8

DATA ANALYSIS

8.1 Introduction

Contradictory questions have always plagued urban heat and humidity island studies. Some earlier works suggested, for example, that lower relative and absolute humidities are found in urban areas than in the surrounding country side while later work disclosed increased absolute humidities over the urban areas. Both of these contradictory observations, however, may be valid in particular circumstances. The former is caused by the rapid run-off and the lack of evapotranspiration in highly urbanized sectors. The second circumstance can occur when urban combustion and industrial cooling processes as well as many planted trees, add large amounts of water vapor to the atmosphere.

This thesis has not been designed to settle such contradictory questions as the above, but to indicate that such contradictions may be correct depending on such factors as distribution and specific location of measurements. That is, any area of the size under consideration, unless absolutely flat and without surface differentiation, has many microclimates. Each microclimate in turn varies not

only with the constant change in the state of the atmosphere, but also with the nature of the ground and the activity of the city. Any information collected is thus representative of the site and situation at which measurement occurred.

Thus, henceforth, our assessment is for the entire City of Winnipeg, situated in Latitude $49^{\circ}54'N.$, Longitude $97^{\circ}08'W.$, midway between the Pacific and Atlantic Oceans, at the confluence of the Red and Assiniboine Rivers, 230.74m above sea level. The mixing ratio and temperature data analysis represents only the climatic variations for the fixed point locations on the itinerary at which the raw measurements were recorded. No conclusions will and can be drawn regarding the variations of the above climatic parameters for areas not traversed by the itinerary. As the commencement and termination of temperature and dew point data acquisition for this study closely paralleled the invasion of the drought area, centred in South Dakota, into the Eastern Prairies-Northwestern Ontario Regions and its eventual dissipation in early May, 1977, the forthcoming analysis and discussion shall be representative only for the above period of time for which the data was collected (see Section 4.9).

Cluster selection and subsequent statistical analysis of the cluster data will proceed according to the format outlined in the previous chapter.

The examination of the various cluster analysis dendrograms will yield the final data groupings for which further statistical analysis is warranted. The selection method applied to achieve the above goal is as follows.

The dendrogram produced by the cluster analysis with the following masked climatic parameters opacity, pressure, wind speed and wind direction, will be compared to the dendrogram which was generated with no masked variables. Cluster case alterations will be noted. Next, the dendrogram with only one of the above four variables masked will be examined with the no mask plot. The process repeats itself until all the possible combinations, 15 in number, are analyzed. Clusters with the least internal variability will be selected.

A similar procedure will be undertaken with respect to the 15 dendrograms generated from the linear interpolated surface to 500mb radiosonde data matrix for Winnipeg.

The final choice from each data matrix will also be compared. However, as the estimated radiosonde data was calculated from and for the time 00Z and 12Z, only traverses which were standardized to the comparable times of 0900 and 1700 hours will be compared. The end result will be the cluster organization on which statistical analysis will be performed. The cells chosen will be labelled according to air mass properties. The six possible classifications are

cA,cmA, mA, mP, mT and cT. Wherever applicable, a distinction will be made in a cluster between those traverses which were undertaken when the prevailing climatic and/or synoptic conditions were such as to either prevent vegetative budding or cause a permanent cease of photosynthesis, and those traverses which were undertaken when the prevailing climatic and/or synoptic conditions were such as to encourage and maintain a vegetative ecotone.

The selection of clusters for analytic purposes shall follow. However, the procedure will deviate slightly from that discussed in the previous chapter.¹ No longer will all fusions of a sub-cluster which has rejected the null hypothesis be analyzed as a whole. Nor will all the various significant fusions of a sub-cluster which has

¹ The need for change became apparent only after a considerable number of statistically analyzed clusters were compared for similarities of trend form and three dimensional imagery. In fact, analysis had progressed well into the continental Tropic air mass sub-cluster zone when it was noticed that trend formulae were more powerful for clusters which had a fewer number of traverse component. For the latter, the slopes between troughs, plains and ridges on three dimensional plots were of greater inclination. Moreover, special features, such as cold sinks and moisture peaks, were of greater intensity. Dominant bluffs replaced the gentle curved summits which were prevalent on those plots which had been constructed from data groups composed of more than 15 traverses.

Upon re-examination of the cluster data, it was noted that, in the majority of cases, a small number of traverses yielded such an extremely large Kruskal-Wallis test statistic that it maintained a significant alpha for all sub-clusters of which it was a component of. Hence, to remove the undesirable noise from the data analysis, a new procedure for selecting clusters for further statistical examination had to be formulated.

accepted the null hypothesis be analyzed. Instead, statistical examination will be restricted to those fusions which carry the most significant weight within their sub-cluster grouping regardless of their cyclic position in that sub-cluster grouping. Furthermore, if two mutually exclusive cycles, each yielding large test statistic values, are fused, further analysis will only proceed if the resultant H value is greater than either of the two values prior to fusion. If the Kruskal-Wallis statistic decreases, the two fusions will be treated as unique. As long as the test statistic H increases, the number of mutually exclusive groupings fused are irrelevant.² Wherever pertinent, change in the climatic parameters listed above, stability and the kinetic energy due to the velocity difference between the surface and 950mb level, will be examined in order to locate differences which might explain for H value variations.

The following example best illustrates the above procedure and the reasoning associated with it.

² Note that large test statistic values carry with it critical alpha values that approach infinite zero. This critical level alpha, known also as the probability level and significance level, is the smallest significant level at which H_0 , the null hypothesis, would be rejected for the given observations. The critical level should not be confused with type 1 error probability alpha which was set at 0.05 for this thesis. The latter represents the maximum probability of rejecting a true null hypothesis. As long as the critical level is less or equal to the type 1 error level, the null hypothesis is rejected.

Table 8.4.1.3a consists of traverses undertaken during cold maritime Arctic air mass (mAk) engulfment. It is the leftmost portion of the second major cluster group. The latter incorporates 65 itineraries. The cycle number, the actual change of error sum of squares at fusion, d_1 , the Kruskal-Wallis test statistic H corrected for ties and its corresponding significance are listed on the left. The data is representative of the temperature variable only as there is only 2 significant mixing ration fusions in the 32 cycles.

Note that the H value for cycle 239, 166.109, is quite low for a 35 traverse fusion especially when it is compared to the chi-square of either cycles 159 or 161. Respective values of the latter are 273.109 and 262.442. The latter two cycles are not only mutually exclusive. Each member traverse fusion prior to these cycles yielded H values which did not regress. That is, when traverse 9 was fused to cycle 59 components, the test statistic increased 72.892 units from 169.514. When traverse 222 was added, the value jumped another 20.036 units. A similar reaction was noted for the union of cycles 69 to 75, thus forming cycle 159.

Whenever another group of traverses were added to these cycles, the H value declined sharply. For instance, when cycle 161 and 139 were joined, the test statistic yielded 118.842 which had a significance of only 0.662.

Likewise, when cycles 108 and 159 were combined to form cycle 201, the previous high H value of 273.109 fell to 137.801. A drop of 135.308 units.

From the above results, two hypotheses can be deduced. Either cycles 159 and 161 contribute the most weight to cycle 239 as a unit or they contribute the most information as two unique entities.³ The former deduction is false for upon the uniting of these cycles, the chi-square declined to 199.447. However, the latter deduction proved quite valid. When cycle 239 was tested with the traverse components of cycles 159 and 161 removed or masked from the Kruskal-Wallis test calculations, the chi-square fell to 93.812. This value had an associated critical alpha level of 0.986. The null hypothesis that all the k population distribution functions are equal was therefore accepted.

³ Although there are four groups of paired traverses in Table 8.3.2.1 that have critical alpha values well below the set level of significance of 0.05, they shall not be considered for further examination. The reasons why cycles 1, 4, 17 and 34 shall be excluded lie in the inconsistencies one finds in nonparametric texts and articles regarding the size of k random samples required for the Kruskal-Wallis Test. For instance, Conover (1980, pages 236-237) states that for two samples, the statistic in question is equivalent to the Mann-Whitney test whereas Marascuis (1977) states otherwise. Both the above authors and those dealing with this dilemma provide adequate theories backing their particular hypothesis. However, all agree that the chi-square approximation of the Kruskal-Wallis test increases satisfactorily when the random sample size n is greater or equal to 5 and k is greater or equal to 3. Therefore, the decision rule taken here shall be that further statistical analyses will be conducted on cycles where k is equal or greater than three.

The usage of the above procedure will terminate once a representative selection of air mass type traverse fusion groups has been collected. Further statistical analysis will proceed according to the outline discussed in the previous chapter.

To aid in the interpretation of the results, trend surface analysis maps and their three dimensional counterparts shall be constructed.⁴ The former is a multivariate statistical technique that seeks to isolate broad scale variation or trends from local variations. This is achieved by fitting a trend function to a set of data values using a least-square criterion. That is, if X and Y are the locational rectangular co-ordinates of the data, the sum Z, the areally-distributed variable, is such that the sum of squared deviations of X with respect to Y, or vice versa, is minimized. The equation describing the trend surface may be linear to polynomial. The higher the order of the surface, the greater the minimization. However, the increasing value of the coefficient of determination⁵ is frequently an index indicating when to stop increasing the

⁴ Trend surface analysis maps are one of several map electives supported by the Symap(1976) computer package. The generated Z functions of order 6, were incorporated into the G3D Procedure of SAS/Graph (1981, pages 97-101) in order to obtain the three dimensional equivalent. For the required procedures and formulae, refer to the above references.

⁵ The coefficient of determination, R^2 , is the proportion of the variation in the original map accounted for by the trend surface.

surface complexity. When R^2 is maximized, most of the pertinent information has been utilized in the calculation of the trend formula.⁶

To ensure that questions pertaining to the validity of using a multivariate statistical technique on known nonparametric data are kept to a minimum, neither the raw temperature or mixing ratio data from the selected fusion groups nor their corresponding Kruskal-Wallis rank sums per itinerary location will be utilized in the calculation of the Z function. Instead, a coding system based upon the critical alpha levels obtained between itinerary location population pairs using the Kruskal-Wallis Multiple Comparison test statistic, was devised. The code values range from 1 to 11 and their distribution is symmetrical.

For a comprehensive understanding of this coding system, refer to Tables 7.4.4.1 and 7.4.4.2, pages 197 - 198. The smallest inequality to be satisfied by paired comparisons of Table 7.4.4.2 data is 125.88. This is for the fixed alpha of 0.05. From Table 7.4.4.2 it can be seen that there are 55 locations or 27 pairs of locations plus one nonpaired location which can not meet this criterion. The largest mean rank sum of this group is 258.67 for location 75 whilst the lowest is 136.50 for location 44.

⁶ For further discussion on trend surface analysis, equations and examples, refer to Harbough et al. (1967, pages 62-87) and Mather (1976, pages 117-173).

The respective difference on comparison is 122.17. Thus all locations which have no critical alpha level listed in Table 7.4.4.2 are given a code 6.

There are five pairs which have critical levels equal to 0.05 and only two pairs with significance levels of 0.025. The high portion of this group composed of locations 71,2,5,57,73,54 and 116 shall be coded 7 whereas the low portion made up of locations 84,83,15,42,105,43 and 101 shall be coded 5.⁷ Respective mean rank sum ranges are 268.50 through 260.50 and 132.00 through 107.33.

The above process would have been continued until all the critical alpha levels of Table 7.4.4.1 would have been coded.

The high and low portion codes per critical alpha level for subsequent analysis have been listed in Table 8.1. Also shown are their associated symbols which will appear on

⁷ The critical alpha zones 0.05 and 0.025 have been combined to form a single coded unit because calculations based upon the old chosen, now defunct, cluster fusion groupings had shown that very few multiple comparisons yield critical alphas of 0.025. The same held true for critical alpha values of 0.005. The latter was joined with 0.001 critical levels.

When the old three dimensional plots of the trend surface maps were analyzed, it was discovered that the locations yielding 0.025 and 0.005 significance levels usually were the transitional areas between plains and steep ridges or troughs and steep ridge walls. The combination of these two levels had little noticeable affect on the plots. In fact, less computer resources and units were utilized on combination.

the Symap trend surface analysis maps.

TABLE 8.1

CODE ASSIGNMENT FOR CRITICAL ALPHA LEVELS OF
KRUSKAL-WALLIS MULTIPLE COMPARISON RANK SUMS DATA

CRITICAL ALPHA	PORTION CODE		SYMAB SYMBOLISM	
	HIGH	LOW	HIGH	LOW
<0.050		6		++++
≥0.050	7	5	XXXX	====
≥0.010	8	4	0000	'-'-'
≥0.001	9	3	0+0+	----
≥0.0005	10	2	0AVX	''''
≥0.00005	11	1	HHHH	LLLL

In the concluding portions of Chapter 8, emphasis shall be placed upon generalized summation. Parameters which have influenced not only the primary sub-cluster selection but also the end results will be disclosed. Questions dealing with the spatial and temporal relationship between temperature and mixing ratios shall be answered.

8.2 Dendrogram Selection

The use of the masking facility of procedure Correl as a means of indirectly obtaining a local optimum 253 cycle cluster proved to be quite effective. As could be expected, however, both the 15 traverse and 15 radiosonde cluster analyses yielded unique dendrograms. Only one

sub-cluster, that composed of stable cA and cMA air masses, showed remarkable similarity between different dendrograms including those generated by radiosonde data. This unexpected finding is significant because the radiosonde data for all layers from the surface to 500mb, was linearly interpolated from data gathered at The Pas, Manitoba, Bismarck, North Dakota and International Falls, Minnesota. Therefore scrutinous investigation of the climatic parameters causing this is warranted. Note that this sub-cluster indicates that linear estimation of upper air data for a particular location can yield representative results. It will be shown later that such situations only occur if all stations involved in the calculation have similar synoptic conditions. Once a synoptic condition alters at any of the meteorological stations used in the generation of the estimate, representativeness becomes questionable.

The examination of this sub-cluster will also indicate the logical difficulties or obstacles encountered in determining whether or not a particular sub-cluster should be the parent sub-cluster from which traverse fusions would be selected for further statistical investigation.

The manner in which 25 traverses, both cA and cMA, were fused by nine different clustan jobs each with varied masked climatic variables is listed in Table 8.2.1. The computer

job name, the number of traverses fused, TF and the climatic variables to be masked are listed on the left. Respective codes for wind direction, wind speed and opacity are WD, WS, and OP. Traverse codes are listed vertically at the top. Asterisks appear under those variables masked per job and those traverses which are fused as a unit. Capital letter S replaces the blanks for those Clustan-1C2 computer runs which yield dendrograms with parallel fusions. Blanks under a specific traverse indicate no association with prior fusion members.

TABLE 8.2.1

CLUSTAN-1C2 JOB FUSION VARIATION OF cA AND cMA TRAVERSES

JOB NAME	TF	WVO DSP	12322122222222222212122222					
			0191010001111180910000					
			7091223893456734585601					
CT253M00	25		SSSSSSSSSSSSSSSSSSSSSSSSSSSS					
CT253MOP	24	*	SSSSSSSSSSSSSSSSSSSSSSSSSSSS					
CT253SOP	23	**						
CT253DOP	17	* *						
CT253M03	17	***						
CT253MOS	17	*	SSSSSSSSSSSSSSSSSSSS					
CT253MSD	17	**						
CT253MOD	23	*						
RSONDE	12		1	12	22	1	2	21
			3	31	11	3	1	13
			H	HH	HH	H	H	HH

The most noticeable trait of the above table is its similarity with cycle 225 of Table 8.3.1.1. Traverses 1 through 217 are always fused as a unit regardless of the

number of climatic parameters masked or the manner in which the climatic parameters were combined prior to masking. Observe also that traverses 195 through 201 either form a unit which shall be shown in the following section to yield a significant H value or they are not clustered at all. Traverses 183 and 204 are not fused with any of the above major components once variable masking is initiated. Recall that in Section 8.1 it was decided that traverses such as these two traverses would not be statistically analyzed because of their negative effect on the calculation of the H value. That is, when fused with the highly significant group 195 through 206, the null hypothesis was accepted rather than rejected. The radiosonde cluster dendrogram also excludes traverses 183 and 204 as well as traverses 195 and 218. Examination of both the prevailing climatic variables recorded for each traverse and the linear interpolated radiosonde data for the days on which traverses were conducted reveal the reasons why the above discrepancies have occurred.

Traverse 183 through 201 were taken when continental maritime Arctic air engulfed the research zone whereas itineraries 1 through 217 were conducted through continental Arctic. The former group in turn could be classified into a moist or dry category. The mean traverse temperature and mixing ratio for itineraries 183 and 204 were -7.9°C . and 0.8662 g/kg . These parameters were 4.1°C . and 0.1629 g/kg

greater than the calculated mean for fusion 195 through 201 and approximately 13.8°C. and 0.5572 g/kg greater than the average estimate for CA traverses 1 through 217. Respective virtual temperature² of the air between the surface and the 950mb level for T183 and T204 was -7.0°C. and -10.6°C. Within eight hours, at the commencement of T184, cold maritime Pacific air had reoccupied all pressure levels from the surface to 500mb. The mean adjusted virtual temperature for the lowest layer at the beginning of T184 was in excess of 4.8°C.

Similarly, though inversely, at the commencement of traverse 205, the mean adjusted virtual temperature had fallen 5.0°C. By December 6, 1976 at 0600 hours, CA air was dominant at all pressure levels. The estimated mean virtual temperature was approximately -26.2°C. Ice crystals were reported from 6.55 A.M. to 8.14 A.M. by the Winnipeg International Airport.

Hence, traverses 183 and 204 are unique. They were made in moist continental maritime Arctic.

² Virtual temperature is a fictitious meteorological parameter. It is the temperature that dry air must have in order to have the same density as the moist air at the same temperature. As moist air is less dense than dry air, virtual temperature is always greater than the actual temperature. The difference, however, is only a few degrees. Virtual temperature is used as a corrective function for detailed accurate prognoses.

Traverses 195 and 218 were not fused on the radiosonde dendrogram with the remaining cMA itineraries because the estimated kinetic energy available for vertical air parcel displacement due to the velocity difference between the surface and the 950mb level was extremely low for both.³ Respective values in Newtons per meter squared are 0.00025 and 0.4559. These values are negligible when compared to the approximate mean calculated for the cA traverses. That is, 3.4648 N. per m².

Magnitudes, however, of the above parameter are of no consequence when atmospheric conditions are such that vertical air displacement is suppressed. Inversions connote absolute stability and hence turbulent forces are minimized. Such was the calculated hypothesized case for each of the traverses listed in Table 8.1.1. The estimated dQ_{se}/dz for the latter traverse group was 0.0175. The greatest dQ_{se}/dz , 0.0619, was recorded for traverse 183. The pseudoequivalent potential temperature increased 10.53°K. in 164.4 meters: the largest increase noted in the research.

Unfortunately, no actual data exists for either the Winnipeg Meteorological monitoring site or the research zone which can either dispute or validate these assumed calculations. Furthermore, the above estimates may be

³ For formulae and discussion, see Gossard et Hooke, 1975, pages 188-189.

correct for areas similar in nature to radiosonde sites, such as Winnipeg's meteorological monitoring site. For urbanized areas, however, such as industrial-manufacturing sectors, the Central Business District, commercial shopping conglomerations and high density residential zones, these figures become quite questionable. Each of the latter urban morphological sites are not only capable of generating their own unique microclimates but are also contributors to the uniqueness of an urban circulatory system.

Referring to the no masked variable dendrogram CT253M00, Table 8.2.1, traverses 195 and 218 were fused on cycle 64 with $d1$ equal to 0.012. Their union was unique as opacity rather than wind speed was the contributing fusive force. Respective opacities, in tenths, and windspeeds, in kilometers per hour, are 8 and 14.83 for the former and 9 and 31.51 for the latter. The prevailing wind directions were 172° for traverse 195 and 180° for traverse 218.

Although the difference in windspeed was 16.68 km per hour, the temperature variances were similar, being 0.478 for T195 and 0.466 for T218. For both itineraries, the maximum temperatures were located on Portage Avenue between Donald and Main while the minimum temperatures were located at point 33, on the Highway 101-mid Portage Overpass. Respective minimum and maximum temperatures for T195 and T218 were -9.1, -12.2 and -7.7, -11.4.

All prospects of similar comprehensive subcluster analysis were eroded by the extreme traverse fusion variability within each of the subclusters regardless of whether the subclusters were taken from the radiosonde dendrogram or from one of the several traverse-climatic parameter masking dendrograms. It soon became apparent with respect to the radiosonde estimates that in future studies, the following procedures should be adopted. Radiosondes should be launched simultaneously upwind, within the urban heat island generating area and downwind of the research zone, with the commencement of each traverse. Only then can true upper air profiles for the research area be constructed. If the above procedure is economically and physically impossible, the traverses should commence at local times corresponding to 00Z and 12Z: the times upper air stations launch radiosonde equipment. This will eliminate the need for a double linear interpolation of the radiosonde data is not required. That is, the first interpolation is for 00Z or 12Z using 3 or more upper air meteorological monitoring stations while the second interpolation is for the hours between 00Z and 12Z. If both of the above procedures can be carried out, then the results of both should be analyzed. The question of whether these results are comparable will now be addressed.

Wind direction and wind speed are two of the main climatic parameters determining the spatial and temporal

variability of both temperature and mixing ratio, especially within the time period September 21st-March 21st, (Sections 1.5, 2.1 and 6.2). Furthermore, since opacity can affect variability as shown by the example above, the dendrogram printed for the cluster analysis utilizing the total number of continuous variables 198 (no climatic variables being masked) should be chosen as the logical basis for subcluster selection and subsequent statistical analysis.

Nkemdirim(1977) listed both the above parameters among the most important determinants of heat island variability for Calgary, Alberta, and added to this list the heat emission from fuel consumption. Moreover, Kamst et al.(1980) singled out the latter most influence as the primary local diurnal wind variation control during the summer season in the Kwinana Industrial Region, 32 km southwest of Perth, Australia. A similar control could not even be attributed to the regions' topography. The latter ranges from coastal plains in the northern part to sand hills of heights 70 meters in the southern extremities.

Such a choice of dendrograms, however, would be contradictory to the hypothetical assumptions maintained throughout this thesis. It has been continuously emphasized that no assumption, whether climatological or statistical, would be made without adequate substantiation.

It is known that the urban temperature and humidity islands interact with the general air flow and if such a flow is absent, the city's own circulation motion is set into motion (Landsberg, 1974, pages 738-744). Kiruma (1976) indicated that the chief factors influencing this circulation are non-uniform heating from below, whether natural or anthropogenic, momentum and heat diffusion, atmospheric stability, prevailing winds and the non-linear effects of advection. Increased roughness of urban surfaces result in the deceleration of the wind. Mass convergence tendencies thus are replaced by turbulent uplift. The outcome is a change in the wind direction and an increase in the wind speed for the flow must re-adjust to balance the forces now acting (Oke, 1977, page (35-36)). Shreffler (1978, 1979) shows that convergence in St. Louis is stronger during convective instability than with intense heat islands and intense rural stability. Wind speeds are altered greatly by this occurrence.

Unfortunately, simultaneous differences between urban and rural wind speed and wind direction have never been documented for the research zone. Nevertheless, it shall be shown with the aid of the trend maps that Winnipeg maintains its own unique circulatory system. The wind direction and speed measured at the Airport is for all practical purposes, representative of that location only. This assumption aids in explaining why distinct traverses have

been clustered together. For instance, take traverse 199 of the cA air mass group. During the three hour itinerary, the wind direction was constant, varying no more than 22.5 degrees clockwise. Moreover, prior to the commencement of this traverse, there were nine constant consecutive hours of light northwest winds monitored at the Airport. Yet this traverse had the same temperature and mixing ratio plot as those traverses composing the selected cA fusion group. The latter had wind flows from the south through west quadrants.

It will be shown that a similar occurrence was associated with cA traverse components of cycle 126. Itineraries 218 and 195 were undertaken when southwesterly winds dominated the research zone for a period of 18 hours whereas itineraries 205 and 206 were conducted through a well established northwesterly wind flow. The statistical results and trend maps were similar.

It is therefore apparent that wind speed and direction is representative of the monitoring site only and that opacity can alter quite readily during the commencement and cession of a traverse. Consequently, the dendrogram printed for the cluster analysis utilizing only standardized temperature and mixing ratio data (all climatic variables being masked) will be chosen as the basis for sub-cluster selection and subsequent statistical analysis. Thus, these climatic

variables and the radiosonde data can now be extracted as auxiliary sources of information. They will thus aid in the explanation of results rather than being a portion of the results.

Figure 8.2.1 is a 0.75 times reduction of the original dendrogram. Each subcluster to be examined will also be presented in tabular form similar to that of Table 8.3.1. The latter, as previously stated is the cA and cMA traverse subcluster of the original dendrogram.

Generally speaking, the total error sum of squares of the 253 traverse fusions is 150.125. However, 248 fusions out of the total account for 2.02 percent change in d_1 due to pooled variances while 97.97 percent of the change is attributed to the last 6 fusions. The coefficient increased approximately 49.5 times to reach its maximum value in the last 6 steps. The randomness of the sampling procedure, implemented in order to avoid a subjective preference for any particular weather type or synoptic condition, justifies the coefficient's calculation. That is, each subcluster is unique and thus does not readily unite with other distinct subclusters. A sharp value increase in d_2 indicates that much of the classification system's accuracy has been lost by reducing the number of groups by one at this stage. For example, when the mA subcluster was fused with the cA-cMA subcluster d_2 was

18.41. Respective d_1 values prior to union were 2.416 and 1.461.

Of the total number of traverses, 179 were conducted during stable atmospheric conditions while the remainder, 74, were undertaken during unstable conditions. Approximately 52.2 percent of the air masses within the former group can be further classified as being dry according to the definitions set by Environment Canada (see Section 4.2). The respective percentage for the second classification was 54.8.

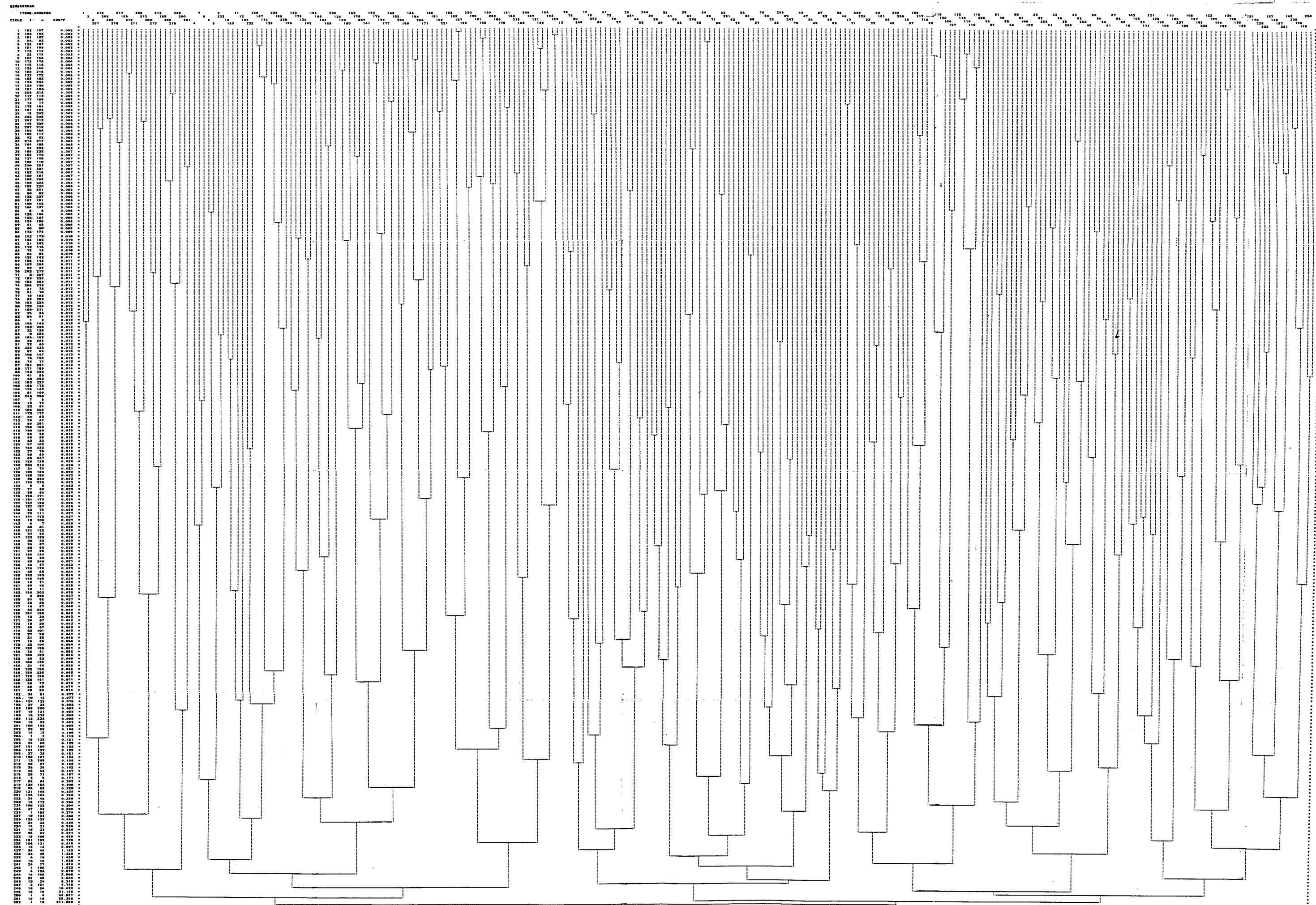
Twenty-nine surveys were conducted when the wind direction recorded at the Winnipeg International Airport Meteorological Station for the standardized traverse hour varied from 001° - 090° . The number of surveys made during wind directions of 091° - 180° , 181° - 270° and 271° - 360° were 78, 71 and 62 respectively. On eight occasions, calm conditions prevailed.

With the exception of the two 0100 LST traverses, the hourly distribution of surveys remained fairly constant. The hourly breakdown for 0900, 1300, 1700 and 2100 LST traverses were 64, 62, 61 and 64 respectively.

Rather than list the subclusters and their associated climatic and statistical attributes here and again when discussion warrants, each subcluster will be analyzed in a

separate section. The introduction of each sub-cluster will contain all pertinent information regarding its position in the master dendrogram, traverse component, radiosonde type and fusion selection for further investigation. The subsequent sections will be aimed at fulfilling the thesis objectives, according to Sections 1.2 and 7.1 through 8.1. The trend will be from one extreme subcluster to the opposite extreme subcluster. That is, the first subcluster to be analyzed will be the cA-cmA group.

FIGURE 8.2.1 : CHOSEN CLUSTER ANALYSIS DENDROGRAM



8.3 Continental Arctic Air Mass Analysis

8.3.1 Fusion Selection

To recapitulate, the first sub-cluster to be statistically analyzed is composed of 25 traverses which were conducted under continental Arctic or continental maritime Arctic air mass conditions. This fusion group is the right most portion of the first major cluster of the chosen dendrogram (all climatic variables masked). Ninety itineraries are incorporated by the latter and represent air mass conditions ranging from cA through to cold mA.

In Table 8.3.1.1, the traverses which were undertaken during cA or cMA air mass engulfment, are coded according to their respective position in the total number of itineraries. Also listed on the left are the standardized traverse hour and the prevailing climatic variables ⁸ station pressure (PPP), in millibars; the wind direction (dd)⁹ wind speed (ff), in kilometers per hour; and

⁸ All the climatic variables that are listed are averages. The respective climatic data that was averaged was monitored at the Airport during the undertaking of a traverse.

⁹ The true direction from which wind is blowing is expressed in compass points. The equivalent, hundreds of degrees codes are:

POINTS	DEGREES	POINTS	DEGREES
N	348.75 - 11.25	S	168.75 - 191.25
NNE	11.25 - 33.75	SSW	191.25 - 213.75
NE	33.75 - 56.25	SW	213.75 - 236.25
ENE	56.25 - 78.75	WSW	236.25 - 258.75
E	78.75 - 101.25	W	258.75 - 281.25
ESE	101.25 - 123.75	WNW	281.25 - 304.75
SE	123.75 - 146.25	NW	304.75 - 326.25
SSE	146.25 - 168.75	NNW	326.25 - 348.75

the total fraction of the celestial dome covered by clouds (N), irrespective of genus type. The latter is coded according to the okta value.¹⁰

The fusion cycle number is listed horizontally on the right of Table 8.3.1.1. The number symbol (#) will appear under those traverses in this table which when fused yield critical alpha values less or equal to the critical type 1 error alpha of 0.05 for both the climatic variables under consideration. An equal sign (=) will indicate the converse of the above. If the null hypothesis is rejected only by temperature data, an unequal sign (≠) will be printed under the respective itinerary grouping. Meanwhile, a hyphen (-) will symbolize that only the mixing ratio data

¹⁰ An okta represents an area of one-eighth of the whole sky. A value of 9 indicates that the sky is obscured or cloud amount cannot be estimated.

As the daily synoptic charts prepared during the data acquisition data period, did not carry the code, N will be determined from the following chart duplicated from Canada, Department of Transport, Meteorological Branch, Tables for Synoptic Codes, Pubn. 63-9028, [Ottawa: Queen's Printer, 1967], one sheet. Both opacity and the amount of cloud present are given in tenths.

		OPACITY								
		1	2	3	4	5	6	7	8	9
		0	0	0	0	0	0	0	0	0
	1	1	1	2	2	2	2	4	8	
A	2	2	2	2	3	4	6	8		
M	3	2	3	4	5	6	8			
O	4	3	4	5	6	6	8			
U	5	5	5	6	6	8				
N	6	6	6	7	8					
T	7	6	7	8						
	8	7	8							
	9	8								

has rejected Ho.

Table 8.3.1.1

CLIMATOLOGICAL AND CLUSTER INFORMATION FOR TRAVERSES
CONDUCTED UNDER cA AND cMA AIRMASS CONDITIONS

TRAV	HR	CLIMATIC VARIABLES				CLUSTER CYCLES							
		PPP	dd	ff	N	2221111111187764432211186	4209654210382473243921	4589952620					
1	9	1000.3	W	34.2	0	≠#		≠	≠				
2	13	1004.3	SSW	20.4	0	≠#		≠	≠		-		
3	17	1003.7	SSW	18.0	1	≠#		≠	≠		-		
207	9	1000.0	WSW	10.3	0	≠#		≠				≠	
210	9	992.6	WNW	15.0	0	≠#		≠				≠	
199	9	992.5	NW	16.3	8	≠##	#			≠	=		
211	13	993.8	NW	12.5	0	≠##	#			≠	=		
202	21	990.7	SW	9.5	0	≠##	#			≠			≠
212	17	994.0	W	7.8	0	≠##	#			≠			≠
203	9	984.1	WSW	12.0	0	≠##	#		#				
208	17	994.0	SSW	11.1	0	≠##	#		#		#		#
209	21	991.5	SSW	8.5	0	≠##	#		#		#		#
213	21	993.5	WNW	2.5	0	≠##	#		#		#		
214	9	994.8	CALM	6.0	2	≠##	=						
215	13	994.7	NE	11.5	8	≠##	=	=					
216	17	994.6	ENE	12.5	6	≠##	=	=			=		
217	21	994.5	ENE	13.5	8	≠##	=	=			=		
183	9	984.5	SW	9.0	0	≠	==			=			
204	13	986.2	NW	25.0	6	≠	==			=			
195	17	991.7	S	14.5	8	≠	==	≠		≠			
218	9	983.5	S	37.0	8	≠	==	≠		≠			
205	9	985.7	WNW	13.0	7	≠	==	≠				≠	
206	17	990.9	WNW	10.0	8	≠	==	≠				≠	
200	13	992.8	NW	18.5	3	≠	=						#
201	17	992.6	WNW	12.0	2	≠	=						#

Statistical information relating to the traverse fusion cycles of Table 8.3.1.1 is found in Table 8.3.1.2.

Together with the cycle identification number, the actual

change in the error sum of squares at fusion (d1) is listed on the left. The Kruskal-Wallis test statistic corrected for ties (H) and its associated critical alpha level (a) are also tabulated for both temperature and mixing ratio.

TABLE 8.3.1.2

STATISTICAL INFORMATION ON TRAVERSES CONDUCTED UNDER
cA OR cmA AIRMASS CONDITIONS

CYCLE	d1	TEMPERATURE		MIXING RATIO	
		H	a	H	a
244	1.4610	175.302	0.0025	109.583	0.851
255	0.2155	404.117	≥0.000005	237.049	≥0.000005
208	0.0980	530.583	≥0.000005	173.349	0.0034
199	0.0810	103.732	0.927	40.880	1.000
169	0.0455	136.614	0.245	46.321	1.000
155	0.0375	462.646	≥0.000005	251.556	≥0.000005
142	0.0320	114.353	0.759	104.272	0.921
126	0.0245	289.418	≥0.000005	39.028	1.000
112	0.0210	234.018	≥0.000005	102.802	0.936
100	0.0180	59.660	1.000	134.200	0.292
83	0.0150	354.600	≥0.000005	155.930	0.0359
78	0.0145	155.210	0.0392	124.560	0.520
72	0.0130	137.887	0.221	111.198	0.824
64	0.0120	184.754	0.0005	57.104	1.000
47	0.0100	258.689	≥0.000005	133.073	0.316
43	0.0090	301.922	≥0.000005	240.708	≥0.000005
32	0.0080	85.255	0.998	84.669	0.998
24	0.0070	151.846	0.058	193.978	≥0.000002
23	0.0070	63.694	1.000	41.297	1.000
19	0.0065	172.172	0.004	46.299	1.000
12	0.0050	197.185	0.000064	51.650	1.000
11	0.0050	198.741	0.000041	172.375	0.0039
8	0.0035	224.137	≥0.000005	148.988	0.074
6	0.0030	226.378	≥0.000005	149.682	0.074

Six distinct, relatively homogenous groups can be detected in Table 8.3.1.2. They are cycles 112, 155, 142, 72, 126, and 11.

Examination of the acceleration of error term d_2 (see Section 7.2.2), suggests that much of the classification system's accuracy has not been lost by reducing the number of groups at the higher cycle levels. For instance, the largest d_2 increase for the data occurred between cycles 112 and 225. From a mean rate of 0.0070, the error term increased to 0.2155.

A similar reaction, though not as drastic, was noted for the fusion of cycles 155 and 142. When the former was linked to the latter, its internal d_2 value increased about 2.4 times. When the resultant cycle, 208, merged with cycle 112, d_2 increased from 0.0605 to 0.1175. This again indicated that no information was being lost.

If information was being lost on higher cycle fusions, then are the calculated Kruskal-Wallis H statistics for both temperature and mixing ratio significant for cycles 55 and 208?

In the forthcoming section, it will be shown that the above six distinct cycles have unique radiosonde characteristics.

A mere glance at the fusion patterns of Table 8.3.1.1 would indicate that there is no relationship between traverse fusions and the time to which the itineraries were standardized. For instance, cycle 208, which registered the

greatest temperature H statistic in the cA - cMA sub-cluster, was conglomerated from 0900, 1300, 1700 and 2100 hour traverses. Respective number were 3, 2, 3 and 4. When these traverses were separated into their particular time group and subjected to the Kruskal-Wallis non-parametric Anova, all group H values were well below that derived for the whole cycle. The largest value, 258.781 was calculated for the 2100 hour distribution.

The most illogical traverse linkage, however, was that of cycle 11. This group was the only traverse pair which yielded significant H values for both temperature and mixing ratio. Respective critical alphas were ≥ 0.000005 and 0.0039.

Traverse component 201 of cycle 11 was conducted during the time period 2100 - 2400 hours, under stable atmospheric conditions whereas its group component, traverse 200, was undertaken during a time when turbulent activity would have been quite strong.¹¹ The estimated dQ_{se}/dz for traverse 201 was 0.0124. As this ratio is greater than zero, the layer is convectively stable and hence absolutely stable. Any

¹¹ Bell (1974, pages 130 - 184), using two and one half years of temperature, lapse rate and wind data from a rural 810 foot tower near Winnipeg, noted that surface heating in the layer closest to the surface is sufficiently strong to dissipate almost all inversions during the day, in all seasons. Only those of advective origin formed during winter days (1100 to 1600) will frequently survive that day and the next night.

orderly isentropic process performed with the air will not destroy this absolute stability.

For example, the amount of work which would be required to interchange vertically adjacent air parcels between the surface and the 950mb layer, against gravity acceleration, would be about 67.2671 N/m^2 during the undertaking of traverse 201 in locales similar to that of the Airport meteorological monitoring site. The kinetic energy available to do this work due to velocity differences between the parcels was estimated at approximately 3.8642 N/m^2 . Hence, to neutralize this layer, thereby assigning a value of one to the Richardson criterion, about 63.4029 N/m^2 must be found.

If the air density of this layer was to remain constant and if other sources of kinetic energy were absent, neutralization would only occur if the horizontal wind velocities within the layer would increase. The surface wind must strengthen from its original value of 15.5 km per hour to 33.9 km per hour whereas the increase at the top of the layer must be approximately 21.7 km/hour. The latter's original speed was 27.7 km/hour.

If the above would not occur, other sources of kinetic energy would have to be introduced. The problem, however, is from what sources would the energy be obtained.

The energy of latent heat of condensation is an inefficient source as CA and cMA air masses are relatively dry. The mean mixing ratio for the above example layer was estimated at 0.4597 g/kg whereas the mean saturation mixing ratio calculated was 0.6589 g/kg. The difference of 0.1992 g/kg would only yield about 107.568 more calories upon condensation at the mean layer dew point temperature -25.2°C.. In other words, approximately 0.0150 N/m² would be added: an insignificant amount compared to that liberated due to increased wind speeds.

The only other major source of energy from which to draw upon would be thermal pollution. Yet, when compared to the world's atmospheric energetic system, this source is also relatively minor.

However, anthropogenic heat production on a local scale might upset the atmospheric circulation much more efficiently than on the global scale. For instance, the energy flux density of a refinery, built on 0.1 km² of land and refining in excess of 6 million tonnes of crude oil yearly, would be approximately 4000 W/m² according to Pankrath(1980). The above estimate is about 2.9 times the solar irradiance on a perpendicular plane at distance (d) from the sun.

As all cities generate thermal pollution, horizontal and vertical temperature gradients tend to be established within

them. Movement and rearrangement aids in the destruction of the stable lapse rate. Potential energy in the layer¹² would thus be converted to kinetic energy. The outcome is the establishment of an air circulatory system.

Therefore, can it be assumed, from the above reasoning, that wind direction and wind speed, when monitored in a rural setting are only representative of that locale and should not be used to describe wind conditions in an urban setting? The expected answer is in the affirmative but for the CA - cMA sub-cluster, the answer is the converse.

There are several strong relationships between variable significance and wind direction in the cycles of Table 8.2.1. The first is quite noticable. Thus all member

¹² If a given amount of the atmosphere has a high temperature, it will have low density but high potential energy. If the air is cold, the air will have high density but low potential energy. The former's energy is due to a higher height: mass and the acceleration of gravity remaining constant.

For example, the three hour averaged respective temperature, mean virtual temperature, mixing ratio and air density for the Airport at the standardized traverse hour of 1700 for traverse 201 were -22.8°C. , -22.74°C. , 0.3587 g/kg and 1.3810 kg/m^3 . The estimated depth of the 992.6mb - 950mb layer was 324.78 gpm. The potential energy of a parcel with volume 1m^3 and mass 1.3810 kg in this layer would be about 4288.012 J..

The respective values for the above climatic variables for a C.B.D. site composed of locales 1-6, 56-69 and 115-127, (refer to Table 5.2.2), are -11.3°C. , -12.69°C. , 0.6762 g/kg and 1.3277 kg/m^3 . The minimal estimated layer thickness would be about 334.65 gpm: a 9.87 gpm increase over the latter Airport z. With constant mass and volume, the potential energy of the C.B.D. locality would be at a minimum of 4413.905 J.. Note, a 125.893 J. increase.

components of cycle 142 did not yield significant Kruskal-Wallis H statistics for any of their respective fusions. Note that cycle 126 components also had N codes of 7 and 8.

For further examination, the traverses listed in Table 8.2.1 were sorted according to whether the prevailing winds monitored at the Airport were from the following quadrants $168.75^{\circ} - 281.25^{\circ}$, $281.25 - 11.25^{\circ}$. Respective compass point equivalences are south through west and west through north.

Both groups were subjected to the Kruskal-Wallis Test. Respective calculated temperature H statistics and associated critical alpha values were 174.271, 0.0036 and 81.524, 0.999. Mixing ratio estimates for the above wind quadrants were 196.249, 0.00036 and 35.786, 1.000.

On eliminating background noise it was found that traverses with N codes <3 oktas could not be merged with those which had N codes ≥ 3 oktas regardless of wind direction. On merger of such traverses, a reduction of the H statistic was noticed. The reduction was greater for mixing ratios, however. For example, when traverses 195 and 218 were added to the other south through west wind quadrant members, chi-square fell 62.534 units for temperature but 111.226 for mixing ratio. The original critical alpha values for both climatic variables of this grouping were greater than 0.0000005.

The similar reaction was noted in the west through north wind grouping. However, the H statistic did not decrease as substantially because all fusions accepted the null hypothesis at critical alphas of 0.999. This finding indicated that only the separated S-W wind group can yield significant results.

Upon added examination of both groups, it was discovered that there was a large variance discrepancy for each variable between the two wind groups. That is, the temperature variance for the south to west wind group was approximately 4.14 times greater than that for the west-northwest to northwest group. Thus, the spatial temperature and mixing ratio trends for the foremost group were more intense, hence few rank ties were calculated. The reverse held true for the latter group. Although there was a trend present, a greater percentage of the ranks were tied. Distinction, both spatially and temporally, was destroyed. Furthermore, for each itinerary in the south to west wind group, the wind direction per three hour traverse was either constant or varied maximally by 22.5° in a clockwise direction. Moreover, prior to each traverse commencement, the wind direction was constant for at least three hours. These conditions insured the development and maintenance of a distinct temperature and mixing ratio spatial distribution. The influence of standardization was thus also limited. That is, trends were present no matter how greatly the data was altered.

The above conditions were absent prior to and during many of the W - N wind group traverses, especially during the undertaking of traverses 210 and 211 at 0900 and 1300 hours respectively on December 7, 1976. Before the commencement of the former itinerary, a new blast of frigid CA air invaded the research zone dissolving the spatial heat and humidity islands formed and measured on the previous day. The winds throughout these traverses continuously varied from 270° to 316°. Towards the conclusion of traverse 211, the wind shifted from a westerly component to a southern flow. This continual veering was sufficient to neutralize any heat or humidity island trend. That is, cold sinks, for example, formed during the northerly flow disintegrated when a southerly flow was established because this area now fell under the influence of the new urban heat island plume. Similarly, southern areas which were affected by the core heat island during a northern flow became colder as the wind altered to the south.

To test the validity of the above speculations, the Kruskal-Wallis test was again applied to cycle 155. However, traverses 211 and 199 were removed. There was an insignificant decline of 4.089 units for temperature but an increase of 5.419 for mixing ratio. The critical alpha values remained relatively stable.

To this group, traverses 1,2,3 and 207 of cycle 112 were added. The structure of the group was thus similar to that of cycle 225, except for the fact that there were no traverses with N codes ≥ 3 oktas and no traverses with prevailing wind directions between the west and north. The H value again declined for temperature but the value increased drastically for mixing ratio. Respective change amounts were 66.175 and 190.905. The mixing ratio chi-square, 364.254, was the largest recorded for the variable in the cA - cmA sub-cluster. The critical alpha values for both variables were greater than 0.0000005.

Consolidating the above, the following facts become evident:

- (1) No wind direction restrictions govern traverse merging when emphasis is placed on the significance of the temperature variable. The composition of cycle 208 provides adequate proof.
- (2) When traverses are grouped according to the quadrant from which the prevailing winds are blowing, only the (S - W) group yield significant results.
- (3) In order to obtain and maintain high mixing ratio H statistics in the (S - W) group, no traverse must have a N code of ≥ 3 oktas.

As no further information on traverse fusion was derived from the examination of the wind speed parameter and whereas the main objective of this thesis is to present, analyze and delineate statistically-significant spatial and temporal distributions of water vapor as represented by mixing ratios, it was decided that only two fusions would be chosen

for further statistical and climatological analysis. These were the (S - W) wind group and cycle 126.

In summation, although it appears that cluster analysis is biased towards mixing ratio data, the bias is in fact contributed and inherent in the temperature data. The latter assumption is valid for all climatological-meteorological time scales because the characteristic traits of a continental Arctic climate are mainly large annual, daily and diurnal changes in temperature. Changes in mixing ratio values, however, are limited (See Chapter 6)

With 127 fixed reference locations on the chosen research itinerary, each varying temporally and spatially, both within and among sites, temperature variability is drastically magnified. Hence, the temperature error sum of squares, the basis of Ward's Hierarchic Combinatorial Algorithm, remain relatively large, especially when compared to those generated by mixing ratios. For example, the total temperature sum of squares for the chosen (S - W) group was estimated at 12241.0741 whereas that for mixing ratio was 8.9169. On an individual basis, fixed point location 21, the Wellington-Conservatory Road intersection, had the least temperature error sum of squares while the greatest was estimated for the Notre Dame-Dublin site, number 31. Respective values were 50.2880 and 137.0937. The highest

mixing ratio error sum of squares was determined for location 7, the Portage-Sherbrook intersection whilst the lowest was estimated for locale 31, the intersection of Roblin and Highway 101. Respective values were 0.3318 and 0.0230.

Cluster analysis, therefore may be able to distinguish temperature variation between and within locales more readily than it can for the mixing ratio data.

Temperature and mixing ratio distributions may, on the other hand, be influenced by the prevailing winds. This possibility exists and will be further examined in the forthcoming air mass sections.

8.3.2 Airmass Classification

Although it has been consistently stated in the previous sections that the first subcluster of the chosen Clustan-1C2 dendrogram is composed of traverses conducted under cA or cMA air mass conditions, it has not yet been proven that these traverses are in fact representative of this air mass classification. Hence, prior to further statistical and climatological analysis of this subcluster, it will be shown that these traverses are truly representative of their designated air mass classification.

To facilitate this purpose, Table 8.3.2.1 has been constructed. Tephigrams showing mean January CA air mass ascent characteristics for the period 1962-66 at Barrow, Alaska, Norman Wells, N.W.T. and The Pas, Manitoba provided the basic data required for the calculation of the pseudo-equivalent potential temperature (Q_{se}) and mixing ratio (MR) for each of the standard pressure levels: surface, 850, 700 and 500 millibars.⁴ These stations, coded BRW, YVQ and YQD respectively, will be regarded as controls with which comparisons are to be made. The cycle numbers correspond to those given for each traverse cluster grouping listed previously in Table 8.3.1.1. Cycle 126 includes the original itineraries plus traverses 200 and 201. The reasons for these additions have been given previously in Section 8.3.1. The lifting condensation level LCL and its associated temperature LCT as well as the convective condensation temperature for surface air have also been determined and tabulated.

An air mass develops its characteristic properties by remaining over a particular region of the earth for periods long enough that its vertical temperature and moisture distribution soon approaches an equilibrium with the

⁴ Each diagram was taken from Crowe, 1971, pages 268 to 271. It should also be noted that both the tephigrams and resultant calculations are representative of typical CA conditions and should not be regarded as climatological normals.

TABLE 8.3.2.1

cA TEPHIGRAM COMPARISONS

CODE	SFC		850mb		700mb		500mb	
	Qse °K	MR (g/kg)	Qse °K	MR (g/kg)	Qse °K	MR (g/kg)	Qse °K	MR (g/kg)
BRW	247.3	0.2363	270.0	0.6048	281.2	0.8337	290.7	0.1007
	SFC	1021.0mb	LCL	937.3mb	LCT	242.2°K	CCT	292.2°K
YVQ	242.5	0.1751	267.4	0.4063	279.1	0.3205	290.7	0.1068
	SFC	1016.0mb	LCL	967.5mb	LCT	239.8°K	CCT	296.2°K
YQD	251.0	0.3394	268.7	0.5167	280.3	0.3746	292.1	0.1425
	SFC	987.0mb	LCL	942.6mb	LCT	247.9°K	CCT	291.2°K
112	248.8	0.3015	264.0	0.5727	273.6	0.3366	288.9	0.1645
	SFC	991.1mb	LCL	909.7mb	LCT	241.4°K	CCT	291.0°K
155	252.1	0.3859	263.2	0.4938	275.3	0.3613	289.1	0.1457
	SFC	983.5mb	LCL	948.0mb	LCT	247.2°K	CCT	280.4°K
142	247.6	0.2812	265.8	0.7273	281.2	0.5766	295.4	0.3793
	SFC	986.6mb	LCL	965.7mb	LCT	244.4°K	CCT	297.0°K
126	270.4	0.8273	273.1	1.0772	283.9	0.9180	298.1	0.3939
	SFC	982.2mb	LCL	968.7mb	LCT	255.1°K	CCT	287.7°K
72	268.0	1.3459	290.3	1.4511	296.7	1.3447	305.0	0.4415
	SFC	971.0mb	LCL	923.4mb	LCT	258.4°K	CCT	302.5°K

underlying surface. Continental Arctic air masses originate over the snow and ice covered Arctic Ocean and land masses of northern North America and eastern Eurasia. Incoming solar radiation is negligible or nil. The high albedo surfaces reflect much of the insignificant incoming radiation while at the same time, these surfaces are efficient emitters of heat in the form of infrared waves. The only constant supply of heat originates from the warmer

unfrozen water beneath several meters of solid ice. Thermal conduction, however, is slow. Hence, the air is cooled from below. As vertical turbulent heat transfer is insufficient to maintain a normal temperature lapse rate, isothermal conditions or inversions develop near the surface. This development further diminishes the lapse rate, which in turn decreases turbulence intensity. Thus the growth of an inversion is favored. As divergent flow from the central part of the anticyclone spreads the cooled air over large areas, subsidence compensates. Advective clouds, if present at all, are dissolved. The surface radiates freely and the inversion intensifies.

Therefore, the most common attribute of a cA air mass is a strongly developed low level inversion. For the control stations, the inversion extends up to 850mb whilst the lapse rate thence is isothermal. The pattern holds valid for cycles 112, 155 and 72 with the deepest inversion being recorded for the latter. That is, from the surface to the 850mb level, a vertical distance of about 1056 meters, the temperature increased 11.1°C . This corresponds to an increase of 22.3°K in Qse. Note that the above compares favorably with that calculated for control stations BRW and YVQ. Respective change in Qse, from the surface to 850mb, for these control stations is 22.7°K and 24.9°K . Lapse conditions, rather than isothermal, occur above the inversion for cycle 72, however.

The remaining cycles have unique characteristics. For cycle 142 an upper level subsidence inversion was present over a very shallow surface inversion. The rate of change, however, was greater for the latter than for the former inversion type. From the surface to 900mb, a vertical distance of approximately 565 meters, the Qse increased only 7.7°K whilst from 900 to 700 millibars, a distance of about 1955 meter, Qse increased 24.2°K. Respective °K/m are 0.0124 and 0.0136.

This cycle represents a middle stage of a cold air outbreak. As the wind diminishes and becomes very light at the ground, 6.8km per hour in this case, radiational cooling effects a lowering of the air temperature at the ground, while subsidence effects a rising of upper level temperatures.

Cycle 126 is representative of an early cA air outbreak stage. At the surface, the wind is moderate, 15.1km per hour, from the west but with elevation the speed increases with a veering to a northwestern and then a northern direction. Respective wind directions and wind speeds for the remaining standard millibar levels are: 289°, 43.4, 317°, 68.8 and 325°, 109.9.

The temperature either decreases through the first few hundred meters above the ground or remains relatively constant, as is the case for cycle 126. This is the result

of the mixing affected by mechanical turbulence. For this cycle, the temperature has decreased 1.9°C from the surface to the 700mb level.

Typical CA air is further characterized by pronounced absolute stability and convective stability. For both cases the quantity dQ_{se}/dz must be greater than zero. This is quite evident from Table 8.3.2.1. For each control station and cycle, Q_{se} increased between each millibar level. The greatest increase was calculated for the inversion zones of YVQ, BRW and cycle 72 whilst the least was estimated for cycle 155. Respective values are 24.9°K , 22.7°K , 22.3°K and 11.1°K .

The estimated quantity dQ_{se}/dz is fairly constant for all cycles, from the surface to 850mb. Respective values according to tabular position are 0.0136, 0.0122, 0.0157, 0.0124 and 0.0296. The lattermost value is high because cycle 72 had only one radiosonde estimate.

Note also that convective processes for all are ruled out. The convective condensation levels are well above 4500 meters for the controls whilst the minimum level estimated for the cycles was 3439 meters for cycle 155. In order for the surface air of cycle 155 to rise so far from the ground, for example, the air would have to obtain temperatures in excess of 280.4°K : an impossibility.

The lifting condensation levels of cA air masses are all quite low, hardly ever exceeding 900mb. Furthermore, the water vapor content of the air is very low. In fact, if the mixing ratios of Table 8.3.1 were calculated with respect to the saturation vapor pressure over ice rather than over water, the values would be lower. Even over deserts water vapor content is greater than the amounts in these cA air mass soundings. The average mixing ratio at Aswan, Egypt in January, for instance, is estimated by near 4.1g/kg: approximately four times greater than the largest tabular value (Crowe, 1971, page 282)

The chief reason for the low moisture values is found in the low temperatures. The greatest mixing ratio values tend to be located in the inversion zone close to the maximum inversion height. Moreover, supply of moisture from the underly surface is minimal to nil. Even evapotranspiration is an insignificant source when temperatures are so low.

Unfortunately, as no long term monthly cA air mass data has been compiled for any region of the globe, it is impossible to analyze trait variability between a particular outbreak and the long term normal. Emphasis has always been directed towards the tabulation of temperature and precipitation observations on a daily and hourly schedule regardless of the type of air mass dominant during the

recording. Nevertheless, in order to indicate the coldness and dryness of cA air masses, a comparison between the recorded temperature and mixing ratio data for each traverse day and the long term normal for each respective climatological parameter for that day will be undertaken.

The minimum, mean and maximum temperatures recorded at the Airport meteorological site during those traverses conducted under cA air mass conditions were, with the exclusion of traverses 183 and 218, well below the average respective estimates based upon climatological Airport data to 1970.⁵ The average minimum temperature for the November traverses was approximately 17.0°C. below the long term estimate whilst the mean deviated 14.8°C.. The actual mean maximum temperature was -14.3°C. while that computed for the 98 year average was -1.1°C.: 13.2°C. lower.

Similar deviations were estimated for the December itineraries. The mean minimum and mean temperatures were 13.6°C. and 13.5°C. lower respectively while the mean maximum difference was 18.0°C.. The greatest departures from the normal were recorded during this month on the 8th for traverse components of cycle 142. Arctic air held the mean temperature 16.6°C. below early December normals. The minimum and maximum temperatures recorded on this day were

⁵ The data was obtained from the publication Daily Data Summaries, No. 20 - Winnipeg, Manitoba. It was supplied through Environment Canada, Atmospheric Canada.

17.5°C. and 16.3°C. respectively below mean values.

The smallest deviations were calculated for those traverses undertaken during the month of February. Respective differences from the mean minimum, mean and mean maximum long term Airport data were 6.4°C., 6.9°C. and 8.0°C..

As no long term humidity records have been compiled by Environment Canada, the comparison of mixing ratio deviations from hourly normals will be based upon Airport records from 1953 to 1976. These values have been previously documented in Tables 6.1.1 to 6.1.12, pages 139 to 162.

When the mixing ratio deviations were calculated for the 0900, 1300 1700 and 2100 standardized hours, all were well below the 95 percent confidence intervals.⁶

⁶ Although the general assumption prevalent throughout this thesis has been that no hypotheses will be formulated regarding the traverse data sample distributions, the spatial distributions of the climatological parameters under investigation or the temporal variability of these climatic parameters, without supporting evidence and although it has been proven in Chapter 7 that the data under investigation is nonparametric in nature, the hypothesis regarding monitoring site temperature, dew point and other humidity variable distributions hypothesized by Environment Canada, Atmospheric Environment, will be assumed valid for this comparison. That is, the Department advocates that when climatological parameters such as the above are obtained at fixed locations according to standard W.M.O. procedures, these parameters have approximately normal distributions. Hence parametric statistics can be employed. With reference to Figures 6.1.1 to 6.1.12, it can be seen that this hypothesis is valid for temperature, dew point, absolute humidity, mixing ratio and saturation deficit for the periods November to March but for the remaining months, the assumption is true only for the former most and

Mixing ratios estimated for 0900 and 2100 hour traverses approached the lower respective 95 percent confidence intervals whilst those estimated for either the 1300 or 1700 hour undertakings deviated greatly.

November continental Arctic traverses registered the greatest departures, ranging from a mean maximum of 2.4305 g/kg for 1700 hour traverses to a mean minimum of 1.9735 g/kg for 0900 hour traverses. For December itineraries, the 1300, 1700 and 2100 hour deviations were rather constant, averaging 1.0587 g/kg below the 23 year estimate interval. The 0900 hour estimate was 0.795 g/kg below the average value. February traverses registered the least departures, ranging from a high of 0.8089 g/kg for 1700 hour traverses to a low of 0.55 g/kg for 0900 hour traverses.

Parameter comparisons of traverses 183 and 218 proved unique. Although their mean temperatures were greater than the long term average, their mixing ratios were below the 95 percent confidence intervals. Respective temperature departures from the 98 year means were 2.5°C. and 12.8°C. whilst the respective mixing ratio deviations from the lower limits were 1.6168 g/kg and 2.1727 g/kg.

In summation, continental Arctic air masses are very cold, very stable and very dry. If the data recorded in Table 8.3.1 was plotted on Rossby diagrams, the graphs would

latter most climatic parameters.

all be located at the lowest left hand corner paralleling the ordinates.

8.3.3 The Analytic Conclusions

Similarities and dissimilarities are evident upon the examination of the trend analysis Symaps 8.3.3.1 through 8.3.3.2. They do not only exist between the same climatic parameter trends but also between the two climatic variables investigated. No generalizations can be formulated which would indicate or predict what type of trend would be generated by the sixth-degree polynomial equation or where the basic form, viz a maximum, stationary ridge, a rising ridge, a minimax and the inverted forms of the latter types would be situated. Each climatic parameter trend surface has its own particular uniqueness: an uniqueness more prevalent between the temperature trends than between temperatures and mixing ratios of the same cycle. Are these surface analysis trends representative of the true climatic conditions which prevailed during the undertaking of each component cycle traverse or has the usage of a nonparametric statistic camouflaged the true situation? In order to answer these questions, refer to the statistic comparison section of each map, located in the uppermost right hand corner.

As stated previously, the Kruskal-Wallis H statistic, calculated for both the temperature and mixing ratio

variables of the chosen south-to-west wind quadrant, Symaps 8.3.3.1a and 8.3.3.1b respectively, and that estimated for Cycle 126 temperature data, Symap 8.3.3.2, had critical alpha values well in excess of -15 decimal places. The most significant level was $1.5341E-24$ for the south-to-west mixing ratio data whilst the least, $9.1159E-15$ was estimated for Cycle 126. Yet the latter, computed from 507 cases of data has a definite trend form composed of all 11 comparison codes whereas the former calculated on 1270 cases has a maximum code 8 region. Similarly, the basic heat island pattern for the south-to-west group which could be classified as a broadened maximum ellipse, is of comparison code 9.

The above lack of a definite higher code trend surface based upon Kruskal-Wallis comparison statistic results for the south-to-west fusion can be traced to the large number of outliers in the data and the spacing of these outliers. Data point spacing in trend analysis is critical. Points should be equally distributed though they need not be regularly spaced. The reason being that closely spaced points exert undue influence on trend surface configurations. That is, when the sum of squared deviations are minimized, the trend surface will tend to be fitted so that it passes nearer to a dense cluster of closely spaced data points than to isolated data locales.

In Cycle 126, there are 11 locales with a code 11: areas designated H on Symap 8.3.3.2. The relative frequency is 0.0866 and is the second highest outside of the insignificant comparison grouping of '++++'. This group in turn is divided into two distinctive zones. The first, with the exclusion of site 68, Portage-Main intersection, is composed of C.B.D. locations 64 through 70 whereas the second, sites 114 through 118, form the southern fringe area of the Central Business District. Respective mean relative distances between each data recording site are 0.20 km and 0.62 km. The former distance is approximately one-half that calculated for the south-to-west sites designated H and almost one third that estimated for the mixing ratio H locales. The second average distance can not be compared with either of the two south-to-west group climatic variables because neither of the two have sites 114 through 118 in code 'HHHH'. For the temperature data, location 119 has a code of 10 whereas 117 is coded 8. The remaining sites are all in the insignificant zone. For the mixing ratio data, 119 is coded H, 118 is designated a 9, 117 is given code 8, 114 is a 7 and the remainder are insignificant.

Outliers therefore aid in the calculation of extremely high critical alpha values but do not yield information for trend surface configuration. Respective unit spread between the highest and lowest mean rank sums for both the temperature and mixing ratio data of the south-to-west group

and Cycle 126 temperature data are 733.77, 744.35 and 410.88. Cumulative frequencies for codes greater or equal to 10 are 0.0709, 0.0866 and 0.1417 respectively. The difference between the highest and the lowest mean rank sums for Cycle 126 is 135.89. This is about 40.71 units less than that for the south-to-west temperature data and approximately 80.61 units less than that estimated for the mixing ratio data.

In summation, high critical alpha values for the Kruskal-Wallis H statistic do not necessarily connote very strong surface trend polynomial configurations.

The corresponding estimated ANOVA statistics for the chosen data fusions are listed directly below the Kruskal-Wallis statistic information. This parametric equivalent of the latter is just as robust¹⁷ however, the power¹⁸ of the F statistic varies in strength. The F ratio is considerably greater than the Kruskal-Wallis test for Cycle 126 and slightly greater for the south-to-west temperature data. For the mixing ratio data of the latter group, the F ratio is less than the calculated H statistic. Conover (1980, page 237) indicates that such an occurrence will arise when data which contains many outliers is

¹⁷ Robustness is the ability of a statistical method to retain its accuracy regardless of the distribution shape. That is, normal, bimodal or skewed.

¹⁸ Power is the ability of a significance test to disconfirm or reject the null hypothesis when the null hypothesis should in fact be disconfirmed. That is, when it is wrong.

subjected to an ANOVA test.

But why such a large F ratio discrepancy between the two temperature data groups?

Of the three assumptions that must be met if analysis of variance is to be done appropriately, the least worrisome with respect to this data would be observation independence. Each recorded value on the traverse is a separate piece of information, not affected by one another. For both temperature and mixing ratio, the location of the monitoring site and the meteorological and anthropogenic controls acting at the site influence the recorded values. Adjacent temperatures only control one another at a micro-meteorological scale. Here minute pressure differences can instigate eddy formation. Turbulence in turn invokes circulation.

Temperatures, of course, affect mixing ratio values by setting an upper maximum limit but mixing ratios can only influence one another through the establishment of either horizontal or vertical advection or convection.

Randomly sampling cases at randomly selected sites guarantee independent observations. Note that for all three trend maps, the point distribution coefficient is constant at 0.97. The spatial distribution of the data points is therefore random (Symap User Reference Manual, 1976, Section III, pages 27-28).

Normality tends not to matter greatly as the size of each group increases (Blalock Jr., 1972, pages 220-222). But, as previously stated, neither the temperature nor the mixing ratio data of both selected fusions have normal distributions. When the Kolmogorov-Smirnov Goodness-of-Fit test¹⁹ was run on both the S-W group and Cycle 126, the results indicated that only the mixing ratio data had an empirical distribution function close enough to indicate normality. The two tailed probability was 0.189. The absolute maximum difference was 0.0305 whilst the critical value for 1270 cases was approximately 0.0380.

¹⁹ The Kolmogorov-Smirnov Goodness-of-Fit test is the non-parametric alternative to the Chi-squared test for goodness-of-fit introduced in Section 7.3. Because it was designed for ordinal data, expected frequencies per group need not be calculated. The latter procedure is a requirement for the SPSS version of the Chi-squared goodness-of-fit test. Moreover, the only assumption for the Kolmogorov-Smirnov test is that the sample be a random one.

This routine tests whether or not the observed data could reasonably have come from a completely specified hypothesized distribution function $F^{\circ}(x)$. The function could be uniform, normal, Poisson, Beta and so forth.

The null hypothesis H_0 is that there is no difference between the observed data distribution function $S(x)$ and the theoretical distribution $F^{\circ}(x)$. The two tailed alternative is that the data and the hypothetical distribution differ.

The test statistic T is the absolute maximum difference between the cumulative distribution functions $F^{\circ}(x) - S(x)$ at any given level.

All $S(x)$'s were nevertheless closer to the normal distribution function than to the uniform distribution function. The Kolmogorov-Smirnov Z^{20} for the above mixing ratio group was 18.534 for the uniform distribution but only 1.935 for the normal distribution. The foremost Z was totally significant as the maximum absolute difference was 0.5201 whilst the critical value was again 0.0380.

As the Kolmogorov-Smirnov test revealed little new information regarding the influence of the normality assumption on the generation of the F ratios and surface trend configurations for the temperature data of both Cycle 126 and the south-to-west traverse union, especially when applied to the data as a unit, it was decided that each code classification would be tested separately for normality. The generated results which were worth the computer costs are listed in Table 8.3.3.1. For each code classification, listed on the left, the absolute maximum difference, the critical region and the 2-tailed probability for both the south-to-west and cycle 126 temperature data

The decision rule for this thesis shall be as follows. The null hypothesis shall be rejected at the level of significance α 0.05 if the T test statistic exceeds the critical value $1.36/\sqrt{[n+\sqrt{(n/10)]}$ (Conover, 1980, page 462).

For additional information, examples, etc., refer to Conover (1980), pages 344-353.

²⁰ The Z parameter is determined from the largest absolute difference. The larger the value of Z , the less likely it is that the observed and theoretical distributions are similar.

are tabulated.

Table 8.3.3.1

KOLMOGOROV-SMIRNOV GOODNESS-OF-FIT TEST FOR
TEMPERATURE DATA OF S-W GROUP AND CYCLE 126

CODE	S - W GROUP			CYCLE 126		
	MAX DIFF	ABS REGION	CRITICAL 2-TAILED PROB	MAX DIFF	ABS REGION	CRITICAL 2-TAILED PROB
HHHH	0.1443	0.1674	0.1640	0.0802	0.2003	0.9400
OXAV	0.1448	0.2414	0.5560	0.1786	0.2497	0.3340
O+O+	0.1332	0.2939	0.8700	0.2149	0.3758	0.6360
OOOO	0.1084	0.1031	0.0370	0.1270	0.2099	0.1270
XXXX	0.1183	0.1494	0.2130	0.0900	0.2497	0.9770
++++	0.0799	0.0775	0.0560	0.0502	0.1313	0.9560
++++	0.0848	0.0820	0.0410	0.1003	0.1366	0.2890
====	0.1129	0.1494	0.2590	0.1584	0.2497	0.4830
'-''	0.0546	0.1031	0.6920	0.1506	0.2099	0.3240
----	0.1782	0.2939	0.5490	0.1790	0.3758	0.8370
''''	0.1097	0.2414	0.8630	0.1884	0.2497	0.2970
LLLL	0.1057	0.1674	0.5150	0.1759	0.2003	0.1310

The null hypothesis was accepted for all 11 code zones of Cycle 126 temperature data though rejected by the south-to-west data zone codes 8 and lower 6. The respective 2-tailed probability of the estimated maximum absolute difference for the latter zones was 0.0370 and 0.0410. When code '++++', the insignificant combinatory group was analyzed as a whole rather than split into an upper and a lower portion, the absolute maximum difference became 0.0767: the critical region value became 0.0576 for an alpha of 0.05 while the 2-tailed probability was 0.003.

Note that the cumulative frequency of these Ho rejecters is 0.5708. In other words, approximately 57% of the south-to-west temperature data used in the calculation of the F ratio is non-normal in distribution.

Yet the insignificant comparison zone '++++' on both the temperature and mixing ratio symaps 8.3.3.1a - 8.3.3.1b for the south-to-west fusion are relatively similar with respect to orientation. The only major deviation occurs in the vicinity of the University of Manitoba. The heat island ellipse in this area, codes 'XXXX' and 'OOOO' combined, encompasses an approximate area of 8.44 km² whereas the area of the mixing ratio ellipse is about 6.30 km². As the minor axes of both are relatively constant at 0.95 km west, the area difference, 2.14 km² is the result of code '++++' fluctuations.

Which of the above code 6 trend configurations is the most representative of the actual situation? For the temperature data, the insignificant zone is non-normal whereas for the mixing ratio variable, the data is of a normal distribution function. The maximum absolute $F^{\circ}(x) - S(x)$ distance of the latter's insignificant grouping which also has a similar high relative frequency of about 0.4409, was 0.0494. With a test statistic of approximately 0.0592, the 2-tailed probability of the Kolmogorov-Smirnov test was 0.158. Hence, the null hypothesis was not rejected.

According to the statistical surface trend analysis measures²¹ generated by Symap(1976)²² the sixth order trend surface of each variable for each data cluster analyzed is of a very good fit. The coefficient of determination²³ varies from a maximum of 0.8738 for the south-to-west temperature data to a minimum of 0.8140 for the mixing ratio data of the same grouping. The coefficient's value of Cycle 126 temperature data was 0.8192. Respective correlation coefficients, the square root of the former values are 0.9348, 0.9022 and 0.9051. Hence, there also is a good trend association between variables.

²¹ Recall that trend analysis is a parametric method for using independent samples to test the null hypothesis that several means are all equal, when the order of the means has been predicted prior by the experimental hypothesis. That is, one has made a prediction as to which cell mean will be highest, which second highest, and so forth until all cell positions have been accounted for. The predicted hypothesis arises from a multiple comparison technique, the latter of which, in turn can only be employed if the null hypothesis of a statistic testing the order of non-predicted means, is rejected. Chapter 7 depicts such a flow chart.

²² The Symap trend measures are listed directly below the ANOVA table in the upper right corner of each trend map.

²³ The coefficient of determination assesses the goodness of a trend fit. It is the total sum of squares $St1$ accounted for by the trend function, Sd . The computation equation is $[1 - (Sd/St1)]$.

A perfect fit of a trend function to the data points, a very improbable situation, would yield a coefficient of one. As the variation in the data increases, the trend function's representation decreases, and the coefficient becomes smaller. When a value of zero is obtained, no polynomial trend relation exists.

The trend statistics also indicate that the F ratio is fairly robust regarding the normality assumption. Scheffe(1967,pages 331-337) concludes that the effect of normality assumption violations is slight,as in the above cA-cmA clusters, only if inferences about the mean are made. When inferences about variances however are made extremely dangerous results can occur.

But inferences about variances have already been made. Recall that one of the basic assumptions of the Kruskal-Wallis non-parametric anova test is that all of the k population distribution functions should be equal. Therefore,to validate homoscedasticity and to indicate whether the differences in the k samples are due to chance variations which are to be expected among random samples from the same sample,each selected variable cluster grouping was subjected to the Squared Ranks Test for Variances.²⁴

There are three assumptions for the Squared Ranks Test. All samples are random from their respective populations. There must be mutual independence between and within samples. The measurement scale is at least interval.

²⁴ This test detects differences in variability or dispersion rather than location: an objective fundamental in preliminary climatological studies (Sundborg,1950,pages 225-226)

It is analogous to the Kruskal-Wallis statistics discussed in Sections 7.4.2 and 7.4.4.

The calculation of this statistic is rather simple though may require coding of data whenever N becomes quite large. From each observation, subtract its k sample mean and take the absolute value. Rank the differences from smallest to largest or vice versa, assigning average ranks in case of ties, again as described in Section 7.4.2. Square each rank. Compute the sum of squares of the ranks for each k sample observation member.

The test statistic is:

$$T_2 = 1/D^2 \left(\sum_{j=1}^k S_j^2 / n_j - \bar{N}(S)^2 \right)$$

where

n_j = number of observations in sample j

$N = n_1 + n_2 + \dots + n_k$

S_j = the sum of the squared ranks in sample j

$\bar{S} = 1/N \sum_{j=1}^k S_j$ = the average of all the squared ranks

$$D^2 = N(N+1)(2N+1)(8N+11)/180$$

The null hypothesis $H_0: \sigma_1 = \sigma_2 = \dots = \sigma_{12127}$ is rejected if T_2 exceeds the 1-alpha quantile of the Chi-square distribution with degrees of freedom, k-1. If and only is

H_0 is rejected, multiple comparisons can be made as described in Section 7.4.4. D^2 replaces S^2 in the multiple comparison formula of the latter section. T_2 replaces H .

The following example best illustrates this rather new statistical technique. The data consists of the first five locations of Table 7.3.1. It is the same as that used in the Kruskal-Wallis multiple comparison example of Section 7.4.4. Respective means for locations 1 through 5 are -18.41°C. , -19.57°C. , -20.73°C. , -19.36°C. , and -19.60°C. . Example measurements and calculations are given in Table 8.3.3.2.

Table 8.3.3.2

THE SQUARED RANKS TEST FOR VARIANCES
(FIRST FIVE LOCATIONS OF TABLE 7.3.1)

k	ABS(X-u)			RANK			(RANK) ²			S _j	S _j ²
1	2.88	1.86	1.02	15	14	11	225	196	121	542	293763.9991
2	1.28	0.34	0.93	12	4	10	144	16	100	260	67599.9999
3	0.53	0.11	0.65	7	1	8	49	1	64	114	12996.0000
4	0.47	0.17	0.29	5	2	3	25	4	9	38	1444.0000
5	1.31	0.51	0.81	13	6	9	69	36	81	286	81795.9999
SUM										1240	45759.9999

N = 15

S = 1240/15 = (N+1)(2N+1)/6 = 82.6667

D⁴ = 15(16)(31)(131)/180 = 1/N - 1 $\sum_{i=1}^N R^4 - \bar{n}(S)^2 = 5414.6667$

T2 = 1/5414.6667 [457599.9999/3 - (15(82.6667)²)] = 9.2391

The null hypothesis for the above is accepted for the critical alpha 0.05 value for k=5, 11.07, that is, the value of T2 is less than 11.07. All k populations are therefore identical both with respect to their means and their variances (See Section 7.4.2)

The null hypothesis was accepted by both the south-to-west temperature and mixing ratio data. The former's calculated test statistic was 40.6866 whereas the latter's was estimated at 73.8181. The respective probabilities for both were 1.000. D² and N(S)² were constant at 2.3176E+11 and 3.6796E+14 respectively. The sum S_j²/n_j for k 1 through 127 was 3.7739E+14 for temperature and 3.8507E+14 for mixing ratio.

For the temperature data of Cycle 126, however, the null hypothesis was rejected. However, it should not be forgotten that Cycle 126 traverse components 218 and 195 were undertaken when southwesterly winds dominated the research zone for a period of 18 hours whereas itineraries 205 and 206 were conducted through a well established northwesterly wind flow. When the Squared Ranks test for variance was run on each of the above components, the null hypothesis was accepted rather than rejected. Respective T2 values were 38.7846 and 42.9874: both indicating probabilities of 1.000.

If the above results are ignored and multiple comparison tests are run on Cycle 126, as a unit, the result proves rather quite interesting. In fact, the theory that Winnipeg possesses its own circulatory system is again validated.

To begin with, note that the N code for Cycle 126 was 8 overcast conditions. Variances were thus expected to be less than that calculated for the south-to-west temperature data. This was, however, not the case. The variances for both the temperature and mixing ratio data were greater for Cycle 126 and its component traverse fusions than for the south-to-west wind group. Moreover, the higher codes 'HHHH' through to '++++' had variances which were always less than that estimated for the code zones '++++' through to '.....'. This can be seen by examining the variances for

each comparison zone listed under the Heat or Mixing Ratio Island heading on Symaps 8.3.3.1a through 8.3.3.2. Hence, it could be stated that the locations within the lower code zones vary greater than those within the urban heat or moisture island.

Returning to the Squared Ranks Test results for Cycle 126, T_2 was found to exceed the alpha 0.05, 126 degree of freedom value of 154.3021 by 12.4529 units. The critical alpha value was approximately 0.0088. Respective values of $N(S)^2, D^2$ and S_j^2/n_j were $3.7813E+12, 5.9533E+09$ and $4.7740E+12$.

The multiple comparison procedure yielded similar inferences regarding k sample variance differentiation as did the similar Kruskal-Wallis routine for the k sample means. That is, the greater portion of comparisons are insignificant more so for the variance than for the mean data tests. Forty-six pairs plus the one lone location had mean variance rank sum differences which could not satisfy the inequality equated in Section 7.4.4. Those which did are listed in Table 8.3.3.3 along with their multiple comparison significance and locational codes, their position in the former Kruskal-Wallis multiple comparison test and their group pooled variances.

Table 8.3.3.3

SIGNIFICANT MULTIPLE SQUARED RANKS TEST COMPARISONS FOR
CYCLE 126 TEMPERATURE VARIANCE

CODE	LOC	K-W CODE	POOLED VARIANCE	K-W CODE	LOC	CODE
''''' (2)	50	6	0.035	4	103	OXAV
	108	6		5	102	(10)
	79	6		1	34	
	107	6		1	34	
	107	6		1	35	
'-''- (4)	94	8	0.062	1	33	OOOO
	60	6		1	38	(8)
	93	8		1	37	
==== (5)	114	11	0.211	1	40	XXXX
	106	6		1	36	(7)
	78	6		3	43	
	112	6		5	15	
	117	11		4	45	
	113	7		6	104	
	125	8		1	39	
	77	6		5	46	
	81	6		4	46	
	80	6		6	9	
++++			1.120			++++

Even with only 14 significant pairs, there is a partial inverse relationship between the Kruskal-Wallis and Squared Ranks multiple comparison test results. The relationship, however, is restricted to only those locales which registered a Kruskal-Wallis comparison code of 5 or less. The corresponding respective Squared Ranks comparison codes are equal to or greater than 7.

Moreover, this relationship is more valid for Kruskal-Wallis code 1 sites than for any other. That is, with the exception of locales 103 and 102 which yielded the greatest mean squared ranks differences of 202476.25 and 196268.00, the next seven consecutive sites all had code 1 Kruskal-Wallis labels. Locations 30 through 32 were the only sites of the latter statistical grouping which had variances that did not differ.

These sites had one trait in common. No matter whether the prevailing winds were from the south or from the northwest, anthropogenic heat acquirement would be always minimal. The lands traversed by these winds were consistently flat, snow clad, stubble agricultural fields.

The trajectories of the 295° and 304° winds of traverses 205 and 206 respectively towards each of the upper significant code sites of Table 8.3.3.3, with the exclusion of locales 15, 16 and 9, were directed over similar terrain. The addition of anthropogenic heat again would have been minimal.

When the winds however were southerly, the distance between the monitoring location and the anthropogenic heat generation area determined in which multiple comparison zone the site would be placed. Moreover, whenever rural and urban land classification types are juxtaposed, and the traversed area is perpendicular to the prevailing winds, the

intermediate situated locales would have the highest temperature variances. Consequently, these areas had the highest calculated mean sum of squared ranks: a code designation of 10. In other words, if the monitoring site was located in the boundary area of the urban heat island or within several of the wind tunnels which bisect the urban heat island, variances between means would be high.

Location 103, situated at the Highway 101-Pembina Cloverleaf entrance, and 102, situated at the exit of the above, had the highest mean sum of squares values. Respective values were 203,189.00 and 192,293.50. Both are perpendicular to the prevailing southern winds and downwind of the residential community of St. Norbert. The minimal hypothetical heat loss generated by this community of about 2100 during those traverses conducted when the prevailing wind was from the south would be approximately $8.52E+07$ Btu's. This is equivalent to about 461 gallons of Bunker 'C' fuel oil (See Appendix A)

Whereas no information what-so-ever is available on even the most fundamental surface boundary parameters such as surface roughness or average substrate densities and specific heats, and whereas basic radiosonde data does not exist either, it is impossible to determine the dispersion rates of the St. Norbert heat island or the dimensions of the heat island spread along the x, y and z axes. All that

is apparent from the data is that the heat loss from this community is sufficient to influence the temperatures of locations 1.8 km. north of the settlement when winds are from a southerly direction. On the average, the temperatures monitored at locales 102 and 103 were approximately 1.2°C. warmer than those logged for locations 30 through 32 during traverses 195 and 218. The only difference between these two groups is that there is no urban community south of the latter. In fact, when the prevailing winds were between 281.25° and 304.75°, the temperature difference between the two was averaging about 0.42°C.

It should also be noted that the temperature differences obtained for the multiple comparisons of location 102 and 103 with sites 30 through 32 for the southern traverse component of Cycle 126 are statistically significant whereas those calculated for the northwest prevailing wind traverses 205 and 206 were not. The critical alpha value for the foremost location comparison varied between 5.88E-07 and 1.44E-07 whilst that for 103 varied between 0.0027 and 0.0005.

There is also a tendency that anthropogenic heat displaced by southern winds stabilize temperature variation between adjacent fixed point monitoring locations within similar sectors of the same traverse. Not a single

multiple squared ranks comparison group,7 through 10,or any portion there of,had an among sums of squares greater than 1.0°C.. Nor had any a within sums of squares larger than 0.7°C.. The least of the within groups sum of squares,0.08°C.,was calculated for the most northwestern traverse locations,37 and 38 whilst the largest value,0.66°C.,was that for location fusion (34,35).

The former group's variation in temperature was slight because the prevailing southerly winds displaced a smaller quantity of anthropogenic heat over a larger area. That is,the only heat that these winds could acquire and disperse was restricted to that generated by two residential community committee areas (CCA) known as Assiniboine Park and St. James-Assiniboine.²⁵ And even so,only that generated

²⁵ All the following land category estimates were obtained from the City of Winnipeg,Development Plan Review,Planning Research, The City of Winnipeg Land Use-1971,by Community Committee Area, September,1972,unless otherwise referenced.

Approximately 84.2, or 104.5 km² of the total Assiniboine Park CCA area is either vacant,agricultural or underdeveloped land. The residential land use category accounts for about 7.5, of the total area whilst that devoted to parks,schools,cemeteries and so forth is 3.6,. Respective percentage in decreasing land use category importance are industrial,2.5;public utilities,1.4;public buildings,0.6 and commercial,0.2.

The St. James-Assiniboine CCA has a similar land use percentage structure. Underdeveloped and vacant land accounts for 67.1, of the total area of 109.3 km². To this,approximately 84, of the public utility area may be added as this percentage constitutes maintained flightpath zones. The latter category has a total area of 10.7 km². Residential land use again has the second highest area percentage. The respective value is 12.3 The remaining

by the western sectors of each CCA.²⁶ Winds with northern trajectories over these western CCA portions traverse on the average 5.9km of urban environment and 6.1km of agricultural land before they arrive at site destinations 36 through 40.²⁷ This trajectory, therefore, assures adequate moderation.

Variation however among traverses can become quite large even if the degree difference between the prevailing winds is only a matter of a few degrees. For example, during traverse 195, the prevailing wind has a direction of 172°. It was therefore parallel to the western portions of the Perimeter Highway. Although the amount of heat acquired and displaced by the wind was proportionate to the traffic

area land use category percentages in descending importance are parks, schools, cemeteries, 5.5; industrial, 2.9; commercial 2.0 and public buildings, 0.6.

Although the commercial area of St. James-Assiniboine is 2.13 km² whilst that of Assiniboine Park CCA is 0.3 km², approximately 0.65% of the area is devoted to parking (City of Winnipeg, Planning Division, Committee on Environment, Shopping Centres 1976, December, 1976)

²⁶ Although both CCA's parallel the Assiniboine River for almost 9.84km east of the western portion of the Perimeter Highway, flightpath zoning by-laws for Runway 36 of the Winnipeg International Airport and the position of the Assiniboine Park-Assiniboine Forest-Tuxedo Golf Course Recreation Complex ensure that the two CCA's will continually be bisected into an eastern and a western sector.

The latter recreational zone with an approximate area of 4.94 km² totally segregates the western portion of the Assiniboine Park CCA from the rest of the city proper (Personal communication, Jim Mansell, Clerk, Parks and Recreation, City of Winnipeg, December 29, 1982, 1225hrs). The minimum width of this zone is about 1.65 km whilst the

flow on the Highway, a cumulative effect was instigated by the flow. That is, the heat liberated from car exhaust at location 31 would influence temperatures and mixing ratios from that locale onwards. Heat liberated at location 32 would be added to whatever was transmitted from the downwind areas.

The average temperature increase per location due to this process between locations 31 through 36 was approximately 0.17°C. When the orientation of the traverse became perpendicular to the prevailing winds at location 37, a drop of 0.51°C. was registered.

maximum is approximately 2.42 km.

The former by-law also sets restrictions on the type of construction allowed south of the threshold area of Runway 36. This includes buildings in the western sectors of the above recreation area. That is, for every 15.24 meters one proceeds southward from the southern boundary of the 1.3 km² threshold rectangular area of Runway 36, the maximum vertical increase allowed is 0.3048 meters (Personal communications, A. Schwartz, Supervisor, Aviation Control Tower, Winnipeg International Airport, December 29, 1982, 1225hrs; Art d'Entremont, Supervisor, Airport Licenses and Inspection, Winnipeg International Airport, December 29, 1982, 1000hrs).

Both the above foster the establishment and maintenance of a non high-rise residential corridor and a 'wind tunnel' between the Airport property boundary and the Assiniboine River-Recreational Complex. The average length and width are 1.42km and 1.19km respectively.

This 'wind tunnel' is quite evident on both the SAS G3D plots and the Synap trend maps. For the former, it is positioned between X co-ordinates 7.2 and 9.7. The

During traverse 218, the prevailing winds, however, were 180°. No pattern existed. Temperatures fluctuated randomly, with the greatest increase registered between locations 34 and 35: 0.56°C.. The reason for such an increase in less than 0.74km is that location 35 is directly downwind of the Unicity Fashion Square. This Regional Shopping Center has a greater area devoted to buildings than any other in the City of Winnipeg: approximately 28.3, of the total area of 0.16km² (City of Winnipeg, Planning Division, Committee on Environment, Shopping Centres-1976, December, 1976). The estimated heat loss during November 23, 1976, the day traverse 218 was conducted, was calculated at 4.88E+07 Btu or 241.9 gallons oil equivalent (see Appendix B)

When examining the among and within groups sums of squares for traverses 205 and 206, the northwesterly prevailing wind component of Cycle 126, it was noticed that both variations were larger than their southern counterparts. The former was approximately 4.3 times greater whilst the within group sums of squares was about 6.8 times as great. Only location grouping (45,46) had compatible results. Respective among and within variations were 0.06°C. and 0.05°C..

corresponding Symap column range is 33 through 48.
²⁷ The northern boundary of the St. James-Assiniboine sector is taken as Saskatchewan Avenue whilst that of the Assiniboine Park CCA sector, also known as Charleswood, is taken as Ridgewood Avenue.

The reasons again for such an occurrence was traced to their locational site. Both are wedged between residential sectors. Even though the population density of the windward sector is quite low, 0.16 persons per km², the effect is very noticable.²⁸ The temperature differences between locations 44 and 45 for traverses 205 and 206 were 0.21°C. and 0.85°C. respectively. The 0.64°C. spread probably arose from an increase in residential energy consumption. Table 8.3.1.1 indicates that pressure, wind direction and speed and parameter N were relatively similar for both traverses. The only difference being that traverse 205 commenced at and was standardized to 1700 hours whilst traverse 206 started at and was standardized to 2100 hours.

Unlike for the above analysis, climatological information can not be used as an aid in explaining why locations 9, 15 and 16 have multiple squared ranks comparison codes 7 or why any of the locations registering codes 1 through 5 have such

²⁸ The windward sector corresponds to Census Tract 51. The total area is 2.46 km² of which 1.4, is residential. Greater than 85, of the remaining area is vacant or agricultural. Approximately 6, or 0.9 km² is public cemetery land. The remainder is commercial of which the greatest proportion is of the ribbon type paralleling Keewatin Street.

The above population census tract information was obtained from the City of Winnipeg, Planning Research Branch, internal publication entitled Population Density (per Gross Acre) by Census Tract - 1971 All other information was obtained from person communications with various departmental Planners.

codes. All these locales are situated well within the urban heat island influence zone. Logical explanation can only be derived from the examination of traffic flow charts for the city.

Locations 14 through 17 are situated within the St. James Bridge-Century Underpass corridor. In 1976, this transportation network had the greatest traffic flow count in the city and it has since increased drastically (Personal communication, Ed Guertin, Transportation Research Analyst, Streets and Transportation Department, City of Winnipeg, December 30, 1982, 1100hrs) The flow, moreover, is relatively constant. That is, the average week day count during 1976 between 0700-1900 hours was approximately 76740: roughly 1.6 times that logged for the Portage-Main intersection. Only 10% of this flow occurs between the morning peak hours 0730-0830 whilst about 13.2% occurs between the evening peak hours 1630-1730. The area therefore has a relative perpetual congestion problem. In fact, during the rush hours, a volume-capacity ratio greater than 1.0 is obtained.²⁹ Thus whenever temperatures and

²⁹ The City of Winnipeg, Streets and Transportation Division, defines the practical capacity of an intersection as the maximum traffic volume that can be discharged by an intersection under normal climatic and street conditions with most of the vehicles being able to clear the intersection without more than an one signal cycle. Where the volume to capacity ratio exceeds 1.0, congestion occurs, causing delay in flow. When the value ranges between 0.75 and 1.0, as in the St. James Bridge-Century Underpass Corridor, conditions are acceptable though they are apt to deteriorate quite suddenly.

mixing ratios are recorded at monitoring sites located within the St. James Bridge-Century Underpass Corridor it is highly probable that the data collected is representative of an exhaust based micro-climate. The effects are quite discernible in the chosen cA-cmA air mass fusion group data. They are however more pronounced for those traverses undertaken through rush hour conditions. For those traverses not conducted during the time span 1700-2000 hours, the effects have distinct wind directional traits.

For all rush hour itineraries of the S-W union, see Table 8.3.1.1, the temperature difference between locations 14 and 15, a distance of approximately 0.48 km with an elevation decline of 0.43 m, is 0.53°C . whereas that between 15 and 16, a distance of approximately 0.45 km with an elevation increase of 0.5 m is -0.14°C . The respective differences for traverse 205 is 0.94°C . and -0.35°C . Note that the changes are more pronounced during a northwesterly wind flow with overcast conditions, though in both, the areas under the overpass are heat sinks.

The missing ratio variable behaves in a similar fashion. For the S-W group the respective differences between the above locales are 0.0176 and -0.0091 g/kg whereas that for traverse 205 are 0.0391 and -0.0026 g/kg.

When traverses were conducted during non rush hour traffic, the heat sink reverses to a cold air sink only when

the prevailing winds are from the south. Moreover, the differences are greater when the skies are clear. The temperature change between locations 14 and 15 for the S-W traverse group is -0.58°C . whereas that between 15 and 16 is 0.24°C .. For traverses 195 and 218 respective differences are -0.22°C . and 0.13°C .: half that of the above rush hour example.

A heat dome however exists over location 16 for traverse 206. The temperature differences between locations 15-16 and 16-17 are 0.48°C . and -0.53°C . Locations 14 and 15 had equal temperatures of -12.8°C .. Recall that location 16 is situated near the center of the St. James Bridge. A 10 km/hour wind was not strong enough to disperse this exhaust micro-climate.

With respects to the variations of the mixing ratio variable, no definite pattern exists. For the S-W fusion there is a steady decline whereas for southern wind components of Cycle 126, a mixing ratio island is situated between locations 14 and 17. The internal variation is approximately 0.0072 g/kg whereas the change at the northern and southern boundaries of the humidity island are 0.1223 and -0.1325 g/kg respectively.

In summation, although a great deal of time has been devoted in examining the probable causes of temperature and mixing ratio variation for those multiple square ranks

comparison locales registering either code 1 or codes 7 through 10, the inferences made about variances for both the Kruskal-Wallis Nonparametric ANOVA and the parametric ANOVA proved to be valid. Recall that the null hypothesis of the Square Ranks Test that the k populations are identical was accepted by the S-W traverse union as well as each of the separate wind directional based traverse components of Cycle 126. Rejection only occurred when Cycle 126 was analyzed as a whole. Though the variation was thus artificially created being not necessarily inherent in the data, the results nevertheless indicated that the majority of the data variates in a similar fashion at each locale. The exception being that for peripheral locations situated within a 180°-360° zone.

The final statistical proof which indicates that the application of parametric tests on nonparametric cA-cmA air mass data does not lead to misleading results, lies in the statistical significance of each trend function derived for Symaps 8.3.3.1a through 8.3.3.2. The F ratios calculated are totally, without question, significant.³⁰

³⁰ Henceforth, the following formula shall be used to compute Symap trend F ratios: $R^2(n-m-1)/n(1-R^2)$ where m equals the number of terms in the trend component and n is the total number of data points (Green, 1978, pages 66-71). Although adopted because of its simplicity, the value generated should be viewed as a gross estimate. The inherent errors lie not in the formula but in the manner in which Symap (1976, Section III, Elective 38 and Section V, pages 32-45) calculates the degrees of freedom and sums of squares for variation sources due to the trend regression and deviations from the trend regression. That is, the total sum of squares variation

Although a great deal of time has been devoted in proving the obvious, that is, that the cA-cmA air mass data under examination was statistically significant no matter what type of statistic was applied, the following facts were uncovered:

- (1) both temperature and mixing ratio outliers aid in the calculation of extremely high critical alpha values for the Kruskal-Wallis H statistic but they do not yield necessary information required for the fitting of a very strong surface trend polynomial configuration equation.
- (2) only the mixing ratio data of the S-W group had an empirical distribution close enough to indicate normality. The temperature data of both the two fusions examined were nevertheless closer to the normal distribution than to the uniform distribution. It will later be shown that this was one of the main parameters which influenced the high F ratio calculation. That is, as the Kolmogorov-Smirnov Z value increases for the normal distribution, decreasing for the uniform, the

remains constant no matter at what order the trend equation is calculated for. This method used by the package is in direct contradiction to the referenced materials. Harbough et al. (1967, pages 61-70), Meyer (1976, Chapter 14) and Snedecor et al. (1976, pages 460-465), to name only a few, all indicate that as the trend surface polynomial equation increases in complexity, the degrees of freedom and sums of squares are proportional to the overall totals. The following best illustrates this procedure.

The total number of data points in each of the Symap figures in this section is constant at 180. Thus the total degrees of freedom is $n-1$ or 179. The degrees of freedom for variation source due to linear regressional components ($Bx + Cy$) are 2 whereas that due to deviations from linear are $179-2$ or 177. When a quadratic relation is derived, respective degrees of freedom would be 3 and 177. The latter value is correct because one must consider the deviations from both the linear and the quadratic forms. As there are five derived components, ($Bx + Cy + Dx^2 + Exy + Fy^2$), there are $179-5$ or 174 degrees of freedom. Symap however, registers 176. Variation due to cubic regression, components ($Gx^3 + Hx^2y + Ixy^2 + Jy^3$) only, would yield 4 degrees of freedom whereas that due to

- F ratio becomes inversely proportionate to the H statistic.
- (3) even though the Squared Ranks Test for Variance statistic proved that the k populations of both the S-W fusion and the component traverse portions of Cycle 126 are identical, by analyzing the latter as a unit, hence generating variance as the traverse components represented two different air flows, it was shown that variation among and between locales along the traverse itinerary is restricted to those areas which are peripheral in the southern, western and northern sectors.
 - (4) the degree of temperature and mixing ratio variation between and among peripheral locations situated in the above sectors depends not only upon the wind direction but also upon the orientation of these locations to both the wind and anthropogenic heat sources. The least variation occurs when there is no juxtaposed urban-rural architecture and hence no anthropogenic influence. Wind direction does not become an influencing factor then. When anthropogenic heat is added downwind of the monitoring site, orientation with respect to the wind direction becomes the main determinant. Locations which are parallel to the wind flow vary greater than those locales which are perpendicular.
 - (5) anthropogenic heat stabilizes variation. That is, variation still exists, though it does not fluctuate as greatly. This is particularly true when the wind direction is from a southern direction.

Linear + Quadratic + Cubic would yield 179-9 or 170. Note that the sum of these two degrees of freedom equal the previous order's error degree of freedom. The respective D.F. for an order 6 trend would therefore be 6 and 159. Symap however registers 6 and 172.

The calculations for the sums of squares follow the same procedure. With each increase in trend complexity, the total sums of squares for that particular order equals the previous order's error sums of squares. Symap again does not do this. Although the sums of squares vary from order to order+1 trend equation, it is not known what portion of the overall sums of squares derives from a linear or a quadratic or a sixth degree trend polynomial equation. Hence, it can not be determined at what level most of the variation is explained due to the regression. Thus, even R^2 values are effected.

- (6) urban situated locales which register high Squared Rank Multiple Comparison Codes, such as locations 9, 15 and 16, have continuous traffic congestion problems. Temperature and mixing ratios vary differently with different wind flows for all hours except for those hours which are designated rush hours.
- (7) the least amount of temperature and mixing ratio variation for the cA-cMA air mass data occurred in the eastern traverse sectors under overcast conditions when the wind was from the northwest. Traffic exhaust combined with a steady heat flow from the city proper and upwind meat processing plants, such as the Canada Packers-Swifts-Burns complex, not only moderated the temperature and mixing ratio data but also maintained a stable environment. The similar occurrence was noted for locations along the Pembina Strip which were downwind of the Manitoba Sugar Beet Plant.

Symap 8.3.3.1a

ca: S - W Wind Direction Group -- Temperature.

SYMAB 8.3.3.1A

STATISTIC COMPARISONS

KRUSKAL-WALLIS NON-PARAMETRIC ANOVA
CASES 1270
H CORRECTED FOR TIES 337.897
CRITICAL ALPHA VALUE 5.6881E-21

PARAMETRIC ANALYSIS OF VARIANCE

SOURCE DF SS MS F F PROB
BETWEEN 126 4664.5318 37.0201 3.452
WITHIN 1143 12241.0741 10.7096 1.2666E-22
TOTAL 1269 16905.6055

KRUSKAL-WALLIS MULTIPLE COMPARISONS

TRENDS ARE BASED ON SIGNIFICANCE LEVELS OBTAINED WHEN PARAMETER RANK VALUES FOR SAMPLES I AND J ARE COMPARED.

MAXIMAL ALPHA VALUES ARE ACHIEVED WHEN EXTREME LOCATIONS ARE COMPARED. FOR INSTANCE, WHEN ANY SAMPLE I PARAMETER VALUE LOCATED WITHIN AN AREA DEFINED BY ... IS SUBTRACTED FROM ANY SAMPLE J PARAMETER VALUE LOCATED WITHIN AN AREA DEFINED BY 'MHM', THE DIFFERENCE OBTAINED IS GREATER THAN THE MINIMAL VALUE REQUIRED FOR AN ALPHA OF 0.00005. ALL SAMPLES WITHIN THE SAME AREA YIELD INSIGNIFICANT ALPHA VALUES ON COMPARISON.

SYMAB ERROR MEASURES:

STANDARD DEVIATION 1.08
VARIATION EXPLAINED
BY SURFACE (6 DF) 0.1300E+04
VARIATION NOT EXPLAINED
BY SURFACE (173 DF) 0.2095E+03
TOTAL VARIATION 0.1509E+04

DETERMINATION COEFFICIENT 0.8612
CORRELATION COEFFICIENT 0.9280
RATIO OF MEAN SQUARES, F 5.9633
F PROBABILITY TOTAL

DISTRIBUTION COEFFICIENT OF POINTS IS RANDOM AT 0.97

Table with columns: RI - RJ, SIGNIFICANCE, FREQUENCIES CLASS, RELATIVE. Rows include MHM, OXAV, O+O, OOO, XXXX, and INSIGNIFICANT.

SUBCLUSTER: CONTINENTAL ARCTIC
CYCLE : SOUTH TO WEST WIND DIRECTION GROUP
VARIABLE: TEMPERATURE (C.)

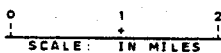
AVERAGE SYNOPTIC CONDITIONS:
N CODE (OKTA) 0
SURFACE WIND DIRECTION (000 TO 360) 231
SURFACE WIND SPEED (KM/H) 10.00
STATION PRESSURE (MB) 995.6
STABILITY, SURFACE-950MB: DOSE/DZ 0.0151

STATISTICS:
MEAN -22.4
STANDARD DEVIATION 3.6499
STANDARD ERROR 0.1024
MAXIMUM TEMPERATURE RECORDED FOR GROUP -14.5
MINIMUM TEMPERATURE RECORDED FOR GROUP -32.7
MAXIMUM RANK AND LOCATION 947.97 # 67
MINIMUM RANK AND LOCATION 214.20 # 39

HEAT ISLAND RANGE (C)

Table with columns: CODE, MEAN, VAR, RANGE, VAR, MEAN, CODE. Rows show temperature ranges for codes MHM, OXAV, O+O, OOO, XXXX.

OUTPUT MAP RATIO 1:62,113



Sympap 8.3.3.1b

cA: S - W Wind Direction Group -- Mixing Ratio

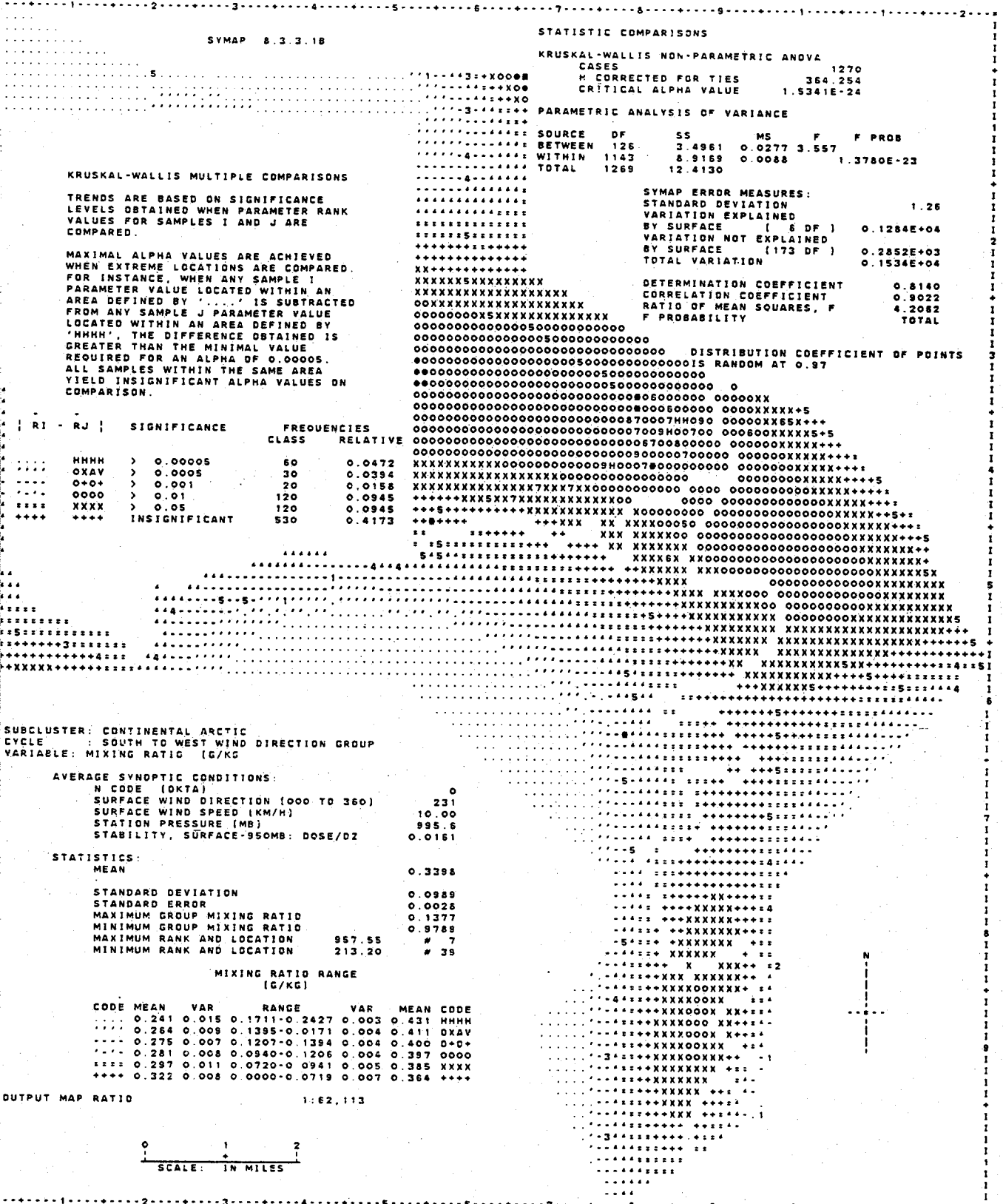
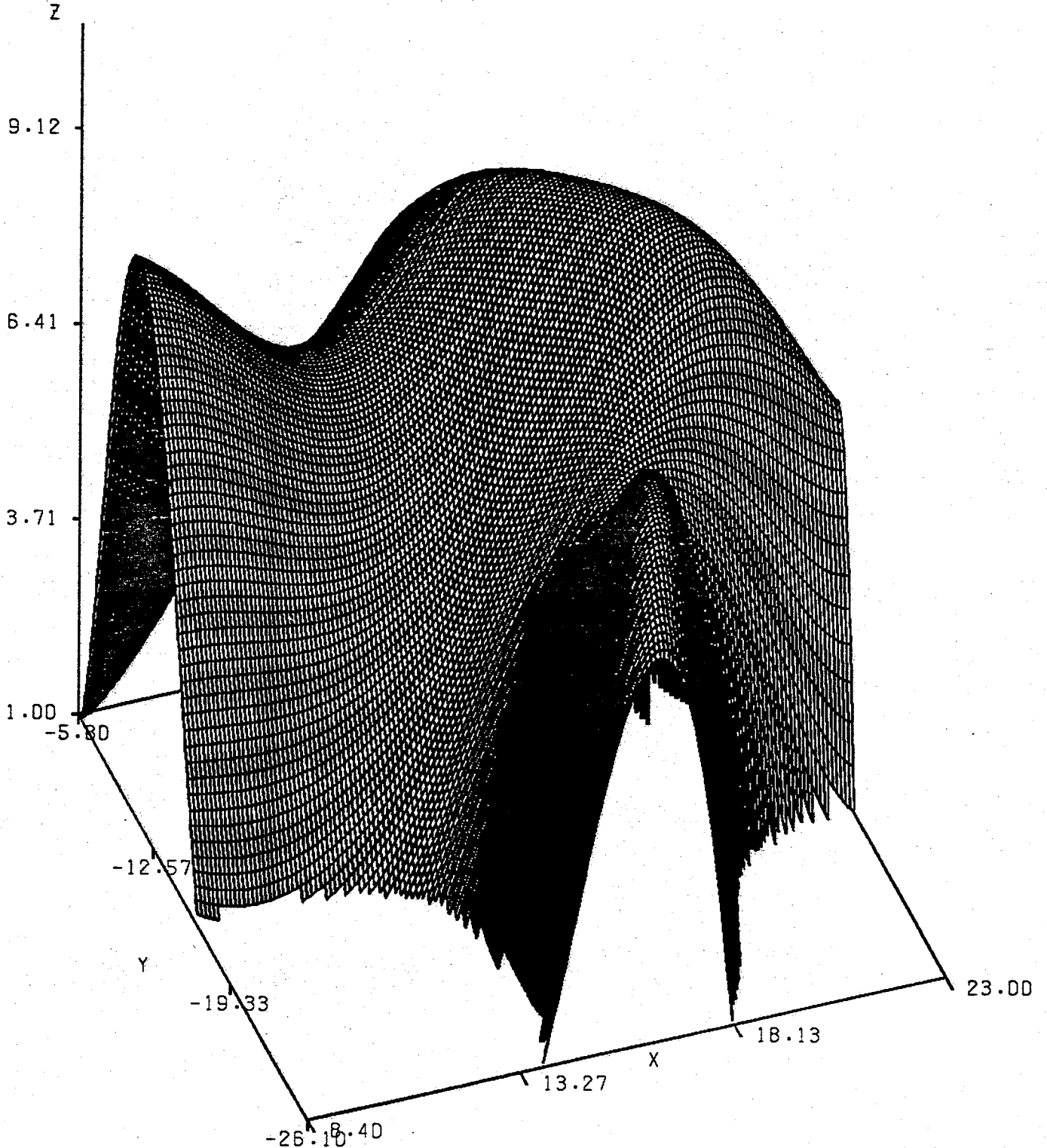


FIGURE 8.3.3.4A

3-DIMENSIONAL VIEW OF FIGURE 8.3.3.1A		Z VALUE		HEAT ISLAND RANGE
Z VALUE		Z VALUE		
<2.00		>9.54		
2.00	- 2.89	-	9.11 - 9.54	6.2 C. - 7.6 C.
2.89	- 3.78	-	8.22 - 9.11	5.0 C. - 6.2 C.
3.78	- 4.67	-	7.33 - 8.22	4.8 C. - 5.0 C.
4.67	- 5.56	-	6.44 - 7.33	3.7 C. - 4.8 C.
5.56	-	-	6.44	2.0 C. - 3.7 C.
				0.0 C. - 2.0 C.

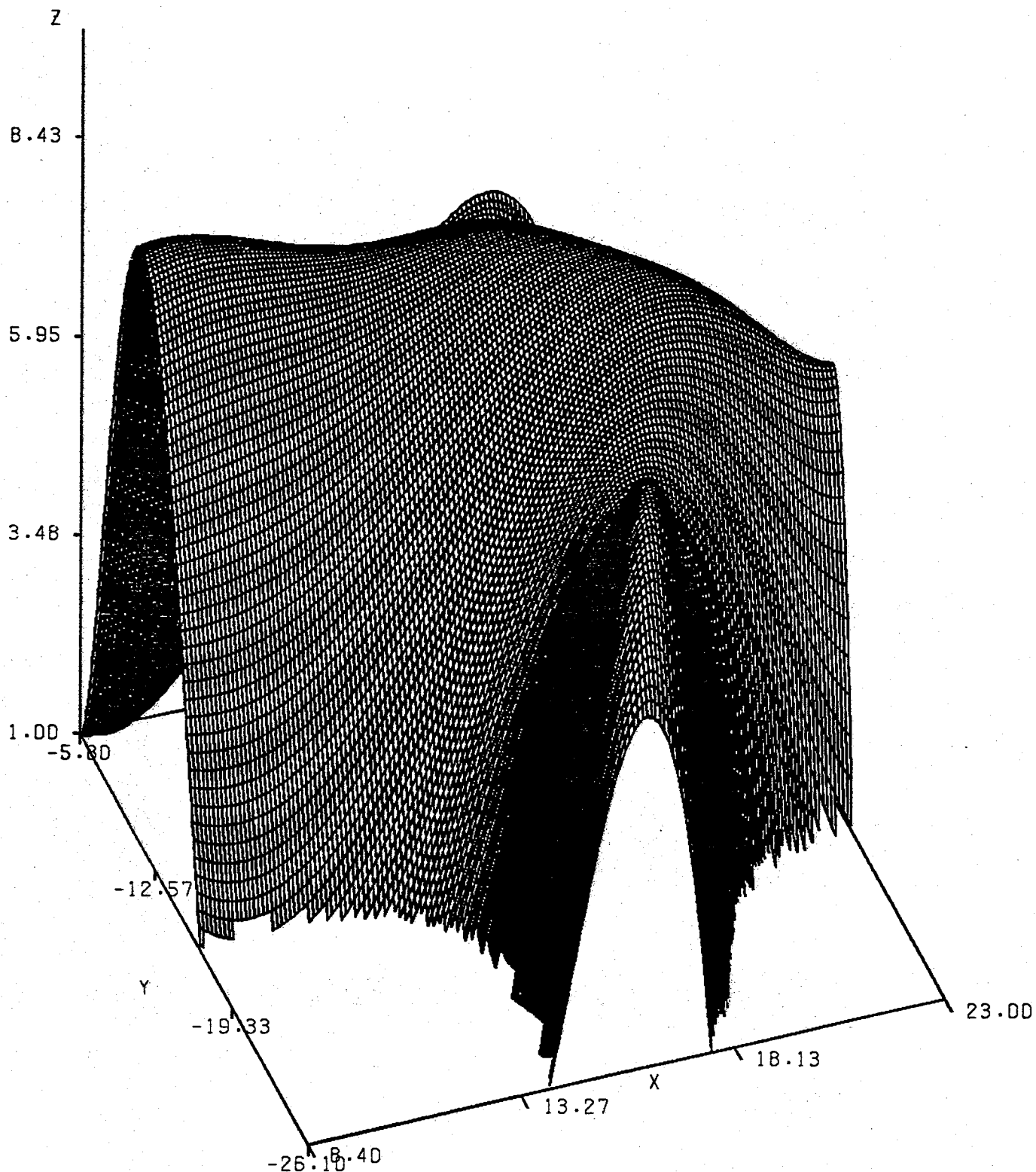


TILTED AT AN ANGLE OF 70 DEGREES
 ROTATED AT AN ANGLE OF 20 DEGREES
 DIRECTION: SW FROM Y-X AXIS INTERCEPT

FIGURE 8.3.3.4B

3-DIMENSIONAL VIEW OF FIGURE 8.3.3.1B

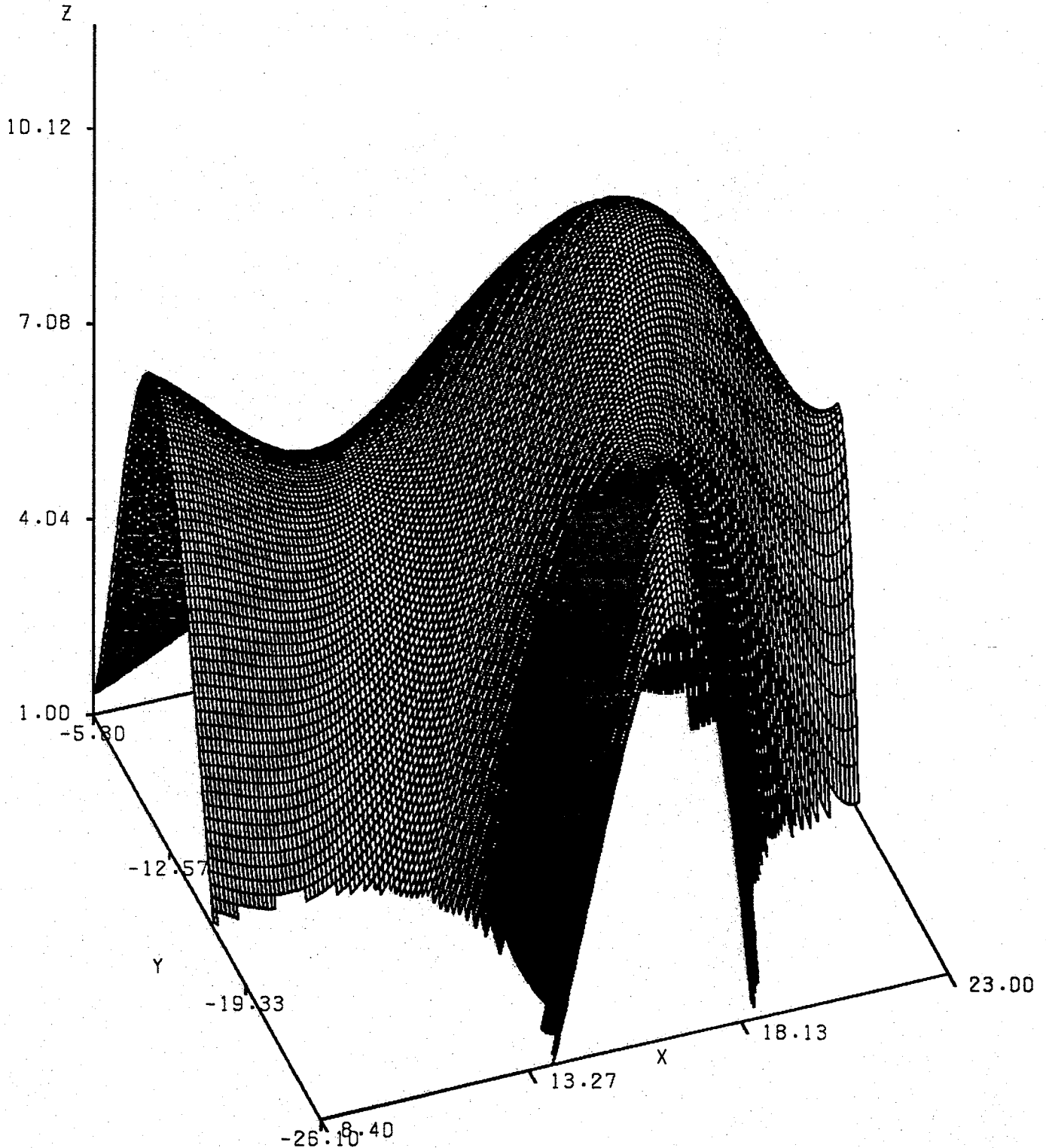
Z VALUE	-	Z VALUE	MIXING RATIO RANGE
<2.00	-	>9.54	0.1711 - 0.2427
2.00 - 2.89	-	9.11 - 9.54	0.1394 - 0.1711
2.89 - 3.78	-	8.22 - 9.11	0.1207 - 0.1394
3.78 - 4.67	-	7.33 - 8.22	0.0940 - 0.1207
5.56	-	6.44	0.0000 - 0.0720



TILTED AT AN ANGLE OF 70 DEGREES
 ROTATED AT AN ANGLE OF 20 DEGREES
 DIRECTION: SW FROM Y-X AXIS INTERCEPT

FIGURE 8.3.3.5
3-DIMENSIONAL VIEW OF FIGURE 8.3.3.2

Z VALUE	-	Z VALUE	HEAT ISLAND RANGE
<2.00	-	>9.54	2.7 C. - 4.1 C.
2.00 - 2.89	-	9.11 - 9.54	2.2 C. - 2.7 C.
2.89 - 3.78	-	8.22 - 9.11	1.9 C. - 2.2 C.
3.78 - 4.67	-	7.33 - 8.22	1.4 C. - 1.9 C.
4.67 - 5.56	-	6.44 - 7.33	1.0 C. - 1.4 C.
5.56	-	6.44	0.0 C. - 1.0 C.



TILTED AT AN ANGLE OF 70 DEGREES
 ROTATED AT AN ANGLE OF 20 DEGREES
 DIRECTION: SW FROM Y-X AXIS INTERCEPT

SYMAP 8.4.3.1

Early cMaw to mAk Transformation -- Temperature

SYMAP 8.4.3.1

STATISTIC COMPARISONS

KRUSKAL-WALLIS NON-PARAMETRIC ANOVA
 CASES 508
 M CORRECTED FOR TIES 268.908
 CRITICAL ALPHA VALUE 4.1989E-12

PARAMETRIC ANALYSIS OF VARIANCE

SOURCE	DF	SS	MS	F	F PROB
BETWEEN	126	963.0792	7.6435	2.941	
WITHIN	381	990.3050	2.5992		7.2415E-10
TOTAL	507	1953.3842			

KRUSKAL-WALLIS MULTIPLE COMPARISONS

TRENDS ARE BASED ON SIGNIFICANCE LEVELS OBTAINED WHEN PARAMETER RANK VALUES FOR SAMPLES I AND J ARE COMPARED.

MAXIMAL ALPHA VALUES ARE ACHIEVED WHEN EXTREME LOCATIONS ARE COMPARED. FOR INSTANCE, WHEN ANY SAMPLE I PARAMETER VALUE LOCATED WITHIN AN AREA DEFINED BY '...' IS SUBTRACTED FROM ANY SAMPLE J PARAMETER VALUE LOCATED WITHIN AN AREA DEFINED BY 'MHMH', THE DIFFERENCE OBTAINED IS GREATER THAN THE MINIMAL VALUE REQUIRED FOR AN ALPHA OF 0.00005. ALL SAMPLES WITHIN THE SAME AREA YIELD INSIGNIFICANT ALPHA VALUES ON COMPARISON.

SYMAP ERROR MEASURES:

STANDARD DEVIATION 1.13
 VARIATION EXPLAINED
 BY SURFACE (6 DF) 0.1375E+04
 VARIATION NOT EXPLAINED
 BY SURFACE (173 DF) 0.2285E+03
 TOTAL VARIATION 0.1603E+04

DETERMINATION COEFFICIENT 0.8575
 CORRELATION COEFFICIENT 0.9280
 RATIO OF MEAN SQUARES, F 5.7814
 F PROBABILITY TOTAL

DISTRIBUTION COEFFICIENT OF POINTS
 IS RANDOM AT 0.97

RI - RJ	SIGNIFICANCE	FREQUENCIES CLASS	RELATIVE
HHHH	> 0.00005	20	0.0394
OXAY	> 0.0005	38	0.0709
O+O+	> 0.001	12	0.0236
OOOO	> 0.01	36	0.0709
XXXX	> 0.05	48	0.0945
++++	INSIGNIFICANT	204	0.4016

SUBCLUSTER: EARLY CMAW TO MAK TRANSFORMATION
 CYCLE : ENO
 VARIABLE: TEMPERATURE (C.)

AVERAGE SYNOPSIS CONDITIONS:

N CODE (OKTA) 0
 SURFACE WIND DIRECTION (000 TO 360) 180
 SURFACE WIND SPEED (KM/H) 17.03
 STATION PRESSURE (MB) 990.3
 STABILITY, SURFACE-950MB: DOSE/DZ 0.0186

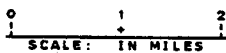
STATISTICS:

MEAN 1.9
 STANDARD DEVIATION 1.9229
 STANDARD ERROR 0.0715
 MAXIMUM TEMPERATURE RECORDED FOR GROUP 5.0
 MINIMUM TEMPERATURE RECORDED FOR GROUP - 7.8
 MAXIMUM RANK AND LOCATION 478.88 # 65
 MINIMUM RANK AND LOCATION 47.00 # 36

HEAT ISLAND RANGE (C)

CODE	MEAN	VAR	RANGE	VAR	MEAN	CODE
....	- 0.78	5.134	3.97-5.80	0.568	4.12	MHHH
....	- 0.24	4.487	3.52-3.98	0.604	3.73	OXAY
....	- 0.02	3.394	2.98-3.51	0.455	3.53	O+O+
....	- 0.43	3.596	2.18-2.97	0.979	3.39	OOOO
....	- 0.87	2.313	1.01-2.15	0.924	3.02	XXXX
....	- 1.49	2.478	0.00-1.00	1.373	2.45	++++

OUTPUT MAP RATIO 1:62,113



8.3.4 Symap Comparisons

Rather than dwell upon the differences and similarities between the two temperature Symaps and between the temperature and mixing ratio Symaps of the S-W fusion, here and again for each of the other five air mass studies, they will be briefly introduced, leaving more detailed discussion for later publications. The reason being, that the same features are reoccurrent.

There is only one major difference between the various Symap and SAS G3D plots and that is that under overcast conditions, the major heat island core of comparison zone 11, designated 'HHHH' on Symap 8.3.3.2, has shifted from the C.B.D. outlier cases and has become consolidated in the vicinity of the major meat packing plants of Winnipeg. The cloud cover was therefore either sufficient to deflect outgoing radiation from the processing plants back down to the monitoring height or the winds in the locale were very light hence preventing heat dispersion.

This occurrence is neither an error or an exception. That is, with the exception of heat losses from refrigeration, boilers, ventilation of buildings and smokehouses, heat rates are constant for the meat processors (Personal communication, Joe Magro, Mechanical Superintendent, Canada Packers Inc. Plant, Winnipeg, January 3, 1983, 0900 hrs.). The estimated heat losses for this particular

company per source during the year 1976, combined from the sources Kiln Dryer, Dowtherm Boiler, Hog Singer and Refinery Cooling Tower, is approximately $1.05E+10$ Btu per month. With the exception of the hog singer which operates 6 hours per day for 5 days, the remaining sources of heat are 24 hour operational outputs.

The heat losses for the Swift plant were similar to that of Canada Packers. That from the Schneider and East-West Packer plants contribute approximately 0.3 of that of Canada Packer's output. The total estimated generated heat loss in the area would be at a minimum of $2.415E+10$ Btu/month (Personal communications, Joe Magro, Mechanical Superintendent and Gene Poluha, Project Engineer, Canada Packers Inc. Plant, Winnipeg, January 4, 0900 hrs.)

Hence, there is a constant heat output even though when skies are clear, the above condition does not exist. Instead, the basic heat island pattern of Symap 8.3.3.1a was of code 9, designated 'O+O+'. The broadened maximum ellipse stretched from the northwestern C.B.D. sectors through the meat processing area well into the Windsor Park residential sector. The major axis was approximately 7.9km whilst the minor axis which paralleled the prevailing mean wind direction, 231° , was about 1.7km.

Just as bewildering is the fact that no significant mixing ratio trend can be detected during overcast

conditions. This is again odd because the rate of water vapor release from the meat processing plants is again constant at approximately $1.30E+05$ litres per day.

The mixing ratio pattern of Symap 8.3.1.1b was in all respects similar to that of its associated S-W temperature trend. The only major difference being that the mixing ratio comparison code '0000' occupies the combined temperature area coded '0+0+' and '0000'.

Turning to the three dimensional representations of the corresponding Symaps, the following traits become apparent:

- (1) the advection of southwestern air is prevalent in all cases. Infiltration occurs well into the residential sectors of Fort Rouge where it becomes effectively blocked by the generated heat and mixing ratio islands.
- (2) the University of Manitoba exists as a separate heat and humidity island under clear conditions but is joined to the major heat core during overcast conditions.
- (3) the steepest temperature and mixing ratio cliffs are constantly located along the Pembina Highway commercial-residential corridor. The slope differentiation between the windward and leeward sides are relatively constant being on the average 0.76 times sharper on the latter. For the S-W group the windward and leeward temperature changes were 3.53°C./km and $-4.66^{\circ}\text{C./km}$ whilst those for Cycle 126 were 1.49°C./km and $-2.51^{\circ}\text{C./km}$, respectively.
- (4) the St. James - Century Underpass traffic corridor discussed in the previous section, appears only on the temperature plots, regardless to the N code conditions.
- (5) the St. James-Assiniboine and Charleswood residential sectors have a unique parabolic temperature and mixing ratio trend. The slopes vary according to the wind direction with the greatest being on the leeward side. During the northwestern flow of Cycle 126 the respective temperature changes were 0.64°C./km and

-0.80°C./km whereas that during southern flow were
1.89°C./km and -2.17°C./km.

8.4 Continental Maritime Arctic Warm to to Maritime Arctic Cold Air Mass Analysis

8.4.1 Fusion Selection

In this section it will be shown that traverses belonging to the same air mass classification, but of a different order, cannot be fused to a single cluster and yet retain their original Kruskal-Wallis significant critical alpha levels. Though, traverses belonging to the same air mass category and of the same warm (w) or cold (k) order, can be fused with the resultant critical alpha level still being greater than or equal to 0.05. If, however, the H statistic so calculated upon fusion, remains relatively constant or becomes lower than either of the component cycle's values, information is being lost and the cycle should be discarded. When the H value increases, either a true trend exists or several outliers have emerged. The latter, as shown in the previous section, lacks any sort of usefulness and thence the fusion should also be ignored.

It has also been shown in Section 8.3 that climatic variable variation need not be constant or similar when significant traverse cycles are fused. Recall, for instance, Cycle 80. Although the prevailing Airport winds were SW during two component traverses and NW for the remaining two, the critical alpha value increased to greater than 0.000005. Only the variance was affected and even so, only for 14 peripheral fixed locational sites.

A similar outcome was noted for the cMA to mAk transformation air mass traverses to be discussed. In fact, climatic parameters f and N were also included with little influence being noted on the resultant fusion. However, prior to any more discussion of the above, background information and generalizations must be noted down.

The second subcluster to be statistically analyzed is composed of 65 traverses. This subcluster is united to the previously discussed cA-cMA subcluster at Cycle 250. The change in the error sums-of-squares, d_1 , at fusion, however, was the third largest recorded out of the total 253 unions. The respective value of 18.872 adequately indicates that this subcluster is unique in several respects though similar to the cA-cMA fusion in others.

In Table 8.4.1.1 the traverses which were undertaken during the early and later cMA to mAk air mass transformation stages are coded according to their respective position in the total 253 conducted itineraries. Numbering 35, the early stage itineraries all have similar air mass characteristic curves which deviate from those of the cA only in the slant of the curve. That is, due to the increased mixing ratio content, the curve is no longer parallel to the Q_d ordinates of the Rossby diagram. Inversions, though, still exist.

For the later 30 stage cMA to mAk transformation traverses, especially the true mAk cluster, Cycle 80, the surface inversion has dissipated and has been replaced by the unusual neutral to unstable condition in the lower 350 meters.

Also listed in both this Table on the left are the standardized traverse hour and the prevailing Airport climatic variables, station pressure (PPP), wind direction (dd), wind speed (ff) and the total fraction of the celestial dome covered by clouds, irrespective of genus type, code N.³¹

The Clustan-1C dendrogram reproduction for each portion of Table 8.4.1.1 is given in Tables 8.4.1.2a and 8.4.1.2b respectively. The ordinates are the traverse codes whilst the abscissa are the fusion cycle numbers. The number symbol (#) will appear under those traverses in this table which when fused yield critical alpha values less or equal to the critical type 1 error alpha of 0.05 for both the climatic variables under consideration. An equal sign (=) will indicate the converse of the above. If the null hypothesis is rejected only by temperature data, an unequal sign (≠) will be printed under the respective itinerary grouping. Meanwhile, a hyphen (-) will symbolize that only the mixing ratio data has rejected Ho.

³¹ See Chapter 8 footnotes 8 through 10 for a recapitulation of valid climatic information concerning these parameters.

Statistical information relating to the traverse fusion cycles of Table 8.4.1.2a is found in Table 8.4.1.3a while that of Table 8.4.1.2b is found in Table 8.4.1.3b. Together with the cycle identification number, the actual change in the error sum of squares at fusion (d1) is listed on the left. The Kruskal-Wallis test statistic corrected for ties (H) and its associated critical alpha level (a) are also tabulated for both temperature and mixing ratio.

TABLE 8.4.1.1

CLIMATOLOGICAL INFORMATION FOR TRAVERSES CONDUCTED UNDER
THE VARIOUS cmAw TO mAk AIRMASS TRANSFORMATION STAGES

EARLY STAGES						LATER STAGES					
TRAV	HR	CLIMATIC VARIABLES				TRAV	HR	CLIMATIC VARIABLES			
		PPP	dd	ff	N			PPP	dd	ff	N
4	9	990.0	WSW	1.8	0	138	21	972.3	WSW	29.7	8
7	21	985.5	S	12.5	0	140	13	985.9	WNW	22.2	8
8	1	981.9	S	22.5	2	141	17	987.1	NW	11.6	8
221	21	964.6	WSW	26.0	4	142	21	988.3	WNW	7.9	8
5	13	988.9	S	7.8	1	139	9	984.3	W	30.1	8
6	17	986.8	S	9.0	0	179	9	980.7	NNW	44.0	8
9	9	982.4	S	31.8	0	167	9	978.5	S	27.8	8
222	9	973.0	NNW	30.1	8	172	13	986.8	NW	42.6	8
124	9	984.3	NNW	32.0	3	173	17	989.5	NNW	34.3	8
128	9	993.6	SSW	16.2	0	174	21	991.2	NNW	41.7	8
143	9	988.6	NW	22.7	8	152	13	998.5	ENE	10.7	8
151	9	1000.0	SE	6.0	7	228	9	992.8	S	22.7	1
159	9	997.7	ENE	11.6	8	231	21	987.9	SE	24.6	5
155	9	990.6	S	27.3	8	156	13	986.2	SSW	25.5	8
166	21	1003.2	S	19.5	0	171	9	984.3	WNW	42.6	8
154	21	997.5	SSE	11.6	7	234	17	994.4	N	17.1	0
160	13	998.0	ENE	14.4	8	176	13	974.9	WNW	21.8	1
161	17	999.7	ENE	13.4	8	190	21	976.8	WSW	19.9	1
162	21	1001.7	ENE	12.1	5	184	13	982.9	SW	14.8	0
175	9	976.7	S	28.7	8	188	13	979.3	W	19.5	0
180	13	985.2	N	32.0	8	185	17	982.9	SSW	13.0	0
181	17	988.7	N	25.5	8	177	17	974.5	W	8.8	5
197	17	983.0	S	20.4	8	189	17	978.2	WSW	13.9	6
198	21	980.5	S	16.7	7	178	21	973.7	WNW	16.7	8
223	13	978.8	NNW	29.7	8	153	17	998.4	E	9.7	7
163	9	1006.6	S	6.8	7	227	21	993.5	N	9.3	0
187	9	980.3	SSW	21.8	0	235	21	996.0	ENE	11.1	0
196	13	986.3	SSW	23.6	8	164	13	1005.8	S	10.7	1
219	13	974.2	S	42.6	7	165	17	1004.8	SSW	9.3	0
220	17	968.1	S	35.2	8	186	21	982.8	SSW	14.8	0
182	21	989.6	NNE	24.1	8						
191	9	996.9	NNW	23.6	8						
194	21	997.1	WNW	14.4	3						
192	13	996.9	NNW	22.2	8						
193	17	997.5	NNW	16.7	8						

TABLE 8.4.1.2a

EARLY cmAw - mAk AIRMASS TRANSFORMATION TRAVERSE DENDROGRAM

TRAV

CYCLE

2222221111111111199977666554321141
 33211098876555310721759829124676
 91293164111910978

4	≠ =	≠						
7	≠ =	≠	≠			-		
8	≠ =	≠	≠			-		
221	≠ =	≠	≠					
5	≠ =	=	≠		≠		≠	
6	≠ =	=	≠		≠		≠	
9	≠ =	=	≠		≠			
222	≠ =	=	≠					
124	≠ =	=		=				
128	≠ =	=		=			≠	
143	≠ =	=		=			≠	
151	≠=	≠=		≠		=		
159	≠=	≠=		≠		=		
155	≠=	≠=		≠		≠		
166	≠=	≠=		≠		≠		
154	≠=	≠=			=			
160	≠=	≠=			=		=	≠
161	≠=	≠=			=		=	≠
162	≠=	≠=			=		=	
175	≠=	≠	=		≠			
180	≠=	≠	=		≠	=		
181	≠=	≠	=		≠	=		
197	≠=	≠	=				=	
198	≠=	≠	=				=	≠
223	≠=	≠	=				=	≠
163	≠=	=	=					
187	≠=	=	=	=		-		
196	≠=	=	=	=		-		
219	≠=	=	=	=	=			
220	≠=	=	=	=	=			
182	≠=	=			=			
191	≠=	=			=	=		≠
194	≠=	=			=	=		≠
192	≠=	=			=	=		#
193	≠=	=			=	=		#

TABLE 8.4.1.2b

LATER cmAw - mAk AIRMASS TRANSFORMATION TRAVERSE DENDROGRAM

TRAV

CYCLE

222211111111111188877754433211

32118885443210041096065496230

255196335275476

138	≠	=	=		=			=	
140	≠	=	=		=			=	
141	≠	=	=		=	=			
142	≠	=	=		=	=			
139	≠	=	=				=		
179	≠	=	=				=		
167	≠	=		=		=			
172	≠	=		=		=			
173	≠	=		=					-
174	≠	=		=					-
152	≠≠	≠=		=					
228	≠≠	≠=		=				=	
231	≠≠	≠=		=				=	
156	≠≠	≠=		=			=		
171	≠≠	≠=		=			=		
234	≠≠	≠=		=					
176	≠≠	≠	≠			=		=	
190	≠≠	≠	≠			=		=	
184	≠≠	≠	≠			=	=		=
188	≠≠	≠	≠			=	=		=
185	≠≠	≠	≠			=	=		=
177	≠≠	≠	≠						
189	≠≠	≠	≠			#			#
178	≠≠	≠	≠			#			#
153	≠≠		≠	≠					
227	≠≠		≠	≠	≠				
235	≠≠		≠	≠	≠				
164	≠≠		≠	≠				-	
165	≠≠		≠	≠				-	
186	≠≠		≠	≠					

TABLE 8.4.1.3a

 STATISTICAL INFORMATION ON TRAVERSES CONDUCTED UNDER
 EARLY cmAw - mAk AIRMASS TRANSFORMATION STAGES

CYCLE	d1	TEMPERATURE		MIXING RATIO	
		H	a	H	a
239	1.0065	166.109	0.010	9.614	1.000
231	0.3400	134.966	0.276	30.383	1.000
222	0.1960	77.683	1.000	60.156	1.000
219	0.1360	138.953	0.203	47.180	1.000
213	0.1100	208.721	≥0.000005	26.332	1.000
201	0.0825	137.801	0.223	53.538	1.000
196	0.0720	118.842	0.662	57.512	1.000
184	0.0540	164.853	0.011	33.417	1.000
181	0.0525	142.573	0.148	24.739	1.000
171	0.0465	152.538	0.054	11.614	1.000
161	0.0390	262.442	≥0.000005	136.107	0.254
159	0.0380	273.109	≥0.000005	19.890	1.000
151	0.0340	168.593	0.0068	62.372	1.000
150	0.0340	92.754	0.988	24.908	1.000
139	0.0310	85.119	0.998	15.293	1.000
117	0.0225	198.959	0.000038	32.482	1.000
108	0.0200	147.076	0.097	102.947	0.934
97	0.0170	242.406	≥0.000005	129.386	0.400
92	0.0170	108.339	0.870	100.078	0.957
91	0.0165	56.064	1.000	61.949	1.000
77	0.0140	100.945	0.951	179.206	0.0013
75	0.0140	187.598	0.00031	41.080	1.000
69	0.0125	136.772	0.241	41.172	1.000
68	0.0125	139.038	0.202	45.702	1.000
62	0.0115	117.427	0.695	163.558	0.014
59	0.0110	169.514	0.0059	115.693	0.734
51	0.0100	138.105	0.217	150.153	0.070
42	0.0090	100.460	0.954	25.321	1.000
34	0.0080	184.925	0.0005	30.320	1.000
26	0.0075	145.850	0.109	88.119	0.996
17	0.0060	170.716	0.0049	72.795	1.000
16	0.0060	220.054	≥0.000005	14.459	1.000
4	0.0020	182.483	0.00076	185.538	0.00045
1	0.0015	184.556	0.00054	71.040	1.000

TABLE 8.4.1.3b

STATISTICAL INFORMATION ON TRAVERSES CONDUCTED UNDER
LATER cmAw - mAk AIRMASS TRANSFORMATION STAGES

CYCLE	d1	TEMPERATURE		MIXING RATIO	
		H	a	H	a
232	0.3675	263.013	≥0.000005	17.502	1.000
225	0.2135	277.798	≥0.000005	20.285	1.000
215	0.1150	37.839	1.000	34.077	1.000
211	0.1010	189.766	0.00021	30.355	1.000
189	0.0615	83.527	0.999	6.107	1.000
186	0.0565	47.451	1.000	61.183	1.000
183	0.0535	202.538	0.000019	33.656	1.000
153	0.0360	293.198	≥0.000005	52.371	1.000
145	0.0325	180.268	0.0011	69.786	1.000
142	0.0320	284.756	≥0.000005	37.947	1.000
137	0.0305	67.592	1.000	31.443	1.000
125	0.0240	27.813	1.000	59.263	1.000
114	0.0215	82.830	0.999	56.958	1.000
107	0.0200	210.947	≥0.000005	45.903	1.000
106	0.0195	112.605	0.798	114.883	0.752
84	0.0155	123.055	0.558	127.049	0.457
81	0.0150	59.285	1.000	112.233	0.805
80	0.0150	276.944	≥0.000005	187.525	0.000313
69	0.0145	48.599	1.000	110.749	1.000
76	0.0140	127.360	0.449	63.285	1.000
70	0.0125	54.684	1.000	56.147	1.000
56	0.0110	128.342	0.425	138.040	0.219
45	0.0090	138.559	0.210	69.622	1.000
44	0.0090	80.059	1.000	139.985	0.186
39	0.0090	120.679	0.617	28.964	1.000
36	0.0080	51.109	1.000	162.259	0.011
22	0.0070	140.631	0.176	127.597	0.443
13	0.0055	102.604	0.937	78.041	1.000
10	0.0045	228.734	≥0.000005	169.996	0.0055

As with the cA - cmA dendrogram cluster, Table 8.3.1.1, the greatest proportion of traverses listed in Table 8.4.1.1 were undertaken when the wind direction, logged at the

Airport, varied between 168° and 349°. The cumulative frequencies for the cA - cMA air mass group and the early and later stages of the cMAw - mAk air mass transition were 0.84, 0.74 and 0.77, respectively. When this wind quadrant is further sub-divided into the S - WSW and W - NNW sectors, there is a quite noticeable similarity between the cA - cMA and later cMAw - mAk traverse frequencies. For the latter cluster group, approximately 36.7 percent of the undertaken traverses were conducted when the wind blew between 168° and 259° whilst about 40.0 percent were undertaken when the wind direction fluctuated between 259° and 349°. The reverse occurred for the early cMAw - mAk cluster. 0.23.

As the cumulative frequency for the S - WSW wind sector increased, the difficulty in selecting the major trend related fusions, magnified. This became quite apparent when the Cluster - 1C dendrogram results, as recorded in Tables 8.4.1.2a and 2b, were ignored and a trial in error process based on a climatological variable analysis, was initiated.

Kruskal - Wallis nonparametric ANOVA tests were run on traverse fusions of each transitional group which had been segregated prior to the analysis according to their standardization hour. The null hypothesis was accepted for both stages for the hours of 0900 and 1300. The calculated H values for the early and later stages at 0900 hours were

51.686 and 36.917 whilst those for 1300 hours were 45.411 and 49.696. The H statistic for the mixing ratio variable did not reach a value of 19.000 for both stages.

For 1700 hour traverses, early stage members registered an insignificant 34.347 for temperature while the later stage group had a significant value of 198.741. The critical alpha value of the latter was 0.00039. Although there were 8 traverses clustered to form this group, there was no wind directional agreement. The approximate direction covered was 293°: from the east through to the north. Mixing ratio data again did not reject the null hypothesis for both stages.

The 2100 hour itinerary fusions of both transformation states were significant but only for the temperature variable. Moreover, the calculated H was highest again for the later stage group. Being 222.494, the critical significance level was 2.81E-07. The respective H and significance of the early cmAw - mAk stage were 152.461 and 0.054. No wind direction agreement existed either. In fact, the direction covered increased to 304°.

When the 1700 and 2100 hour traverses were united, the temperature H value decreased to 145.992 for the early stage but increased dramatically to 386.244 for the later stage. The significance of the former was 0.108 whilst that of the latter was total. The mixing ratio data again did not register a significant H value.

Keeping the above results in mind, the traverses of each group were catalogued according to their N code value for a similar Kruskal-Wallis analysis. The two cmAw - mAk stages reacted differently. Whereas there was no differentiation between the Kruskal - Wallis statistic for each of the N code zones (0 , <6 , ≥5) of the early stage, as N approached a code of 0, the later stage's critical alpha value approached the alpha value of 0.05. Though insignificant, the H value calculated for clear condition undertaken traverses of the later stage was 141.558. The respective critical significance was 0.163.

Once the climatic variables wind speed and direction were added to the stepwise analysis, it immediately became apparent from the results of the early stage traverse grouping which fusions would yield the most trend information. Two groups existed. The first was composed of traverses undertaken under clear skies. The prevailing winds were from the south though the speeds had to be either less than 10 km/hr or greater than 15.0 km/hr. The standardized hour of each component member did not play a significant role. The traverse combination with the above characteristics were traverse fusion (5,6,9,166). The H value calculated was 269.908. The significance was well in excess of -12 decimal places (see Symap 8.4.3.1) Note that this conglomeration with the exclusion of traverse 166 is in fact Cycle 97 of Table 8.4.1.2a. From Table 8.4.1.3a, it is

shown that Cycle 97 has a lower H value when traverse 166 is left out of the calculation even though the significance is still greater than 0.000005. Even Cycle 161 has a lower H value.

The second group consisted of traverses 151,155 and 175. Though this fusion was not represented in Table 8.4.1.2a, it had several common traits. All were conducted under overcast morning conditions when the wind direction logged at the Airport varied between the Northeast and South.

When the whole early cmAw - mAk stage, Cycle 239, was tested without the above fusion groups, the H value fell from 166.109 to 84.630. From a marginal significance of 0.010 to total insignificance. With the inclusion of only fusion (151,155,175), the H value increased to 127.142. The critical alpha value being 0.455, now. Removing traverse union (5,6,9,166) from cycle 239 resulted in a relatively similar result. The new H value was 121,640, its significance being 0.593. When these two fusions were combined, the H was 262.678 which was the highest calculated when Table 8.4.1.3a is examined. Remember, that Cycle 159 is composed of similar members and thence can not be used in the comparison.

Therefore, the two early cmAw - mAk transition stage fusions to be further analyzed statistically will be (151,155,175) and (5,6,9,166).

From Table 8.4.1.1, it becomes quite apparent that only two unique situations occur. Either the traverses conducted were undertaken under overcast conditions or they were not. That is, the skies of the alternative, were clear. Recall from the early portions of this section that significant H values were only calculated for those traverses standardized to 1700 and 2100 hours. For the cloudy occurrence grouping, only 9 traverses have such traits: both a N code of 8 and 1700 or 2100 standardization hours.

Using wind direction quadrants as references, non significant H values were obtained for both variables whenever traverses 235 and/or 141 were fused with those traverses within the wind quadrants WSW - WNW. The values H ranges from 94.157 through to 136.642 for the temperature variable and from 94.766 through to 124.255 for mixing ratio. When the WSW - WNW group, traverses 142, 177, 189, 178 and 138 were subjected to the Kruskal - Wallis test, the H value became 225.266 for temperature and 94.766 for mixing ratio. The former was significant whilst the latter was not. To see which of these 5 carry the most information, wind speeds were used as a categorizing device. That is, the traverses were sorted according to the wind speed. Traverse 142 which had the lowest speed of 7.9 km/hr was paired first with the second lowest, then the third lowest and so on. Then traverses (142, 177) were paired with the lowest of the remaining itineraries. The process

continued until all the 5 traverses formed a unit. A similar process was then initiated but the speeds were of decreasing order. Out of 52 combinations the only combination which yielded both a significant temperature and mixing ratio H value was traverse fusion (177,189,178). This fusion is merely Cycle 80 of Table 8.4.1.2b. The corresponding H values for temperature and mixing ratio were 276.944 and 187.525, respectively.

When Cycle 80 is removed from any of its component cycles of higher order, the H value calculated is no longer significant for either of the two climatic variables under examination. Note that from Cycle 211 downwards, only Cycle 80 is composed of significant traverse groups.

The selection for the later cmAw - mAk traverses conducted under clear skies is Cycle 183 fused with traverses 188 and 190. The H value calculated has increased over that of the lone Cycle 183 by 46.781 units. The reasons behind this grouping, however, can not be traced by utilizing any of the Airport climatic conditions listed in Table 8.4.1.1. Instead, reference was directed towards the hypothetical vertical radiosonde estimates averaged for the group. It should be noted that although some reasons for the particular fusion can be detected from the vertical data parameters, they are by far not the only possible explanations.

All the traverse members of this fusion have the same neutral lapse rate between the surface and 950mb level. Moreover, the amount of kinetic energy available due to the velocity difference between the two levels, is greater than that of any other early or later cmAw - mAk fusion. For example, the approximate estimate of the work required in the adiabatic exchange of two adjacent air parcels separated by 1 meter for the traverse grouping (5,6,9,166) is $8.1912E-04$ kg/m sec² whilst that for the particular fusion in question would probably be in the vicinity of $3.0908E-04$ kg/m sec². Now note, the wind shear energy of the former was estimated at $4.8310E-06$ kg/m sec² while that of the latter was $1.2391E-05$ kg/m sec². In other words, there is about 2.56 times more energy in the wind shear of traverse fusion than in the itinerary grouping (5,6,9 166). Also notice that it requires less energy for parcel displacement for the former than for the latter, roughly two-thirds less. All that can be seen is that the plots of temperature and mixing ratio variation with location are similar for the traverse components. The Clustan - 1C package picks this up.

When this fusion is removed from the total clear sky traverse calculation, the H value falls to 52.410 from 249.319. From a critical significance value of $8.6304E-10$ to total insignificance.

The two later stage cMAw - mAk traverse fusions to be examined will therefore be Cycle 80 and Cycle 183 fused with traverses 188 and 190.

8.4.2 Proof of Airmass Classification

Tephigram data, either graphical or tabular, depicting surface through to 500mb level cMA and mA air mass characteristics, for the Canadian Prairie stations, does not exist in a complete form. Upton(1961) has analyzed and estimated ten-day moving averages of temperature as well as the mode and the 75 percent sample range of wet-bulb potential temperature for the main four air masses affecting the region, but the results were restricted to the standard millibar pressure levels, 850, 700, 500 and 400. Harley(1962) established actual Qw ranges for mA, mP and mT air masses, yet again, the estimates were restricted to upper millibar levels.

Hence, the surface through 850mb traits are unknown and cannot be determined. Questions such as, are ground inversions, caused by cooling of stagnant air, common for cMA and/or mA air masses or are winds sufficiently strong to encourage and maintain turbulent mixing, thereby either elevating the inversion or preventing an inversion from forming, remain unanswered. Moreover, the depth of a subsidence inversion, if at all present, can not be determined.

Therefore,as no current papers have been published regarding this theme,the qualitative data required for the proof of the radiosonde estimates for the selected dendrogram traverse clusters, will be based upon Willett's(1933) differential classification of air masses,as well as Showalter's(1939) extended analyses of Willett's classification. The results,although out of date,are the most complete information obtainable to date.

To facilitate the proof that the selected fusions are indeed cmAw and mAk,Table 8.4.2.1 has been constructed as well as the Rossby profiles of each of the selected fusions: diagrams R8.4.2.1 through R8.4.2.6. The pseudo-equivalent potential temperature (Q_{se}) and mixing ratio (MR) for each of the standard pressure levels,surface,850,700 and 500 have been calculated for each of the two reference stations, Seattle,Washington and Ellendale,North Dakota. The respective codes for the above stations in Table 8.4.2.1 are SEA and ELL. The early cmAw traverse fusions shall be coded according to their N code. EN0 will designate fusion (Cycle 97 + T166) whereas EN8 will be used for selection (T151,T155,T175). For the later cmAw - mAk transitional stages,LN0 will represent Cycle 80 while LN8 will be the code for union (Cycle 183 + T188 + T190)

The lifting condensation level (LCL) and its associated temperature (LCT) as well as the convective condensation

temperature (CCT) for surface air, have also been determined for each of the above selections for each standard millibar surface.

TABLE 8.4.2.1

cmAw - mAk TEPHIGRAM COMPARISONS

CODE	SFC		850mb		700mb		500mb	
	Qse °K	MR (g/kg)	Qse °K	MR (g/kg)	Qse °K	MR (g/kg)	Qse °K	MR (g/kg)
SEA	291.4	4.4400	275.3	0.9070	278.0	0.3420		
	SFC	1020.3mb	LCL	955.8mb	LCT	276.5°K	CCT	278.2°K
ELL	281.7	2.9999	297.0	2.5175	290.0	1.0953	306.5	1.0396
	SFC	981.8mb	LCL	938.2mb	LCT	269.0°K	CCT	290.4°K
EN0	278.2	2.2345	288.2	1.6063	298.4	1.1460	305.8	0.3875
	SFC	991.3mb	LCL	903.0mb	LCT	264.5°K	CCT	298.0°K
EN8	272.9	1.7086	285.7	2.2012	294.2	1.2791	303.8	0.6765
	SFC	990.9mb	LCL	907.8mb	LCT	261.2°K	CCT	298.4°K
LN0	281.5	1.6008	289.3	1.9217	294.8	1.1078	305.1	0.4370
	SFC	992.8mb	LCL	774.1mb	LCT	257.9°K	CCT	296.5°K
LN8	284.6	2.5147	287.7	2.2662	294.4	1.4811	299.4	0.2844
	SFC	975.5mb	LCL	848.1mb	LCT	265.1°K	CCT	286.9°K

The SEA sounding is a typical average for Willett's Polar Pacific (Pp) air mass designation. Known as mA in Canada, the local source region, similar to that of cA, in Siberia, the Arctic Ocean and Alaska. The trajectories of the air mass, however, deviate, depending mainly on the intensity and the southward movement of the Aleutian Low.

With increasing intensities, more air is drawn in from the source regions. Wave formation along the Polar Front, situated near 60°N , intensifies. The initial waves generally move rapidly southeastward along the front at velocities varying between 48 to 73 km per hour. Each successive wave extends its effects farther southward mainly due to the fact that there is superseding by additional waves. With crests lengths of approximately 1600 km, moving at a relative constant velocity of 1280 - 1930 km per day during winter, the series lasts from 5 to 7 days (Taylor, 1943, pages 128 - 129)

For the SEA reference, the Pp maritime trajectory was approximately 3025 km. The average velocity was 52.1 km per hour. The results of the 2 to 3 day prolonged heating and moistening of the lower air mass layers, that is surface to the 950mb level, is convective instability. Within this layer's depth of approximately 588.3 gpm, Q_d increased from 280.1°K to 280.8K whereas Q_{se} decreased to 289.5°K from 291.4°K . Moreover, the convective condensation temperature is -2.95°K lower than the actual surface temperature of 281.15°K . Hence, convection usually becomes initiated once the Pp air mass has reached the North American coast. The LCL of 955.8 mb is the lowest recorded not only in Table 8.4.2.1 but it is also lower than any of the cA tabulations. Condensation will occur at 463.4m above the surface.

The mixing ratio is quite high in the convective layer, varying between 4.44 g/kg at the surface to 3.282 g/kg at the 950mb base. The former is approximately 3.4 times greater than that of Pp air after a days traverse from Alaska's Beaufort Sea coast to Fairbanks whereas the latter is 1.6 times as great.

Total absolute instability exists between 950 - 850 mbs. The layer's depth is 882.5 gpm. dQ_{se}/dz is -0.0093 for the 950 - 900 mb zone and -0.0233 for the 900 - 850 mb level. The respective dQ_d/dz values are -0.0038 and -0.0143. The rate of Q_d decrease is greater than that of Q_{se} between the 950 and 850 mb bases but dQ_{se} is always larger than dQ_d .

The base of the 850mb level is also the upper limit of turbulent mixing. The depth of mixing was thus approximately 1451 gpm. From 900 to 850 mb, the temperature decreased 10.3°K., whereas that of the dew point was 11.7°K. There is a concurrent mixing ratio decline of 1.3554 g/kg.

Above this point, the air is cold and dry: characteristics of the original cA air mass. The Q_{se} difference for Barrow, Alaska and Seattle between the 850 and 700mb levels are -5.3°K. and -3.2°K., respectively. Moisture wise, the mixing ratios of Seattle at these levels are closer to those of Norman Wells and The Pas (see Table 8.3.2.1) The difference averaging at 0.4455g/kg and 0.0056g/kg for the above respective millibar zones.

However, the major difference between upper level cA and upper level mA is that subsidence intensifies Q_{se} for the former. Not only are the dQ_{se}/dz values relatively constant for cA air masses, they are also consistently large, fluctuating only between subsidence zones. This is not the case for pure Pp air. Although both Q_{se} and Q_d increase for the SEA reference from 800mb to lower pressure levels, dQ_{se}/dz values are inconsistent. For example, this ratio ranges from a high of 0.0043 for the 800-750 level to a low of 0.0004 for the upper adjacent 750-700mb zone. Even though absolute stability exists, it fringes on the neutral.

As advancing Pp air masses are usually warmer than the coastal air, especially during the winter season, it passes over the coastal air rather than displacing the coastal air. Due to the convective instability of the lower layers, this lifting, magnified when passing over mountainous regions, trigger heavy precipitation. Heat liberated from condensation fortified with dynamic heating on the air mass' descent on the leeward side of the Rockies, aids in stabilizing the lower levels of the air mass.

If the northern interior Plains are dominated by a current outbreak of cA air, the descending Pp air mass will pass over the cA because of the density differences between the two. When the above occurs, blizzard conditions are initiated.

On the other hand, when the air dominating the Plains is of a backflow cA, Pp readily intermixes. This intermixing is facilitated by the instability of Pp's upper millibar zones. That is, the instability is apt to initiate vertical divergence. The surrounding air masses thereby lose their stability whereas the Pp air mass gains.

When the invading Pp air mass enters a former col zone and the dynamic anticyclone of the Great Basin of the Western United States is of declining intensity thereby reducing subsidence modification of the upper Pp levels, Pp progresses eastward, stabilizing at the lower levels because of radiational cooling and contact cooling.³² The convective instability is thus transferred upwards whereas the top most millibar zones retain their original source characteristics of dryness and absolute stability.

Transitional forms of modified Pp are designated Npp in the United States but cMA in Canada.

³² The intense anticyclone of the Great Basin is extremely spasmodic with respects to occurrence and intensity. When its occurrence is infrequent, subsidence modification effects on Pp air are limited to the upper most levels. When, on the other hand, the anticyclone is persistent and intense, the modified Pp is warmer and dryer at all levels than either the original Pp air mass or cA. At all times, this type of Pp air mass, classified as Pb, is very stable. When Pb is forced aloft on contact with cA, its dryness does not allow precipitation nor cloud to develop. Ground fogs plus pollution are however acquired in the lower levels on Pb movement eastward.

The Ellendale sounding, taken from Taylor (1943, page 134) is of a Pp air mass which has traversed the North Pacific for 2 days and the land mass of North America prior to its arrival at Ellendale for 2 days, also. It is not the same Pp that was referenced in the SEA case, though it is a representative example of one of the modification possibilities. The variety of transformations, however, are endless.

The Ell data of Table 8.4.2.1 immediately indicates the continental influence. An intense inversion, though very shallow, occupies the first 696.5 gpm above the ground. Shallow in the sense that it is approximately 0.56 the height of the average inversion depths for the three cA reference stations of Table 8.3.2.1. The temperature increase is approximately 7.7°K. or 0.0111°K. per meter. The latter rate is roughly double that of the cA examples.

Notice also that unlike the cA mixing ratio estimates taken through the inversion layer, there is no discontinuity in the respective transformation Pp layer. That is, the mixing ratio remains at or about 3.0g/kg which is of course greater than that registered for the cA data by a factor of approximately 8.6 at the surface and about 4.8 at the top of the inversion zone.

From 900 to 750 mb., convective instability occurs. dQ/dz declines from the inversion rate of 0.0213 to 0.0020

whereas that of dQ_{se}/dz falls from 0.0223 to -0.0003. Note, that the latter is bordering along the neutral.

The temperature of the Lifting Condensation Level, 269.0°K., located 313.9 gpm above the surface, is greater than the CA reference stations' mean of 243.3°K. by 25.7°K. though only 7.5°K. lower than the corresponding SEA value. The LCL is 938.2 mb which is similar to that of CA Barrows example.

Though the mixing ratio has declined by approximately 1.2868 g/kg from the base of the convective unstable layer to the top of this layer, it is still quite high, being approximately 1.5792 g/kg greater than for the similar millibar zone of the average CA reference stations.

The absolute unstable layer located between the 900 and 850 mb level for the SEA example is situated in the ELL between the the 750 and 700 mb zones. Within the 533.3 gpm zone, dQ_{se}/dz is 0.0125 whilst that of dQ_d/dz is 0.0092. The former ratio is 0.0037 units less than the average absolute unstable layer's value for SEA while the latter is exactly similar. Hence, pure Pp air is more unstable. Note also that in the SEA case, approximately 875 gpm are absolutely unstable while that of the ELL is roughly one-sixth of the depth: 533.3 gpm.

Millibar levels below 700 are all absolutely stable. dQ_{se}/dz are, furthermore, parallel to the CA station values for this zone than for the SEA example. In other words, neutrality is out of the question.

The Q_{se} value of $296.8^{\circ}K$. at the base of the absolute stable layer is approximately $21.0^{\circ}K$. greater than that of the SEA case. Within 1342.1 gpm, the ELL value increases $9.7^{\circ}K$. whilst that of the SEA example increases only $4.35^{\circ}K$. in 2557.8 gpm.

At the 500 mb mark, the Q_{se} value for ELL is $15.3^{\circ}K$. greater than that of the CA example's average for the same millibar level. The latter value is $291.2^{\circ}K$, the reason being that the ELL mixing ratios are continuously higher at all levels than any of the CA reference stations. Referring again to the 500 level, the mixing ratio is 1.0396 g/kg for ELL whilst only 0.1168 g/kg for the combined CA stations. In fact, the mixing ratio for SEA at this level, 0.2504 g/kg, is about 0.7892 g/kg less than that of the ELL case.

The high water vapor content at the 500 mb level for ELL, as well as throughout the whole sounding, is due to turbulence caused by high wind velocities as the winds cross the Rockies. This turbulence aids in dissipating the remnants of the clouds which formed in the convective and absolute unstable layers of the air mass, such as those of the cumulus gender and/or the high clouds, cirrus nothus and cirrus densus which arise from the anvils of cumulus nimbus.

All layers of EN0 are absolutely stable with dQ_{se}/dz showing no signs of neutrality. Values range from a high of 0.0168 at the top of the surface inversion to a low of 0.0029 at millibar levels at and below 700. The surface inversion was formed by cooling from below as the mixing ratio shows little discontinuity in the layer. There is also a very weak frontal inversion 2208.5 gpm above the surface. The top limit is located at the 750 mb zone. Q_d increases $4.0^\circ K$. from the 800 mb level value of $284.0^\circ K$. whereas the mixing ratio increases from 1.2397 to 1.2759 g/kg. The frontal inversion is also quite stable as dQ_{se}/dz increases from 0.0062, estimated for the 800 mb level, to 0.0082. Since neither Q_d nor the mixing ratio have increased drastically, the air mass overriding the cmAw is probably of the same type.³³

Comparing EN0 with Cycle 72 of Section 8.3.2, the main difference lies in the mixings ratio. The former is approximately 0.8886 g/kg moister than the latter at the surface though with vertical distance, the difference decreases. Respective differences for the 850, 700 and 500 mb levels between the two are 0.1552, -0.1987 and -0.0540

³³ The parent air mass of the EN0 sounding was of mAk type which moved on to the Oregon coast in the vicinity of North Bend on March 29, 1976 at 0900z after a 2.5 day trajectory from the Aleutian Island - Alaska coast.

The overriding cmAw air mass was the successive wave, reaching the northern California-southern Oregon boundary area, a day latter. Unlike the former, it was relatively more stable with higher upper wind velocities.

g/kg. The LCL is lower for EN0 by 20.4 mbs but the LCT is greater by 6.1°K.. The convective condensation temperature is also lower for EN0 by approximately 4.5°K.

Comparing the EN0 and EN8 soundings shows that the latter's surface inversion is not only of stronger intensity but it is also accompanied by a moisture inversion. dQ_{se}/dz for the surface to 950 mb level is 0.0208 or approximately 0.25 stronger than that of EN0. The depth of the temperature inversion is relatively similar being 8.34 gmp lower than that for EN0. The moisture inversion, however, extends for another 427.1 gpm, reaching a maximum value of 2.2963 g/kg at the 900 mb level.

On the whole, the sounding of EN8 shows greater stability than that of EN0, but both no longer have the characteristic CA curve of being parallel to the ordinate Qd axis. The greater moisture content in the lower levels migrates the characteristic curve in a counterclockwise direction at these levels.

The LCL difference between EN0 and EN8 is a mere 4.8 mbs whilst that of LCT is 3.3°K.. The CCT estimates are equal being 298.0°K. for EN0 and 298.4°K. for EN8.

The surface inversion for LN0 is present though not as intense. With a dQ_{se}/dz of 0.0123, it is approximately 0.25 less intense than the surface inversion for EN0 and 0.59

less intense than that for EN8. Moreover, although each zone registers stable dQ_{se}/dz values, they are not consistent. That is, from the surface-950 mb to the 950-900 mb level, dQ_{se}/dz falls from 0.0123 to 0.0023. It then rises to 0.0053, falling again to 0.0039 for the 900-850 mb zone. The fall continues to 0.0021 for the next level rising to 0.0041 for 750-700 mbs. Back to 0.0034 and for the 600-500 mb zone, a value of 0.0049 is calculated. This trend was not seen in any of the previous soundings, no matter what the classification was.

In the LN8 sounding, the inversion no longer exists. It has been destroyed by rapid cooling from below and turbulent mixing, both the effects of increased wind velocities. dQ_{se}/dz for the surface-950 zone is 0.0006: stable though bordering the neutral. Note that the CCT, 286.9°K., is only 2.3°K. greater than the surface temperature. Convection, however, would probably be checked because directly above this layer is 1577.3 gpm of stable atmosphere. The top zone, 850-800 mb, has a dQ_{se}/dz of 0.0074.

From 800 mbs upwards, the differences between adjacent Q_{se} values decrease decreasingly, so that by the 600 mb zone, neutral conditions exist. dQ_{se}/dz for the 700-600 mb zone is 0.0001.

The characteristic curve for LN8 is unique. It does not parallel the ordinate axis as in the case of the cA and cmAw categories nor does it have a similarity with the mAk Ellendale example. The only trait that distinguishes this fusion group as being members of a mAk classification is the fact that convective instability is present and that the CCT is lower than the actual surface temperature. These traits are only duplicated in the mAk air mass radiosondes of Seattle and Ellendale.

Comparing the recorded temperature and mixing ratio data between each traverse day and the long term normals for each respective climatological parameter for that day, shows that the climatic parameters under investigation deviate not only from the 95 percent confidence values calculated for that period but also fluctuate greatly between component fusion member estimates. The trend analyses, nevertheless, were similar for the components of each fusion group.

Of the EN0 traverse fusion, only the day on which traverses 5 and 6 were undertaken had near normal temperature tendencies. The minimum registered for the day, -8.6°C ., was -0.3°C . warmer than the 99 year minimum average whilst the mean, -1.7°C . and the maximum, 5.3°C ., were greater than the respective long term averages by 1.6°C . and 3.1°C ..

The remaining days during which EN0 traverses were conducted could be classified as climatically juxtaposed, i.e., the minimum, mean and maximum temperatures for Traverse 9 were all outside of the upper 95 percent limits for each category whilst those for Traverse 166 were outside the lower limits. The confidence intervals of the former were (-9.7°C., -6.9°C.), (-4.6°C., -1.8°C.) and (1.0°C., 3.4°C.) while the day's corresponding temperatures were -0.3°C., 5.2°C. and 10.6°C..

For T166, the minimum, mean and maximum logged Airport temperatures were -16.6°C., -8.2°C. and -7.8°C.. These values deviated from the tabulated averages by -13.8°C., -10.4°C. and -7.5°C., respectively. In fact, the difference between the lowest 99 year minimum temperature registered for that day and the actual minimum was 4.0°C.. The former was -20.6°C. and it was recorded in 1936.

Utilizing the computed 24 year climatic variable data tabulated in Tables 6.1.1 through 6.1.12, a similar fusion component inconsistency for mixing ratio was noted. The mixing ratios for T5 and T7 were outside the upper 95 percent confidence values by 0.4299 and 0.3465 g/kg respectively whereas that of T9 was well within the limits (2.9010, 3.4705 g/kg).

The influence of the drought was reflected in the mixing ratios of T166. The traverse's value at 2100 hours, 1.9840

g/kg, was almost one-half that registered for the same hour based on 24 years of data. In other words, the actual value was 1.9228 g/kg below the lower 95 percent confidence interval value.

Traverses 151 and 155, components of fusion EN8, were conducted during days which registered cold, below normal temperatures. During the former, smoke generated by burning marshes, engulfed the city, restricting visibilities. The only clear period during the day arrived between 1721 to 2255 hours. Smoke and haze reinvaded the city again after. During the former traverse, rain showers of an inconsistent duration occurred between the hours of 1808 and 2220. Only a trace was registered at the airport.

The deviations of the minimum, mean and maximum temperatures logged at the Airport during T151 from the calculated 95 percent confidence intervals based on 100 years of data for the respective temperature type were -10.97°C ., -7.60°C ., and -4.50°C ., at the lower level. Those of T155 were -3.57°C ., -2.36°C ., and 0.41°C ..

The remaining fusion component of EN8, traverse 175, was conducted under exact opposite temperature conditions. That is, the temperature throughout the day was above normal. The respective minimum, mean and maximum upper confidence limits were -6.17°C ., -1.34°C ., and 2.68°C ., whilst the actual respective temperatures for each category were -5.40°C ., 0.30°C ., and 5.9°C ..

The only uniform climatic trait for this group was the dryness of the air. The pooled mixing ratio was 1.4716 g/kg or approximately 3.2753 g/kg outside of the lower 95 percent confidence limit. Recall from Chapters 5 and 6 that both October and November were the sunniest and driest on record.

The erratic traverse combinations also occurred for LN0. Below normal temperatures were recorded for traverses 235, 164 and 165 whilst above normal temperatures existed for the remaining components. The lowest minimum temperature of the former group was 11.80°C. below the lower confidence limit of -2.65°C. while the respective mean and maximum values deviated from their 100 year comparisons by 14.65°C. and 11.40°C. respectively.

For the above normal traverse combinations of LN0, the registered pooled minimum, mean and maximum temperatures were 4.02°C., 5.64°C. and 8.45°C. above the pooled upper confidence limits.

Though the temperatures fluctuated drastically from one traverse day to the other for LN0, the dryness persisted. The lowest mixing ratio, 1.2293 g/kg was registered for traverse 235 whilst the highest, 2.1981 g/kg was for T227. The former was 0.8609 g/kg outside the lower limit while the latter was 0.8741 g/kg. Note, that as the cMAw traverses were replaced by the mAk classification, the mixing ratio, although still low, approached the 95 percent confidence limits.

Traverse components of LN8 all were undertaken during above normal conditions. The greatest difference occurred on the day traverses 177 and 178 were conducted. The minimum, mean and maximum confidence intervals calculated were (-7.63°C. to -5.70°C.), (-3.11°C. to -1.34°C.) and (0.65°C. to 2.68°) whilst the registered respective temperatures were 0.10°C., 5.3°C. and 10.4°C.. The respective deviates outside the upper limits for T189 were 0.21°C., 2.23°C. and 4.13°C..

With respect to the mixing ratios of the LN8 union, the 1700 hour traverses were within the 95 percent limits, 2.1198 to 2.7116 g/kg whilst the 2100 traverse, 178, was slightly over the upper limit by approximately, 0.0052 g/kg.

In summation, increasing mixing ratios, lowering convective condensation temperatures and destabilizing millibar layers proceed cMAw to mAk transformations. The EN0 cluster was approximately 0.8886 g/kg moister than Cycle 7.2 of Section 8.3.2 at the surface even though both fusions were of the same class. The CCL of the former was, furthermore, lower than the latter by 4.5°K.. Under overcast conditions, early cMAw to mAk transformations are more stable than their clear counterparts, usually with a moisture inversion accompanying the stronger surface inversion. Later stage transformations under clear conditions are marked with reduced surface inversion strength. dQ_{se}/dz for LN0 was estimated to be

0.25 less intense than that calculated for EN0 and 0.59 less than that for EN8. When mAk air masses engulf the city, the surface inversion layer no longer exists, being destroyed by rapid cooling from below and turbulent mixing: both the effects of increased wind velocities. Convective condensation temperatures are near to the actual surface temperatures. For the LN8 case, the CCT was only 2.3°K. greater. Although absolute instability may or may not exist as in the SAE or ELL references, layer neutrality is present, hence, indicating convective unstable possibilities.

With respect to the surface temperatures and mixing ratios of the selected dendrogram fusions, erratic traverse temperature combinations existed for all excluding LN8 whereas the mixing ratios were all below the 95 percent confidence intervals excluding again fusion LN8. The latter had traverses which were conducted under above normal temperature conditions while the mixing ratios registered were all within or slightly above the confidence limits.

8.4.3 The Analysis

Nonparametric statistics can readily distinguish temperature and mixing ratio trends evident in fusions which are not members of the same cluster subset though part of the overall cluster whereas their corresponding parametric counterparts can not. For example, when the cA S-W fusion was united with the cmAw Cycle 126, the Kruskal-Wallis H statistic calculated for temperature, 179.310, was significant at a critical alpha value of 0.0013. The corresponding ANOVA F ratio was 0.965 which has a probability of 0.5923. The respective degrees of freedom and sum of squares for the latter's between and within error sum of squares were (126, 4548.1911) and (1651, 61756.4160).

Although the mixing ratio data generated an H value below the 95 percent probability level, the same relationship existed between the two types of statistical techniques. The H value was 148.221 which was significant at 0.086 whilst the F ratio, 0.488, was totally insignificant. The respective degrees of freedom and sum of squares for both the between and within error sources were (126, 3.4695) and (1651, 101.5294).

The above example was not an unique case. Other fusions registered similar results. When, for instance, the cA S-W fusion was linked to the EN0 group, the calculated temperature H, 182.224 had a critical alpha level of 0.0008

whereas the F ratio, 0.320, was again totally insignificant. The ANOVA sum of squares for the between error source with 126 df. was 5537.4828 whilst that for the within source with 1651 df. was 226940.3101.

Both statistical techniques accepted the null hypothesis for the mixing ratio variable, but again, the nonparametric test results were closer to rejection alpha of 0.05. The H statistic generated was 118.131 which had a critical alpha value of 0.679 whilst the F ratio of 0.020 had a probability of 1.000. The between sum of squares and the within sum of squares were 3.4838 and 2242.0058 respectively.

The above nonparametric-parametric relationship, moreover, was not restricted to traverse groups bearing similar climatic situations. The cA S-W group fusion to the mAk LN8 group yielded a temperature H value of 197.180 and a mixing ratio H value of 203.331. Both were significant, the former at a critical value of 0.000053 the latter at 0.000016. The corresponding generated F ratios, 0.211 for temperature and 0.099 for mixing ratio, were both totally insignificant. The between and the within degrees of freedom for both climatic variables were 126 and 1524. The respective sum of squares for temperature were 4959.2771 and 283915.8662 whilst the corresponding values for the mixing ratio variable were 7.7519 and 283915.8662.

There were also no result parallelisms between the two statistical procedures for any fusion cluster outside of the original cA - cMA air mass classification. Infact, the more complex the urban - rural differential, the greater the gap between non - parametric and parametric results. For example, when 50 traverses which were conducted under continental Tropic air mass conditions were fused and analyzed, the Kruskal-Wallis H statistic corrected for ties yielded a value of 163.506. With 6350 cases, it was significant at 0.014. The F ratio, on the other hand, was estimated at 1.326. This result based on the same data base was now totally insignificant.

It became quite apparent after prolonged investigation that the climatic elements of an urban - rural area are composed on many intertwining facets, each determined by a common set of controls. Mixing ratio and temperature variations are meerly the effects of the basic five climatic controls solar radiation, interfaces, and earths' geodetic constants. Air masses with their specific properties and air currents are sub-controls, which inturn themselves are modified by land-sea configuration and topography.

To the above controls, surface architectural differences between the two environments magnifies the uniqueness of the mixing ratio and temperature islands. The canyon affect of the urban architecture promotes greater shortwave absorption

due to a reduced outward reflection. This is accomplished through greater internal side reflection and absorption. The thermodynamic properties of urban construction material ensure that this increased shortwave energy potential is maintained by converting it into heat storage. This heat will be slowly released through infra - red emission, especially during low solar altitudes. But infra-red radiation is also prevented from escaping by being re-absorbed by the canyon and/or re - emitted by the polluted atmosphere. Hence, the urban heat island.

Water vapor in the rural setting originates mainly from evapotranspirational processes. The rate varying according to the interface's saturation vapor - air differentiation, the wind speed, the soil moisture conditions, and the vegetation specie cover.

In the urban zone, anthropogenic sources of water vapor add to that already present in the lower atmospheric layers. The result, is the urban humidity island.

All the above processes act differently in different locations. Where inflow of air occurs due to pressure differences, a mesoscale circulation occurs. Hence, a heat island and humidity island within the larger islands. The statistical results documented in this thesis indicate that these differences are also evident under cA -cMA air mass conditions, though the magnitudes are reduced.

Nevertheless, it has been indicated that parametric statistics can not be employed on non - homogeneous environmental data. Each urban - rural data zone has its specific mixing ratio and temperature distributions. To group the whole urban - rural mesoclimate as an unit for the investigation of climatic parameter similarity will result in climatological untruths and climatological vagueness. These features were quite evident in the literature review of Chapter 3.

Since, this thesis was not designed to parallel the known, but rather to indicate the variability of mixing ratio and temperature variation between and within an urban - rural environment, through the use of statistics, further analysis of the urban and rural mixing ratio and temperature islands formed under different air mass conditions will not be discussed here. Results pertaining specifically to climatological aspects will be published at a latter date.

To sum up, analysis indicated that departures from the underlying normality assumptions of the sample can affect the computed parametric statistical results substantially and it is this departure which yielded the incongruencies between the two types of statistics. The degree of incongruency depends upon the cumulative frequency of the non-normal distributed data in the sample.

8.5 Conclusion

The analyses of the various air mass classifications may be regarded as unique. Through the use of statistical investigation we have shown alternatives to the standard unanimous arguments which state that the urban humidity island is conditioned by or contingent upon the urban heat island.

In the case of Winnipeg, moisture deficits are not present. Mixing ratio islands do exist under cA - cMA air mass conditions and that the various moisture zones are significant even if the climatological differences between them are less than 1.0g/kg. Furthermore, mixing ratio spatial forms do not necessarily parallel those of temperature. Anthropogenic sources influence the initial mixing ratio spatial pattern but the urban orientation together with climatological and meteorological parameters such as wind velocity and opacity, are the predominant pattern developers.

These analyses also have indicted that statistical alteration from the parametric to the non-parametric branch have drastically modified the resulting conclusions. The undetected and insignificant temperature and mixing ratio regimes become exposed with non-parametric statistics.

CHAPTER 9

Summation

A bench mark derived from the literature field had to be established in order to facilitate and perpetuate rational internal and external result comparisons. For three reasons, logic dictated the choice of anticyclonic cA and cMA air mass classifications. Firstly, these were the only major air masses under which research was undertaken by the literature investigators. Secondly, collected data, whether logged at a stationary locale or via mobile traverses, have consistent symmetric bell - shaped normal distribution curves with minimal skewness and kurtosis. A normal temperature and mixing ratio data distribution would guarantee a parallelism between parametric and non - parametric statistic conclusions. This aspect of normality is therefore the primary trait of a cA - cMA bench mark air mass. As air mass complexity increases, the discoveries of this thesis though often contradictory with the generalizations of the literature field, can be compared with the original cA - cMA findings in order to discover what degree of change occurred in the spatial and temporal distributions of mixing ratio and temperature.

Thirdly, the effects of vegetative ecotones would be removed from the analyses thereby allowing investigation of

the data to be directed towards finding out the degree of influence anthropogenic moisture and heat sources would have upon the spatial and temporal distributions of the research parameters under investigation.

This thesis's primary contention revolved around whether or not an urban humidity island exists. For the case of Winnipeg, the answer lies in the affirmative. However, in order to discover statistical significance in mixing ratio data, the seasonal maximum magnitude of this humidity parameter must be taken into account. One must not disregard information because parameter values are of a decimal format. The approach taken in the thesis is contrary to the general train of thought so prevalent in the literature field. That is, researchers, on the average, appreciate data not of a proper fraction form. If a researcher's data is consistently fractional it has usually been ignored especially when a secondary variable in the analysis is relatively quite large. For the mixing ratio data collected for this thesis, statistical significance commenced at the second decimal place. The following data assessment best clarifies the above supposition.

A representative mixing ratio humidity island logged during cA air mass intrusion was estimated at 0.2427g/kg. (see Symap 8.3.3.1b) The average mixing ratio over a 23 year span during winter conditions as previously defined is

0.7717g/kg.. Air mass type has been disregarded for the latter season. Using equations of proportionality; the average temperature of -15.74°C . for the above winter season and barring unit measurements, the equivalent heat island value for the above mixing ratio humidity island value would be 5.01°C .. The latter would be significant at or above 0.0005.

If averages are ignored and replaced by the actual parameter values recorded at the Airport simultaneously as the traverse undertakings, the equivalent heat island would increase 57.3, to 7.88°C .. This calculation is 0.27°C . greater than the actual urban heat island registered for the cA, S - W cluster (see Symap 8.3.3.1a) A one-to-one correspondence which initially was undetectable³

The second finding deals with the debatable literature generalization that heat island development and retention approaches a maximum under clear, calm, cold cA nights. During cloudy, windy periods, only a minimum heat island can be detected, if at all.

Although there are many clusters, sub - clusters, and individual traverse studies which provide evidence contradicting the above literature findings, Symap 8.3.3.2 of Cylce 126 clustering is one of the most dynamic.

Though the air mass in question was of a modified cMA form with respect to temperature and mixing ratio, the surface to 950mb stability was equal to that expected for cA air. The calculated $dQSE/dZ$ was 0.0168 for the former while that for the latter, as represented in Symap 8.3.3.1, was 0.0161. Moreover, in both cases, the winds were moderate from the SW - WSW. The only climatological parameter that was different was opacity. Cycle 126 had an okta value of 8 which signifies sky obscurity by clouds.

Note the different heat island pattern that was generated by the conditions. It is a pattern exemplifying anthropogenic - climatic interactions. That is, escaping longwave radiation is reflected back downwards while the stable surface layer prevents turbulent exchange.

In future publications, it will be shown that under cloudy conditions, as in the above example, industrial sites and other heat generating complexes replace the urban CBD as the predominant urban heat island cells. This in itself is another point that contradicts the established literature generalizations.

A similar climatological variable independence is also evident with respect to the once thought permanent reciprocal relation between mixing ratio and temperature. When meteorological conditions are such that

- (1) wind velocities average either 34.72km/hr at 193.1° or 35.25km/hr at 323.0° with okta values less than 2 for the former but greater than 6 for the latter.
- (2) winds do not exceed 20.0km/hr from the S - SW quadrant though pressure must be in excess of 1003.0mb.
- (3) a low pressure system approaches from the S - SW with moderate advective winds ranging from 15.0 - 25.0km/hr and pressure decreases below 988.5mb

the mixing ratio humidity island develops independently of the urban heat island.

Sublimation is the fundamental cause of this varied spatial mixing ratio pattern especially with regards to the for most point (1). Automobile exhaust heat as well as liberated heat from other anthropogenic - mechanic sources combined with pressure exerted by high wind speeds upon structural form impact, fosters sublimation of available free water vapor with no apparent intermediate liquefaction. This process is non static in nature, reversing on windward exposures as long as heat energy is available. This usage of heat maintains a lower heat island effect in the designated areas. Icing occurs permanently on the non - mechanical turbulent leeward sides.

Cycle 36 of the later cmAw - mAk transformation stages had conditions representative of the above. The alpha value was insignificant for temperature but significant at 0.011 for mixing ratio. In fact, deviations from the routine itinerary during traverses 173 and 174 in the CBD zone

indicated that areas in seclusion where air flow was reduced though not terminated and areas where horizontal flow was deflected vertically due to the perpendicular architecture, registered higher mixing ratios. The deviation averaged +0.2015g/kg.. The greatest increase during these exploratory undertakings was logged in the col zone between fixed point locales 67 - 68 on Portage Avenue. The value was 0.4618 g/kg..

During calm days and nights, conditions specified under point 2, mixing ratio sources can easily be identified. Due to the extreme lower air mass layer stability, sublimation occurs instantaneously on vapor release. In Cycles 56 and 24, mixing ratio humidity islands were registered at sewer outlets, heavy traffic intersections, and in the vicinities of major water based industries, such as sugar processing plants, laundromats, car washes, to name but a few. Ice fog was noted on the strip charts in each case. It should be also emphasized that point 2 conditions okta value remains insignificant: a unique occurrence.

Urban architecture again plays the dominant force in advective 'warm air' processes. Perpendicular areas to the wind log greater values for mixing ratio than do parallel zones.

In conclusion, as the air mass characteristics become more complex, the bench mark statistical traits of cA - cMA

air no longer hold valid. For mA air mass data, rural fixed point locale measurements were normal whilst urban measurements were not. Non-parametric statistics showed that both were significant whereas the equivalent parametric deduced the contrary for the latter. The dilemma generated was either to run equivalent though alternative type successive statistics for each analysis or to backtrack the research to a non-parametric cluster analysis technique. Rationality dictated the latter. Possible further investigation lies with an expanded hybrid version of a non-parametric clustering technique based upon Worsley(1977), Sneath(1979) and Ramey(1983). However, it will not be introduced until its robustness has been tested against the major frequency curves. It should be noted that the only reason why parametric tests are so robust is because the statistic in question is always tested against the normal distribution.

APPENDIX A

Hypothetical Estimation of St. Norbert Heat Generation

As neither comprehensive nor authoritative energy consumption data have ever been accumulated for Winnipeg, all forth noted estimates are hypothetical. They have been based upon what ever information was obtainable from the various Federal, Provincial and City agencies.

All energy consumption units are in British thermal units, here to abbreviated Btu. To obtain the corresponding SI joule unit, multiply the given Btu value by the conversion factor 1055.07.

The City of Winnipeg, Development Plan Review, Research Branch (1978, pages 30-34) estimated the total residential energy consumption of Winnipeg, 1976-1977, as $38.00E+12$ Btu. Component energy mode consumptions are $26.6E+12$ for natural gas, $3.04E+12$ for fuel oils of various types and $8.36E+12$ for electricity. Coal usage constitutes another $0.092E+12$ Btu.

Approximately 98.85, of all Manitoban dwellings use natural gas as a space heating fuel rather than an utility energy source (Statistics Canada, Gas Utilities, CS 55-002/18-1 through 18-12, 1976). Transplanting this percentage for the Winnipeg case minutely reduces the above natural gas Btu volume to $26.3E+12$.

Fuel oil and coal consumptions remain constant whereas the contribution of electricity as a principal heating fuel is reduced to approximately $0.41E+12$ Btu or roughly one-twentieth of the above estimate. The reason for such a reduction can be traced to the fact that only 4.91% of Winnipeg's 1971 occupied dwellings used electricity for space heating (Statistics Canada, Population and Housing Characteristics by Census Tracts, Winnipeg, 1971, CS 95-753, Table 2). The total estimated residential space heating energy consumption would therefore be approximately $29.84E+12$ Btu for the whole city.

The estimated 1976 annual energy consumption for space heating for the Province of Manitoba, according to the Central Mortgage and Housing Corporation (1976, pages 28-29) is $44.2E+12$ Btu or 239 million gallons of oil equivalent. As there were 330,800 dwelling units at the time in Manitoba, the average hypothetical consumption per dwelling would be about $13.36E+07$ Btu.

In 1976 there were some 197,305 private dwellings in the City of Winnipeg (Statistics Canada, Census of Canada, Winnipeg, CS 34-002). The total consumption for the city would therefore be in the vicinity of $26.36E+12$ Btu.

The above estimate difference of $3.48E+12$ Btu is equivalent to $1.92E+07$ gallons of Bunker 'C' fuel oil: the most common fuel oil in use in Manitoba (Government of Manitoba, Department of Industry and Commerce, Manitoba

Community Reports, 1976). As the average CNR oil tanker car holds 142,000 gallons, approximately 132.5 cars would be required to hold this energy oil equivalent difference (Personal communication, Ken Knutson, Yardmaster Clerk Aid, Symington Yards, Canadian National Railways, December 7th, 1982, 1000 hours).

Therefore, rather than speculating further on the representativeness of the above two estimates, the average value of the above, $28.10E+12$ Btu, will be taken as the space heating consumption value for Winnipeg. This amounts to $1.42E+08$ Btu per dwelling.

The cumulative total heating degree days for Winnipeg is approximately 10679 (Labelle et al., 1966, pages 31-32). A heating degree day is the number of degrees the mean daily temperature is below 18°C . The number is zero whenever the inequality is not satisfied. Hence, the average space heating energy consumption per degree day for Winnipeg is $2.63E+09$ Btu or 13336.37 Btu per dwelling.

The average number of heating degree days during Cycle 126 was 59.03. Thus the hypothetical minimal energy consumption during Cycle 126 was $1.56E+11$ for the residential sector or 787,245.93 Btu per dwelling.

When Cycle 126 is broken up into its northwestern and southern traverse components, the respective minimal energy consumptions for the city as a whole would be $1.69E+11$ and

1.42E+11 Btu's. The former's average number of heating degree days was 64.30 whilst the latter's was 53.77. The energy consumption rates per dwelling for the above are 857,528.60 and 717,096.63 Btu's.

There were 313 constructed single detached and single attached households in St. Norbert in 1975 and 281 constructed apartments or flats (City of Winnipeg, Department of Environmental Planning, Research Branch, Winnipeg CMA Housing and Population Projections by Community Committee and Census Tracts and Traffic Zones, 1971-96, February 1977, pages 20 and 24 respectively). The community would have therefore burned approximately 4.68E+08 Btu's of space heating fuel or about 2528 gallons of oil equivalent during Cycle 126 as a whole. For group 218 and 195, the consumption would have been 5.09E+08 or 2753.36 gallons of oil whereas for fusion 205 and 206 the usage would have been 4.26E+08 or 2302.46 gallons.

Whereas over 50% of the homes and apartment blocks in St. Norbert were constructed during the energy awareness period 1961-1971 and whereas the majority of the dwellings in this community have been classified as 'good', let us assume that the respective R values for ceilings and walls are constant at 11 and 10 (Government of Canada, Central Mortgage and Housing Corporation, 1974 Survey of Housing Units, Cross-tabulation of Dwelling Units and Households, Survey Area No.23, Winnipeg, NHA 5146-23 Weir et al., 1978, Map D, page

42;Energy,Mines and Resources Canada,Keeping the Heat In,August 1976,pages 35-36). R or thermal resistance is a measure of the resistance to heat flow either of a material of any given thickness or of a combination of materials. The value can be determined by multiplying the material's thermal resistivity $1/k$,where k is thermal conductivity,see Section 2.3,by the unit thickness.

The total minimal estimated space heat loss per dwelling would vary between approximately 20 to 30 percent of the above calculated energy consumption,depending upon the life style of the occupant(s) as well as the elongation and orientation of the dwellings with regards to the sun's seasonal altitude,wind directions and speeds,air infiltrations and so forth (Ibid.,pages 6-7,92-94;Government of Manitoba,Department of Energy and Mines,Conservation and Renewable Energy Branch,Housing Standards Summary,August 1981 Aho,1981,Chapter 3) The minimal expected heat loss therefore during Cycle 126 for St. Norbert would be about $0.94E+08$ Btu's or 506 gallons of Bunker 'C' oil. Respective loss per dwelling would be $1.58E+05$ Btu's or 0.85 gallons oil equivalent. Corresponding losses for the northwestern fusion would be $1.02E+08$ Btu's or 171,505.72 per dwelling whilst that for the southern grouping would be $0.85E+08$ or 143,419.33 per dwelling.

APPENDIX B

Hypothetical Estimation of Unicity Fashion Square Heat Loss

During the period November 16, 1976 - December 15, 1976, approximately 5.21×10^6 cubic feet of natural gas was consumed for space heating (Personal communication, James Park, Maintenance Supervisor, Unicity Fashion Square, December 7, 1976, 1010hrs). During this period, there were approximately 1744.74 heating degree days below 65°F . The energy consumption therefore per heating degree day during this period would have been a hypothetical 2987.84 cubic feet of natural gas.

There were 49.92 heating degree days during November 23rd, 1976: the day on which traverse 195 was conducted. Thus the energy consumption would have been 1.49×10^5 cubic feet or 1.49×10^8 Btu equivalent (Personal communication, Ken Wilson. Commercial Marketing, Greater Winnipeg Gas Corporation, December 15, 1976, 1030hrs).

The maximum allowable heat loss, under the most probable adverse climatological conditions, incorporated into the blueprints of Unicity could not be obtained nor determined from the HVAC plans because the plans were missing (Personal communication, R. Wesche, Mechanical Engineer, Abuugav and Sunderland, Calgary, Alberta, December 15, 1976, 1300hrs). The estimated heat loss or the estimated energy conservation

potential for such a regional commercial store was therefore taken to be 30, (Government of Canada, Energy, Mines and Resources, Conservation and Renewable Energy Branch, Building Series, Publication No. 1, Patterns and Levels of Commercial and Industrial Consumption: A Case Study of Metropolitan Toronto, Chapter 2 and Appendix C, 1979) Hence, the hypothetical heat loss during traverse 218 would have been in the vicinity of $4.48E+07$ Btu or 241.9 gallons oil equivalent.

This estimate might seem quite high but one should keep in mind that the loading docks are heated and Unicity's HVAC system was designed such that any excess pressure in the complex would be immediately released by roof ventilation apparatus.

APPENDIX C

DATES ON WHICH TRAVERSES WERE CONDUCTED

The following list contains the dates on which the traverses mentioned throughout this thesis were undertaken. The format used is year - month - day followed by the traverse number.

76 - 02 - 04	T1	,	T2	,	T3
76 - 03 - 13	T4	,	T5	,	T6
76 - 04 - 01	T8	,	T9		
76 - 09 - 21	T124				
76 - 09 - 27	T128				
76 - 10 - 04	T138				
76 - 10 - 05	T139	,	T140	,	T141 , T142
76 - 10 - 13	T143				
76 - 10 - 18	T151	,	T152	,	T153 , T154
76 - 10 - 19	T155	,	T156		
76 - 10 - 25	T159	,	T160	,	T161 , T162
76 - 10 - 26	T163	,	T164	,	T165 , T166
76 - 11 - 01	T167				
76 - 11 - 02	T171	,	T172	,	T173 , T174
76 - 11 - 08	T175	,	T176	,	T177 , T178
76 - 11 - 09	T179	,	T180	,	T181 , T182
76 - 11 - 15	T183	,	T184	,	T185 , T186
76 - 11 - 16	T187	,	T188	,	T189 , T190
76 - 11 - 22	T191	,	T192	,	T193 , T194
76 - 11 - 23	T195	,	T196	,	T197 , T198
76 - 11 - 29	T199	,	T200	,	T201 , T202
76 - 11 - 30	T203	,	T204	,	T205 , T206
76 - 12 - 06	T207	,	T208	,	T209
76 - 12 - 07	T210	,	T211	,	T212 , T213
76 - 12 - 08	T214	,	T215	,	T216 , T217
76 - 12 - 13	T218	,	T219	,	T220 , T221
76 - 12 - 14	T222	,	T223		
77 - 04 - 12	T227				
77 - 04 - 13	T228	,	T231		
77 - 04 - 21	T234	,	T235		

THE CITY OF WINNIPEG



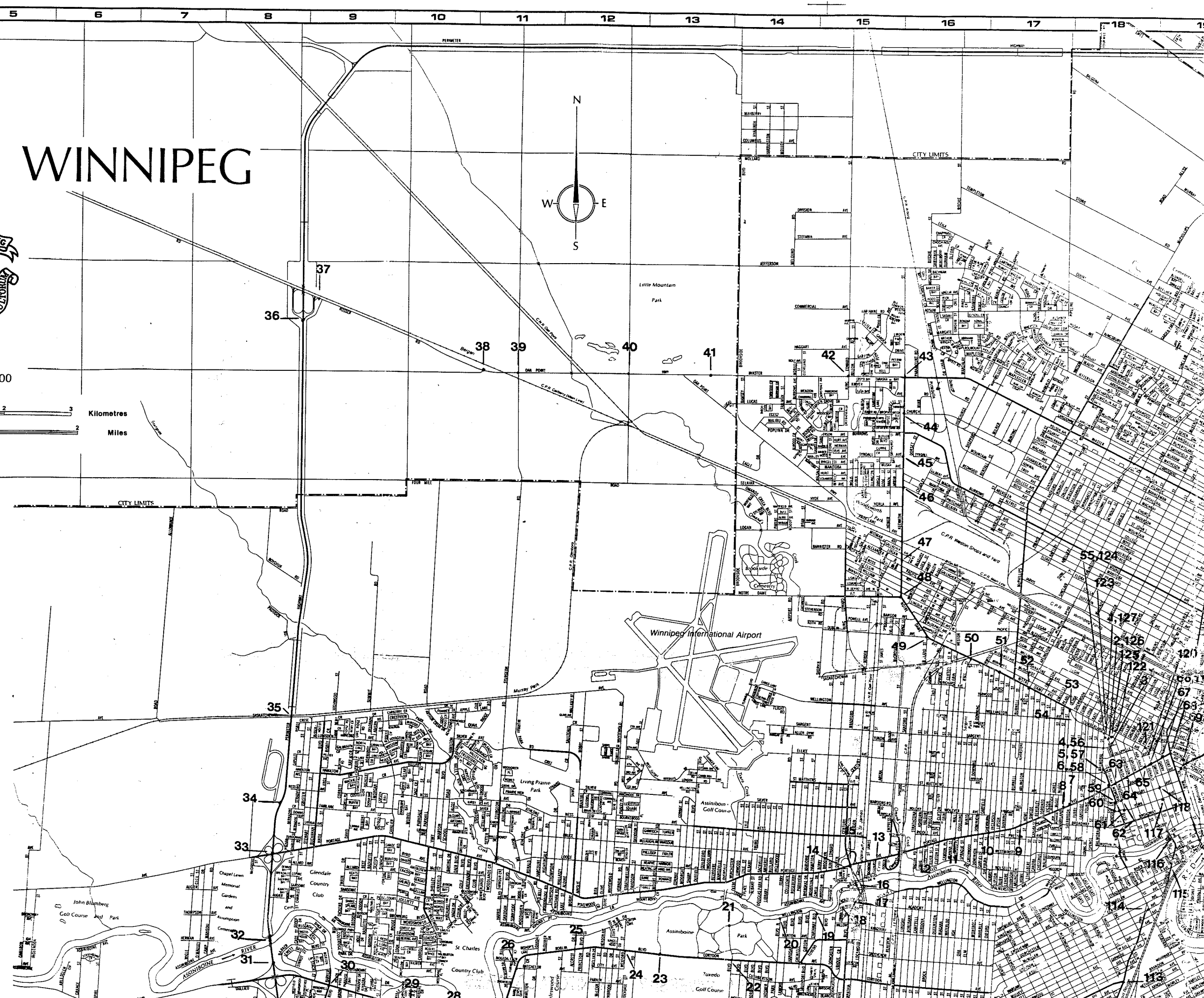
Scale 1:50000



TABLE 5.2.2

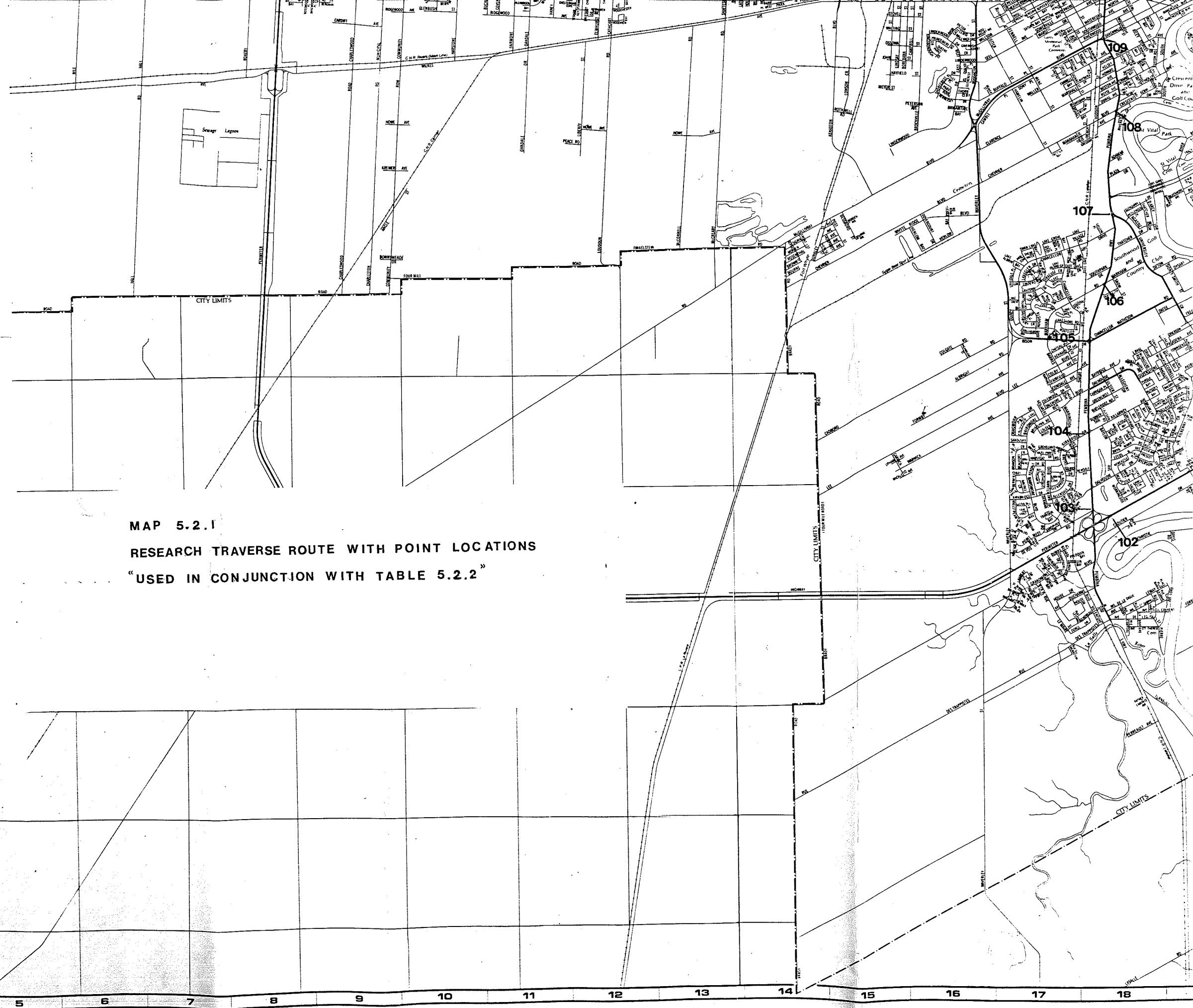
POINT LOCATION, DISTANCE AND TIME INFORMATION

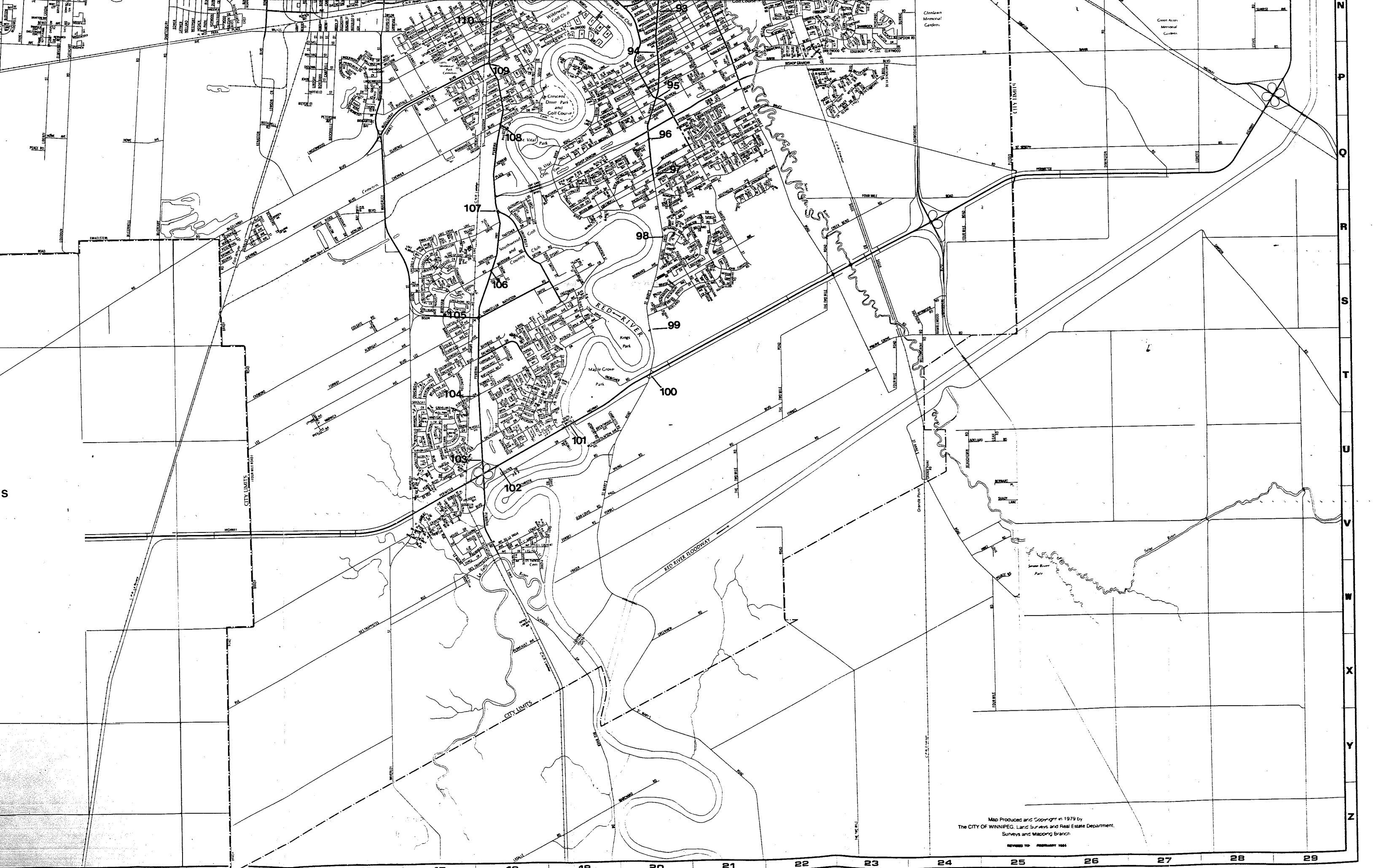
POINT	LOCATION	D (km)	T (sec)
1	Home Driveway	0.00	0.0
2	Driveway-Kennedy	0.03	3.2
3	Kennedy-Sargent	0.13	12.8
4	Sargent-Balmoral	0.10	9.6
5	Balmoral-Ellice	0.35	35.2
6	Colony-Portage	0.29	28.8
7	Portage-Sherbrook	0.60	59.2
8	Portage-Maryland	0.01	9.6
9	Portage-Arlington	0.68	67.2
10	Portage-Sherburn	0.48	48.0
11	Portage-Wall	0.24	24.0
12	Portage-Valour Rd.	0.24	24.0
13	Portage-Tylehurst	0.81	80.0
14	Portage-onto Cloverleaf	0.63	62.4
15	Cloverleaf-Century	0.48	48.0
16	Century-mid Bridge	0.45	44.8
17	Kenaston-Academy	0.32	32.0
18	Academy-Wellington	0.28	25.6
19	Wellington-Chataway	0.68	67.2
20	Wellington-Park Bd.	0.50	49.6
21	Wellington-Conservatory Rd.	0.77	76.0
22	Conservatory Rd.-Corydon	0.48	48.0
23	Corydon-Zoo Entrance	0.56	56.0
24	Roblin-Waxford	1.61	160.0
25	Roblin-Alcrest	0.48	48.0
26	Roblin-Batchelor	0.97	96.0
27	Roblin-Grant	0.81	80.0
28	Roblin-Pepper Loaf Cr.	1.29	128.3
29	Roblin-Community Rd.	0.64	64.0
30	Roblin-Dale	0.97	96.0
31	Roblin-Hwy. 101	0.74	73.6
32	Hwy. 101-mid Bridge	0.48	48.0
33	Hwy. 101-mid Portage Overpass	1.24	123.3
34	Hwy. 101-Downs Entrance	1.29	128.3
35	Hwy. 101-Saskatchewan	0.74	73.6
36	Hwy. 101-on to Hwy. 221	6.28	624.2
37	Cloverleaf-Hwy. 221	0.48	48.0
38	Hwy. 221-Grain Elevator	2.41	240.0
39	Hwy. 221-Sturgeon Rd.	0.97	96.0
40	Hwy. 221-Hwy. 7	0.97	96.0
41	Inkster-Drainage Ditch	2.41	240.0





49	Notre Dame-Dublin	0.87	86.4
50	Notre Dame-Wall	0.68	67.2
51	Notre Dame-Sherburn	0.53	52.8
52	Notre Dame-Arlington	0.50	49.6
53	Notre Dame-Maryland	0.64	64.0
54	Cumberland-Sherbrook	0.16	16.0
55	Cumberland-Balmoral	0.48	48.0
56	Balmoral-Sargent	0.19	19.2
57	Balmoral-Ellice	0.35	35.2
58	Colony-Portage	0.29	28.8
59	Memorial-St. Mary	0.21	20.8
60	Memorial-York	0.16	16.0
61	York-Vaughan	0.10	9.6
62	Vaughan-St. Mary	0.16	16.0
63	Vaughan-Portage	0.26	25.6
64	Portage-Edmonton	0.10	9.6
65	Portage-Donald	0.29	28.8
66	Portage-Smith	0.10	9.6
67	Portage-Fort	0.19	19.2
68	Portage-Main	0.10	9.6
69	Portage-Westbrook	0.37	36.8
70	Westbrook-Water	0.15	14.4
71	Water-mid Bridge	0.63	62.4
72	Provencher-Alneau	1.03	102.4
73	Provencher-Des Meurons	0.60	59.2
74	Provencher-mid Bridge	0.23	22.4
75	Provencher-Archibald	0.39	38.4
76	Archibald-Plinquet	0.42	41.6
77	Plinquet-Dawson Rd.	0.32	32.1
78	Dawson Rd.-Dugald Rd.	1.16	115.3
79	Dawson Rd.-Maion	0.58	57.6
80	Dawson Rd.-Hwy. 59	0.97	96.0
81	Hwy. 59-Maginot	0.45	44.8
82	Hwy. 59-Botourney	1.13	112.3
83	Hwy. 59-Cottonwood	0.97	96.0
84	Hwy. 59-Paterson	0.81	8.1
85	Paterson-Lochmore	0.39	38.9
86	Paterson-Westmount	0.16	16.0
87	Westmount-Hwy. 1	0.27	27.2
88	Hwy. 1-Lakewood	0.93	92.8
89	Hwy. 1-Archibald	0.68	67.2
90	Hwy. 1-mid Bridge	0.81	80.0
91	Hwy. 1-St. Anne's Rd.	0.90	89.6
92	Hwy. 1-St. Mary's Rd.	0.66	65.6
93	St. Mary's Rd.-Glenview	0.32	32.0
94	St. Mary's Rd.-Poplarwood	0.48	48.0
95	St. Mary's Rd.-Dunkirk	0.71	70.4
96	St. Mary's Rd.-Bay Avalon	0.97	96.0
97	St. Mary's Rd.-Woodlawn	0.64	64.0
98	St. Mary's Rd.-Riverside	0.97	96.0
99	St. Mary's Rd.-Hwy. Exit Sign	2.15	214.4
100	St. Mary's Rd.-Hwy. 101	0.81	80.0
101	Hwy. 101-mid Bridge	1.61	160.0
102	Hwy. 101-on Cloverleaf	1.61	160.0
103	Cloverleaf-Pembina	0.16	16.0
104	Pembina-Killarney	1.29	128.3
105	Pembina-Matherson	0.97	96.0
106	Pembina-Markham Rd.	1.29	128.3
107	Pembina-University Cres.	1.13	112.3
108	Pembina-Chevrier	1.45	144.2
109	Pembina-McGillivray Bd.	1.00	99.2
110	Pembina-Point Rd.	0.64	64.0
111	Pembina-Underpass	0.90	89.6
112	Pembina-Stafford	0.48	48.0
113	Pembina-Grant	1.0	99.2
114	Pembina-Corydon	1.22	121.3
115	Donald-Stradbroom	0.74	73.6
116	Donald-mid Bridge	0.50	49.6
117	Smith-York	1.03	102.4
118	Smith-St. Mary	0.19	19.2
119	Smith-Portage	0.37	36.8
120	Smith-Ellice	0.10	9.6
121	Smith-Notre Dame	0.06	6.4
122	Notre Dame-Edmonton	0.55	54.4
123	Notre Dame-Balmoral	0.21	20.8
124	Balmoral-Cumberland	0.10	9.6
125	Cumberland-Kennedy	0.06	6.4
126	Kennedy-Home Driveway	0.02	1.6
127	Home Driveway	0.03	3.2





Map Produced and Copyright in 1979 by
The CITY OF WINNIPEG, Land Surveys and Real Estate Department,
Surveys and Mapping Branch
REVISED TO FEBRUARY 1985